Electrophysiological analysis of the epithelial H^+/oligopeptide transporter, PepT1

Lorraine Anne Beattie
Wolfson College

Thesis submitted for the degree of
Doctor of Philosophy
University of Oxford



Department of Human Anatomy and Genetics
Michaelmas Term 2001

Electrophysiological analysis of the epithelial H^+/oligopeptide transporter, PepT1

Lorraine Beattie, Wolfson College, University of Oxford

D.Phil Thesis submitted Michaelmas Term 2001

The characteristics of transport by the epithelial, proton-coupled oligopeptide transporter, PepT1, have been investigated in PepT1 expressing *Xenopus laevis* oocytes using electrophysiological techniques.

Membrane depolarisations and inward currents have been measured in response to various dipeptide substrates, including structurally modified and charged peptides. The latter part of this study has focussed on the role of phorbol esters on the regulation of PepT1-mediated peptide transport.

I have shown that transport of neutral peptides is dependent on both pH and membrane potential. In addition, the carboxyl terminus plays an important role in substrate recognition and binding, as when blocked, the affinity of the substrate is reduced 10-fold. The importance of position of charge within a dipeptide on substrate binding has also been investigated using dipeptides where the charged amino acid residue is present at either the amino or carboxyl terminus. The results showed that the apparent order of affinity reversed upon extracellular acidification, thus charged residues within the peptide play an important role in substrate binding.

The acute regulation of the oligopeptide transporter has been examined by studying the effects of phorbol esters on the transport of a neutral peptide, Gly-Gln. The active ester, PMA, was shown to decrease both the K_a and the I_{max}. Immunocytochemical studies have confirmed the electrophysiological findings.

All truth passes through three stages: first, it is ridiculed; second, it is violently opposed; and third, it is accepted as self-evident."

Arthur Schopenhauer (1788-1860)

Acknowledgements

There are a number of people who have made this thesis what it is:

First and foremost I would like to thank my supervisor, Richard Boyd, for his guidance and constant enthusiasm even for the smallest of my achievements. I would also like to thank Dr. Alan Chipperfield for encouraging me to stay in science, and for introducing me to Richard Boyd.

A big 'thank you' to Corinna for teaching me everything I needed to know about oocytes and to John for teaching me electrophysiology. Yoshi, Michael, David and Sarah also deserve a 'thank you' for making the CARB lab such a fun place to work, and for all those trips to the pub for 'one pint', which inevitably turned into 'two, three…'. And of course, Bob, a technical genius, without whom some of these experiments may never have been completed.

The Wellcome Trust deserve a mention for the financial support that enabled me to complete this thesis.

No acknowledgements would be complete without a big thank you to my parents and sister for their support and encouragement over the years. And finally to Steve for his unwavering love and encouragement and belief in my abilities.

Declaration

All of the experiments and data analysis presented in this thesis are wholly my own work.

Lorraine Beattie

December 2001

List of Contents

Chapter 1 – Introduction 1

1.1 Membrane potential and membrane transport 1

1.1.1 The cell membrane 1

1.1.2 The membrane potential 2

1.1.2.1Generation of membrane potential 5

1.1.2.1.1Role of the Na^+K^+ATPase 5

1.1.2.1.2Role of K^+ 5

1.1.2.1.3Calculation of E_{K^+} 6

1.1.2.1.4Role of Na^+ 6

1.1.2.1.5The role of Na^+ and K^+ in the generation of membrane potential 7

1.1.2.2 The Goldman-Hodgkin-Katz equation 7

1.1.3 Membrane Transport 9

1.1.3.1 Methods of membrane transport 9

1.1.3.1.1 Diffusion 9

1.1.3.1.2 Carrier-mediated transport 9

1.1.4 Electrogenic transport 10

1.1.4.1 Electrogenicity 10

1.1.4.2 Na^+K^+ATPase 12

1.1.4.3 SGLT1 12

1.1.4.4 hCAT-2A and hCAT-2B 12

1.2 Proton-coupled oligopeptide transport 13

1.2.1 History of intestinal protein absorption 13

1.2.2 Mechanisms of peptide transport 14

1.2.3 Cloning of peptide transporters 16

1.2.4 Localisation of PepT1 18

1.2.4.1 Tissue localisation 18

1.2.4.2 Cellular localisation 20

1.2.5 Functional characteristics of PepT1 20

1.2.5.1 Electrogenicity and H^+-dependence of peptide transport 20

1.2.5.2 Substrate specificity 21

1.2.5.3 Stereospecificity of PepT1 21

1.2.5.4 Stoichiometry of PepT1 22
1.2.6 Methods used to study PepT1 22
1.2.6.1 Brush border membrane vesicles 23
1.2.6.2 Cell lines 23
1.2.6.3 Expression systems 23
1.3 The *Xenopus laevis* oocyte expression system 24
1.3.1 Historical background 24
1.3.2 Oocytes as protein synthesis factories 24
1.3.3 Advantages of using *X.laevis* oocytes 24
1.3.4 Disadvantages of using *X.laevis* oocytes 25
1.4 Aims of this thesis 26

Chapter 2 – Materials and Methods 27
2.1 Preparation of the PepT1 plasmid 27
2.1.1 Making competent cells 27
2.1.2 Transformation of competent cells 28
2.1.3 Amplification of transformed cells 29
2.1.4 Extraction of plasmid 29
2.2 Synthesis of mRNA from a cDNA clone 30
2.2.1 Preparation of the template DNA 30
2.2.2 Phenol-chloroform extraction and ethanol precipitation of DNA 31
2.2.3 Removal of template DNA 33
2.2.4 Termination of the reaction and recovery of the RNA 33
2.2.5 Determination of concentration of the RNA 33
2.3 Preparation of *Xenopus laevis* oocytes 36
2.3.1 Isolation of *X.laevis* oocytes 36
2.3.2 Defolliculation of *X.laevis* oocytes 38
2.3.3 Injection of cRNA 38
2.4 Electrophysiology of *Xenopus laevis* oocytes 42
2.4.1 The whole system – an overview 42
2.4.2 Pulling microelectrodes 42
2.4.3 Preparation of microelectrode holders 43
2.4.4 Assembly of microelectrode and holder 44
2.4.5 Bath perfusion 47

2.4.6 Preparing the electrodes for recording 47
2.4.7 Impaling an oocyte 48
2.4.8 CA-1B high performance oocyte clamp 48
2.4.9 The digidata 1200 series interface 49
2.4.10 The chart recorder 49
2.4.11 Data acquisition 49
2.5 Immunocytochemistry of *Xenopus laevis* oocytes 51
2.5.1 Preparation of oocytes for whole-mount immunocytochemistry 51
2.5.2 Mounting bisected *X.laevis* oocytes 52
2.5.3 Viewing oocytes with the confocal microscope 53
2.6 Experimental solutions 55
2.7 Materials 55
2.8 Calculation of kinetic constants 55
2.9 Data expression and statistics 55

Chapter 3 – Voltage and pH dependence of oligopeptide transport through PepT1 56
3.1 Introduction 56
3.2 Effect of Xaa-Ala peptides on membrane voltage 56
3.2.1 Phe-Ala, Trp-Ala and Tyr-Ala 56
3.2.2 General observations 58
3.2.3 Response to 0.5mM Phe-Ala, Trp-Ala and Tyr-Ala 58
3.2.4 Response to 0.5mM Gly-Ala, Leu-Ala, and Ala-Ala 63
3.3 Transport of Gly-Gln 66
3.3.1 Effect of Gly-Gln on membrane voltage 66
3.3.2 Voltage clamping of Gly-Gln transport 66
3.3.3 Dose-response curves for Gly-Gln transport 70
3.4 pH dependence of peptide transport by PepT1 73
3.4.1 Transport of Leu-Ala 73
3.5 Summary of Chapter 80

Chapter 4 – Analysis of transport induced by native and carboxyl terminus modified peptides 81

4.1 Introduction 81

4.2 Responses induced by Phe-Tyr in PepT1 expressing oocytes 82

4.3 Responses induced by Phe-Tyr in control oocytes 82

4.4 Responses induced by Phe-Tyr-NH_2 in PepT1 expressing oocytes 88

4.5 Responses induced by Phe-Tyr-NH_2 in control oocytes 92

4.6 Comparison of responses induced by Phe-Tyr and Phe-Tyr-NH_2 92

4.7 Dose-response curves of Phe-Tyr and Phe-Tyr-NH_2 transport 92

4.8 Template binding model for PepT1 96

4.9 Summary of Chapter 99

Chapter 5 – Substrate titration is not solely responsible for the effect of pH on charged peptide binding 100

5.1 Introduction 100

5.2 Response to Gly-Asp and Asp-Gly by PepT1 expressing oocytes 101

5.3 Response to Gly-Asp and Asp-Gly at pH 7.5 101

5.4 Response to Gly-Asp and Asp-Gly at pH 5.5 in PepT1 expressing oocytes 107

5.5 Comparison of Gly-Asp and Asp-Gly transport at pH 7.5 and 5.5 112

5.6 Dose-response curves of Gly-Asp and Asp-Gly transport 112

5.7 Summary of Gly-Asp and Asp-Gly experiments 117

5.8 Preliminary experiments with Gly-Lys and Lys-Gly 118

5.9 Summary of Gly-Lys and Lys-Gly experiments 123

5.10 Summary of Chapter 124

Chapter 6 – Regulation of PepT1: The role of phorbol esters 125

6.1 Introduction 125

6.2 Protein kinase C (PKC) 125

6.3 Phorbol 12 myristate, 13 acetate (PMA) 126

6.4 4α-phorbol 12, 13-didecanoate (4α PDD) 126

6.5 Composition of solutions 126

6.6 Effect of PMA on Gly-Gln transport 129

6.6.1 Determining the concentration of PMA and the incubation period 129
6.6.2 Effect of PMA on 2mM Gly-Gln transport 129
6.7 Effect of PMA on Gly-Gln dose-response curves 135
6.8 Control experiments 139
6.8.1 The effect of 4α PDD on Gly-Gln transport 139
6.8.2 The effect of three consecutive pulses of Gly-Gln on transport through PepT1 140
6.8.3 The effect of three consecutive Gly-Gln dose-response curves on K_a and I_{max} 140
6.9 Summary of electrophysiological results 145
6.10 Confocal analysis of PepT1 expression in *X.laevis* oocytes 146
6.10.1 Introduction 146
6.10.2 Effect of PMA and 4α PDD on PepT1 expression determined by FITC 146
6.10.3 Effect of PMA and 4α PDD on PepT1 expression determined by TRITC 147
6.11 Summary of confocal data 153

Chapter 7 – General Discussion 154
7.1 Advantages and disadvantages of electrophysiology 155
7.1.1 Advantages 155
7.1.2 Disadvantages 156
7.2 Evidence for proton dependence of peptide transport 156
7.2.1 Early evidence 156
7.2.2 Evidence presented in this thesis 159
7.3 Structural requirements for PepT1 substrates 159
7.4 Substrate template binding model for PepT1 160
7.4.1 Formulation of the model 160
7.4.2 Experimental evidence supporting the model 162
7.5 Transport of charged peptides 164
7.5.1 Evidence from previous research 164
7.5.2 Evidence from this thesis 164
7.5.2.1 Transport of anionic peptides 164

7.5.2.2 Transport of cationic peptides 166
7.6 Regulation of PepT1 167
7.6.1 Dietary regulation of PepT1 167
7.6.2 Hormonal regulation of PepT1 167
7.6.3 Regulation of PepT1 by PKC 169
7.6.4 Evidence for regulation by phorbol esters 170
7.7 General conclusions and future work 172
7.8 Physiological implications 173

Appendix I – Abstracts 174
AI.1 Analysis of currents induced in PepT1-expressing *Xenopus laevis* oocytes by native and carboxyl terminus modified peptides 174
AI.2 Evidence that substrate titration is not solely responsible for the effect of pH on charged peptide binding in PepT1-expressing *X. laevis* oocytes 175
AI.3 Protein kinase C activation directly alters the kinetics of PepT1-mediated peptide transport 176

Appendix II – Preliminary studies on the transport of N-Formyl-Met-Leu-Phe – A biologically active molecule 178
AII.1 Introduction 178
AII.2 Methods 178
AII.2 .1 Solutions 180
AII.3 Results 180
AII.4 Summary 185

Appendix III- Preliminary experiments investigating the role of intracellular pH on peptide transport 186
AIII.1 Introduction 186
AIII.2 Methods 187
AIII.2.1Electrophysiology 187
AIII.2.2 Radiolabelled influx studies 187

AIII.3 Results 187
AIII.3.1 Electrophysiology 187
AIII.3.2 Radiolabelled influx studies 191

Appendix IV-The 'static head' method to estimate intracellular peptide substrate concentration: A novel electrophysiological application 193
AIV.1 Introduction 193
AIV.2 Reversal potential and the Goldman-Hodgkin-Katz equation 193
AIV.3 Methods 194
AIV.4 Results 194
AIV.5 Summary 198

References 199

List of figures

Figure 1.1	Diagram of the plasma membrane	3
Figure 1.2	Relations between flux and membrane potential	11
Figure 1.3	Schematic diagram of a typical intestinal epithelial cell	15
Figure 1.4	Expression cloning of membrane proteins	17
Figure 1.5	Membrane model of PepT1	19
Figure 2.1	Agarose gel to assess the quality and quantity of linearised DNA	34
Figure 2.2	UV wavelength scan 320-220nm of PepT1 RNA	35
Figure 2.3a	Schematic diagram of a healthy stage VI oocyte	40
Figure 2.3b	Schematic diagram of the Nanoject semi-automated injection system	41
Figure 2.4a	Schematic diagram of the two-electrode voltage clamp set-up	45
Figure 2.4b	Schematic diagram of a microelectrode holder	45
Figure 2.4c	CA-1B high performance oocyte clamp	45
Figure 2.4d	Photograph of the electrophysiology set-up	46
Figure 2.4e	A magnified schematic of the oocyte perfusion bath	46
Diagram 2.4.	Schematic diagram of the bath perfusion system	50
Figure 2.5	Schematic diagram of the light path in the confocal Microscope	54
Figure 3.1a	Voltage trace recorded in response to 1mM Phe-Tyr in a control oocyte	60
Figure 3.2	Voltage traces recorded in response to 0.5mM Phe-Ala, Tyr-Ala, and Trp-Ala at pH 7.5 and 5.5	61
Figure 3.3	Voltage traces recorded in response to 0.5mM Gly-Ala, Leu-Ala, and Ala-Ala at pH 7.5 and 5.5	64
Figure 3.4	Voltage traces recorded in response to the 2mM Gly-Gln at pH 7.5 and 5.5	67
Figure 3.5	Steady state I-V relationship recorded in the presence and absence of Gly-Gln in PepT1 expressing oocytes at pH 7.5	68

Figure 3.6	Steady state I-V relationship recorded in the presence and absence of Gly-Gln in PepT1 expressing oocytes at pH 5.5	69
Figure 3.7	Dose-response curves for Gly-Gln at pH_o 7.5 and pH_o 5.5	71
Figure 3.8a-g	Leu-Ala transport at various pH values	77
Figure 3.8h	Maximal current for Leu-Ala transport plotted at each pH value	77
Figure 4.1	Voltage trace recorded in response to 1mM Phe-Tyr in a PepT1 expressing oocyte	84
Figure 4.2a	Steady state I-V curves recorded in a PepT1 expressing oocyte in the presence and absence of 1mM Phe-Tyr, at pH 7.5	85
Figure 4.2b	Steady state I-V curves recorded in a PepT1 expressing oocyte in the presence and absence of 1mM Phe-Tyr, at pH 5.5	86
Figure 4.3a	Steady state I-V curves recorded in a control oocyte in the presence and absence of 1mM Phe-Tyr at pH 7.5	87
Figure 4.3b	Steady state I-V curves recorded in a control oocyte in the presence and absence of 1mM Phe-Tyr at pH 5.5	87
Figure 4.4.	Voltage trace recorded in response to 5mM Phe-Tyr-NH_2 in a PepT1 expressing oocyte	89
Figure 4.5a	Steady state I-V curves recorded in a PepT1 expressing oocyte in the presence and absence of 5mM Phe-Tyr-NH_2 at pH 7.5	90
Figure 4.5b	Steady state I-V curves recorded in a PepT1 expressing oocyte in the presence and absence of 5mM Phe-Tyr-NH_2 at pH 5.5	91
Figure 4.6	Dose response curves for Phe-Tyr and Phe-Tyr-NH_2 at pH_o 7.5	93
Figure 4.7	Dose response curves for Phe-Tyr and Phe-Tyr-NH_2 at pH_o 5.5	94
Figure 4.8	A template model for substrate binding to PepT1	98
Figure 5.1	Steady state I-V curves recorded in PepT1 expressing oocytes in response to 2mM Gly-Asp and Asp-Gly at pH 7.5	104
Figure 5.2	Currents induced by 2mM Gly-Asp and Asp-Gly at pH 7.5	106
Figure 5.3	Steady state I-V curves recorded in PepT1 expressing oocytes in response to 2mM Gly-Asp and Asp-Gly at pH 5.5	109
Figure 5.4	Relative currents induced by 2mM Gly-Asp and Asp-Gly at pH 5.5	111

Figure 5.5a	Dose-response curves for Gly-Asp and Asp-Gly at pH 7.5	115
Figure 5.5b	Dose-response curves for Gly-Asp and Asp-Gly at pH 5.5	115
Figure 5.6a	Steady state I-V curves in response to 2mM Gly-Lys and Lys-Gly at pH 7.5	120
Figure 5.6b	Normalised values for maximal currents evoked by Gly-Lys and Lys-Gly at pH 7.5	120
Figure 5.7a	Steady state I-V curves in response to 2mM Gly-Lys and Lys-Gly at pH 5.5	121
Figure 5.7b	Normalised values for maximal currents evoked by Gly-Lys and Lys-Gly at pH 5.5	121
Diagram 6.1a	Schematic diagram of PKC	127
Diagram 6.1b	Molecular structure of PMA, an activator of PKC	127
Diagram 6.1c	Molecular structure of 4α PDD	127
Figure 6.1	Peptide induced currents recorded from PepT1 expressing oocytes before and after treatment with the phorbol ester PMA	132
Figure 6.2	Steady state currents induced upon voltage clamping PepT1 expressing oocytes in uptake solution, pH 7.5, before, during and after PMA treatment	133
Figure 6.3	Steady-state I-V relationship in the presence and absence of Gly-Gln before and after incubation with 10nM PMA	134
Figure 6.4a	Steady state I-V curves recorded in response to increasing concentrations of Gly-Gln at pH 7.5	136
Figure 6.4b	Steady state I-V curves recorded in response to increasing concentrations of Gly-Gln after PMA treatment at pH 7.5	136
Figure 6.5a	Dose-response curves for Gly-Gln before and after treatment with the PMA at pH 7.5	137
Figure 6.5b	Maximal currents for Gly-Gln pulses before and after PMA treatment	137
Figure 6.6	Steady-state I-V curves showing the effect of 4α PDD on currents induced by 2mM Gly-Gln and on those recorded in the absence of substrate at pH7.5	141

Figure 6.7a	Dose-response curves for Gly-Gln before and after 4α PDD treatment	142
Figure 6.7b	Maximal current for Gly-Gln pulses before and after 4α PDD treatment	142
Figure 6.8a	Currents induced by three consecutive pulses of 2mM Gly-Gln and those currents recorded in the absence of peptide substrate at pH 7.5	144
Figure 6.8b	Three consecutive dose-response curves evoked by Gly-Gln at pH 7.5	144
Figure 6.9	FITC images obtained by confocal microscopy for control oocytes and those treated with PMA and 4αPDD	148
Figure 6.10	TRITC images obtained by confocal microscopy for control oocytes and those treated with PMA and 4αPDD	150
Figure 7.1	Evidence for proton dependence of peptide transport	158
Figure 7.2	Substrate template-binding model for PepT1	161
Figure 7.3	Inhibition of ^{3}[H]-D-Phe-L-Gln uptake by modified peptides	163
Figure 7.4	Transport of differently charged peptides	165
Figure 7.5	Putative model for effects of phorbol esters on PepT1	171
Figure AII.1	Structure of N-Formyl-Met-Leu-Phe	179
Figure AII.2	I-V curves recorded in the presence and absence of 2mM N-Formyl-Met-Leu-Phe at pH 7.5	181
Figure AII.3	I-V curves recorded in the presence and absence of 2mM N-Formyl-Met-Leu-Phe at pH 5.5	182
Figure AII.4	I-V curves recorded in the presence and absence of 2mM N-Formyl-Met-Leu-Phe at pH 7.5 and 5.5 in a control oocyte	184
Figure AIII.1	Concentration-dependence of Gly-Asp and Asp-Gly in the presence and absence of 25mM sodium acetate at pH 7.5	188
Figure AIII.2	K_i and V_{max} values for ^{3}[H]-D-Phe-L-Gln uptake at pH 5.5	192
Figure IV.1	Peptide induced currents at different clamped voltages in Response to 2mM Leu-Ala between pH5.0-8.0	195
Figure IV.2	Peptide induced currents (E_m=0) by 2mM Leu-Ala expressed As a function of pH_o	196

List of tables

Table 1.1	Concentrations of Na^+ and K^+ in a typical cell	4
Table 2.1	Composition of ice cold cell buffer	28
Table 2.2	Assembly of reaction to linearise template DNA	31
Table 2.3	Reagents used to start transcription reaction	32
Table 2.4a	Composition of Ca^{2+} isolation solution	36
Table 2.4b	Composition of Barth's solution	37
Table 2.5a.	Three-stage program used to make microelectrodes	42
Table 2.5b	Two- stage program used to make injecting microelectrodes	43
Table 2.6a.	Composition of PBS	51
Table 2.6b	Composition of TBSI	52
Table 3.1	Experimental protocol used to investigate the effects of Xaa-Ala peptides in PepT1 expressing oocytes	57
Table 3.2	E_m values for PepT1 and control oocytes	59
Table 3.3	Depolarisations evoked by 0.5mM Phe-Ala, Trp-Ala and Tyr-Ala	62
Table 3.4	Depolarisations evoked by 0.5mM Gly-Ala, Leu-Ala and Ala-Ala	65
Table 3.5	K_a and I_{max} values for Gly-Gln recorded at pH 7.5 and 5.5	72
Table 3.6	Maximal currents evoked by 2mM Leu-Ala recorded at each extracellular pH value	78
Table 4.1	Experimental protocol for the effect of a single saturating concentration of Phe-Tyr at pH 7.5 and pH 5.5	83
Table 4.2	K_a and I_{max} values for Phe-Tyr and Phe-Tyr-NH_2 at pH 7.5 and 5.5	95
Table 5.1	Experimental protocol for the effect of a single saturating concentration of neutral and negatively charged peptides	102
Table 5.2	Maximal current values in response to 2mM Gly-Gln, Gly-Asp and Asp-Gly at pH 7.5	105
Table 5.3	Maximal current values in response to 2mM Gly-Gln,	

	Gly-Asp and Asp-Gly at pH 5.5	110
Table 5.4	Maximal current values in response to 2mM Gly-Gln, Gly-Asp and Asp-Gly at pH 7.5 and 5.5	114
Table 5.5a	K_a values for Gly-Asp and Asp-Gly at pH 7.5 and 5.5	116
Table 5.5b	I_{max} values for Gly-Asp and Asp-Gly at pH 7.5 and 5.5	116
Table 5.6	I_{max} values for Gly-Lys and Lys-Gly at pH 7.5 and 5.5	122
Table 6.1	Composition of uptake solution	128
Table 6.2	Detailed protocol for voltage clamp experiments involving PMA	131
Table 6.3	K_a and I_{max} values for Gly-Gln transport through PepT1 at pH 7.5 before and after PMA treatment	138
Table 6.4	K_a and I_{max} values for Gly-Gln transport through PepT1 at pH 7.5 before and after 4α PDD treatment	143
Table 6.5	Maximum intensity of fluorescence obtained for each experimental condition using FITC	149
Table 6.6	Maximum intensity of fluorescence obtained for each experimental condition using TRITC	152
Table 7.1	Uptake of ^{14}[C]Gly-Sar	168
Table AII.1	Maximal current values obtained in response to 2mM N-Formyl-Met-Leu-Phe	183
Table AIII.1	K_a and I_{max} values for Gly-Asp and Asp-Gly in the presence and absence of 25mM sodium acetate at pH 7.5	190

CHAPTER 1

INTRODUCTION

The aim of this chapter is to provide the background on which the studies presented in this thesis are based. It has been divided into three sections;

1.1 *Membrane potential and membrane transport* where the principles of membrane potential will be discussed as well as an overview of membrane transport.

1.2 *Proton-coupled oligopeptide transport*, where the cellular and molecular mechanisms of peptide transport will be covered detailing the techniques used and the most recent advances on this topic.

1.3 *The Xenopus laevis oocyte expression system,* where the expression system used to study PepT1 in this thesis will be discussed.

1.1 Membrane potential and membrane transport

1.1.1 The cell membrane

The cell membrane separates the intracellular environment from the extracellular environment and is essential for the survival of all cells. It is an extremely thin layer composed of lipids (mostly phospholipids and a little cholesterol), proteins and carbohydrates. It serves as a mechanical barrier whilst also selectively allowing specific substances to enter and leave the cell (Zubay and Salemme, 1988).

The membrane is described as a fluid lipid bilayer embedded with proteins. The lipid bilayer consists mainly of phospholipids that have polar head groups and non-polar tails, with a small amount of cholesterol to prevent the tails from packing together. The proteins can either span the whole membrane or can stud either the intracellular

or extracellular face of the membrane. The lipid bilayer forms the primary barrier to diffusion, whereas the proteins perform more specific membrane functions.

The membrane carbohydrates are only found on the extracellular face of the membrane. They are thought to play a role in the orienting and anchoring of membrane proteins, as well as in cell-cell interactions and recognition and they are also thought to prevent overgrowth of tissue, i.e. they are a means by which the cells guide their growth (Sherwood, 1993). Figure 1.1 shows a diagram of the cell plasma membrane.

1.1.2 Membrane potential

Membrane potential refers to the separation of opposite charges across the plasma membrane. It is the unequal distribution of a few key ions between the intracellular and extracellular environments, and their selective movement through the plasma membrane that are responsible for the electrical properties of the membrane.

Membrane potential is primarily due to the differences in distribution and membrane permeability of Na^+, K^+ and large intracellular anions. In general, cells have a high concentration of K^+ inside compared to the outside, and a low concentration of Na^+ inside compared to a high concentration outside. Table 1.1 shows typical intracellular concentrations for sodium and potassium ions in oocytes and enterocytes.

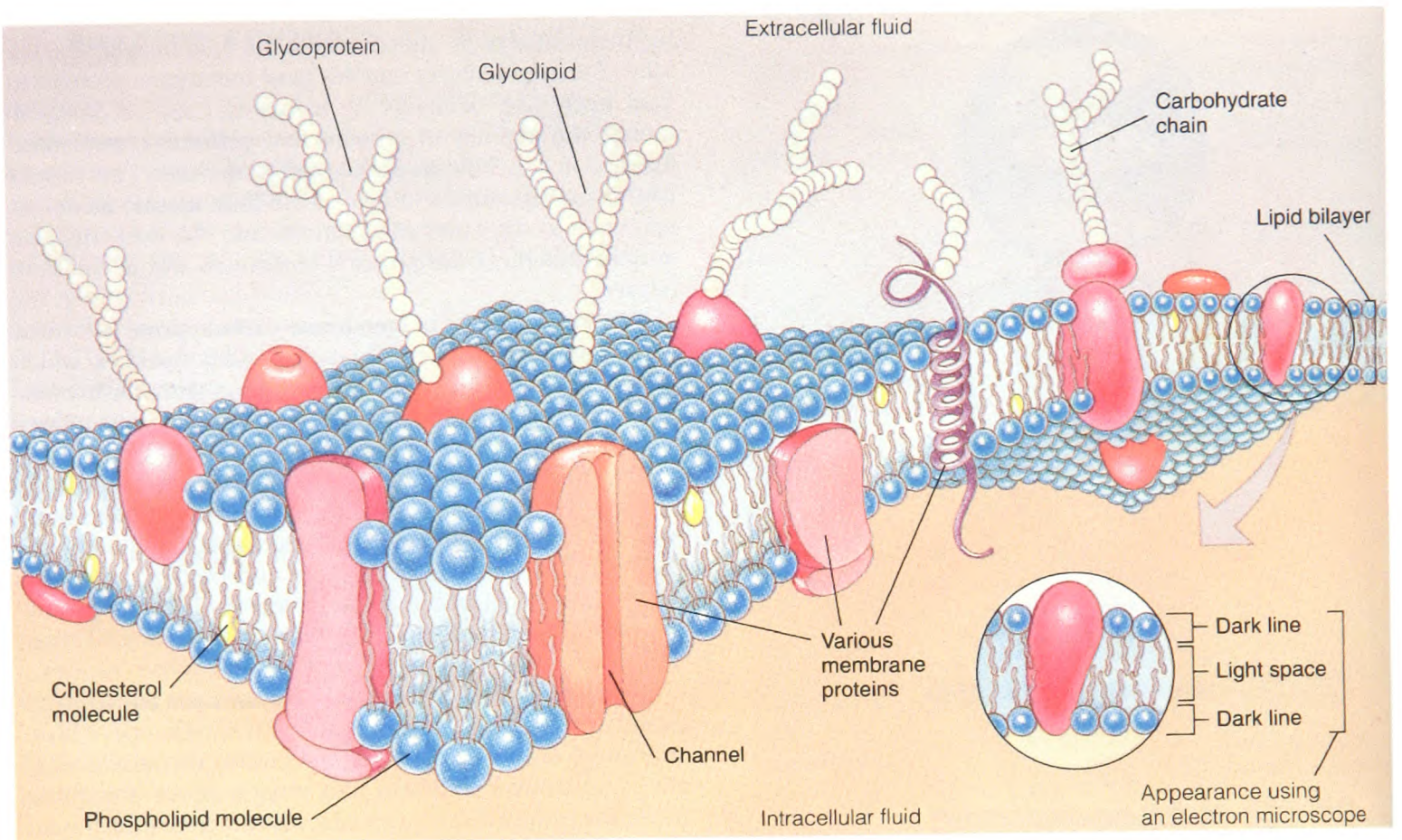


Figure 1.1 Diagram of plasma membrane structure showing all major components of the fluid mosaic model. (Reproduced from Sherwood, 1993)

Ion	Concentration (mM/L)		
	Typical Cell	Oocyte	Epithelial cell
Na^+	5	23	27
K^+	150	110	85

Table 1.1 Concentrations of Na^+ and K^+ in the intracellular environment in an oocyte and enterocyte (values obtained from Weber, 1999, review, and Armstrong, 1975).

1.1.2.1 Generation of membrane potential

1.1.2.1.1 Role of Na^+K^+ATPase

The sodium pump indirectly generates approximately 20% of the membrane potential. It creates potential by the unequal movement of the two ions, namely 3 Na^+ out of the cell, for 2 K^+ into the cell per cycle (Stein 1990). The sodium pump is responsible for maintaining the concentration gradients of Na^+ and K^+, which are responsible for the other 80% of the generation of the membrane potential, E_m, (Sherwood, 1993).

1.1.2.1.2 Role of K^+

Potassium is largely responsible for the generation of membrane potential. This is due to the cell membrane being much more permeable to it than any other ion. The increased permeability to potassium is because at any one time there are more K^+ channels open than for any other ion. The negative intracellular proteins also play a role in membrane potential as they are unable to cross the membrane, and are essentially 'trapped' in the intracellular environment.

As there is a high concentration of potassium ions inside the cell, there is a concentration gradient for movement of potassium out of the cell. As the K^+ leaves, positive charge also leaves the cell, and thus the inside of the cell becomes more negative. An electrical gradient for K^+ also exists, but it is much weaker than the concentration gradient. However, as more K^+ leaves the cell, the concentration gradient gets weaker and the electrical gradient gets stronger. There are therefore driving forces present for the movement of K^+ in both directions. When these two

gradients equal each other, there is no net movement of K^+, and the equilibrium potential of K^+ has been reached, E_{K^+}.

1.1.2.1.3 Calculation of E_{K^+}

The equilibrium potential for any ion, E_{ion}, is calculated using the Nernst equation:

$$E_{ion} = \frac{RT}{zF} \log \frac{C_o}{C_i} \quad \text{or} \quad E = 61 \log \frac{C_o}{C_i}$$

where:

E_{ion} = equilibrium potential for the ion (mV)

61 = a constant that incorporates the gas constant (R), temperature (T), the valence of the ion (z) and Faraday's constant (F)

C_o = the concentration of the ion in the extracellular fluid in mM

C_I = the concentration of the ion in the intracellular fluid in mM

So using the values from table 1,

$$E_{K^+} = 61 \log \frac{5}{150}$$

$$E_{K^+} = 61 \log (-1.477)$$

$$\mathbf{E_{K^+} = -90mV}$$

This calculation is representative of conditions at body temperature. Experiments in this thesis were done at room temperature.

1.1.2.1.4 Role of Na^+

Sodium also has a role to play in the generation of membrane potential. It is a less permeant ion than potassium, but can nevertheless pass through the plasma membrane. In contrast to K^+, Na^+ is in high concentration outside the cell, and in low

concentration inside the cell. This means that there is a strong concentration gradient driving movement of sodium into the cell, thus introducing positive charge to the inside of the cell. This movement of Na^+ into the cell results in an electrical gradient being set up for the movement of Na^+ out of the cell. This electrical gradient is weaker than the chemical gradient, but becomes stronger as more positive charge enters the cell. The concentration gradient decreases with continued movement of Na^+ into the cell. When these two gradients are equal in strength there is no net movement of Na^+ and thus the E_{Na}^+ has been reached. The value for E_{Na}^+ is approximately + 60mV as determined by the Nernst equation, using the intracellular and extracellular concentrations quoted in table 1.1.

1.1.2.1.5 The role of K^+ and Na^+ in the generation of membrane potential

In a typical cell, the large net diffusion of potassium ions out of the cell establishes the E_K^+ of –90mV. The relatively small net diffusion of Na^+ into the cell neutralises some of the potential created by K^+, resulting in a membrane potential of approximately –70mV. The E_m is closer to the equilibrium potential for K^+ due to the greater permeability of the cell for K^+. However, at –70mV, neither K^+ nor Na^+ are at equilibrium and as a result there is leak of both of the ions. The Na^+K^+ATPase controls the leak of these ions and thus all exchanges between the intracellular and extracellular environments are balanced.

1.1.2.2 The Goldman-Hodgkin-Katz equation

However, the most commonly used formula for describing the resting membrane potential is the Goldman-Hodgkin-Katz equation. It takes into account the ion concentrations and permeabilities (Schultz, 1980). Given the conductance properties of the membrane, the ionic distribution across the membrane and the active transport currents for Na^+ and K^+, the resting membrane potential can be predicted using the conductance equation.

$$E_m = \frac{RT}{F} \ln \frac{P_K [K]_o + P_{Na} [Na]_o + P_{Cl} [Cl]_i}{P_K [K]_i + P_{Na} [Na]_i + P_{Cl} [Cl]_o}$$

where

P = permeability of the indicated ion (K^+, Na^+, Cl^-)

R = gas constant

T = temperature (degrees Kelvin)

F = Faraday's constant

This equation gives a potential for the steady-state condition, where the net current leaving the cell is equal to that entering the cell. The membrane potential is calculated as a weighted mean of all of the ions involved, and as stated above in section 1.1.2.1.5, potassium is the major factor in the calculation of membrane potential.

1.1.3 Membrane Transport

1.1.3.1 Methods of membrane transport

1.1.3.1.1 Diffusion

There are two main types of diffusion, (i) through the lipid bilayer and (ii) through a channel.

(i) Diffusion of nonpolar molecules such as O_2 and CO_2 pass through the lipid bilayer moving down their concentration gradient from high to low concentration until a state of equilibrium is reached.

(ii) Diffusion through channels involves the movement of ions such as Na^+, K^+, Ca^{2+} and Cl^- down their electrochemical gradient, again until equilibrium is reached.

1.1.3.2 Carrier-mediated transport

There are three main types of carrier-mediated transport; facilitated, primary active and secondary active transport.

(i) Facilitated carrier-mediated transport. This is a method whereby a carrier, e.g. the GLUT family of glucose transporters (reviewed by Thorens, 1993), can transport specific molecules across the membrane in the direction of their concentration gradient. This type of membrane transport has a transport maximum; i.e. the carrier molecule can become saturated.

(ii) Primary active transport. This is a method of membrane transport where an energy source is required, e.g. ATP. In primary active transport, specific ions or molecules are moved against their concentration gradients. An example of this sort of transport is the Na^+K^+ATPase. This transporter actively transports

Na^+ and K^+ ions against their concentration gradients energised by the hydrolysis of ATP (Kirk *et al*, 1980).

(iii) Secondary active transport. In this case the molecules are transported via a carrier using the concentration gradient established by another transporter, usually the Na^+ gradient of the Na^+K^+ATPase. For example, glucose transport against its concentration gradient is driven by the Na^+ concentration gradient, e.g. SGLT1 (Hediger *et al*, 1987).

1.1.4 Electrogenic transport

1.1.4.1 Electrogenicity

Electrogenic transport occurs as a result of net movement of charge. This movement of charge results in a change to the membrane potential, and as such allows electrophysiological techniques to be used to investigate transport by these transporters. The theoretical basis of electrogenic carrier-mediated transport has been fully considered by Schultz (1980). The major conclusion from the analysis was that the I-V relationship for flux through an electrogenic co-transporter depends on whether the carrier itself is charged. However, the relations between the current flow and membrane potential are only different for electrogenic carrier mechanisms from the constant field Goldman-Hodgkin-Katz equation at extremes of membrane potential. Close to the reversal potential, the curves are experimentally indistinguishable, see figure 1.2.

A number of electrogenic transporters will be discussed, focussing on the sodium pump and other specific solute transporters.

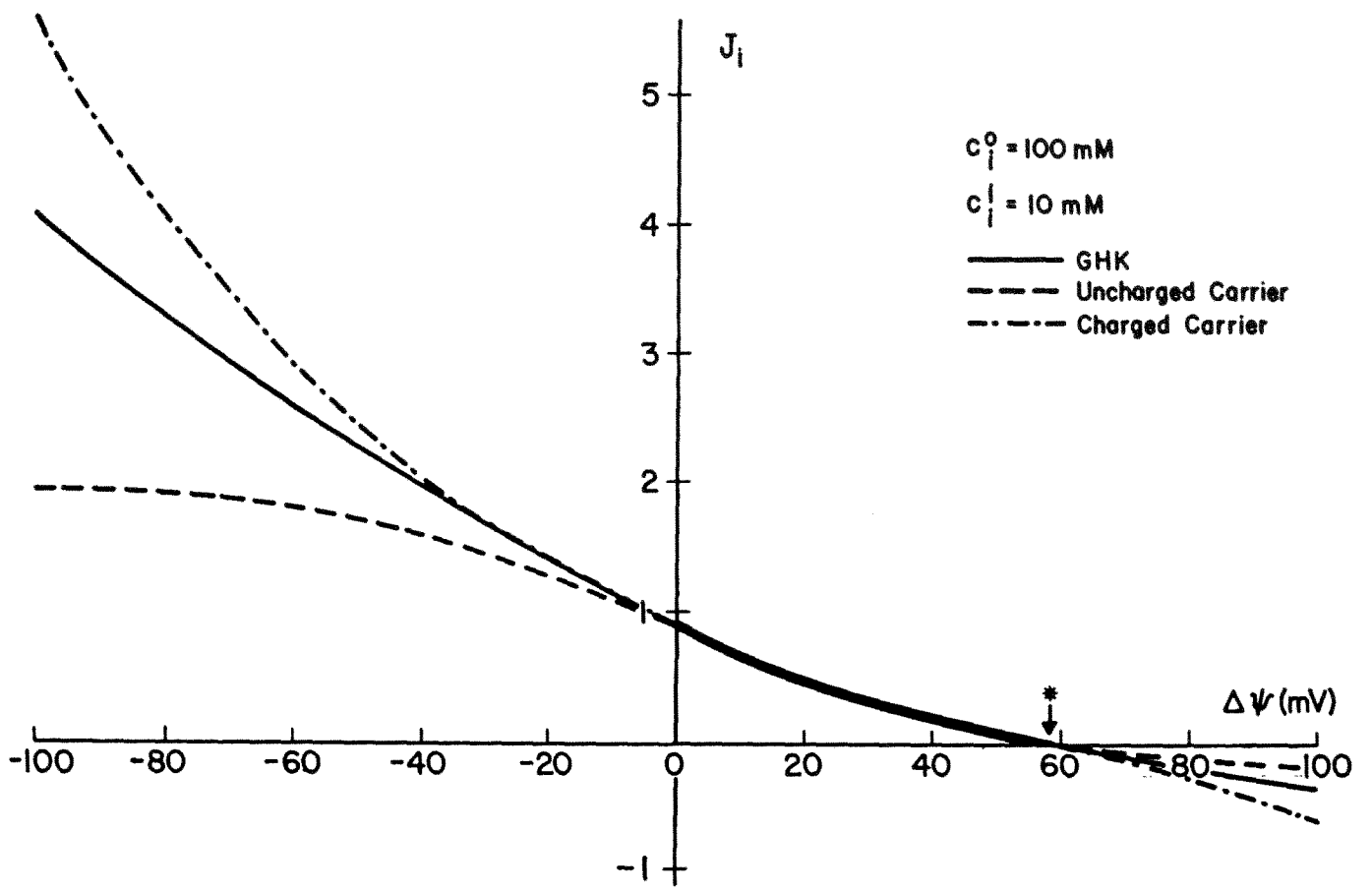


Figure 1.2. Relations between flux, (J_i), and membrane potential, ($\Delta\psi$), predicted by the Goldman-Hodgkin-Katz equation for simple diffusion of a monovalent cation, and for carrier-mediated transport of a monovalent cation by an uncharged or charged carrier. The arrow represents the reversal potential, (reproduced from Schultz, 1980).

1.1.4.2 Na^+K^+ATPase

The sodium pump is one of the most common electrogenic transporters. It is found in the basolateral membrane of epithelial cells, and it transports three Na^+ out of the cell for every two K^+ into the cell, against the sodium and potassium concentration gradients. As a result of this, there is a net efflux of one positive charge leaving the cell during each turn of the pump cycle (Stein, 1990). The sodium pump sets up many of the electrochemical gradients that drive transport of other solutes.

1.1.4.3 SGLT1

The Na^+ -coupled glucose transporter from rabbit small intestine was cloned in 1987 by Hediger *et al.* This transporter was electrogenic due to the net influx of positive charge carried by Na^+ with each glucose molecule. Subsequent studies using *X. laevis* oocytes microinjected with the cRNA for this transporter focussed on measuring the inward currents generated by the sodium-coupled glucose transporter (see figure 1.3 and section 1.3). The currents induced by transport of Na^+ and glucose were biphasic, with a voltage dependent region from +20 to –75mV) and voltage independent from -75 to -150mV, (Birnir *et al*, 1991).

1.1.4.4 hCAT2A and 2B

The CAT family transporters are similar to oligopeptide transporters in that they have different isoforms, much like the oligopeptide transporters, PepT1 and PepT2. Transport of cationic amino acids was for many years thought to occur via a single transporter protein, system y^+, however, now there are known to be several different

transport proteins involved, (Devés and Boyd, review, 1998). One particular family that transports these cationic amino acids is the CAT family, and two members of this family are hCAT2A and hCAT2B (Closs *et al*, 1997). In a recent study using the two-electrode voltage-clamp, Nawrath *et al*, 2000, showed these transporters exhibited both inward and outward currents dependent on the concentration gradient of the substrate amino acid and on the E_m. The two isoforms were shown to have distinct electrical properties and contribute differentially to the transport of cationic amino acids.

1.2 Proton- coupled oligopeptide transport

1.2.1 History of intestinal protein absorption

In the first decade of the 19th Century, investigators began studying a number of substances we now call proteins. By 1820, the nature and importance of protein substances was realised, and in 1838 the term 'proteine' was introduced by G.J. Mulder (Matthews, 1991). By the end of the 19th Century there was an established view of protein absorption whereby protein was absorbed intact through the membrane of the epithelial cells.

At the turn of the 20th Century however, came the discovery trypsin and of 'erepsin', an enzyme which could rapidly break down proteins to amino acids (Cohnheim, 1901), (see Matthews, 1991). The theory of protein being absorbed intact was seriously challenged, and by 1920 the 'classical hypothesis' had been formulated. Proteins were believed to be completely digested by erepsin into constituent amino acids before being absorbed into the epithelial cells by passive mechanisms. This hypothesis was challenged as early as 1921 by Cathcart, who demonstrated the accumulation of intact peptides, however, this study was overlooked.

To further strengthen the classical hypothesis, in the early 1950's active transport of amino acids was demonstrated, and it was concluded that this transport was dependent on Na^+, saturable, and it obeyed Michaelis-Menten kinetics. Some mutual inhibition between some amino acids was also observed, leading to the theory that there were several different transport systems for different amino acids.

It was not until the mid 1950's-60's that work by Newey and Smith, and later Matthews (1968) provided evidence for small peptides being absorbed intact. By the early 1970's the importance of active transport of di- and tripeptides was recognised.

1.2.2 Mechanisms of peptide transport

Epithelial cells are polarised, each having two distinct membranes, the apical membrane and the basolateral membrane. The apical brush border membrane is in contact with the lumen and the basolateral membrane is in contact with the blood. Each membrane contains a different array of membrane proteins; channels, pumps and transporters, all of which aid the transcellular transport of solutes. Figure 1.3 is a schematic diagram of an epithelial cell showing the major pumps and transporters involved in the transcellular transport of protein. In figure 1.3 the Na^+K^+ATPase maintains the Na^+ gradient for the Na^+/H^+ exchanger (NHE3), and the NHE3 in turn maintains the proton gradient for PepT1.

Peptide transport studies have centred mainly on the mechanism of entry into the epithelial cells due to the fact that most peptides are readily hydrolysed upon entry into the epithelial cells, and thus they exit the cell and enter the bloodstream as amino acids. However, Thwaites *et al*, 1993a were able to show exit of intact dipeptides, thus providing evidence of an exit pathway for dipeptides. Terada *et al*, 1999 carried

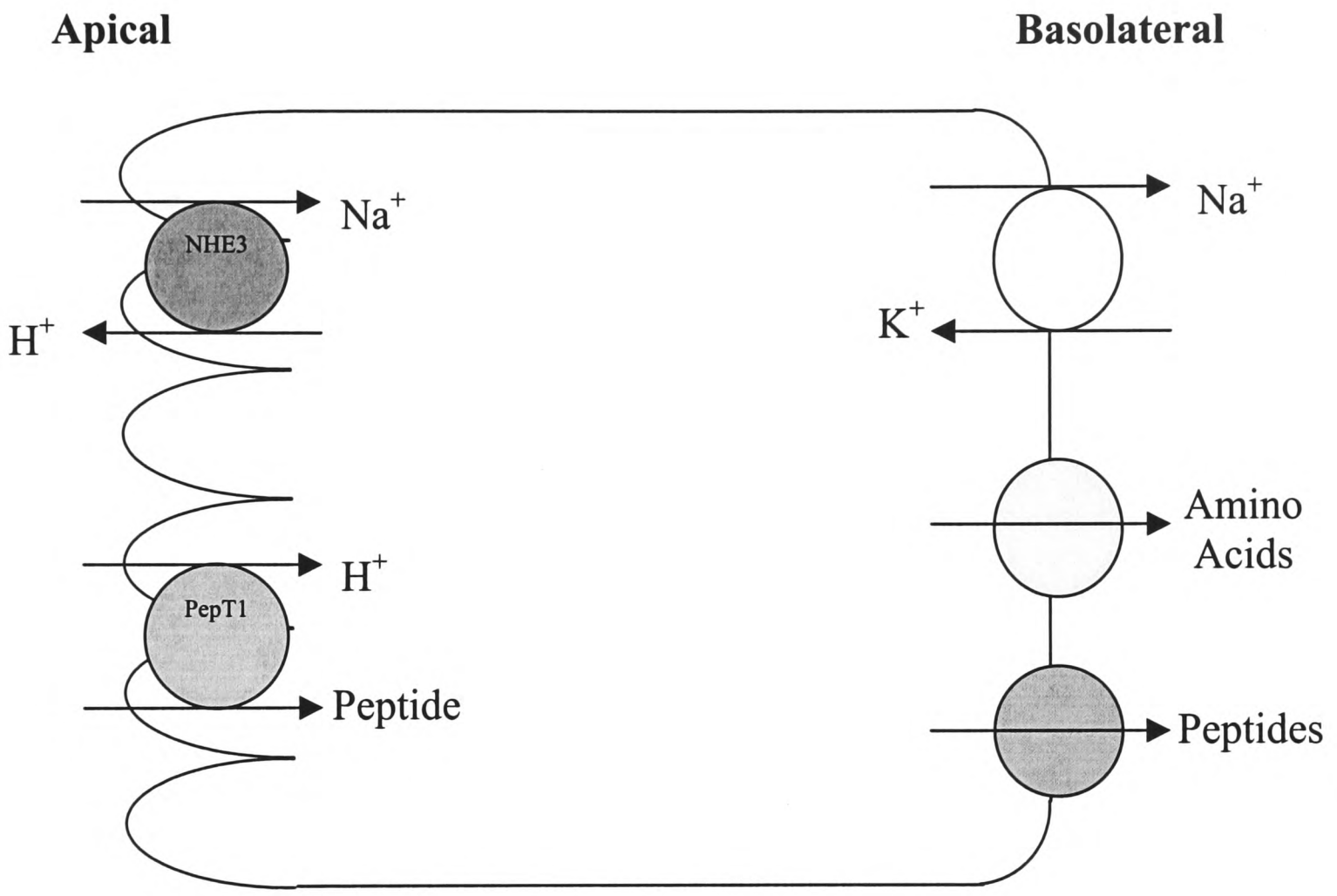


Figure 1.3 Schematic diagram of a typical epithelial cell showing the brush border and basolateral membranes and the pumps and carriers typically found in the epithelial cells of the small intestine which play a role in peptide transport.

out a study on Caco-2 cells to functionally characterise the basolateral transporter and found it to be less sensitive to the pH of the extracellular environment and to be a lower affinity system than PepT1. Dipeptide transport via this transporter did not occur against its concentration gradient. They concluded that a single facilitative transporter existed at the basolateral membrane that worked co-operatively with PepT1 to bring about transepithelial peptide transport.

1.2.3 Cloning of peptide transporters

PepT1 was the first mammalian H^+/oligopeptide transporter to be cloned, (Fei *et al*, 1994). They used a method known as expression cloning, see figure 1.4, which avoided the requirement for any structural information of PepT1. Briefly, the technique involved injecting poly $(A)^+$ RNA from rabbit small intestinal mucosa into *Xenopus laevis* oocytes to test for H^+-coupled peptide transport. A plasmid cDNA library was constructed from the active RNA fraction. Screening a rabbit intestinal cDNA library isolated a peptide transporter cDNA of 2746bp coding for PepT1. This gene coded for a 707 amino acid protein which when microinjected into X.laevis oocytes induced H^+/oligopeptide transport. The expression of this protein in the oocytes resulted in a 63-fold increase in Gly-Sar transport, compared to control water injected oocytes. PepT2 was subsequently identified in human kidney, (Liu *et al*, 1995), and a 729 amino acid protein was identified which induced H^+/oligopeptide transport in transfected HeLa cells. PepT2 was found to share 50% identity and 70% similarity to human PepT1, (Liang *et al*, 1995). PepT1 and PepT2 have now been cloned in many different species; human PepT1 (Liang *et al*, 1995), rat PepT1 (Saito *et al*, 1995), murine PepT1 (Fei *et al*, 2000) and ovine PepT1 (Pan *et al*, 2001), and

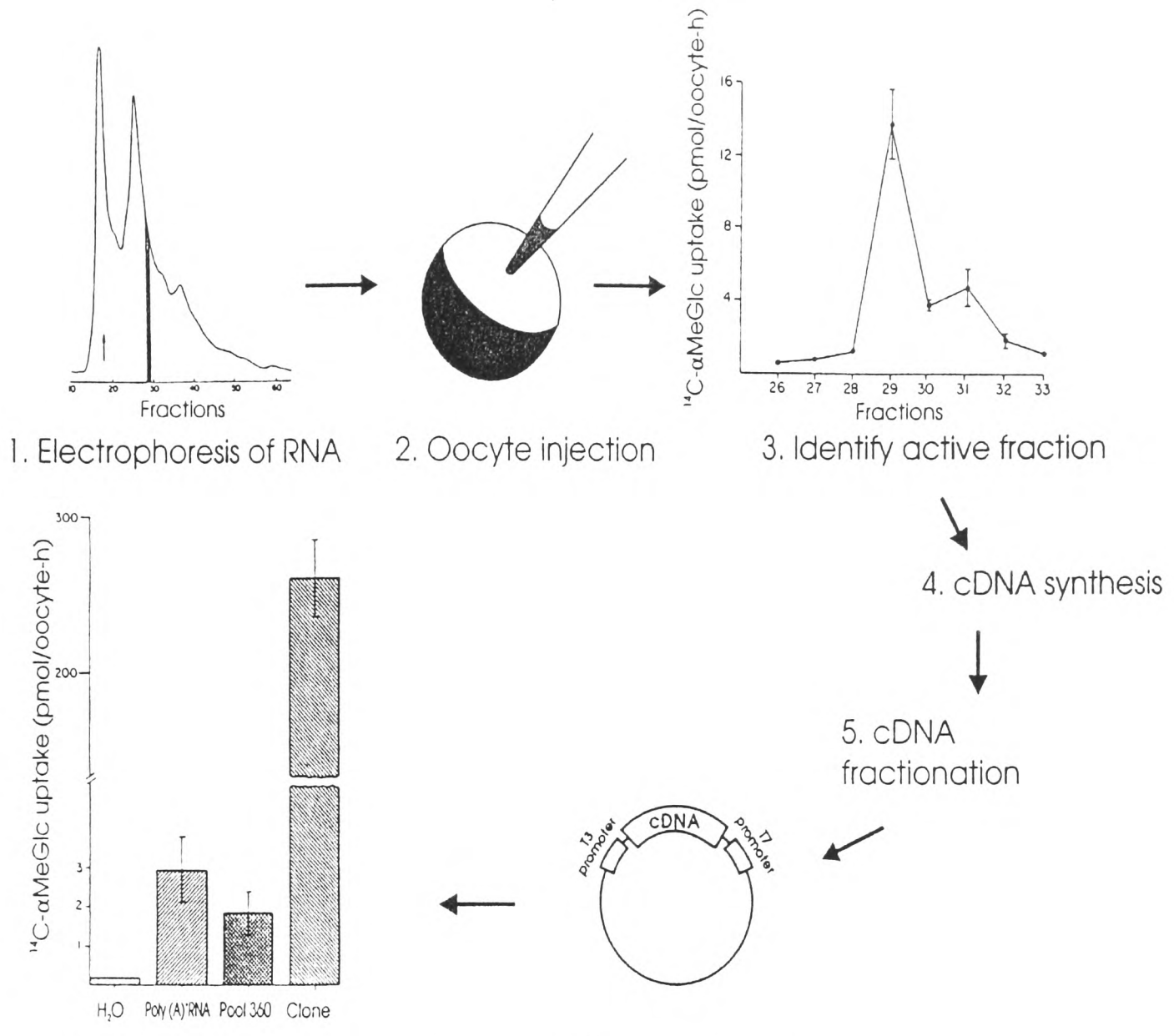


Figure 1.4 Expression cloning of membrane transport proteins using *X.laevis* oocytes (reproduced from Hediger and Rhoads, 1994)

rat PepT2 (Saito *et al*, 1996), rabbit PepT2 (Boll *et al*, 1996) and murine PepT2 (Rubio-Aliaga *et al*, 2000).

In addition a number of other H^+-coupled peptide transporters have been identified; OPT1 in *D.melanogaster* (Roman *et al*, 1998), CPTA and CPTB in *C.elegans* (Fei *et al*, 1998) and PEP2 also in *C.elegans* (Rubio-Aliaga and Daniel, *in press*).

PepT1 and PepT2 both have 12 transmembrane (TM) spanning domains, similar to SGLT1 (Hediger *et al*, 1995). PepT1 is unique however in that it has a large extracellular loop between TM domains 9 and 10 and an intracellular loop which is high in charged residues, see figure 1.5.

PepT1 has little in common with other mammalian transporters, but has some homology with plant and bacterial transporters. PepT1 shows weak similarity to the H^+-dependent CHL1 transporter from plants as well as Dtp, a di/tripeptide transporter from *Lactococcus lactis* and YhiP a putative protein found in *Escherichia coli,* (Hediger *et al*, 1995).

1.2.4 Localisation of PepT1

1.2.4.1 Tissue localisation

PepT1 has been found in many different tissues throughout the body. First reports determined that PepT1 mRNA was present in the intestine, kidney and liver and in small amounts in the brain, (Fei *et al*, 1994). Since then, peptide transporter expression has been found in other tissues including lung, placenta, mammary gland, pancreas and the central nervous system, (Meredith and Boyd, review, 2000). PepT1 has not been found to be the protein expressed in all these tissues, and work is continuing in many cases to identify the peptide transporter present.

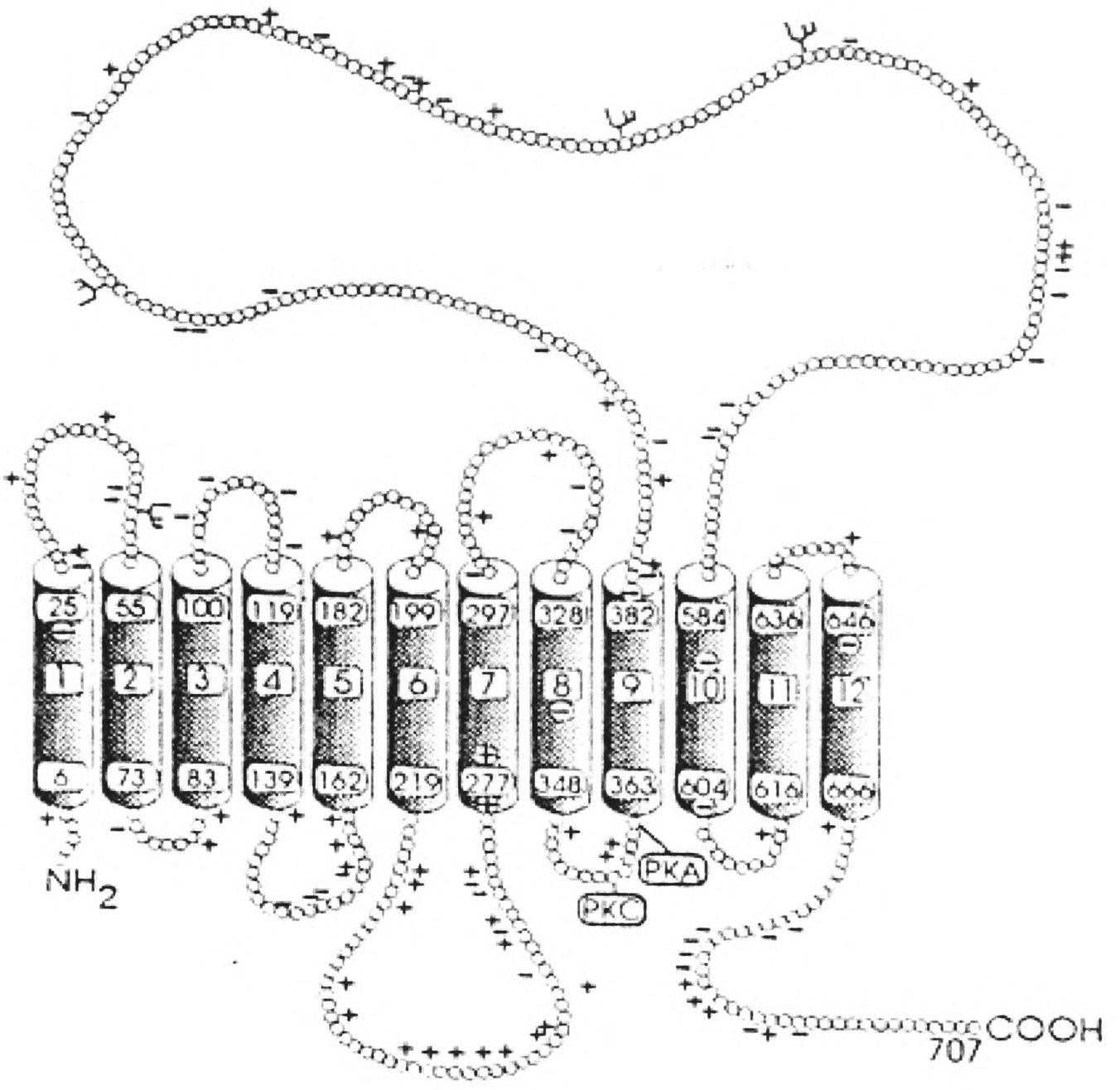


Figure 1.5 Membrane model of PepT1. Transmembrane domains are numbered 1-12, and charged residues are denoted by + and –. Putative PKA and PKC sites are also shown (reproduced from Fei *et al*, 1994).

A more detailed study on PepT1 expression in the intestine showed expression of PepT1 was most abundant in the duodenum and jejunum with lower levels found in the ileum and very low levels found in the colon, (Freeman *et al*, 1995). A subsequent study provided an insight into how PepT1 expression altered throughout development by measuring the levels of PepT1 mRNA in the small intestine of rats. The results showed that PepT1 mRNA was greatest at day 4 and that adult levels of expression were reached by day 28, (Miyamoto *et al*, 1996).

1.2.4.2 Cellular localisation

The lining of the small intestine is arranged into large fold to increase the surface area for absorption. In addition, there are tiny finger-like projections called villi that also greatly increase the surface area available for absorption. PepT1 is found in the epithelial cells of the villi. Various antibody studies, (Ogihara *et al*, 1996, and Sai *et al*, 1996), have shown that expression of PepT1 is regulated and that it is only as the cells leave the crypt and migrate towards the tip of the villi that they express PepT1.

1.2.5 Functional characteristics of PepT1

1.2.5.1 Electrogenicity and H^+-dependence of peptide transport

The first demonstration that peptide transport was electrogenic was by Boyd and Ward in 1982. They showed in the intestine of *Necturus maculosus* that transport of a neutral peptide was independent of Na^+, but that a depolarisation of the membrane occurred. They concluded that peptide transport was dependent on another cation but were unable to identify the ion responsible.

In 1983, Ganapathy and Leibach demonstrated in renal brush border membrane vesicles that an inwardly directed pH gradient played a role in peptide uptake, Gly-

Sar and Gly-Gly uptake were stimulated in the presence of an inwardly directed pH gradient, suggesting coupling of peptides to the transport of H^+. However, it wasn't until later studies where intracellular pH was measured directly that peptide transport was observed to be accompanied by a fall in intracellular pH, (Thwaites *et al*, 1993). This study directly confirmed that peptide transport was coupled to H^+.

1.2.5.2 Substrate specificity

An unusual feature of PepT1 is its ability to transport a wide range of substrates. It can transport all naturally occurring di- and tripeptides irrespective of the charge (Amasheh *et al*, 1997 and Temple *et al*, 1995). It is also accepted that PepT1 can transport β-lactam antibiotics, ACE inhibitors and some anti-neoplastic drugs (Daniel and Adibi, 1993 Wenzel *et al*, 1995 and Zhu *et al*, 2000). Peptides larger than three amino acids long have a greatly reduced affinity for PepT1 and those larger than tetrapeptides are not transported at all.

1.2.5.3 Stereospecificity of PepT1

Boyd and Ward (1982) showed that L-amino acid and not D-amino acid peptides were substrates for the intestinal peptide transporter. In 1995, Lister *et al* showed in isolated loops of rat small intestine that PepT1 could transport dipeptides containing both an L-amino acid and a D-amino acid. This study showed that those peptides composed of L-amino acids were taken up and then rapidly hydrolysed, whereas those containing D-amino acids were less well taken up, but more hydrolysis resistant. Those peptides containing both an L- and a D-amino acid were well transported and hydrolysis resistant. In a more recent study, a synthetic peptide with the peptide bond

replaced with an isosteric thioxo peptide bond showed that PepT1 could selectively bind and transport peptides in the *trans* configuration. (Brandsch *et al*, 1998).

1.2.5.4 Stoichiometry of PepT1

Initial experiments measuring the transepithelial flux of peptide transport in isolated toad intestine suggested that the H^+ : peptide coupling stoichiometry was 2:1 (Abe *et al*, 1987). This stoichiometry was confirmed in a study by Thwaites *et al* in 1993 in Caco-2 cells using a pH sensitive dye to measure the changes induced by application of neutral peptides. In contrast, Temple *et al*, 1995 found in real brush border membrane vesicles that the stoichiometry of H^+ : peptide coupling depended on the substrate charge. The study concluded that neutral, anionic and cationic peptides have a stoichiometry of 1:1, 2:1 and 0:1 respectively. The other major conclusion of this study was that the interior negative potential was the major driving force for peptide entry and that the stoichiometry for the differently charged peptides made sure that the total charge translocated into the cell would remain constant. A third hypothesis was proposed by Amasheh *et al* in 1997 who suggested that the stoichiometry of substrates is independent of charge, as the substrates only bind to PepT1 when they are in their zwitterionic from. This means that the major driving force for peptide entry is pH and not the internal negative potential.

1.2.6 Methods used to study PepT1

There are many different methods used to study peptide transport via PepT1, and three of the most common will be discussed here.

1.2.6.1 Brush border membrane vesicles

Brush border membrane vesicles have been used extensively in the study of PepT1-mediated peptide transport (Ganapathy *et al*, 1997, Takahashi *et al*, 1999, and Temple *et al*, 1995). One advantage of using vesicles is that transport processes can be localised to a particular membrane. This membrane preparation is particularly good for kinetic and substrate binding studies (Temple *et al*, 1996). However, a major disadvantage of this method is the loss of cell cytoplasm that occurs during preparation and the elimination of the basolateral membrane, abolishing interactions that PepT1 may have with other membrane proteins.

1.2.6.2 Cell lines

The Caco-2 cell line is the one most commonly used to study the transport characteristics of PepT1 (Thwaites *et al*, 1993, Wenzel *et al*, 1996 and Bretschneider *et al*, 1999). Caco-2 cells have the advantage of displaying many properties in common with enterocytes such as villi and brush border hydrolases. However, they do express several functional properties that are not native to the *in vivo* situation.

1.2.6.3 Expression systems

Several cell lines have been transfected to express PepT1; LLC-PK1 (Terada *et al*, 1997 and Sawada *et al*, 1999) and CHO (Guo *et al*, 1999 and Han *et al*, 1999). In addition Xenopus laevis oocytes have increasingly been used to study PepT1-mediated transport (Amasheh *et al*, 1997, Balimane *et al*, 1998, Fei *et al*, 1994, Tamai *et al*, 1999 and Temple *et al*, 1998). While these systems express the protein excellently with no interference from any endogenous peptide transporters, the interaction of PepT1 with other cell proteins may be overlooked.

1.3 The *Xenopus laevis* oocyte expression system

1.3.1 Historical background

In 1971, Gurdon and his colleagues demonstrated that oocytes could translate exogenous mRNAs injected into their cytoplasm. Since then, the Xenopus oocyte has been a favoured system for the study of transcript processing and translation. The oocyte was first used to study membrane proteins in the 1970's by Miledi who reported the presence of acetylcholine receptors in the oocyte membrane (Kusano *et al*, 1977). However, it was not until 1987 that Wright and colleagues demonstrated that oocytes could be used to directly study the functional properties of transport proteins as well as being a vehicle for expression cloning, (Dascal, 1987, review).

1.3.2 Oocytes as protein synthesis factories

Oocytes have often been described as 'miniature protein synthesis factories' due to their ability to manufacture many different proteins introduced into the cell via RNA or DNA microinjection. This is because during oogenesis, the immature eggs accumulate a vast cellular store of enzymes. It is estimated that a typical oocyte will contain approximately 200,000 more ribosomes and 10,000 more tRNA molecules than a typical somatic cell.

1.3.3 Advantages of using X.laevis oocytes

Oocytes make an ideal expression system as they can express any exogenous RNA or DNA injected into them (see above). However, they are also ideal for the researcher to work with due to their large size. At approximately 1-1.2mm in diameter they are large enough to see with the naked eye which makes manipulation of the cells easy. Combined with this they are easy to obtain and are abundant, with each frog ovary

containing thousands of oocytes. For electrophysiological purposes, oocytes are an excellent system to work on due in part to their large size, but also because they are robust. Most oocytes can cope with two glass microelectrodes being impaled into them and having experiments carried out for as long as 2 hours.

They are also incredibly versatile with regard to the number of techniques that can be carried out on them. In this study, the major technique was electrophysiology, with immunocytochemistry being a secondary technique, but oocytes can be used in radiolabelled uptake studies as well as HPLC, with several methods being carried out on one cell.

Although oocytes express various endogenous ion channels, transporters and receptors, they are still an excellent model for the characterisation of exogenous transport proteins and receptors. This is due to the endogenous proteins producing currents that are very small in magnitude compared to the exogenous membrane proteins, or because the endogenous proteins exhibit different characteristics to the exogenous proteins (Weber, review, 1999). In this thesis however, the membrane protein investigated was not endogenously expressed in X.laevis oocytes.

1.3.4 Disadvantages of using X.laevis oocytes

Although the advantages of using X.laevis oocytes outweigh the disadvantages, there is a major disadvantage of using *X.laevis* oocytes as the expression model. Oocytes exhibit seasonal variation and as a result sometimes they simply do not survive long enough for experiments to be carried out. This problem usually only occurs during the summer, and can be avoided to some extent by using laboratory bred frogs that are kept in a 12hours light/12hours dark environment.

1.4 Aims of this thesis

The wider aim of this thesis was to more fully understand one of the most fundamental physiological processes – the absorption of dietary protein. More specifically the aims were to characterise the transport protein responsible for the uptake of all naturally occurring di-and tripeptides, as well as many pharmacologically active drugs, (PepT1). The question of how PepT1 is able to accept such a wide range of substrates was addressed, as well as the acute regulation of this protein.

The two-electrode voltage-clamp technique was used to investigate the importance of a free carboxyl terminus on transport by PepT1. Transport of a peptide with a blocked carboxyl terminus, Phe-Tyr-NH_2, was compared with the parent peptide, Phe-Tyr. These experiments enabled me to assess the importance of the carboxyl terminus in substrate recognition.

In Chapter 5, I investigated the importance of the position of charge within a peptide. Previous studies had been carried out on charged substrates, but always with the charged amino acid residue in a fixed position. This study provided valuable insights into how charged substrates are recognised and bound to PepT1.

The latter part of my work focussed on the acute regulation of PepT1. Literature on the subject is sparse, with most research centring on longer-term regulation by the diet or hormones. By combining the two-electrode voltage-clamp and immunocytochemistry the role that phorbol esters play in the regulation of PepT1is becoming clear.

CHAPTER 2

MATERIALS AND METHODS

2.1 Preparation of the PepT1 plasmid

2.1.1 Making competent cells

XL-1 Blue *E.coli* cells were obtained from Stratagene, Amsterdam, and were streaked out onto an agar plate containing tetracycline (agar 2%, tetracycline 12.5µg/ml) and incubated overnight at 37°C with the plate inverted. A single colony was picked from this overnight growth and used to inoculate 10ml of LB broth (25g/l) supplemented with tetracycline in a 50ml polyethylene centrifuge tube. A loose fitting lid was placed on the tube and it was placed in an incubator at 30°C for an overnight incubation with moderate shaking (150cycles/min.). 5ml of this overnight culture was inoculated into 500ml of LB broth supplemented with tetracycline and this was incubated at 30°C in a shaking incubator (195cycles/min) until the optical density at 600nm reached 0.45-0.55. This procedure took 7-10 hours. Once this point was reached, the cells were chilled on wet ice for 2 hours in the cold room. The solution containing the cells was transferred to two sterile 250ml centrifuge pots, and the samples subsequently spun at 2500*g* for 20 minutes at 4°C. The pellets were resuspended in 5ml ice cold buffer (see Table 2.1) and any lumps removed by gently pipetting the cell mixture. The samples were diluted with 250ml of ice cold cell buffer and incubated on wet ice for 45 minutes in a cold room. After incubation the samples were centrifuged at 1800*g* for 10 minutes at 4°C.

The supernatant was removed and the pellets resuspended in 25ml of ice cold cell buffer. The two samples were pooled to give a final volume of 50ml. 11.5ml of 80% glycerol was added to the cell suspension in a dropwise fashion with the solution

swirled constantly. The final concentration of the solution was 15% v/v. The cells were aliquoted into 0.5ml volumes into sterile Eppendorf tubes and stored immediately at -80°C until use.

Ice cold cell buffer	*Concentration (mM)*	*g / litre*
$CaCl_2$	100	14.71
$MnCl_2$	70	8.81
NaOAc	40	5.44

Table 2.1 Composition of ice cold cell buffer. The solution was made up with autoclaved distilled water and the pH was altered to 5.5 with Tris. The solution was filter sterilised before use.

2.1.2 Transformation of competent cells

Transformation of the competent *E.coli* was achieved via the "heat shock" method. A vial of competent E.coli cells were removed from the -80°C freezer and allowed to thaw on wet ice for 10 minutes. A 50µl aliquot of these cells was added to an ice cold Eppendorf tube and 1µl (10ng) DNA was added (PSPORT PepT1 plasmid), the contents were swirled gently and incubated on ice for 30 minutes. The original cDNA was a gift from M.A.Hediger. The sample was then incubated in a PCR machine for 42°C for 1 minute to heat shock the cells and then transferred to ice for 2 minutes. 950µl of LB broth was added to the tube and the contents subsequently incubated at 37°C for 1 hour. 100µl of this final mixture was plated out onto an LB agar plate supplemented with ampicillin (50mg/ml) and allowed to absorb into the agar before inverting the plate and incubating overnight at 37°C.

2.1.3 Amplification of transformed cells

100ml of LB broth containing ampicillin in a 500ml flask was inoculated with a single colony picked from the plate of transformed cells. The opening of the flask was covered loosely with tin foil and the flask was placed in a shaking incubator at 37°C overnight (150cycles/min).

2.1.4 Extraction of plasmid

A Qiagen midi kit (Crawley, West Sussex, U.K.) was used to extract PepT1 plasmid DNA. The broth was divided into two 50ml polyethylene centrifuge tubes and spun at 6000 x *g* for 15 minutes at 4°C to pellet the bacteria. The supernatant was discarded and the pellets resuspended in 4ml of buffer P1 to which 0.05ml of RNase A had been added (from the Qiagen kit). 4ml of buffer P2 was added to each tube and the contents mixed gently by inverting the tubes 4-6 times. This mixture was incubated at room temperature for 5 minutes before 4ml of chilled buffer P3 was added. Buffer P3 was chilled to enhance precipitation of the DNA. The contents of the tube were again mixed gently by inverting and then incubated for 15 minutes on wet ice. The solutions were centrifuged at 20000 x *g* for 30 minutes at 4°C and the supernatant containing the DNA removed to a new tube and centrifuged again at 20000 x *g* for a further 15 minutes at 4°C. The second centrifugation step was carried out to avoid any particulate matter entering the Qiagen tip. Applying 4ml of buffer QT equilibrated a Qiagen tip-100 and the tip was allowed to empty by gravity flow. The recentrifuged supernatant was applied to the column and again allowed to pass through by gravity flow (if there was still evidence of particulate matter then the supernatant was filtered before being applied to the column). The tip was then washed twice with 10ml of buffer QC. The first wash is usually sufficient to rid the

column of any contaminants in the majority of plasmid DNA preparations, but a second wash should be carried out just to be certain of this. The DNA was then eluted with 5ml of buffer QF and collected in a polyethylene centrifuge tube. 3.5ml of room temperature isopropanol was added to precipitate out DNA and the contents of the tube were mixed and centrifuged at 15000 x *g* at 4°C for 30 minutes. The supernatant was carefully decanted. The isopropanol pellet had a glassy appearance and was only loosely attached to the side of the tube. The pellet was washed with 2ml of room temperature 70% ethanol and then centrifuged at 15000 x *g* for 10 minutes. The 70% ethanol removed precipitated salt and replaced the isopropanol making the DNA easier to dissolve. The supernatant was carefully removed and the pellet allowed to air dry for 5-10 minutes (any longer made it harder to dissolve the pellet). The pellet was dissolved in a suitable volume (approx.100µl) of Buffer TE, pH8.0. The yield of DNA was determined by spectrophotometry. A wavelength scan was performed between 320-220nm and the 260/280 ratio was determined. This value should be greater than 1.8, and the closer to 2 it is the better. The amount of DNA present in the sample can be determined via the following equation:

OD 260 x dilution factor x 50 = xµg / µl

The DNA is diluted to a concentration of 1µg/µl with buffer TE and stored at -20°C.

2.2 Synthesis of mRNA from a cDNA clone

2.2.1 Preparation of the template DNA

Preparation of the linearised template was a simple procedure requiring DNA, a restriction enzyme (Not1), water, NEB3 and BSA, all of which were RNase free. See table 2.2 for assembly of reaction.

Reagent	Volume
H_2O	78µl
NEB3	10µl
DNA	10µl
BSA	1µl
Not1	1µl

Table 2.2 Assembly of reaction to linearise template DNA, total volume 100µl.

All the reagents were added to an RNase free Eppendorf tube using RNase free tips and pipettes. Assembly of the reaction was done at room temperature and the reagents were added in the order seen in the table above. The contents of the Eppendorf tube were mixed and then centrifuged briefly at low speed (approx. 2000rpm). The sample was subsequently incubated in a PCR machine for 3 hours at 37°C. The rest of the procedure could be carried out straight after this incubation, or could be commenced the next day if the sample was incubated at 4°C.

2.2.2 Phenol-chloroform extraction and ethanol precipitation of DNA

The DNA was extracted via phenol-chloroform by adding 100µl of phenol:chloroform:isoamylalcohol premix, collecting the top layer after centrifugation, and then adding 100µl of chloroform and again collecting the top layer. The DNA was precipitated by addition of 250µl of 100% ethanol to the tube. The sample was incubated in the freezer at -20°C for at least 15 minutes before being centrifuged at 14000rpm for 15 minutes at 4°C to pellet the DNA. The supernatant

was carefully removed and the pellet washed in 300µl of 70% ethanol and then resuspended in 5µl of RNase free water.

A 1µl sample of this linearised DNA was aliquoted out and run on an agarose gel to assess its quality and quantity. See figure 2.1 for an example of one such gel.

When satisfied that the linearised DNA was of good quality and quantity, the transcription reaction was started. See table 2.3 for reagents and volumes used to set up the reaction.

Reagent	Volume
RNase free H_2O	4µl
Transcription buffer	2µl
2x ribonucleotide mix	10µl
Linearised template DNA	2µl
10x enzyme mix	2µl

Table 2.3 Reagents used to start transcription reaction, total volume 20µl. Reagents were added to an RNase free Eppendorf tube in the order stated above at room temperature.

The contents of the tube were mixed gently by flicking the tube and then the sample was centrifuged for a few seconds at low speed (2000rpm) to collect all the reaction components at the bottom of the tube. The tube was incubated at 37°C in a PCR machine for 1 hour.

2.2.3 Removal of template DNA

When the transcription reaction was complete the template DNA had to be removed. This was achieved by the addition of 1µl RNase free DNase1 to the tube to degrade the DNA present. A further incubation at 37°C for 15 minutes was required to complete removal of the DNA.

2.2.4 Termination of the reaction and recovery of the RNA

At the end of the 15 minute incubation with DNase1, 115ul of RNase free water and 15ul of ammonium acetate stop solution halt the reaction. After being mixed and centrifuged briefly, 150µl of phenol:chloroform:isoamylalcohol premix was added. The top layer was collected and 150µl of chloroform added followed by mixing and centrifugation. The top layer was once again collected and 150µl of isopropanol was added to precipitate the RNA. The tube was incubated at -20°C for at least 15 minutes to allow this precipitation to occur. The RNA was pelleted via centrifugation at 14000rpm at 4°C for 15 minutes. The resultant RNA was resuspended in 10µl of RNase free water and kept frozen until quantitative analysis was carried out.

2.2.5 Determination of concentration of RNA

The quality and concentration of the RNA was determined via UV spectrophotometry. A 1µl sample of the RNA was diluted 100 fold in RNase free H_2O in an RNase free Eppendorf tube. The UV spectrophotometer was used to obtain a wavelength scan between 320-220nm with a speed of 500nm/min. See figure 2.2 for an example of a wavelength scan printout.

Figure. 2.2 is a worked example of determination of RNA concentration.

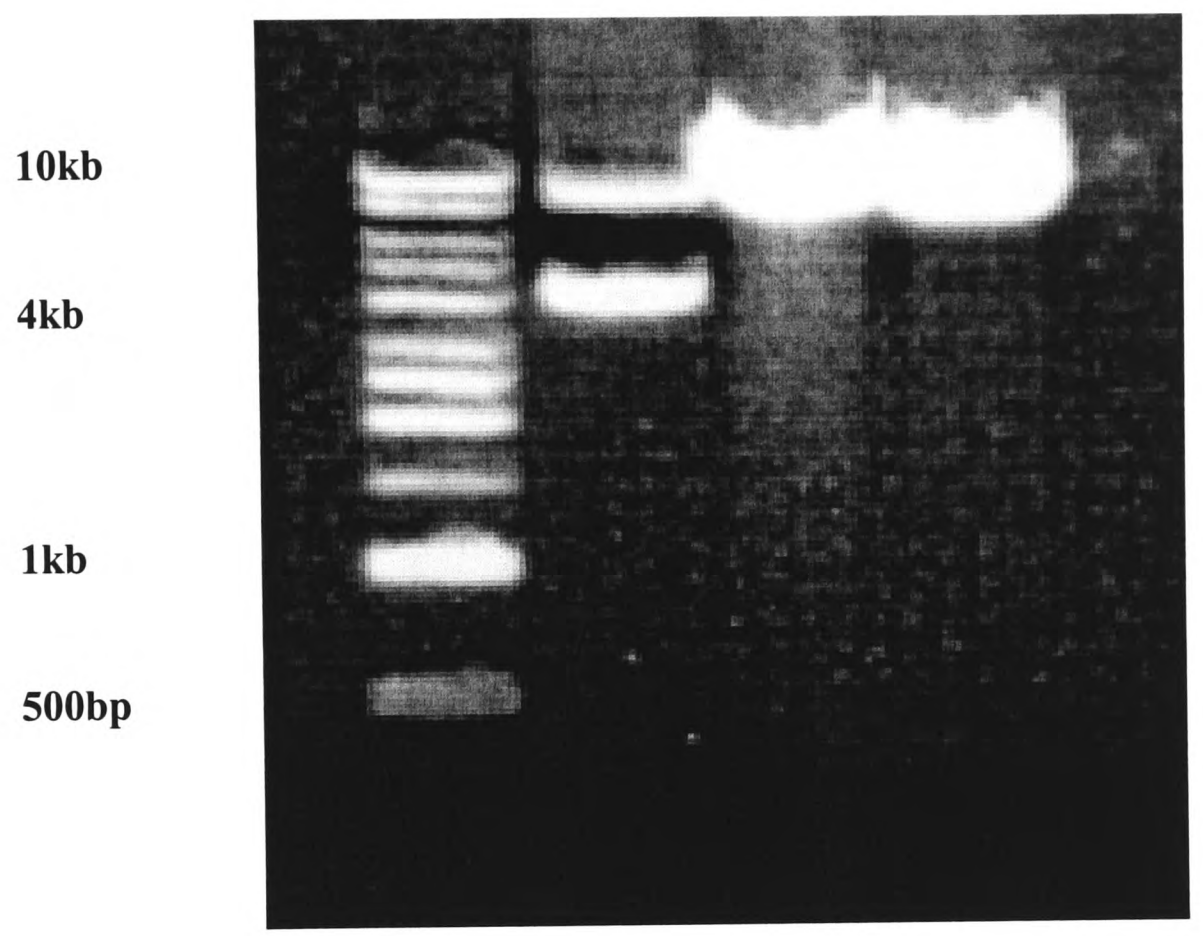


Figure 2.1 Agarose gel to assess the quality and quantity of linearised DNA. . Lane 1 DNA ladder, 500bp-3kb in 500bp repeats, 3-6kb in 1kb repeats and 6-10kb in 2kb repeats, lane 2 uncut DNA, lane 3 linearised DNA, and lane 4 linearised DNA.

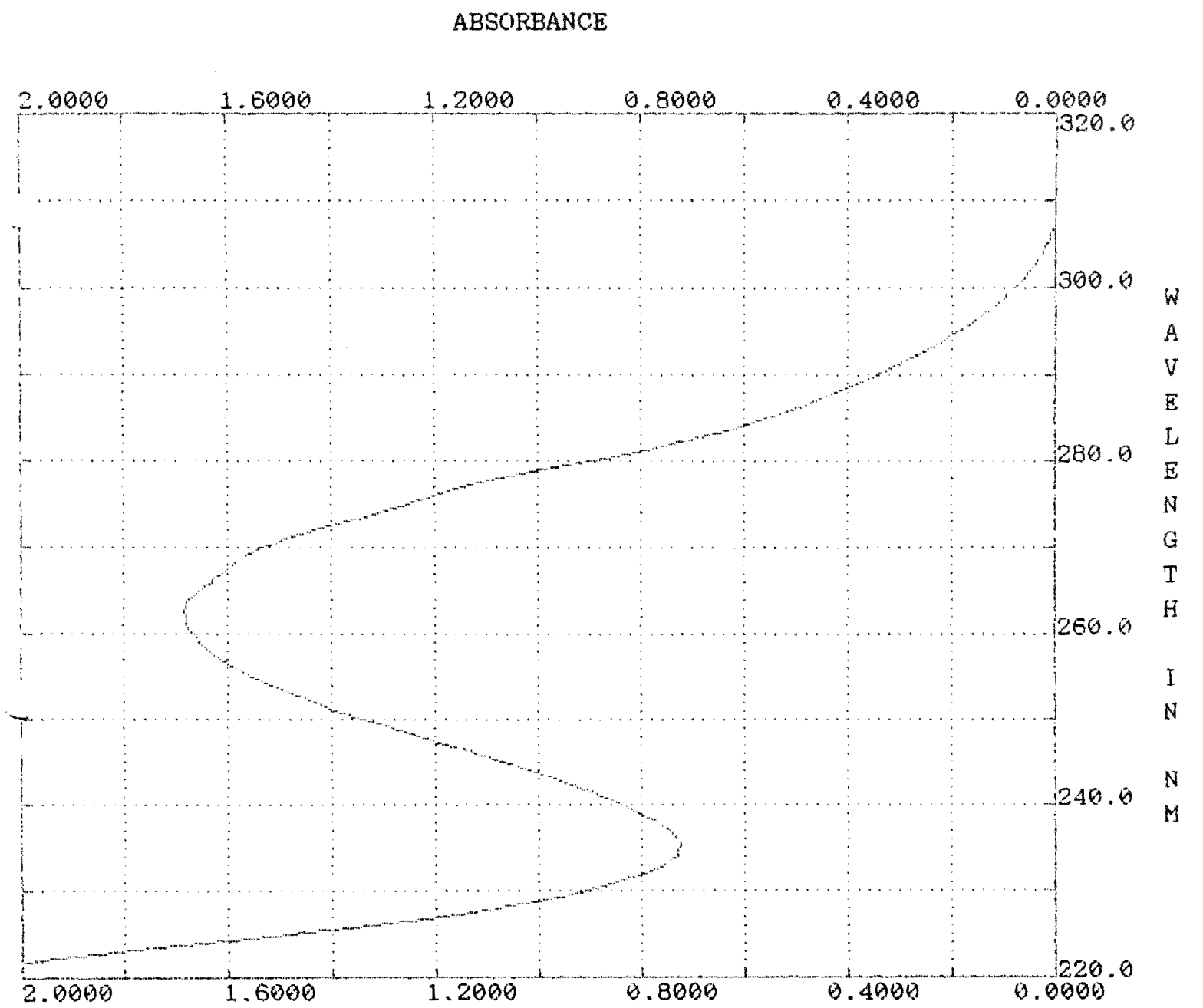


Figure 2.2 UV wavelength scan 320-220nm of PepT1 RNA

1 Abs = 8.5cm

Background = 0 (reading at 320nm)

260 reading = 14.1cm – background (0) ⇒ 14.1/8.5 = 1.66 Abs

280 reading = 7.7cm – background (0) ⇒ 7.7/8.5 = 0.91 Abs

260/280 ratio = 1.66/0.91 = **1.82**

To determine yield, the 260 reading was multiplied by 4 to give the concentration in μg/μl.

∴ 1.66 x 4 = 6.64μg/μl.

The sample was diluted accordingly to reach a final concentration of 1μg/μl.

2.3 Preparation of *Xenopus laevis* oocytes

2.3.1 Isolation of X.laevis oocytes

Xenopus laevis oocytes were isolated from the ovaries of adult frogs, defined as those being ≥ 7.5cm in length (Blades Biological, Kent, UK.). One animal was anaesthetised in 0.2% 3-aminobenzoic ethyl ester, and oocytes were removed by ovariectomy and quickly placed into a 50ml polyethylene centrifuge tube containing 20ml Ca^{2+}free isolation solution (see Table 2.4a). If the operation was the first for the frog, then 2-3 sutures were inserted into the muscle layer and the skin layer to close the wound. The frog was then allowed to recover in a separate tank of water for 3 hours before being transferred back to the home tank. If the operation was the second, then the frog was killed by pithing whilst still anaesthetised in accordance with the Home Office Scientific Procedures Act 1986.

Ca^{2+} free Isolation Solution	*Concentration (mM)*	*ml / litre*
NaCl	80	16ml of 5M stock
KCl	2	10ml of 0.2M stock
$MgCl_2$	1	10ml of 0.1M stock
HEPES	5	5ml of 1M stock

Table 2.4a Composition of Ca^{2+} isolation solution used in the isolation of oocytes.

This solution was made up in autoclaved distilled water and the pH was adjusted with 1M sterile NaOH to 7.6 before use. The final solution was filter sterilised before use.

The ovarian lobes were washed 10 times in 20ml of isolation solution and transferred to a 90mm Petri dish filled with isolation solution where they were separated into clumps of 10-20 oocytes using 4SA tweezers. These separated oocytes were then

transferred via a cut off Pasteur pipette to another 50ml polyethylene tube containing 30mg of collagenase dissolved in 10ml of isolation solution. The oocytes were incubated on a roller mixer for 1 hour at 19°C to digest connective tissue.

The separated oocytes were washed 20 times with 10ml isolation solution to remove the collagenase and a final 20ml wash was made with Barth's solution. The oocytes were then transferred to a 90mm petri dish containing Barth's (see Table 2.4b).

Barth's Solution	*Concentration (mM)*	*ml / litre*
NaCl	88	17.6ml of 5M stock
KCl	1	5ml of 0.2M stock
$MgSO_4$	0.82	4.1ml of 0.2M stock
$CaNO_3$	0.33	0.33ml of 1M stock
$NaHCO_3$	2.4	6ml of 0.4ml stock
$CaCl_2$	0.41	0.41ml of 1M stock
HEPES	15	10ml of 1M stock
pH to 7.6, then add		
Na Pyruvate	0.55g/l	0.55g/l
Gentamycin	0.05g/l	0.05g/l

Table 2.4b Composition of Barth's solution used in the storage of oocytes.

Barth's solution was made up in autoclaved distilled water and was pH adjusted to 7.6 with 1M sterile NaOH prior to the addition of Na pyruvate and gentamycin. The final solution was filter sterilised before use.

2.3.2 Defolliculation of X.laevis oocytes

Once separated and washed the oocytes were sorted into groups of healthy and unhealthy, with the unhealthy discarded. Healthy oocytes were at stage V-VI in development, approximately 1-1.2mm in diameter, with no blemishes on their surface and good distinction between the vegetal and animal poles (see diagram 2.3a).

The healthy oocytes were manually defolliculated. The follicular layer is a one cell thick membrane covering the exterior of the oocyte and must be removed as the individual cells in the layer are electrically coupled to each other and to the oocyte through gap junctions. The follicular layer can therefore interfere with recordings made during electrophysiological procedures. Because of the large size of oocytes, and the ease with which the follicular layer can be visualised (seen under low magnification as a fine covering containing blood vessels), manual defolliculation was done using fine watchmakers forceps. The oocytes were manipulated and agitated until the layer was seen to be removed.

The oocytes were incubated overnight in groups of 50 in 30mm Petri dishes filled with Barth's solution in a cooling incubator with the temperature set at 17°C. This allowed for any deaths that occurred and saved waste of PepT1 cRNA.

2.3.3 Injection of cRNA

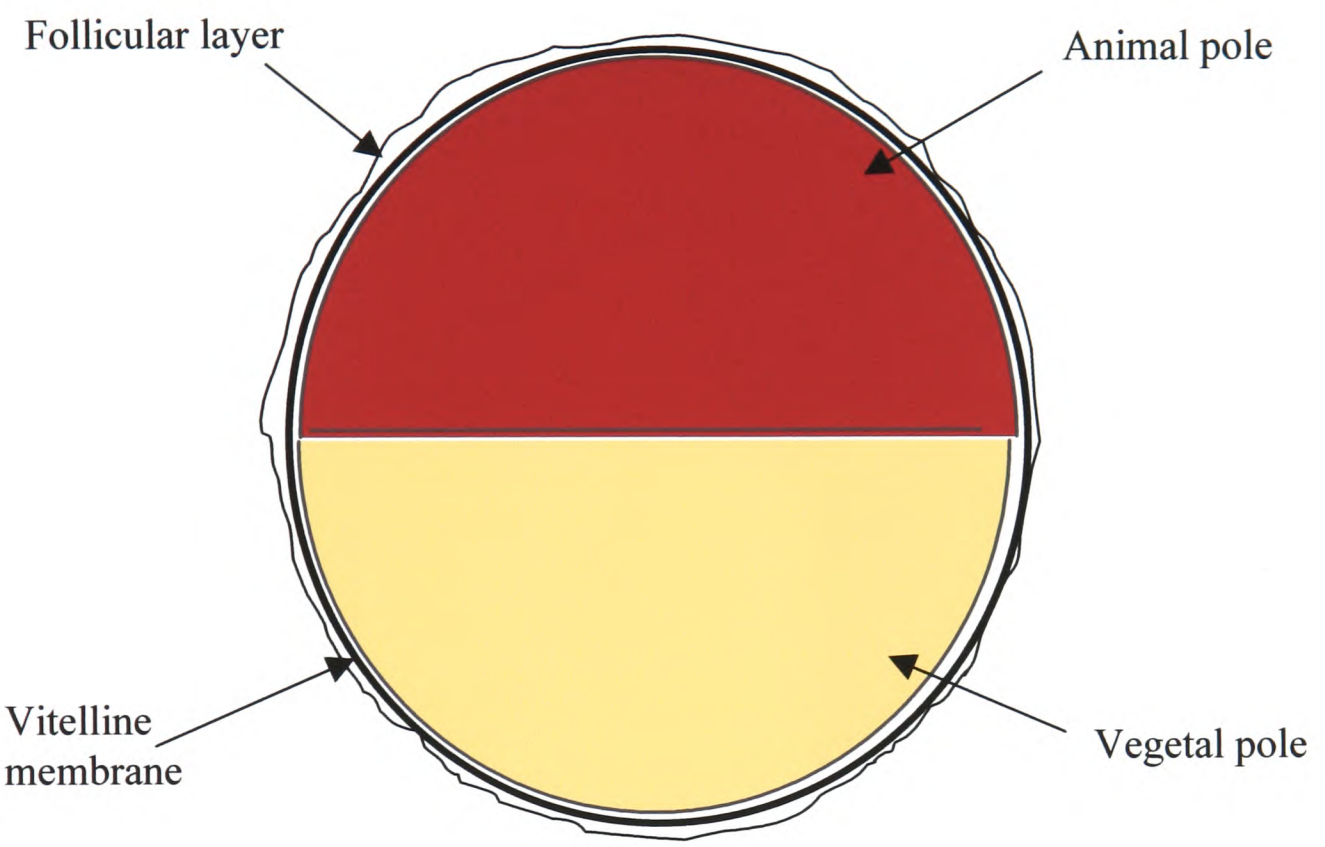
24 hours after isolation the oocytes are injected with PepT1 cRNA. This was carried out using a semi-automated injection system, Nanoject, see diagram 2.3b. The plunger wire of the injection system must be fully extended before use, this was checked by depression of the empty button until a double beep was heard. When the plunger wire was fully extended, it was coated with vacuum grease. An injection

electrode was selected and back-filled with mineral oil and then placed onto the plunger wire and secured in place by tightening the screw (see section 2.4.2 for description of electrode pulling).

An insert was custom-made by Mr. A Klukowski, Dept. Human Anatomy and Genetics, to fit into the base of the microscope (Leica MZ6) and can also be seen in diagram 2.3b. It consists of a circular base with a two-way direction manipulator and a clip to hold the grooved slide in place. The grooved slide makes it easy to position the oocytes for injection. PepT1 cRNA was pipetted onto an upturned lid of a 30mm Petri dish lid and the tip of the injecting microelectrode put into the drop of RNA and the fill button on the microinjector depressed to allow the RNA to be taken up into the electrode. Once the RNA was taken up the tip of the injecting electrode was placed into each oocyte and the inject button depressed once to inject 25nl of RNA (pre-set volume). This process ensures that 25ng of PepT1 cRNA is injected into each oocyte. The same procedure was carried out for the controls, but 25nl of RNase free water was injected instead.

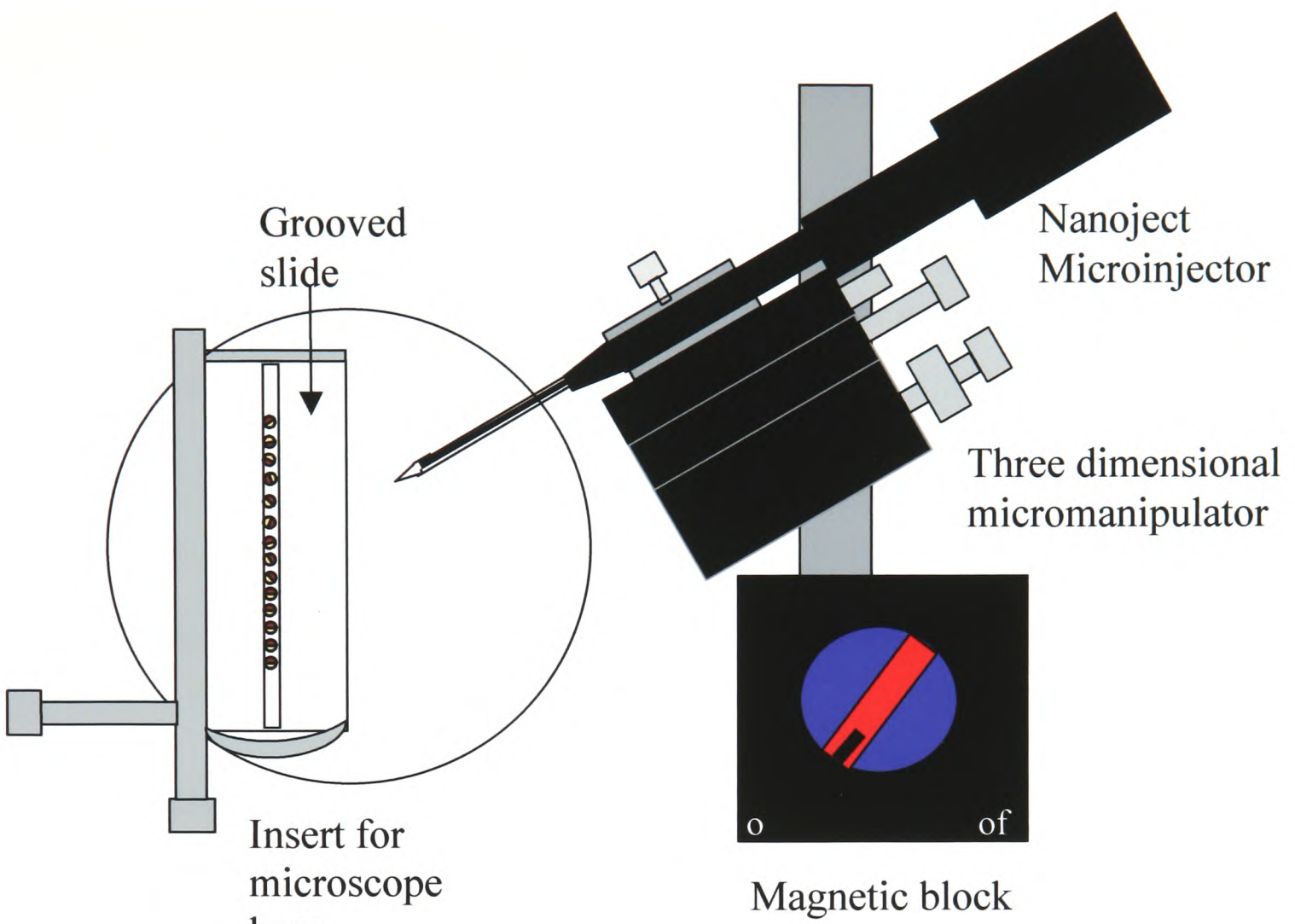
The oocytes were incubated in Barth's solution at 17°C for three days for expression to reach experimental levels with the solution changed daily.

Experiments were carried out on the third day after injection of cRNA. The responses to peptide substrates were assumed to be due to the expression of the exogenous protein. Oocytes have many endogenous ion channels, such as Na^+, K^+, Cl^-, Ca^{2+} and NH_4^+ – of which there are several classes- and all are involved in the maintenance of the oocytes. However, there is no documentation in the literature of any endogenous amino acid or peptide transporters or indeed H^+ channels that may have interfered with the experimental recordings made in this thesis.



a.

Figure 2.3a. Schematic diagram of a healthy stage VI oocyte showing the poles and the vitelline and follicular layers.



b.

Figure 2.3b. Schematic diagram of the Nanoject semi-automated injection system with the custom made insert for the microscope base and grooved slide for *X.laevis* oocytes.

2.4 Electrophysiology of *Xenopus laevis* oocytes

2.4.1 The whole system-an overview

To explain the two-electrode voltage clamp experiments, it is necessary to look at the system as a whole before breaking it down into its constituents. The set-up consists of the microelectrodes and holders, headstages, oocyte clamp, chart recorder, A/D converter and the computer with both pCLAMP hardware and software installed. Diagram 2.4a (from http://faculty.plattsburgh.edu/donald.slish/RecEqu.html) indicates how the system is set up. Diagram 2.4d and e also show the exact set-up of the electrophysiology system in our laboratory.

2.4.2 Pulling microelectrodes

Microelectrodes were pulled using the Model 773 Micropipette Puller (Campden Instruments, Loughborough, UK). Borosilicate glass capillaries (Harvard Apparatus, Kent, UK) with an outer diameter of 1.5mm and an inner diameter of 1.17mm were pulled using a three stage program. See table 2.5a for details of the program.

	Step	Heat Intensity	Heat time	Pull Force	Pull displacement
Parameters	001	23	0	15	3
	002	0	1	0	0
	003	23	0	20	24

Table 2.5a. Three-stage program used to make microelectrodes.

Once pulled the electrodes were stored embedded in blu-tak™ in a Petri dish until required.

Injection electrodes were also pulled using the micropipette puller, however the glass capillaries used were different as was the program. Glass capillaries were purchased from Laser Laboratory Systems, Southampton, U.K. with an outer diameter of 1.14mm and an inner diameter of 0.53mm. Table 2.5b provides the details of the pulling program.

	Step	Heat Intensity	Heat time	Pull Force	Pull displacement
Parameters	001	30	0	40	2.1
	002	25	10	0	0

Table 2.5b Two- stage program used to make injecting microelectrodes.

Once pulled the tips of the electrodes were manually broken to the correct size (an old electrode of good size was used as a template). The microelectrodes were then sterilised in glass Petri dishes for 2 hours at 200°C.

2.4.3 Preparation of microelectrode holders

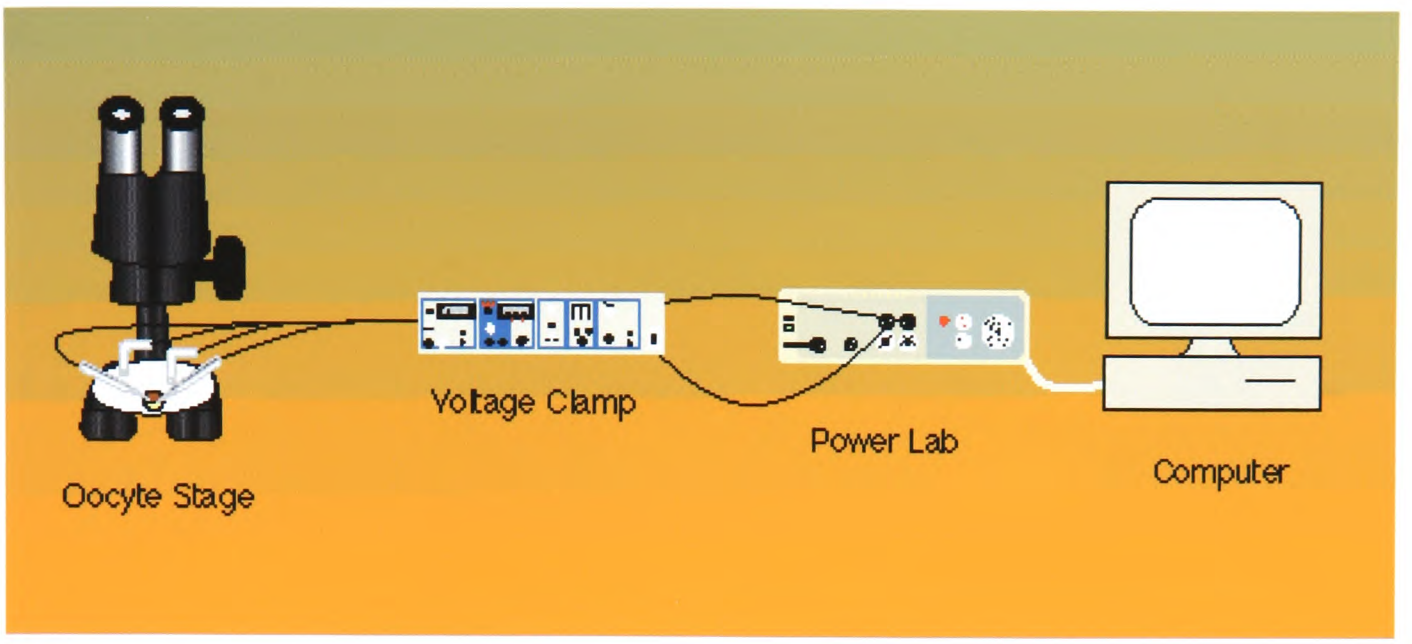
Microelectrode holders were purchased from Dagan Corporation, Minnesota, USA. Straight microelectrode holders with replaceable silver wires were purchased from Harvard Apparatus (diameter of wire 0.25mm). The wires were replaced on a regular basis. Replacement wire was threaded through the rubber washer in the holder and a

series of loops were made in the end to prevent slippage and then the wire was threaded through the rest of the holder, see diagram 2.4b.

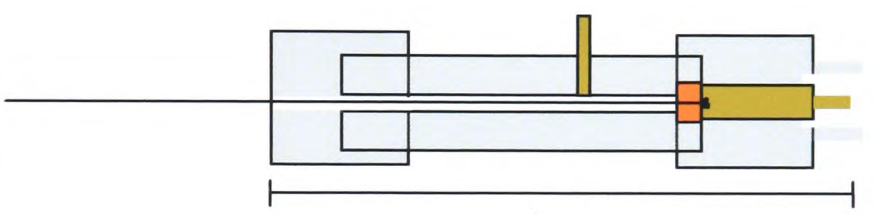
Before use the silver wires in the holders had to be chloridised. The surface of the silver wire was scored with 'wet and dry' sandpaper and then immersed in bleach for 30-60sec. This treatment coated the silver wire in a film of silver chloride that was insoluble to water. When coated the silver wire looked dark grey in colour. The wire was chloridised each morning before starting experiments and then again when the coating disappeared (when the silver wire appeared white in colour).

2.4.4 Assembly of microelectrode and holder

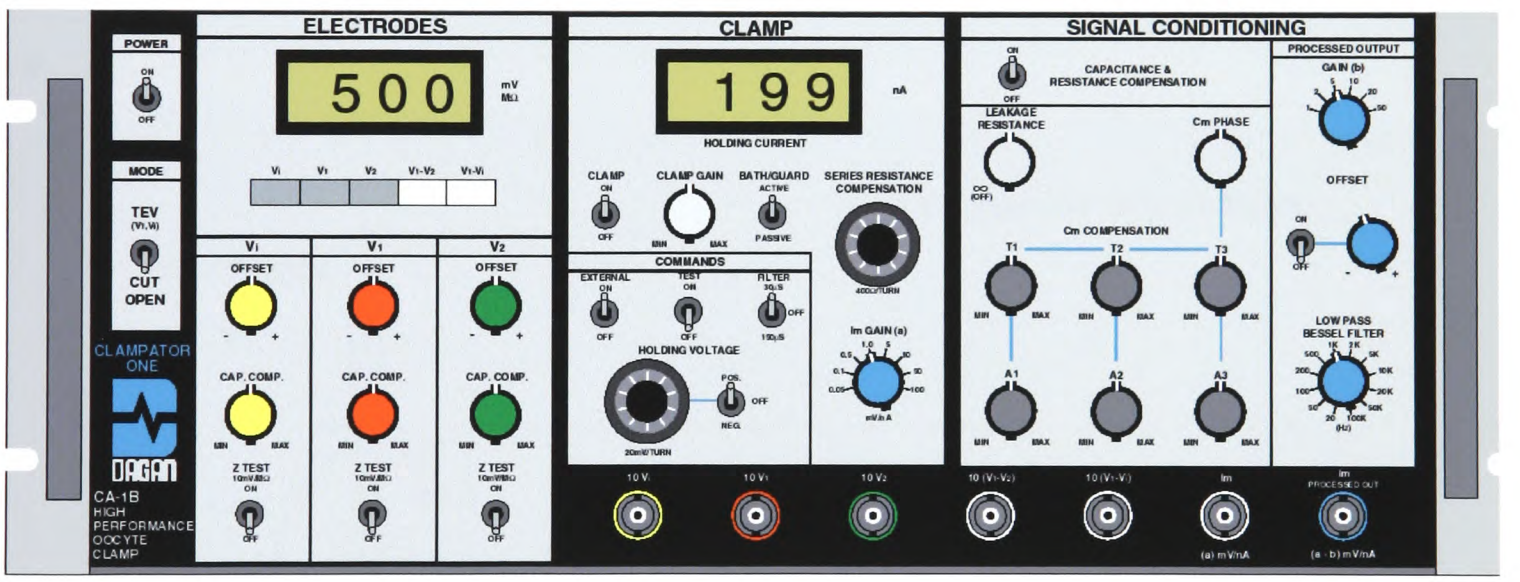
A microelectrode was selected and back-filled with 3M KCl, using a 1ml syringe, a filter (Schleicher and Schuell, London, U.K.) and a Microfil™ (World Precision Instruments, Stevenage, U.K.). A Microfil is a non-metallic syringe needle used for filling microelectrodes. It has a long fine tip that allows filling to occur from as close to the tip of the electrode as possible, helping to eliminate the chances of air bubble formation. The filled microelectrode was then pushed into place in the holder with the coated silver wire inside the electrode. The whole unit was connected to the headstage. The procedure was repeated three times to ensure that an electrode and holder was inserted into each of the three headstages: V_1, voltage recording, V_i, current injecting and V_2, ground/reference.



a.



b.



c.

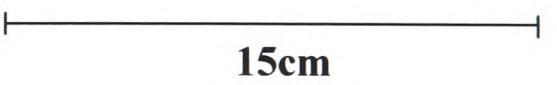
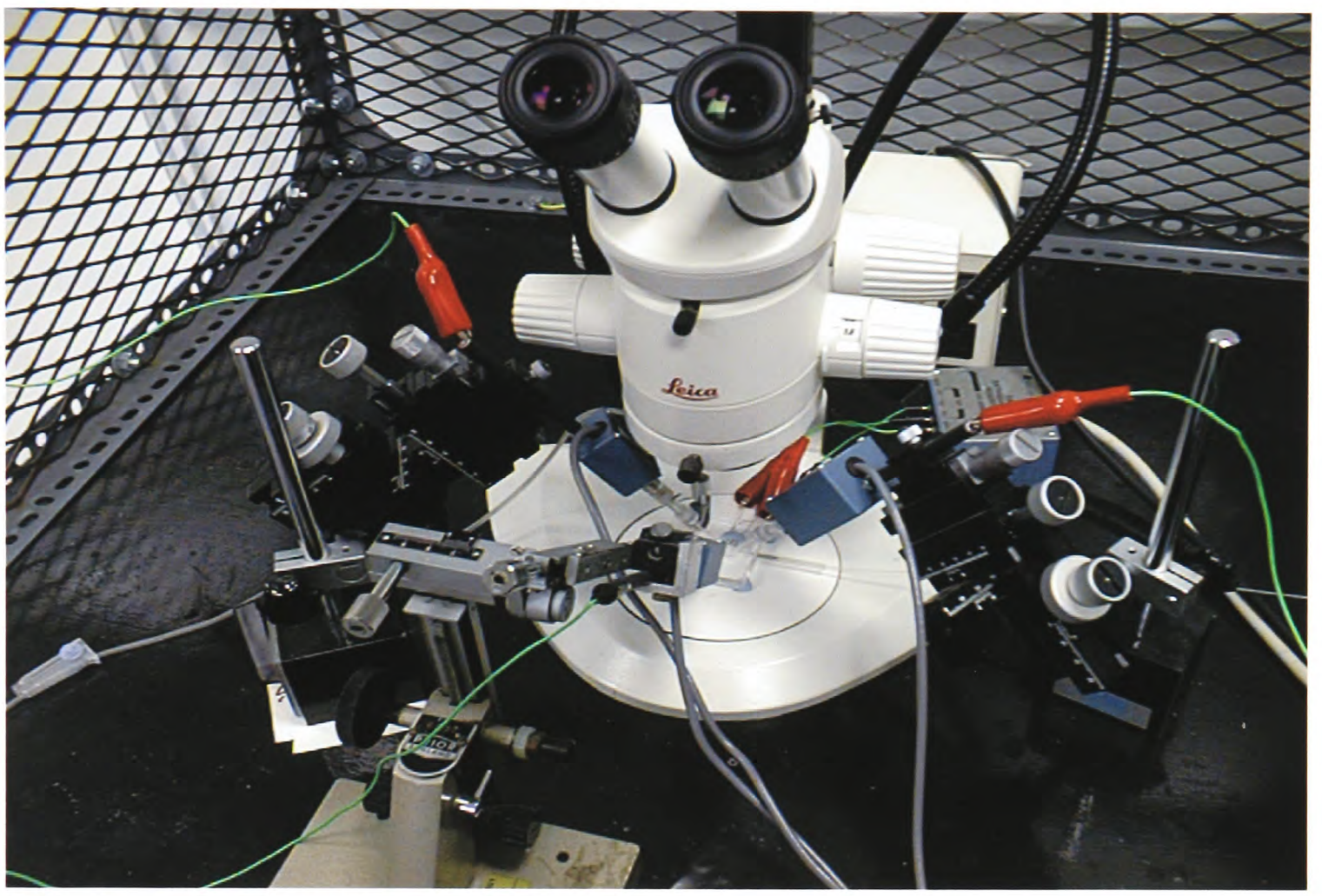


Figure 2.4.

a. Schematic diagram showing all the constituents of the two-electrode voltage clamp set-up. b. Schematic diagram of a microelectrode holder showing: silver wire, rubber washer (orange) and pin for headstage connection. c. CA-1B high performance oocyte clamp with 'electrode', 'clamp' and 'signal conditioning panels'.

d.



e.

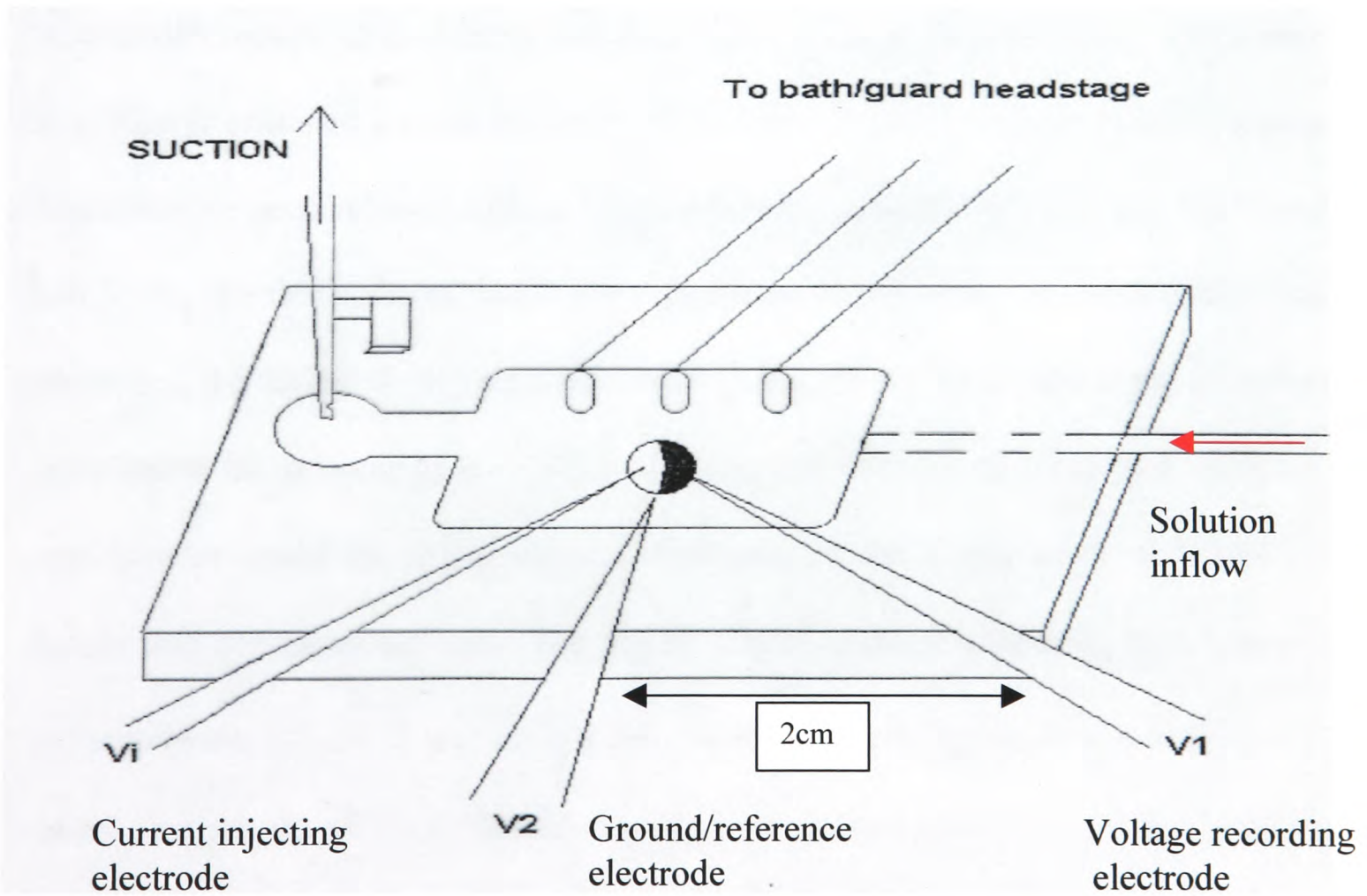


Figure 2.4. d. Photograph of the electrophysiology set-up. e. A magnified schematic of the oocyte perfusion bath.

2.4.5 Bath perfusion

The oocyte bath was custom-made by Mr. A. Klukowski. The bath was oval in appearance and the dimensions were approximately 150mm x 100mm x 1.5mm. The perfusion of the oocyte bath was achieved by a gravity inflow system using 50ml syringes, see diagram 2.4. Each syringe was fitted with a three-way tap, needle and length of tubing. Each length of tubing from the individual syringes passed through a multi-way connector to ensure that all the tubing from the syringes ended up as one single tube running to the oocyte bath. Removal of the solutions from the bath was by suction achieved by a vacuum (via a tap, a long length of tubing and a bottle).

2.4.6 Preparing the electrodes for recording

The resistance of the electrodes had to be measured before they could be used in an experiment. The tips of the electrodes were advanced into the bath solution and the 'Electrode' section of the clamp amplifier was used, see diagram 2.4c. The clamp amplifier is switched on and set in the two-electrode voltage clamp (TEVC) mode. The electrode section has headstage selector buttons, denoted by V_1, V_i and V_2, V_1-V_2 and V_1-V_i, the first three of which were depressed in sequence. As each button was depressed, the digital display showed a reading, this was offset to zero using the offset dials below the selector panel. When all three had been set to zero, each electrode was then be tested for its resistance. Switching on the Z test when each selector button was depressed did this. The digital display showed a value in MΩ, and any value between 0.5-2MΩ was acceptable. If values were higher than that it usually meant that the tip of the electrode was blocked. Alternatively, if a steady reading could not be obtained then it was likely that the tip of the electrode had been broken.

2.4.7 Impaling an oocyte

Following preparation of the microelectrodes and when bath perfusion had been established, an oocyte was introduced into the bath. A healthy oocyte was selected and carefully placed between all three electrodes. The oocyte was then impaled with the V_1 and V_i electrodes by advancing the electrodes through the plasma membrane. The electrodes dimpled the surface of the oocyte first before breaking through the membrane. To ensure that the oocyte had been impaled, the 'electrode' digital display on the clamp should have the reading of the membrane potential, E_m, of the oocyte. The E_m of a healthy oocyte was between -40 and -60mV, see Chapter 3 for a statistical analysis of oocyte E_m. The V_2 or ground electrode was as close as possible to the oocyte without touching it.

2.4.8 CA-1B high performance oocyte clamp

The CA-1B high performance oocyte clamp was purchased from Dagan Corporation, Minnesota, U.S.A. It was used mainly to conduct the voltage clamp experiments, but as stated in section *2.4.6* it was also used in the preparation of electrodes for recording. The middle section of the clamp was designated the 'Clamp' section. This section was the one that executed the voltage commands during the voltage clamp experiments. When an oocyte was impaled, the clamp section was switched to record voltage clamps. To activate a voltage clamp experiment, the clamp switch was turned on, the clamp gain was turned up, the bath/guard was activated and the external command switch was turned on.

2.4.9 The digidata 1200 series interface

The information recorded by the oocyte clamp was in analogue form. The digidata (Axon Instruments, California U.S.A) translates the analogue information from the clamp into digital form which the computer can understand and process.

2.4.10 The chart recorder

The chart recorder (Amersham Pharmacia Biotech, Little Chalfont, U.K.) was connected to the oocyte clamp to receive the voltage output recorded throughout experiments. The recording ensured that there was a record of exactly when substrates were added and voltage clamps were performed. It also served as record of membrane potential and how and when it changed throughout the experiments.

2.4.11 Data acquisition

Data acquisition was achieved by installing pCLAMP (Axon Instruments) hardware into the computer and software onto the hard drive of the PC. For voltage recording only, the Fetchex program was used to record data, and Fetchan was used to analyse the data acquired. In the case of voltage clamping experiments, Clampex was used to record the data whilst Clampfit was used to analyse the data.

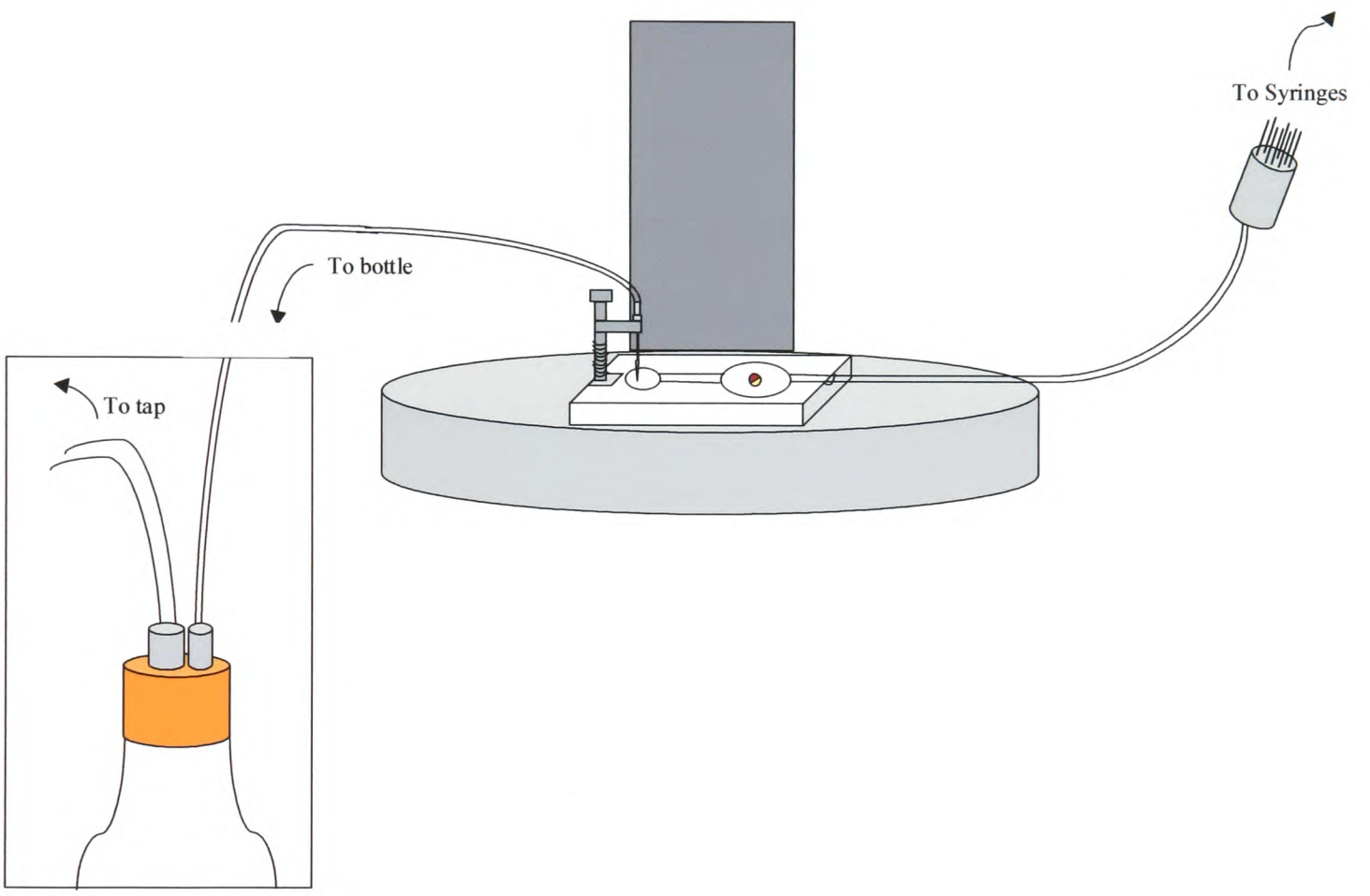


Diagram 2.4. Schematic diagram of the bath perfusion system. Gravity inflow achieved by the use of 50ml syringes, with active suction achieved via tubing attached to a bottle and subsequently a tap.

2.5 Immunocytochemistry of *Xenopus laevis* oocytes

2.5.1 Preparation of oocytes for whole-mount immunocytochemistry

PepT1 and water injected control oocytes were incubated for 30 minutes in experimental media before being removed and fixed in 100% methanol. Fixing was carried out for 4 hours at -20°C in 4ml glass vials. Samples were subsequently rehydrated by a series of PBS (table 2.6a) washes at room temperature. Three washes in total were carried out, the first being a 15 minute wash in 50% methanol/50% PBS and the remaining washes were for 15 minutes in PBS alone. The oocytes were then bisected with a clean, sharp scalpel blade in a Petri dish containing PBS. The samples were transferred to 1.7ml Eppendorf tubes and incubated in blocking buffer (10% goat sera plus 2% bovine serum albumin (BSA) in 0.1M PBS) for 1 hour at room temperature.

pH	ml of A	ml of B	Ratio B/A
7.4	95	405	4.37

Table 2.6a. Composition of buffer in 1 litre of distilled water. Solution A - 0.2M NaH_2PO_4, solution B - 0.2M Na_2HPO_4. 9g of NaCl is added to the above phosphate solution to make 0.1M PBS.

Samples were washed again in Tris buffered saline plus 0.1% igepal (TBSI) (table 2.6b). Three washes were carried out, each of thirty minutes duration, with the samples on a rocker. The oocytes were subsequently incubated for 16-24 hours in primary antibody solution (rabbit antiPepT1), diluted 1:200 in TBSI plus 2% BSA, at 4°C on a rocker for gentle motion, (Hussain *et al*, 2001).

Reagent	Weight (g)
NaCl	80
KCl	2
Tris base	30

Table 2.6b. The above reagents were dissolved in 800ml double distilled water and the pH adjusted to 7.4 with 1M HCl then water was added up to 1 litre and the solution autoclaved. This is a 10x stock. Dilute 10 fold before use then add 0.1% Igepal (v/v).

The samples were washed for 24-36 hours in 500µl TBSI at 4°C with gentle motion and the wash buffer changed every 8-12 hours. The wash buffer was removed and the oocytes incubated in fluorochrome-conjugated secondary antibody (Fluorescin isothiocyanate (FITC) or tetramethylrhodamine isothiocyanate (TRITC)-conjugated goat anti-rabbit, 1:200) for 16-24 hours at 4°C with gentle motion. The samples were subsequently washed for 24-36 hours at 4°C with the wash buffer changed every 8-12 hours. The samples were dehydrated by the addition of 1ml of 50% methanol in PBS at room temperature for 15 minutes. Samples can be stored in methanol at -20°C at this stage if required.

2.5.2 Mounting bisected X.laevis oocytes

Samples were mounted in Murray's Clear (benzyl benzoate/benzyl alcohol, 1:2 v/v) into cavity slides. 3-5 oocyte halves were removed from the Eppendorf tube with a Pasteur pipette and placed into the 0.5ml cavity on the slide. The excess methanol was wicked away using paper towel before the cavity was filled with Murray's Clear. Excess mounting media was also removed by wicking away with paper towel before

the coverslips were put into place, the edges of which were sealed with clear nail polish. Slides were stored at 4°C in a slide storage box.

2.5.3 Viewing oocytes with the confocal microscope

Fluorescing oocyte sections were viewed using a confocal microscope and Leica TCS NT software (see Diagram 2.5a). The argon (FITC) or krypton (TRITC) lasers were switched on 15 minutes prior to use and allowed to heat up. The microscope was set up for visual use and slides were placed onto the microscope stage and a 10x 0.3NA dry objective lens used to find a good sample. When a sample was selected, the objective was changed to UV 20x 0.7NA plan apochromat oil immersion. The oil used had a refractive index similar to that of the glass coverslip (typically 1.51). To obtain an image, the filters on the microscope were changed for scanning, and the software set up with the correct parameters i.e. objective lens, lasers, accumulations etc. and images were collected. Excitation of the fluorochromes occurred at 488nm for FITC and 568nm for TRITC. Optical sectioning of the sample and quantification of the fluorescence were also undertaken using the TCS NT software. These images as well as the fluorescence profiles of the oocytes were saved as Excel spreadsheet files onto a zip disk.

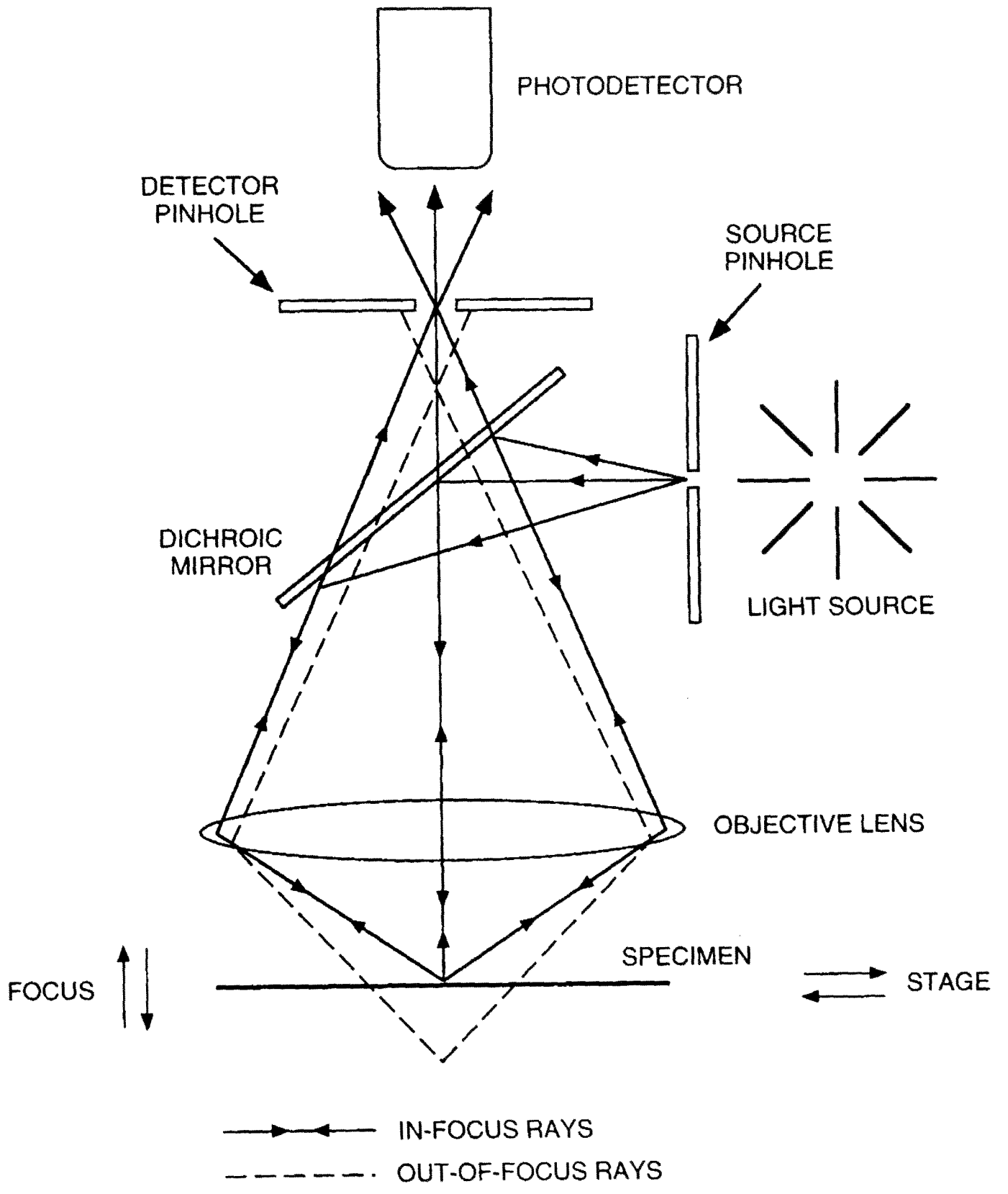


Figure 2.5 Schematic diagram of the light path in the confocal microscope (redrawn from Confocal Microscopy Methods and Protocols, Stephen W. Paddock – part of the Methods in Molecular Biology series).

2.6 Experimental solutions

In all cases when uptake solution is used, the composition is as follows:

95mM NaCl, 2mM KCl, 1mM $CaCl_2$, 1mM $MgCl_2$, 20mM HEPES, or 20mM MES adjusted to the appropriate pH with Tris.

2.7 Materials

All chemicals were from Sigma, Poole, Dorset, U.K. except for Phe-Tyr, Phe-Tyr-NH_2, Gly-Asp, Asp-Gly, Gly-Lys and Lys -Gly which were all from Bachem, St. Helens, Merseyside U.K., Type 1 collagenase from ICN, Basingstoke, Hampshire, U.K. and gentamycin from Fluka, Poole, Dorset, U.K.

2.8 Calculation of kinetic constants

Michaelis Menten curves were fitted using Sigma Plot 2000, according to:

$$V = \frac{I_{max}\,(S)}{K_a + S}$$

where;

I_{max} is the maximum current evoked by peptide transport

K_a is the concentration required to evoke a half-maximal effect

V is the rate of peptide transport for a given S

S is the substrate concentration

2.9 Data expression and statistics

All data are quoted as mean ± s.e.m (standard error of the mean) unless otherwise stated. Voltage traces, I-V curves and concentration response curves are all representative of one individual oocyte. Statistical analyses of the mean values obtained were carried out using the Student's *t* test.

CHAPTER 3

pH AND VOLTAGE DEPENDENCE OF OLIGOPEPTIDE TRANSPORT THROUGH PEPT1

3.1 Introduction

The effect of various Xaa-Ala dipeptides on membrane voltage have been investigated at neutral and acidic pH, as well as a comprehensive study of the transport of neutral peptide Gly-Gln. Voltage responses upon Gly-Gln application were recorded, as were dose-response curves which allowed the estimation of the kinetic parameters of the peptide, namely the K_a and the I_{max}. In addition, the pH dependence of another neutral peptide, Leu-Ala, was investigated over a range of pH values from pH 5.0 - pH 8.0.

All of the experiments and results presented in this chapter were designed to give an introduction to the basic electrophysiology of peptide transport via PepT1, to understand the theory of the experimental apparatus and to provide practice in using the equipment and the computer software required for data analysis.

3.2 Effect of Xaa-Ala peptides on membrane voltage

3.2.1 Phe-Ala, Trp-Ala and Tyr-Ala.

Phe-Ala, Trp-Ala and Tyr-Ala are all aromatic dipeptides. The effects of these molecules were recorded in PepT1 expressing oocytes using a single saturating concentration of 0.5mM at pH 7.5 and pH 5.5. The membrane voltage was recorded throughout the experiment using a chart recorder. The exact protocol can be seen in table 3.1, and the traces recorded during these experiments can be seen in figure 3.1.

Step	Condition
1	pH 7.5 uptake
2	pH 7.5 uptake + 0.5mM Xaa-Ala
3	pH 7.5 uptake
4	pH 5.5 uptake
6	pH 5.5 uptake + 0.5mM Xaa-Ala
7	pH 5.5 uptake
8	pH 7.5 uptake
9	pH 7.5 uptake + 0.5mM Xaa-Ala

Table 3.1 Experimental protocol used to investigate the effects of Xaa-Ala peptides in PepT1 expressing oocytes.

3.2.2 General observations

Before reporting the specific effects of these dipeptides, a few general observations should be noted. The average resting membrane potential, E_m, of healthy oocytes was 48 ± 4.mV, mean ± s.e.m, n = 10. The values recorded control oocytes were not significantly different, see table 3.2. The oocytes usually required at least 20 minutes to reach a steady E_m once they had been impaled with the electrodes. If after this time a substantial voltage was not achieved or a steady level was not reached, then the oocyte was discarded. A depolarisation was always seen upon a change in extracellular solution from neutral to acidic, i.e. pH 7.5 - pH 5.5, regardless of whether the oocytes had been injected with water or PepT1 cRNA, which could be attributed to the opening of an endogenous cation channel. The E_m of the oocytes changed by 14± 3.mV upon extracellular acidification, mean ± s.e.m, n=10. No peptide induced currents were recorded in water injected control oocytes, suggesting that all measurements made were as a result of injection of PepT1 cRNA into the oocytes and its subsequent expression, see figure 3.1a. No currents were observed when the constituent amino acids were applied in place of the peptide, see figure 3.1b. The data presented in figure 3.1 was obtained directly from pCLAMP software (Fetchan), whereas all other voltage traces were obtained from traces recorded by the chart recorder (hence the change in noise level between figures).

In this thesis, transport of dipeptides was defined as either the generation of a depolarisation (voltage responses) or an inward current (voltage clamping) as a result of the movement of positive charge, (H^+), into the oocytes.

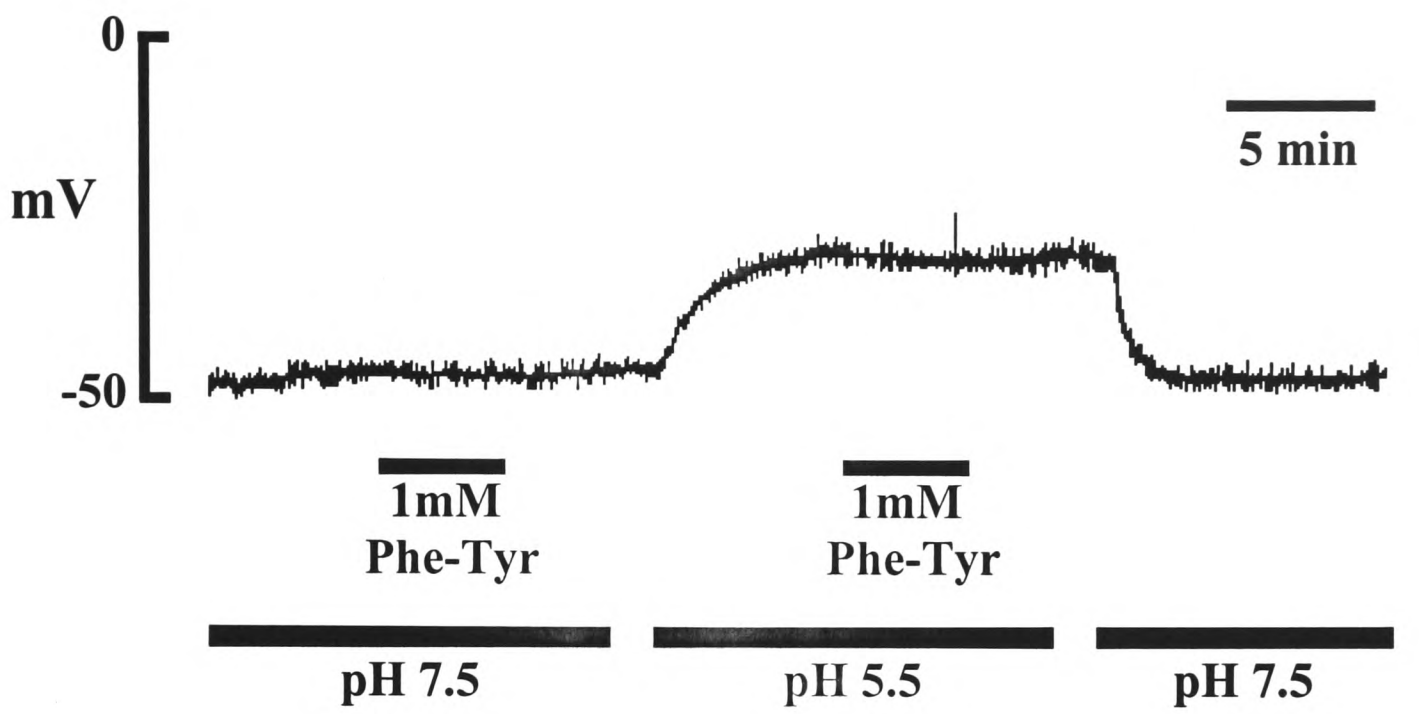
3.2.3 Response to 0.5mM Phe-Ala, Trp-Ala and Tyr-Ala

Exposure to 0.5mM Phe-Ala at pH 7.5, resulted in a depolarisation of 15.0 ± 3.5mV

Condition	Membrane potential, E_m (mV)
PepT1	-48 ± 4mV
Control	-50 ± 5mV

Table 3.2 E_m values for oocytes either injected with PepT1 cRNA or water. The values were not statistically significant from each other, P>0.1, using Student's *t* test, mean ± s.e.m, n = 10.

a.



b.

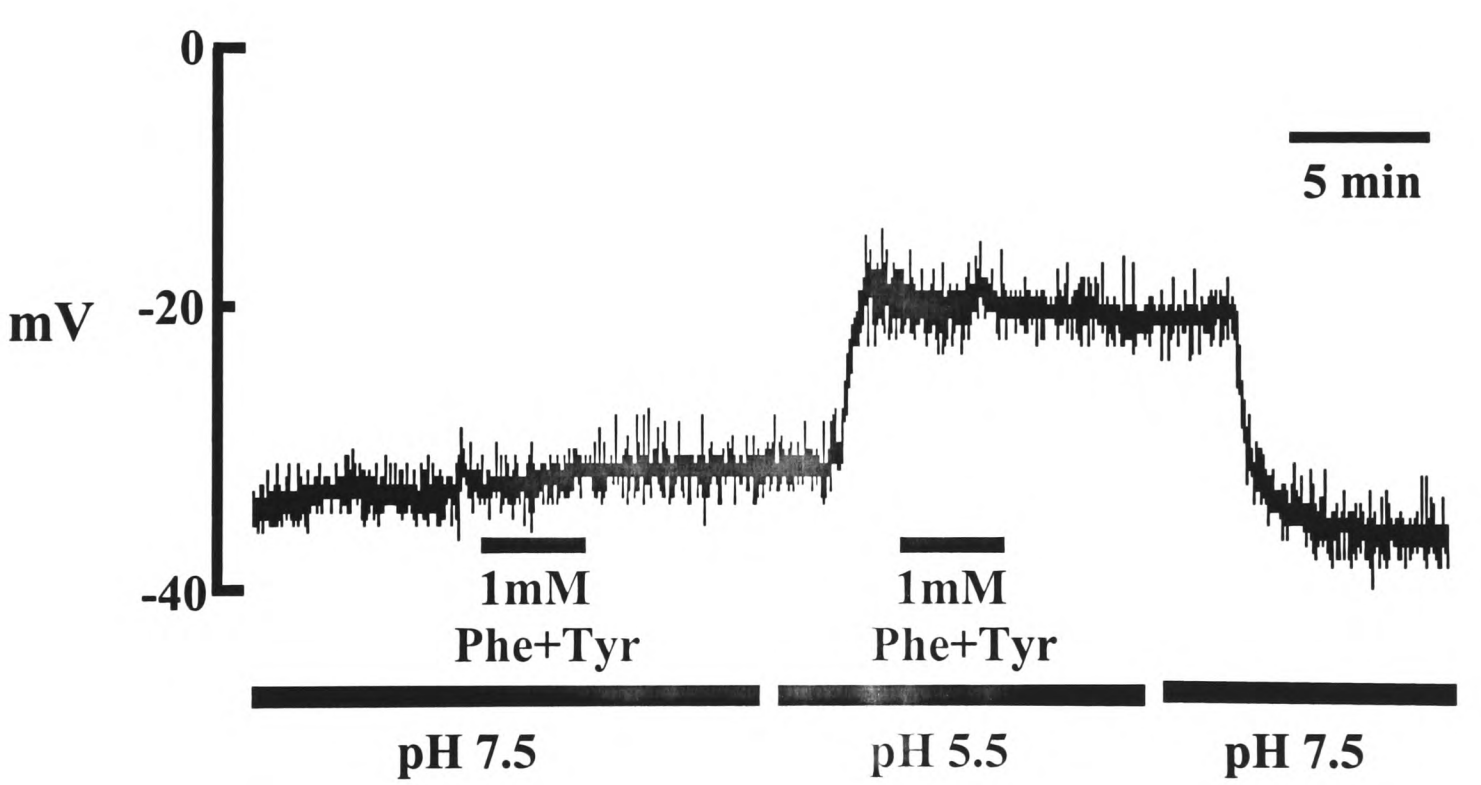


Figure 3.1a Voltage traces recorded in response to 1mM Phe-Tyr at pH 7.5 and 5.5 in a control oocyte. b. Voltage trace recorded **in response to constituent amino acids, Phe and Tyr in a** PepT1 expressing oocyte **(data are representative of one oocyte).**

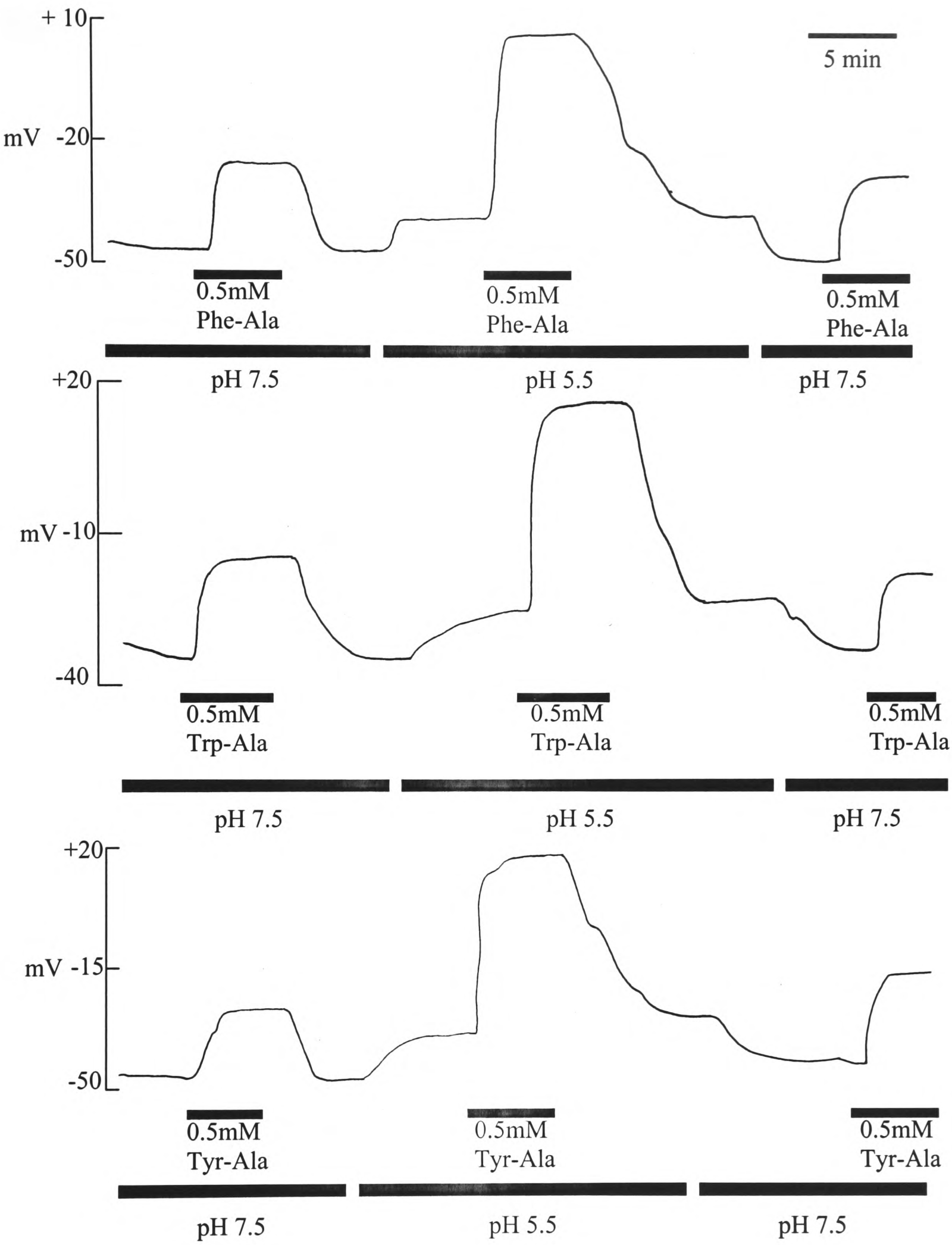


Figure 3.2 Voltage traces recorded in response to 0.5mM Phe-Ala, Tyr-Ala, and Trp-Ala at pH 7.5 and 5.5 in a PepT1 expressing oocyte, (data are representative of one oocyte).

Substrate	Depolarisation (mV) pH 7.5	pH 5.5
Phe-Ala	15 ± 3.5	43 ± 3.0
Trp-Ala	23 ± 6.0	47 ± 1.0
Tyr-Ala	22 ± 1.0	53 ± 2.0

Table 3.3 Depolarisations evoked by 0.5mM Phe-Ala, Trp-Ala and Tyr-Ala in PepT1 expressing oocytes, mean ± s.e.m, n = 10.

compared to 23.0 ± 6.0mV and 22.0 ± 1.0mV for Trp-Ala and Tyr-Ala, respectively. At pH 5.5, all of the depolarisations recorded were greater than those observed at pH 7.5; 43.0 ± 3.0mV for Phe-Ala, 47.0 ± 1.0mV for Trp-Ala and 53.0 ± 2.0mV for Tyr-Ala, mean ± s.e.m, n=10.

There was therefore a 2.8-fold increase in the depolarisation by Phe-Ala as a result of extracellular acidification, compared to a 2-fold increase for Trp-Ala and a 2.4 fold increase for Tyr-Ala. Table 3.3 contains the depolarisation values for the peptides.

3.2.4 Response to 0.5mM Gly-Ala, Leu-Ala and Ala-Ala

These three peptides are aliphatic, and the same protocol was applied for them as for the aromatic peptides. Briefly, the effects of these molecules were recorded in PepT1 expressing oocytes using a single saturating concentration of 0.5mM, at pH 7.5 and pH 5.5. The membrane voltage was recorded throughout the experiment using a chart recorder. Again the exact protocol can be seen in table 3.1. The traces recorded during these experiments can be seen in figure 3.3.

Upon exposure to 0.5mM Gly-Ala at pH 7.5, there was a depolarisation of 27.0 ± 1.0mV compared to 46.0 ± 7.0mV and 42.0 ± 1.0mV for Leu-Ala and Ala-Ala, respectively. At pH 5.5, all of the depolarisations recorded were greater than those observed at pH 7.5; 44.0 ± 5.0mV for Gly-Ala, 50.0 ± 2.0mV for Leu-Ala and 47.0 ± 3.0mV for Ala-Ala, mean ± s.e.m, n=10.

There was therefore a 1.6-fold increase in the depolarisation by Gly-Ala as a result of extracellular acidification, compared to a 1.1-fold increase for Leu-Ala and again a 1.1-fold increase for Ala-Ala. Table 3.4 contains the depolarisation values for the peptides.

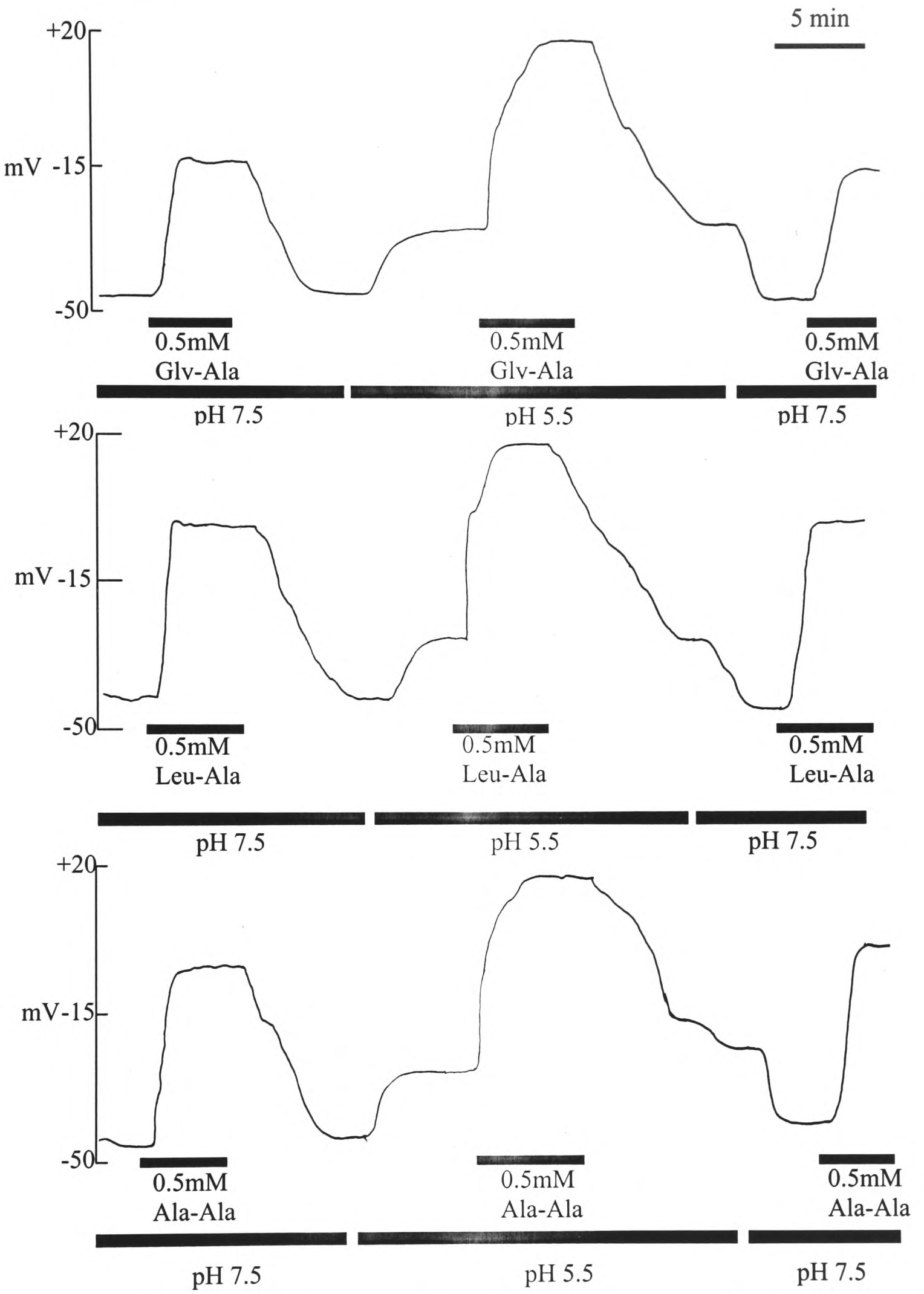


Figure 3.3 Voltage traces recorded in response to 0.5mM Gly-Ala, Leu-Ala, and Ala-Ala at pH 7.5 and 5.5 in a PepT1 expressing oocyte, (data are representative of one oocyte).

	Depolarisation(mV)	
Substrate	pH 7.5	pH 5.5
Gly-Ala	27 ± 1.0	44 ± 5.0
Leu-Ala	46 ± 7.0	50 ± 2.0
Ala-Ala	42 ± 1.0	47 ± 3.0

Table 3.4 Depolarisations evoked by 0.5mM Gly-Ala, Leu-Ala and Ala-Ala in PepT1 expressing oocytes, mean ± s.e.m, n = 10.

Application of standard peptides always caused a depolarisation in PepT1 expressing oocytes as a result of movement of positive charge into the oocytes. This voltage change was greater at pH 5.5 presumably due to an increased proton gradient.

3.3 Transport of Gly-Gln

3.3.1 Effect of Gly-Gln on membrane voltage

The effect of Gly-Gln on membrane voltage was investigated in the same way as the Xaa-Ala peptides, but the concentration of peptide used was 2mM. The same protocol was used as shown in table 3.1, and again the response of the PepT1 oocyte to Gly-Gln was recorded continuously throughout the experiment, see figure 3.4. Exposure to 2mM Gly-Gln at pH 7.5 caused a depolarisation of 60.0 ± 8.0mV compared to 77.0 ± 12.0mV at pH 5.5, mean ± s.e.m, n = 10.

There was a 1.3-fold increase in transport of Gly-Gln as a result of extracellular acidification. These results are similar to those gained with Xaa-Ala dipeptides, but the size of the depolarisations for Gly-Gln were approximately 2-fold greater at pH 7.5, except in the case of Phe-Ala where there was a 4-fold increase. At pH 5.5 the depolarisations were approximately 1.5-fold greater.

3.3.2 Voltage clamping of Gly-Gln transport

The same protocol was used in these experiments as that stated above but two-electrode voltage clamp studies were also carried out. Steady state I-V curves were generated at both pH values in the presence and absence of 2mM Gly-Gln. Briefly, the membrane potential of the oocyte was held at –50mV and stepped from +50mV to –150mV in 10mV increments. Voltage clamp recordings were taken once the E_m of the oocyte had reached a steady state. The data recorded were used to generate

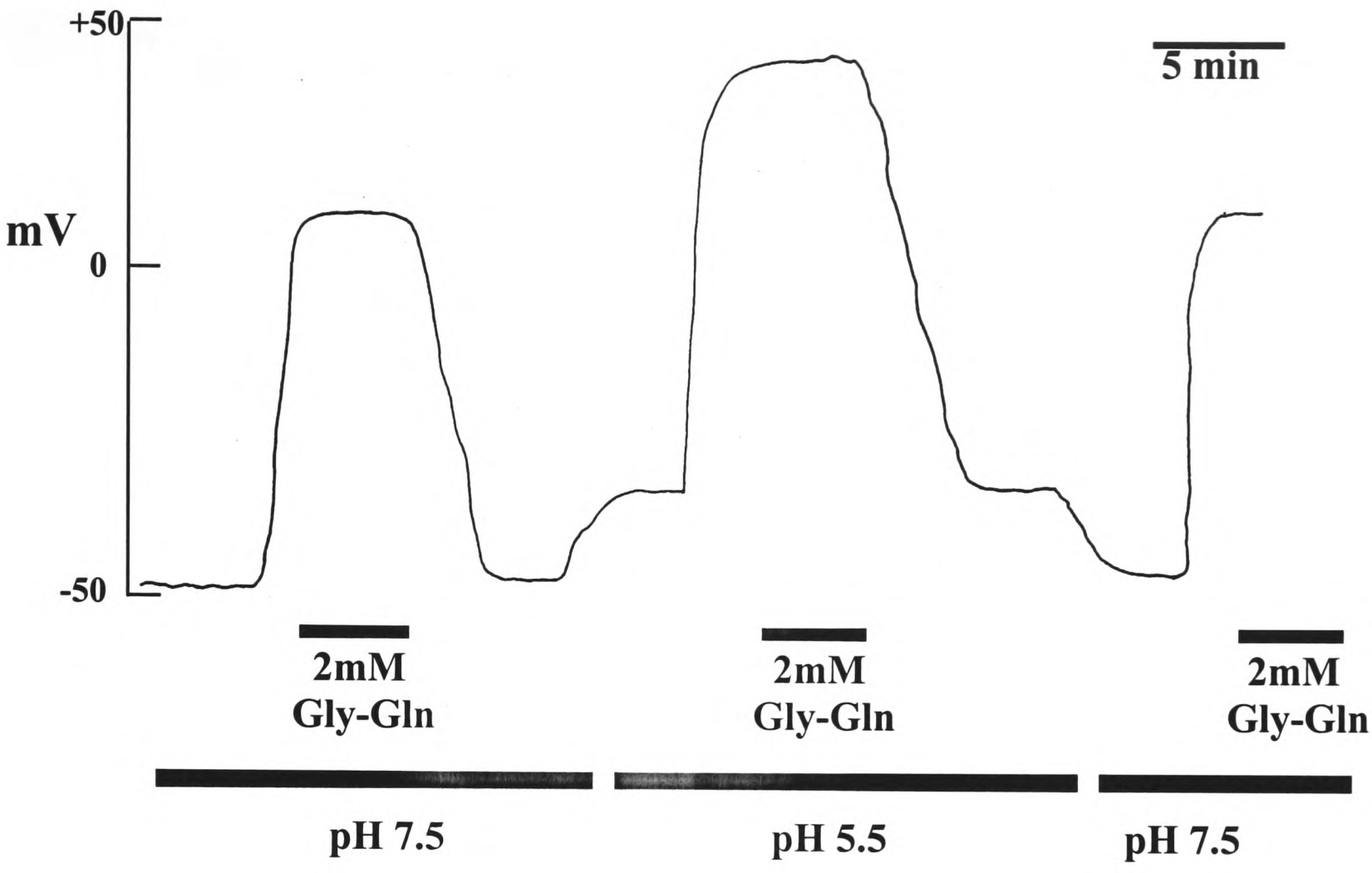


Figure 3.4 Voltage traces recorded in response to the 2mM Gly-Gln at pH 7.5 and 5.5 in a PepT1 expressing oocyte, (data representative of one oocyte).

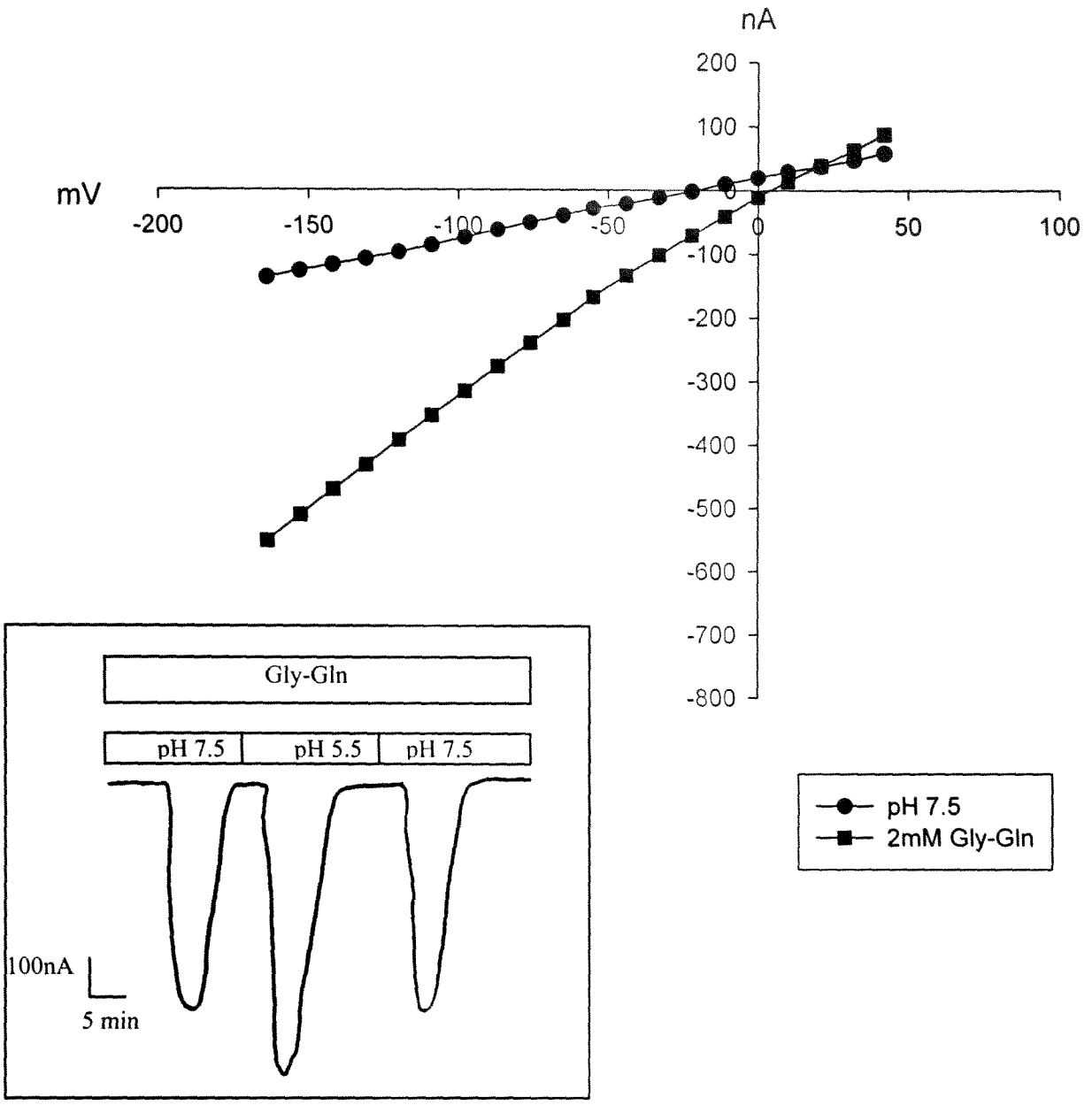


Figure 3.5 Steady state I-V relationship recorded in the presence and absence of Gly-Gln in PepT1 expressing oocytes at pH 7.5, (data representative of one oocyte). Inset: Current trace recorded in a PepT1 expressing oocyte in response to 2mM Gly-Gln at pH 7.5 and pH 5.5.

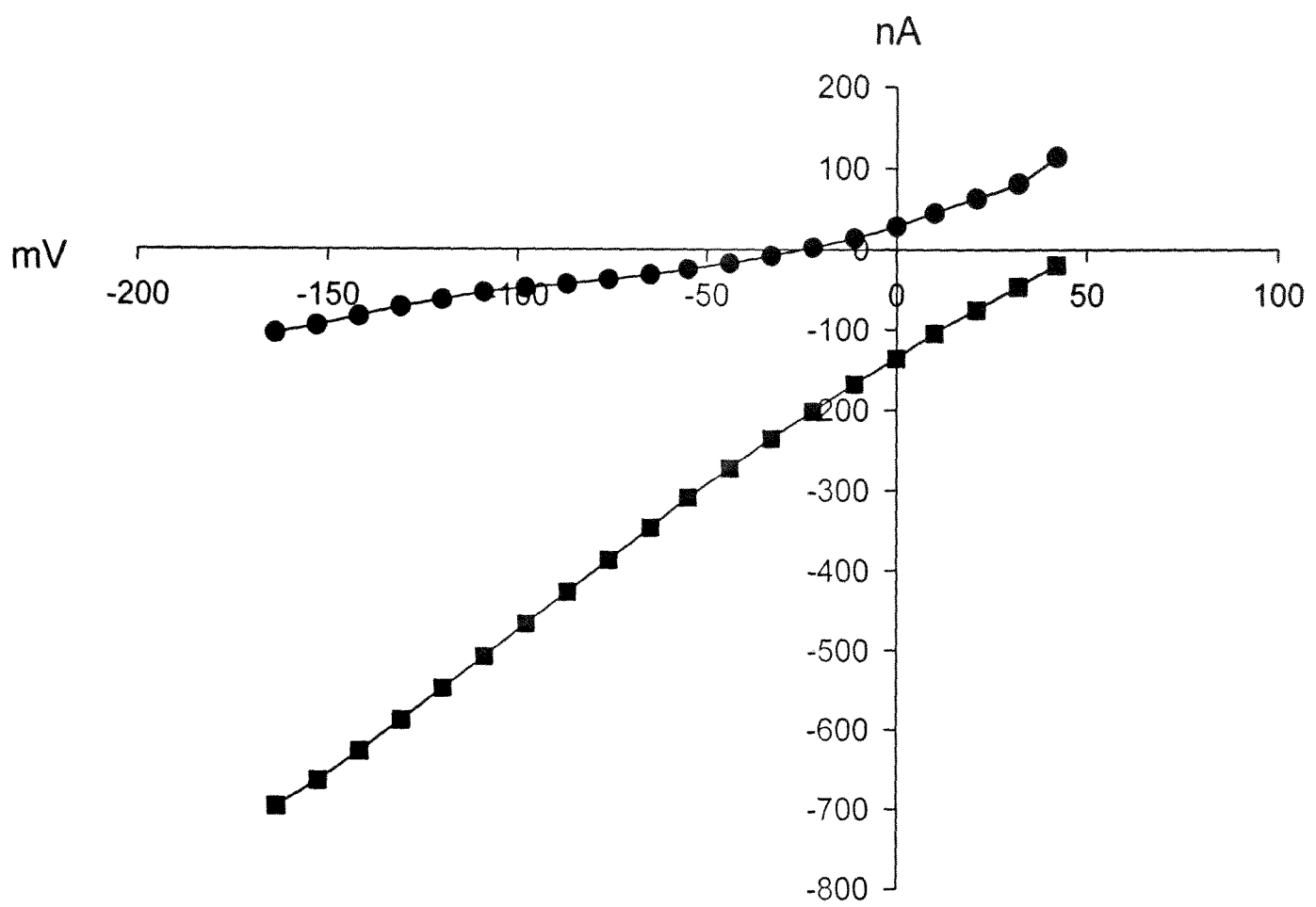


Figure 3.6 Steady state I-V relationship recorded in the presence and absence of Gly-Gln in PepT1 expressing oocytes at pH 5.5, (data representative of one oocyte).

standard I-V curves. Figures 3.5 and 3.6 show typical responses at pH 7.5 and 5.5 with and without Gly-Gln.

Maximal current values were always observed at –150mV. In some cases where dose-response curves were not asymptotic (due to solubility constraints of the peptides), the I_{max} was assumed to be at –150mV. The data presented are that of one oocyte, but are representative of all oocytes tested.

The I_{max} values obtained at pH 7.5 were 414.5 ± 36.2nA compared with 591.0 ± 29.7nA at pH 5.5, mean ± s.e.m, n = 10. Larger currents were obtained at pH 5.5 as expected due to the increased proton driving force for transport into the oocytes. The maximal currents at pH 5.5 were approximately 1.4-fold greater than those currents recorded at pH 7.5.

The reversal potential also changed upon external acidification, but not to the degree expected. The reversal potential for PepT1 has received very little attention in past and recent literature, but in this case the anomaly could be due to a leak current.

3.3.3 Concentration-dependence of Gly-Gln induced currents

Concentration-dependence of Gly-Gln induced currents was carried out at pH 7.5 and pH 5.5 in PepT1 expressing oocytes. The concentrations of Gly-Gln used were 0.5, 1, 2 and 5mM. Figure 3.7 shows typical dose-response curves recorded at both pH values. Inward currents were observed for the substrate at pH 7.5 and pH 5.5, but extracellular acidification caused an increased in the maximal current values obtained. I_{max} values for Gly-Gln were 568.1 ± 12.2nA at pH 7.5 and 771.3 ± 19.5nA at pH 5.5, (mean ± s.e.m, n =10, $P < 0.01$). The currents recorded at pH 5.5 were approximately 1.4-fold greater than that observed at pH 7.5.

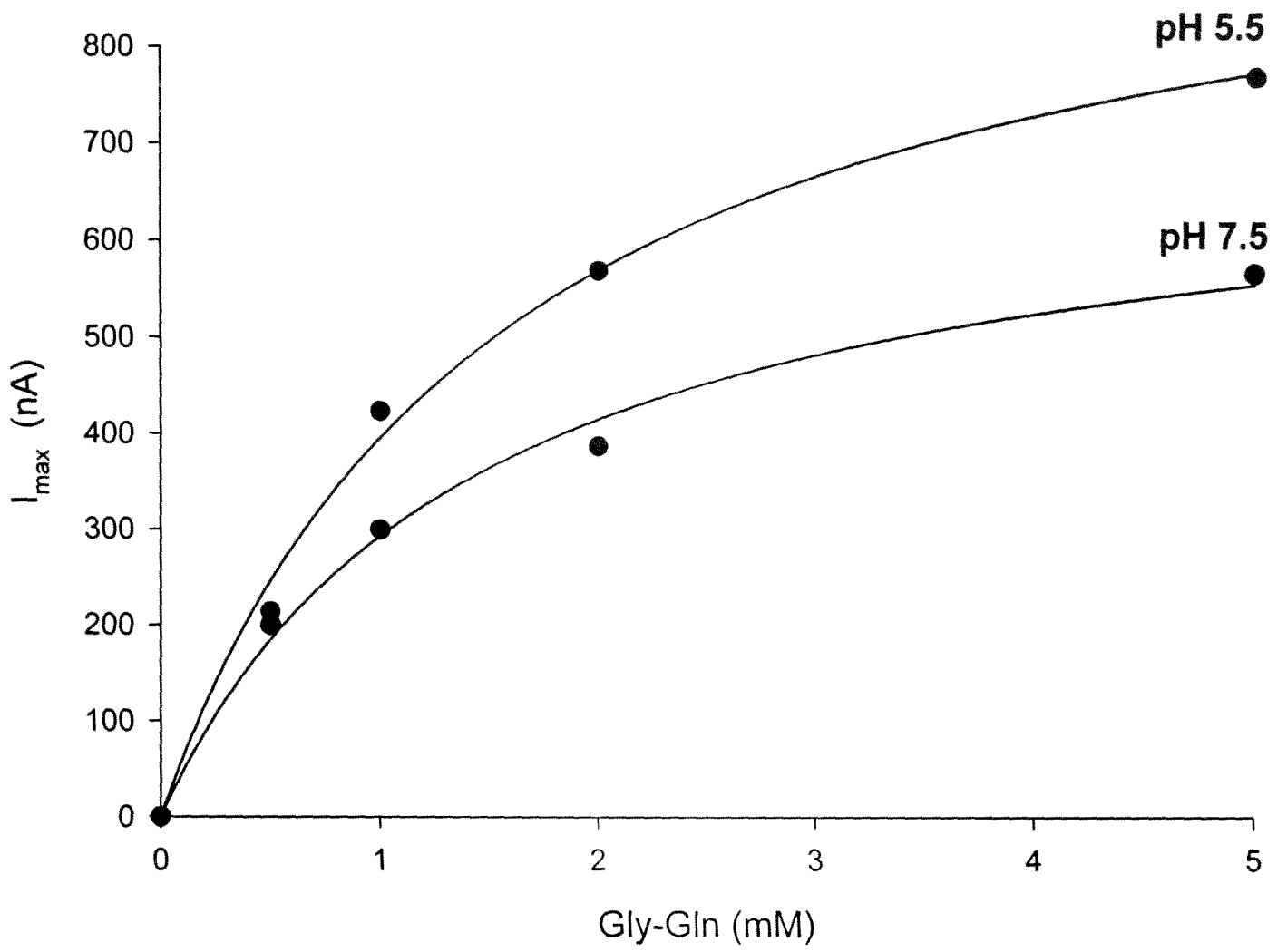


Fig 3.7 I_{max} for the peptide-induced currents at pH_o 7.5 and pH_o 5.5 were plotted as a function of substrate concentration.

Substrate	**pH**	**I_{max} (nA)**	**K_a (mM)**
		mean ± s.e.m	**mean ± s.e.m.**
Gly-Gln	7.5	568.1 ± 12.2	0.8 ± 0.04
Gly-Gln	5.5	771.3 ± 19.5	1.1 ± 0.09

Table 3.5 K_a and I_{max} values for Gly-Gln recorded at pH 7.5 and 5.5 in PepT1 expressing oocytes, mean ± s.e.m, n = 10.

The affinity for Gly-Gln was also altered by the shift in extracellular pH. At pH 7.5 the affinity for Gly-Gln was 0.8 ± 0.04mM, compared to 1.1 ± 0.09mM at pH 5.5, (mean ± s.e.m, n=10,). This is an approximate 1.4-fold decrease in affinity upon extracellular acidification. Again values were statistically significant from each other, $P < 0.01$, using the Students *t* test. The values for the kinetic parameters, I_{max} and K_a can be seen in table 3.5.

3.4 pH dependence of peptide transport by PepT1

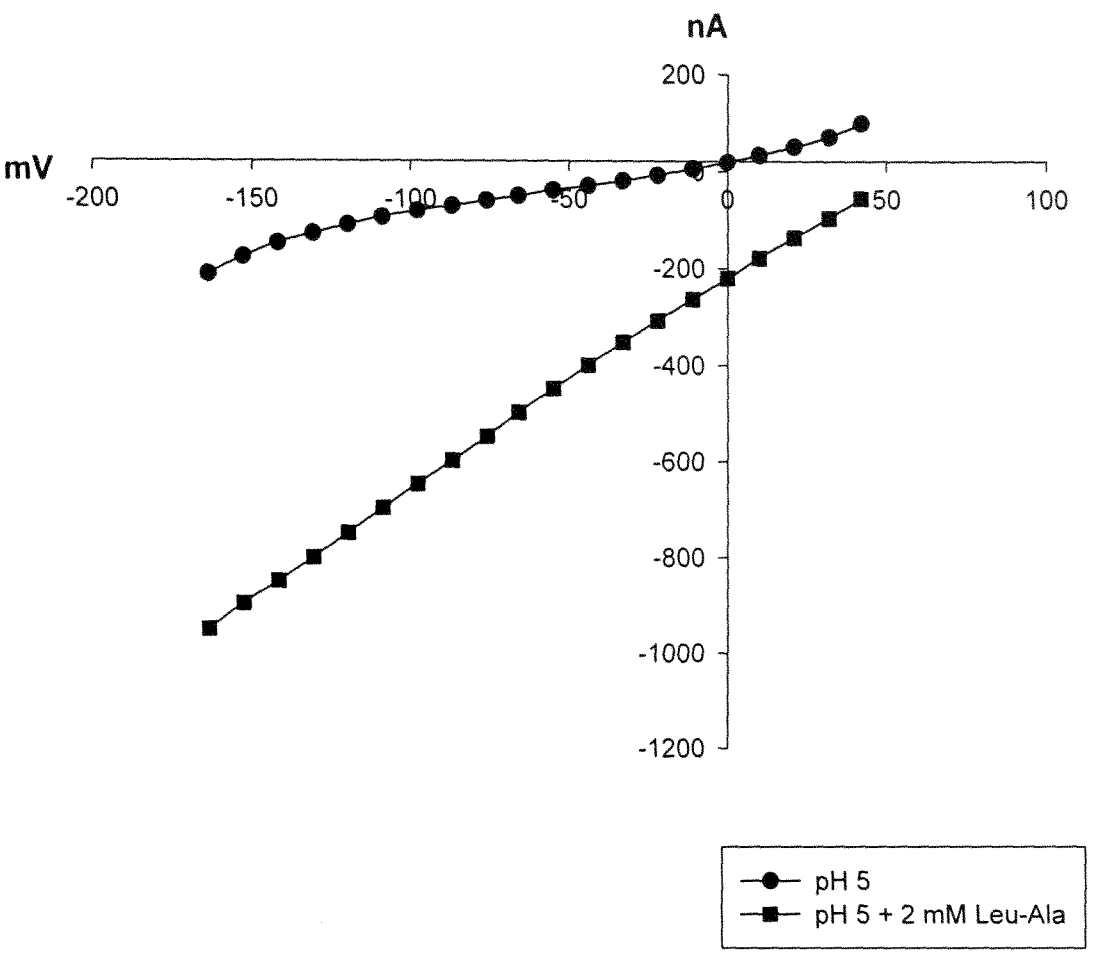
Previous experiments have been carried out at two pH values, and had provided evidence that PepT1-mediated peptide transport was maximal at acidic pH values. This experiment was designed to confirm that the optimal pH for transport of a neutral peptide by PepT1 was close to pH 5.5.

3.4.1 Transport of Leu-Ala

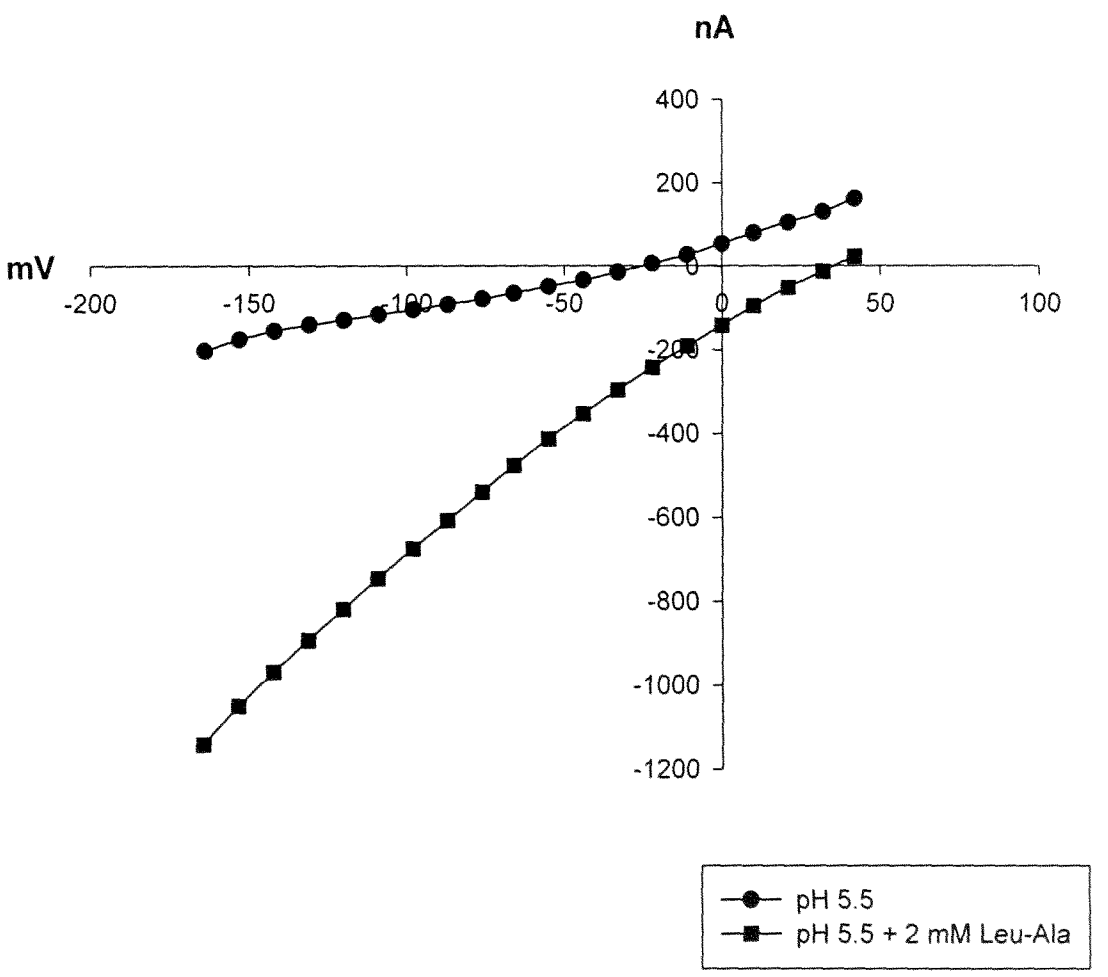
A single saturating concentration of Leu-Ala was used to investigate the effect of extracellular pH on transport of a neutral peptide. The transport of this peptide was recorded at pH 5.0-pH 8.0 in 0.5 pH unit intervals. Steady-state I-V curves were carried out at each pH in the presence and absence of peptide substrate, with the same voltage protocol used, as described earlier. Figure3.8a-g show the I-V curves plotted and figure 3.8h shows the maximal currents obtained plotted against pH.

The I_{max} values for the transport of 2mM Leu-Ala over the pH range indicate that transport by PepT1 is maximal at pH 5.5. The maximal current obtained was 942.9 ± 7.07nA at pH 5.5 compared to 574.4 ± 7.64nA at the most alkaline pH of 8.0. Transport increases from pH 5.0 to pH 5.5 where it reaches it's maximum, 742.3 ± 3.78nA to 942.9 ± 7.07nA, before it shows a slow decline from pH 6.0 to pH 8.0,

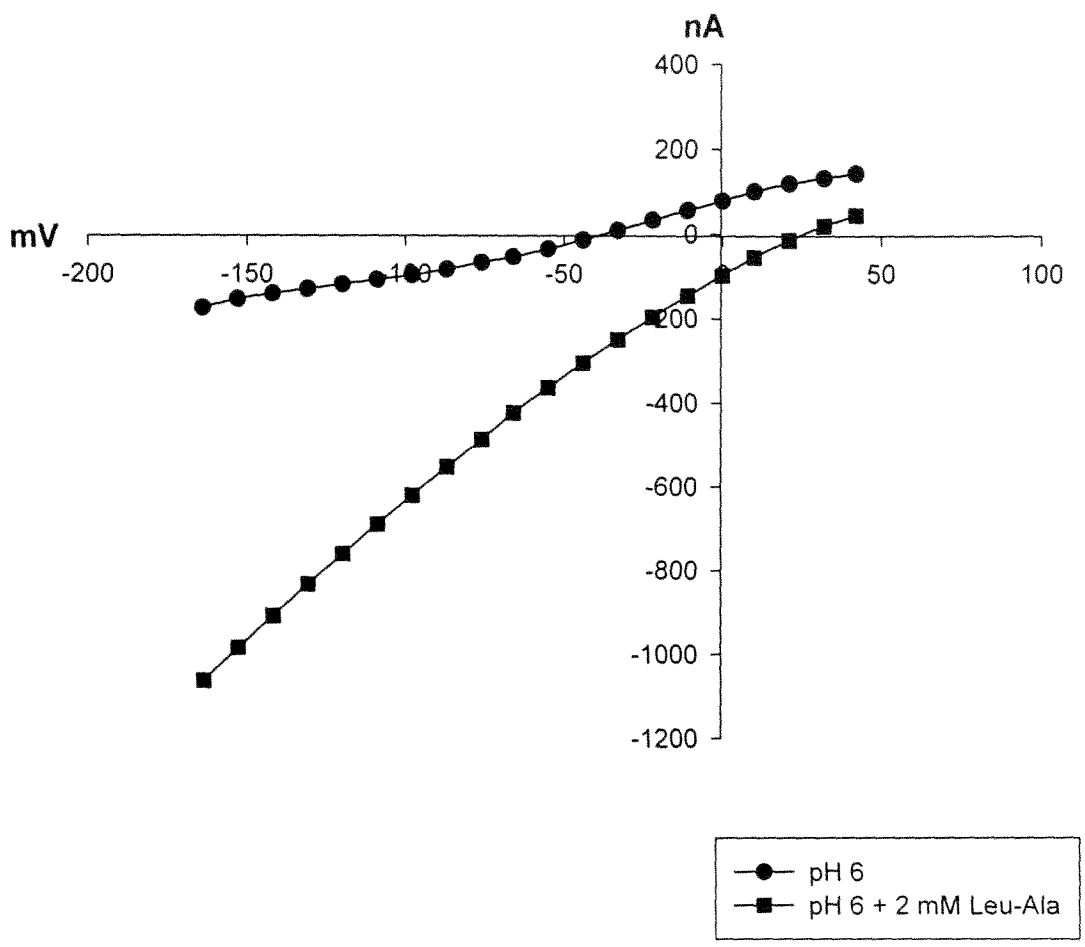
a.


nA
200
mV
-200
-150
-100
-50
0
50
100
-200
-400
-600
-800
-1000
-1200
pH 5
pH 5 + 2 mM Leu-Ala

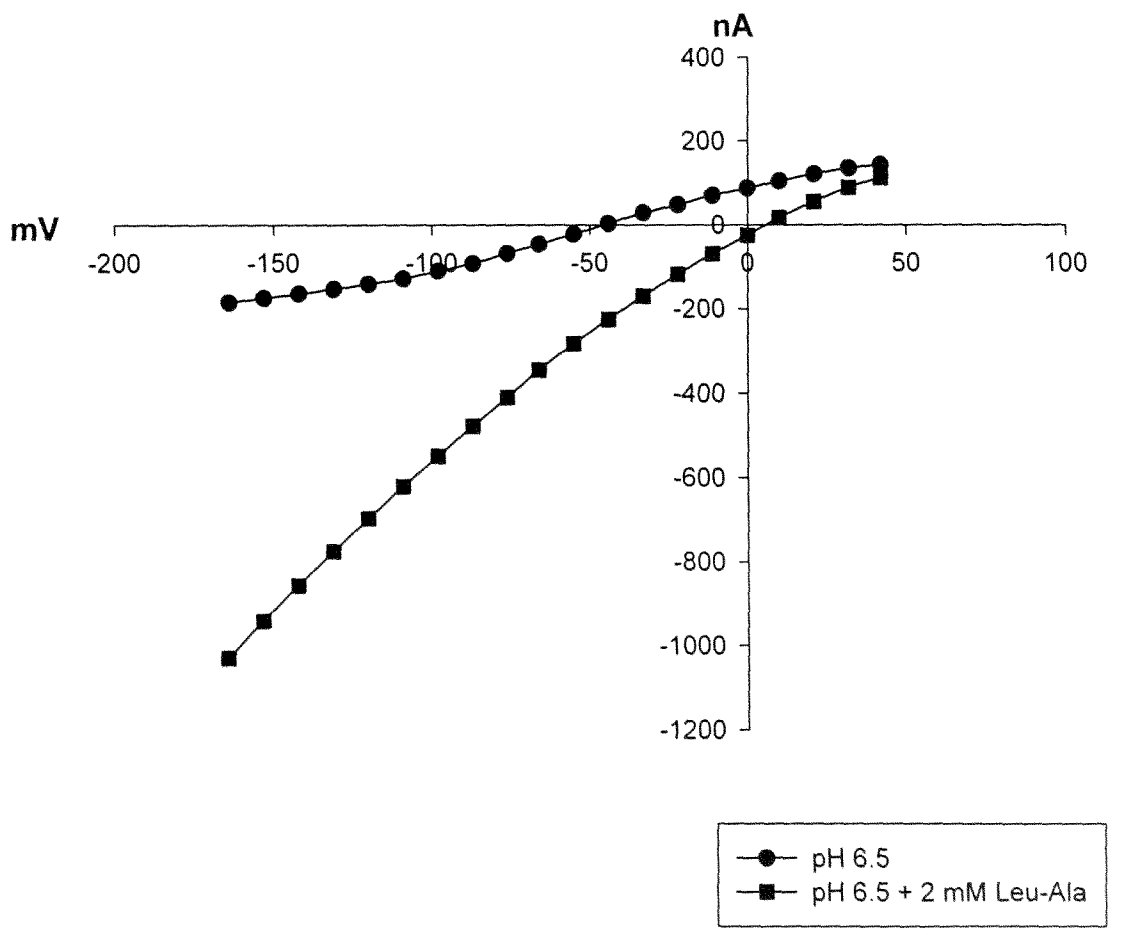
b.


nA
400
200
mV
-200
-150
-100
-50
0
50
100
-400
-600
-800
-1000
-1200
pH 5.5
pH 5.5 + 2 mM Leu-Ala

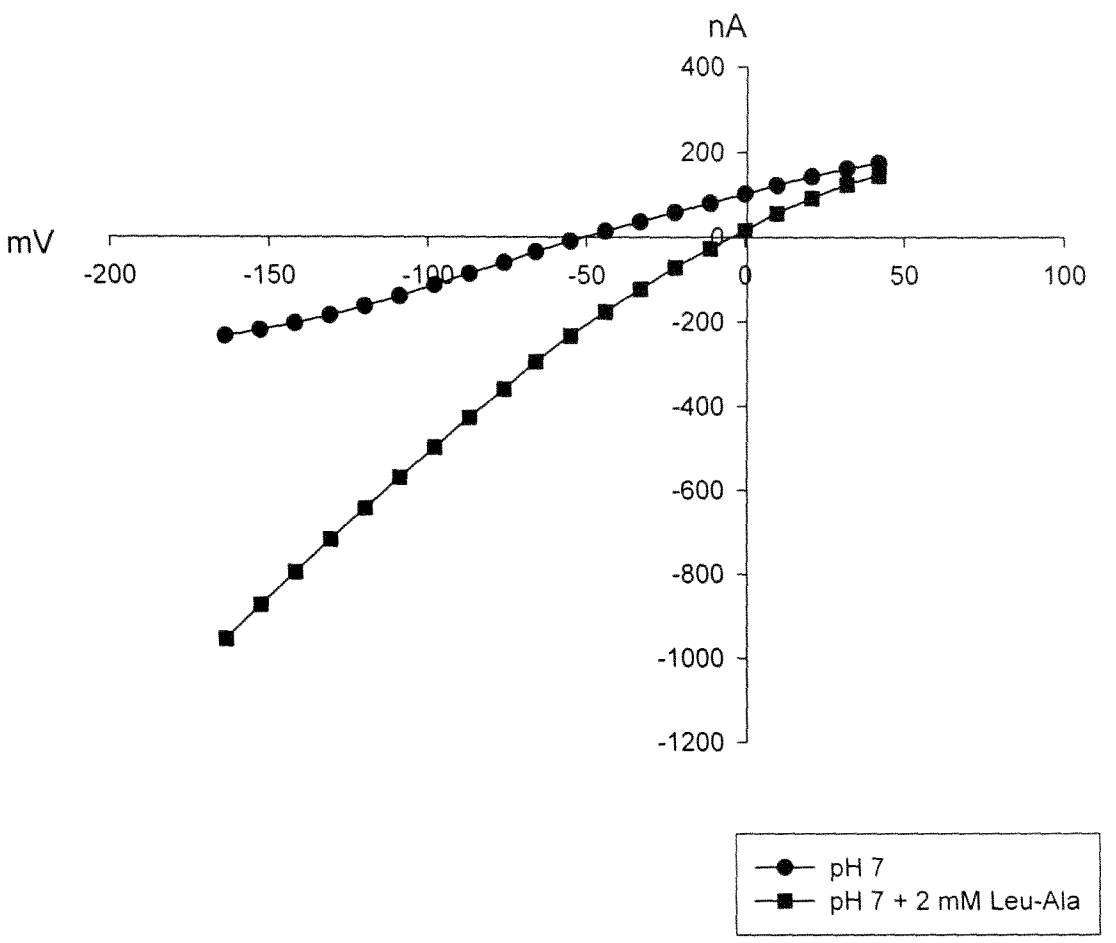
c.


nA
400
200
mV
0
-200
-150
-100
-50
50
100
-200
-400
-600
-800
-1000
-1200
pH 6
pH 6 + 2 mM Leu-Ala

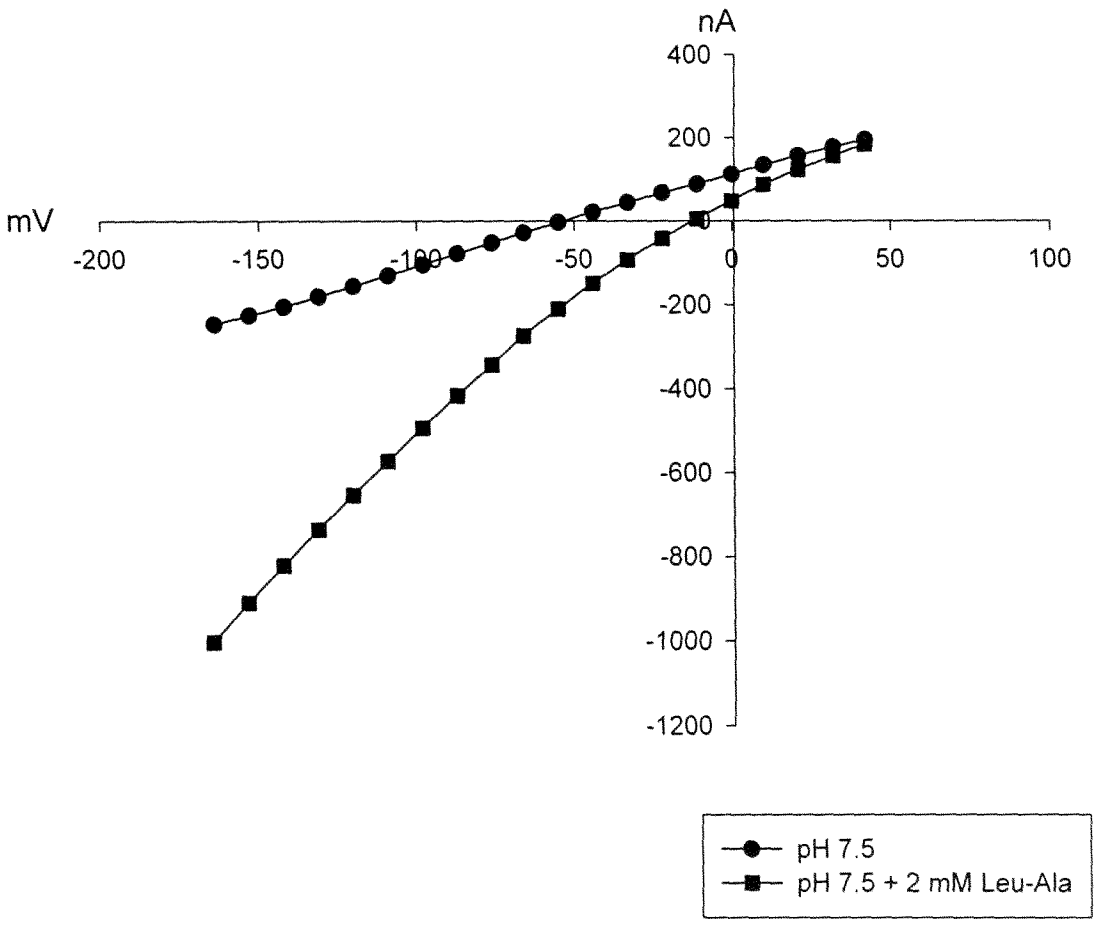
d.


nA
400
200
mV
0
-200
-150
-100
-50
0
50
100
-200
-400
-600
-800
-1000
-1200
pH 6.5
pH 6.5 + 2 mM Leu-Ala

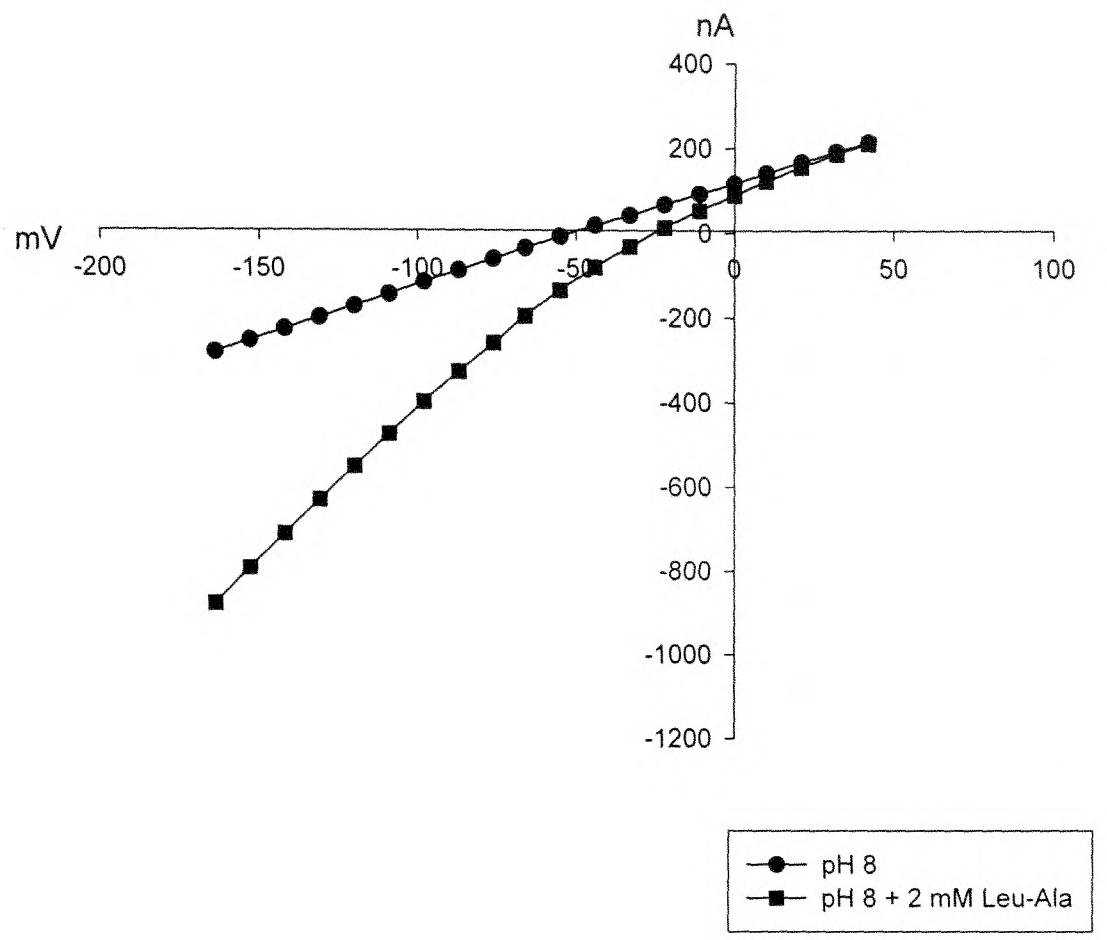
e.


nA
400
200
mV
-200
-150
-100
-50
0
50
100
-200
-400
-600
-800
-1000
-1200
pH 7
pH 7 + 2 mM Leu-Ala

f.


nA
400
200
mV
-200
-150
-100
-50
0
50
100
-200
-400
-600
-800
-1000
-1200
pH 7.5
pH 7.5 + 2 mM Leu-Ala

g.



h.

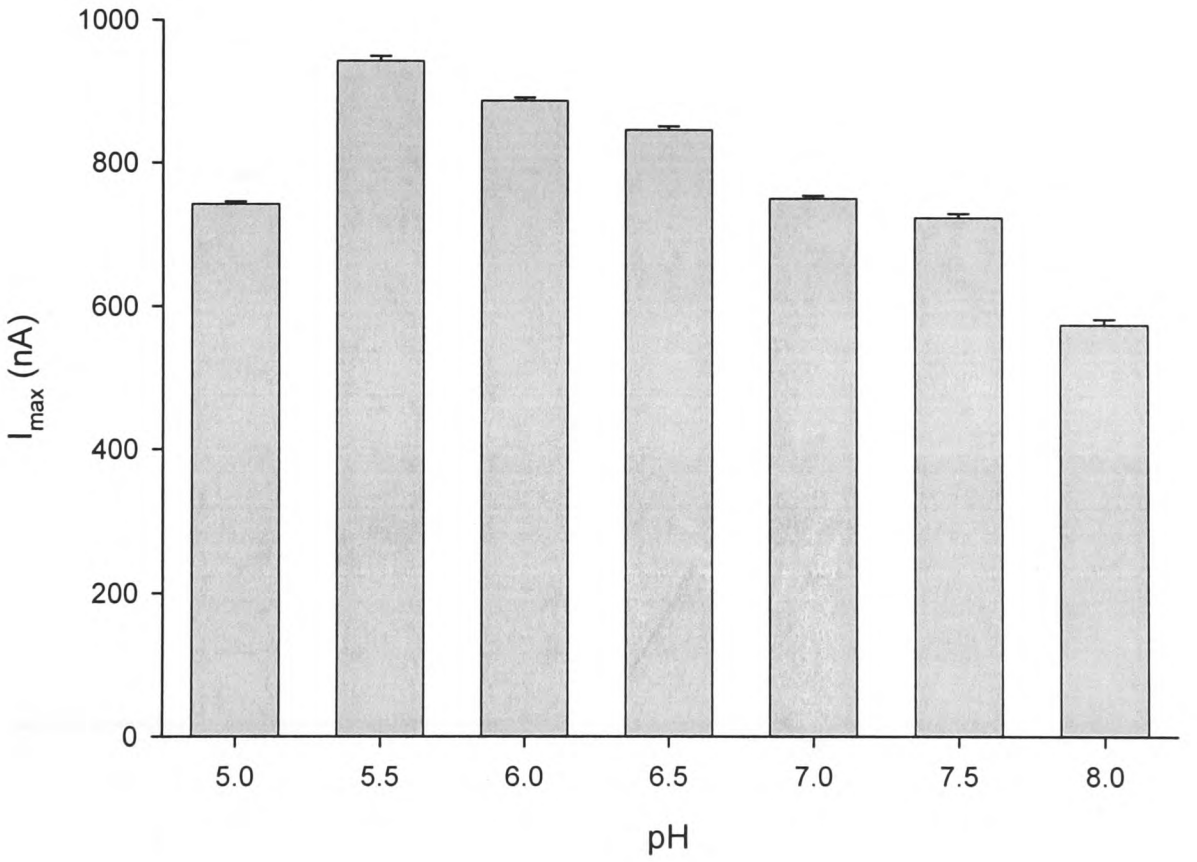


Figure 3.8a-h. Leu-Ala transport at a. pH 5.0. b. pH 5.5. c. pH 6.0. d. pH 6.5. e. pH 7.0. f. pH 7.5. g. pH 8.0. (data representative of one oocyte) h. Maximal current at each pH plotted as a function of extracellular pH, mean ± s.e.m, n = 5.

pH	**I_{max} (nA)**
5.0	742.3 ± 3.78
5.5	942.9 ± 7.07
6.0	887.4 ± 4.48
6.5	846.8 ± 4.66
7.0	750.8 ± 4.23
7.5	724.2 ± 5.72
8.0	574.4 ± 7.64

Table 3.6 Maximal currents induced by 2mM Leu-Ala recorded at each extracellular pH value in PepT1 expressing oocytes, mean ± s.e.m, n = 5

887.4 ± 4.48nA to 574.4 ± 7.64nA, mean ± s.e.m, n = 5. Table 3.6 contains all the maximal current values recorded at each extracellular pH. The same trend was observed whether the experiment was carried out from pH 5.0 – pH 8.0, or pH 8.0 – pH 5.0. See Appendix IV for further analysis of this data.

3.5 Summary of chapter

1. Injection of PepT1 cRNA and subsequent expression of PepT1 had no effect on the E_m of oocytes.

2. No response to peptide substrate was seen in water injected control oocytes.

3. Xaa-Ala dipeptides and Gly-Gln were substrates for PepT1, and their transport was electrogenic due to the cotransport of protons. This was recordable as either a membrane depolarisation or as an inward current.

4. The currents for peptide transport were maximal at –150mV.

5. The optimal pH for transport of a neutral peptide was pH 5.5.

CHAPTER 4

ANALYSIS OF TRANSPORT INDUCED BY NATIVE AND CARBOXYL TERMINUS MODIFIED PEPTIDES

4.1 Introduction

Rabbit PepT1 was cloned in 1994 by Fei *et al* and was reported to be a proton-coupled oligopeptide transporter that could also accept various peptidomimetics such as ACE inhibitors and β-lactam antibiotics, (Boll *et al*, 1994). Subsequent studies centred on the chemical features that substrates for this transporter must exhibit. The first major breakthrough occurred when it was discovered that a peptide bond was not a requirement for a molecule to be a substrate for PepT1, (Temple *et al*, 1998). This report was swiftly followed by an article stating that a distance of >500pm <630pm between the amino nitrogen and the carboxylic carbon was necessary for a substrate to be transported by PepT1, (Döring *et al*, 1998).

A more recent study using radiolabelled peptides has concentrated on the requirement of free amino and carboxyl termini, concluding that the N terminus is the primary site for the binding of di- and tripeptides, (Meredith *et al*, 2000).

In this chapter, the transport of carboxyl terminus modified peptides was analysed. Phe-Tyr and Phe-Tyr-NH_2 transport was measured electrophysiologically in PepT1 expressing *Xenopus laevis* oocytes.

4.2 Responses induced by Phe-Tyr in PepT1 expressing oocytes

Preliminary experiments were carried out using a single saturating concentration of the parent peptide, Phe-Tyr. The PepT1 expressing oocytes were subjected to pulses of 1mM Phe-Tyr at both pH 7.5 and 5.5 and two-electrode voltage clamps were carried out once steady state was reached. The membrane was held at –50 mV and stepped to test voltages of +50mV to –150mV in 10mV increments. Table 4.1 shows the experimental protocol in detail.

Figure 4.1 shows the voltage trace recorded throughout the whole experiment. The voltage changes upon addition of peptide substrate can be clearly seen with a greater depolarisation recorded at pH 5.5, a value of 62mV compared with 33mV at pH 7.5. In a series of experiments the values obtained were 60 ± 10.5mV and 35 ± 8mV, mean ± s.e.m, n = 10, at pH 5.5 and 7.5 respectively.

The steady state I-V curves recorded are shown in figure 4.2a and b. Maximal current values were observed at –150mV at both pH values and for all oocytes tested. The data represented are that of one oocyte, but a similar result was observed for all oocytes.

The I_{max} values obtained at pH 7.5 were 248 ± 11.2nA compared with 446.8 ± 12.7nA at pH 5.5, mean ± s.e.m, n = 10. These results were expected since there was a greater inward proton driving force at pH 5.5, thus greater transport of peptide was observed.

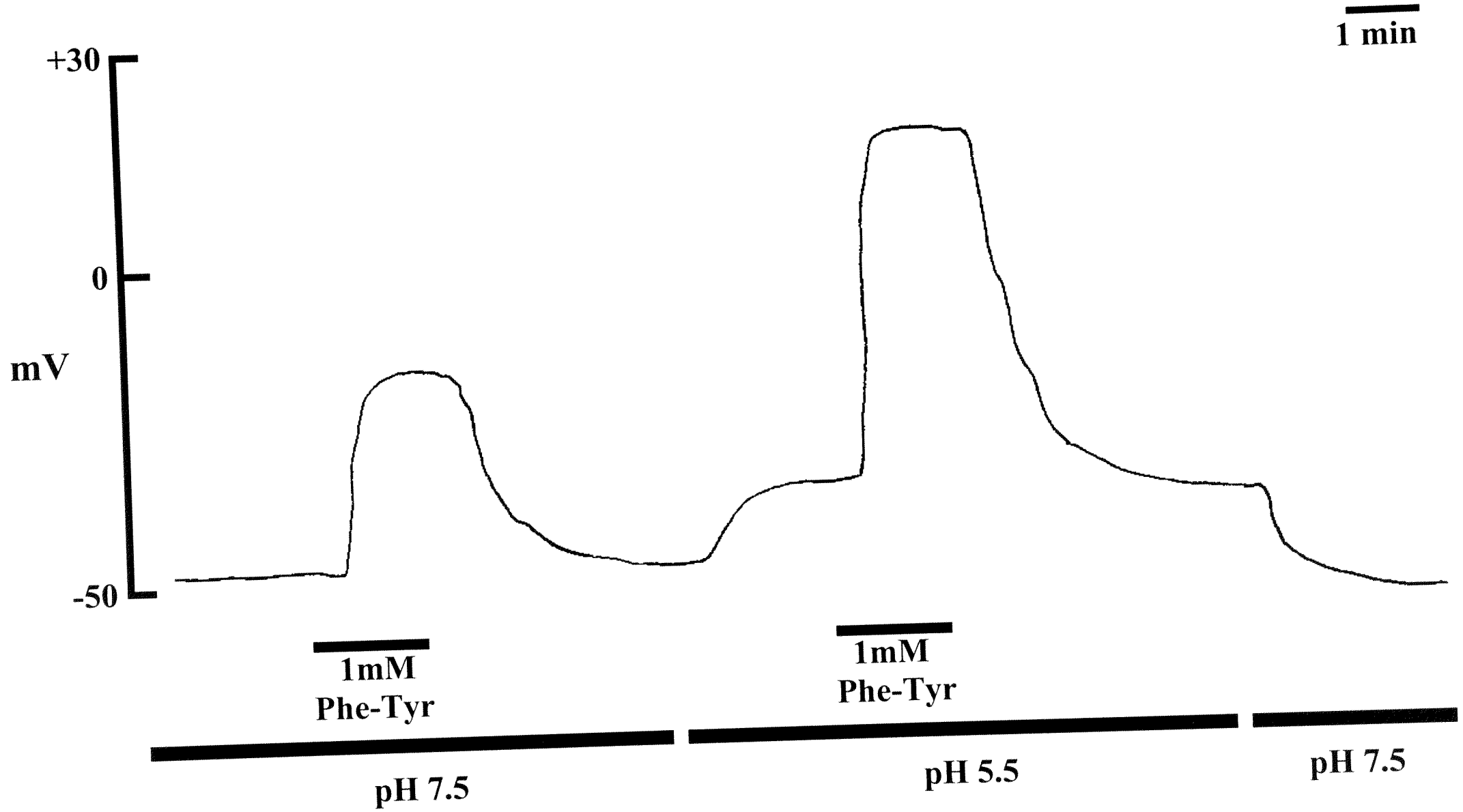
4.3 Responses induced by Phe-Tyr in control oocytes

Control experiments were carried out in water injected oocytes to ensure that all the currents recorded were due to the PepT1 cRNA injected into the oocytes, and not due

Step	Condition
1	pH 7.5 uptake
2	pH 7.5 uptake + 1mM Phe-Tyr
3	pH 7.5 uptake
4	pH 5.5 uptake
6	pH 5.5 uptake + 1mM Phe-Tyr
7	pH 5.5 uptake
8	pH 7.5 uptake

Table 4.1 Experimental protocol for the effect of a single saturating concentration of neutral parent peptide at pH 7.5 and pH 5.5. The same protocol was employed to study transport of Phe-Tyr-NH_2.

Figure 4.1. Voltage trace recorded in response to 1mM Phe-Tyr in a PepT1 expressing oocyte. A continuous voltage recording was made of an experiment with incubations in solutions of pH 7.5 and 5.5, with and without peptide substrate. Steady state I-V curves were carried out immediately before application of substrate, during substrate application and finally after once the substrate had been removed from the media.


1 min
+30
0
mV
-50
1mM
Phe-Tyr
1mM
Phe-Tyr
pH 7.5
pH 5.5
pH 7.5

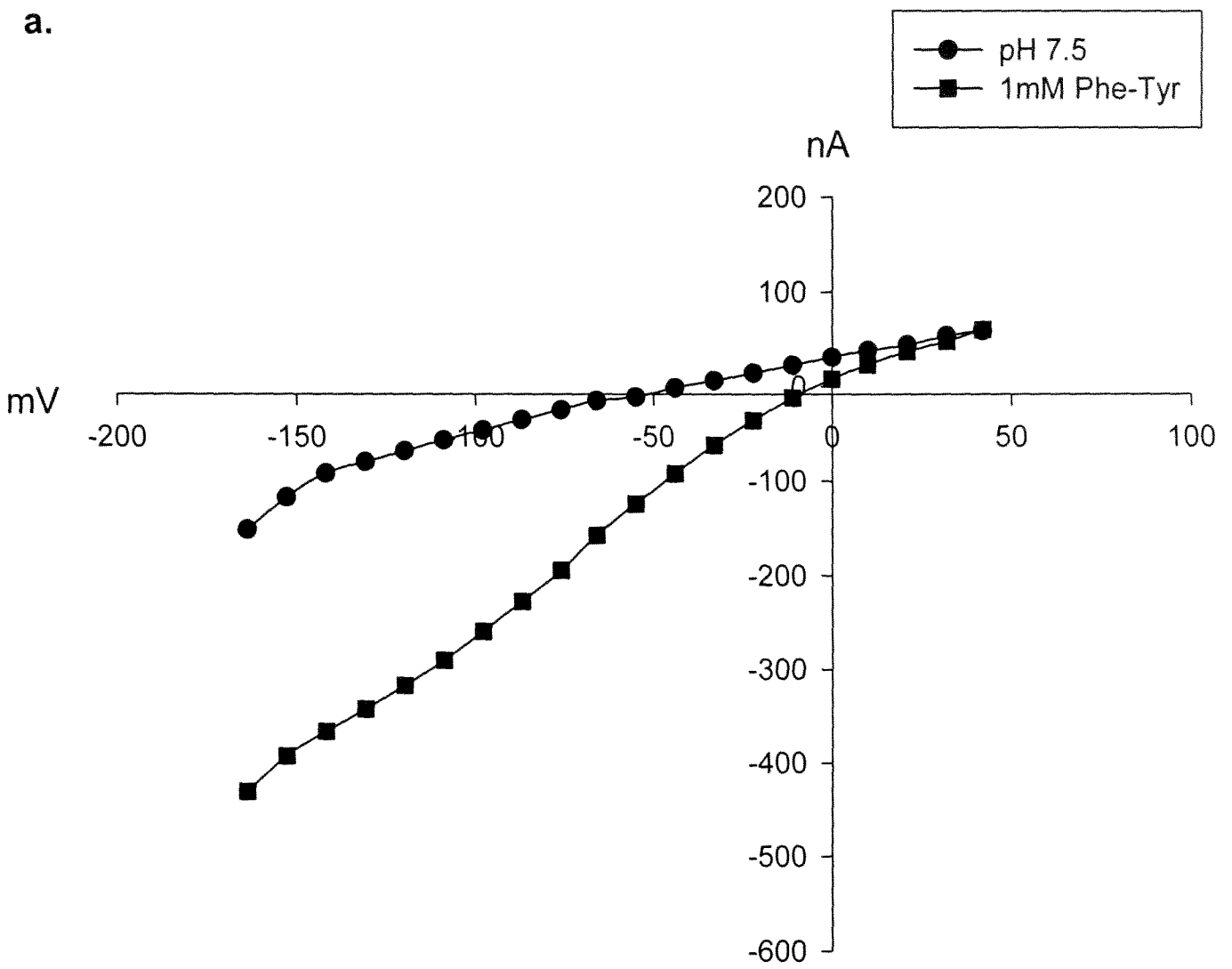


Figure 4.2a. Steady state I-V curves recorded in a PepT1 expressing oocyte in the presence and absence of 1mM Phe-Tyr, at pH 7.5.

b.

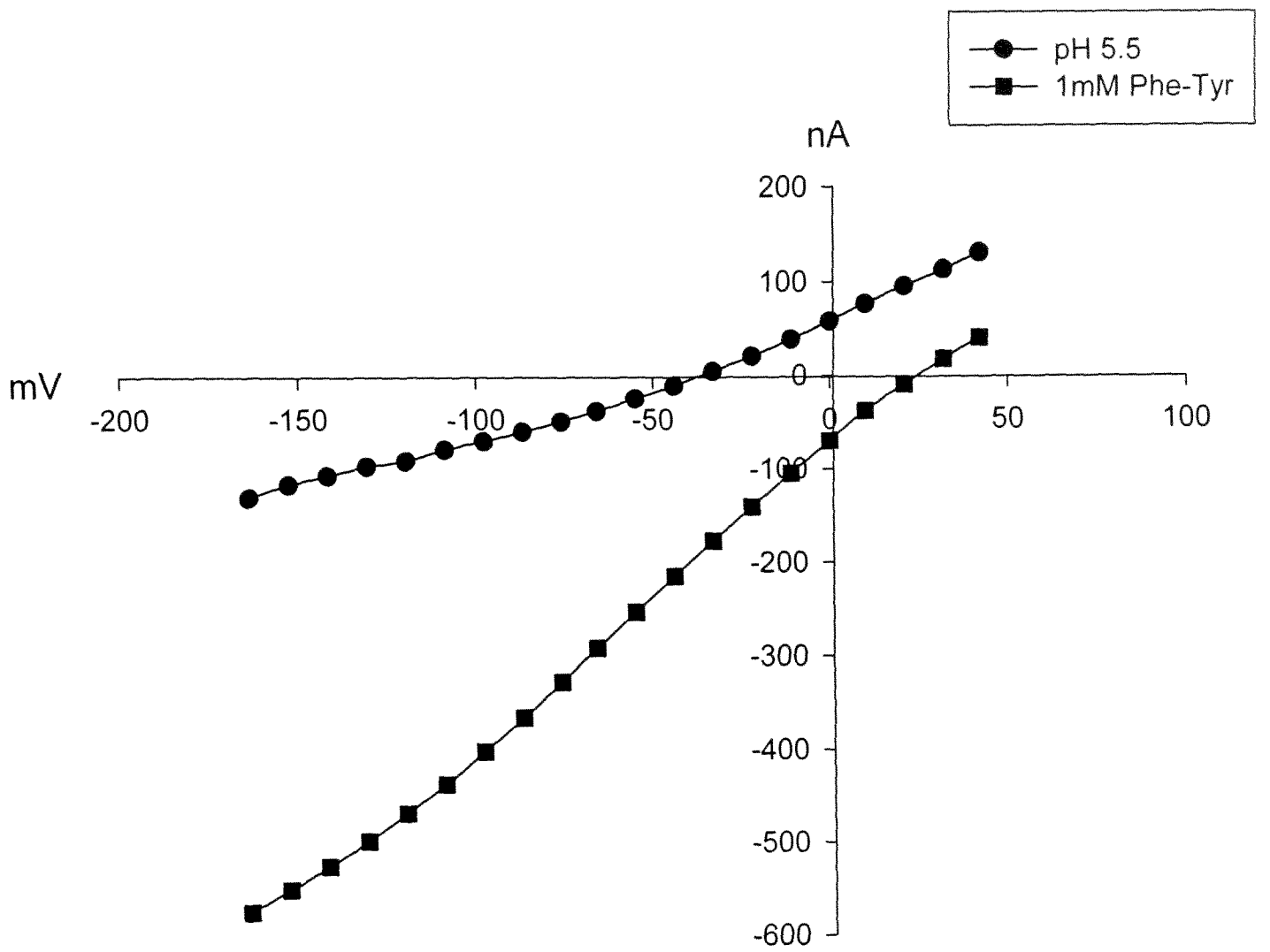


Figure 4.2b. Steady state I-V curves recorded in a PepT1 expressing oocyte in the presence and absence of 1mM Phe-Tyr, at pH 5.5.

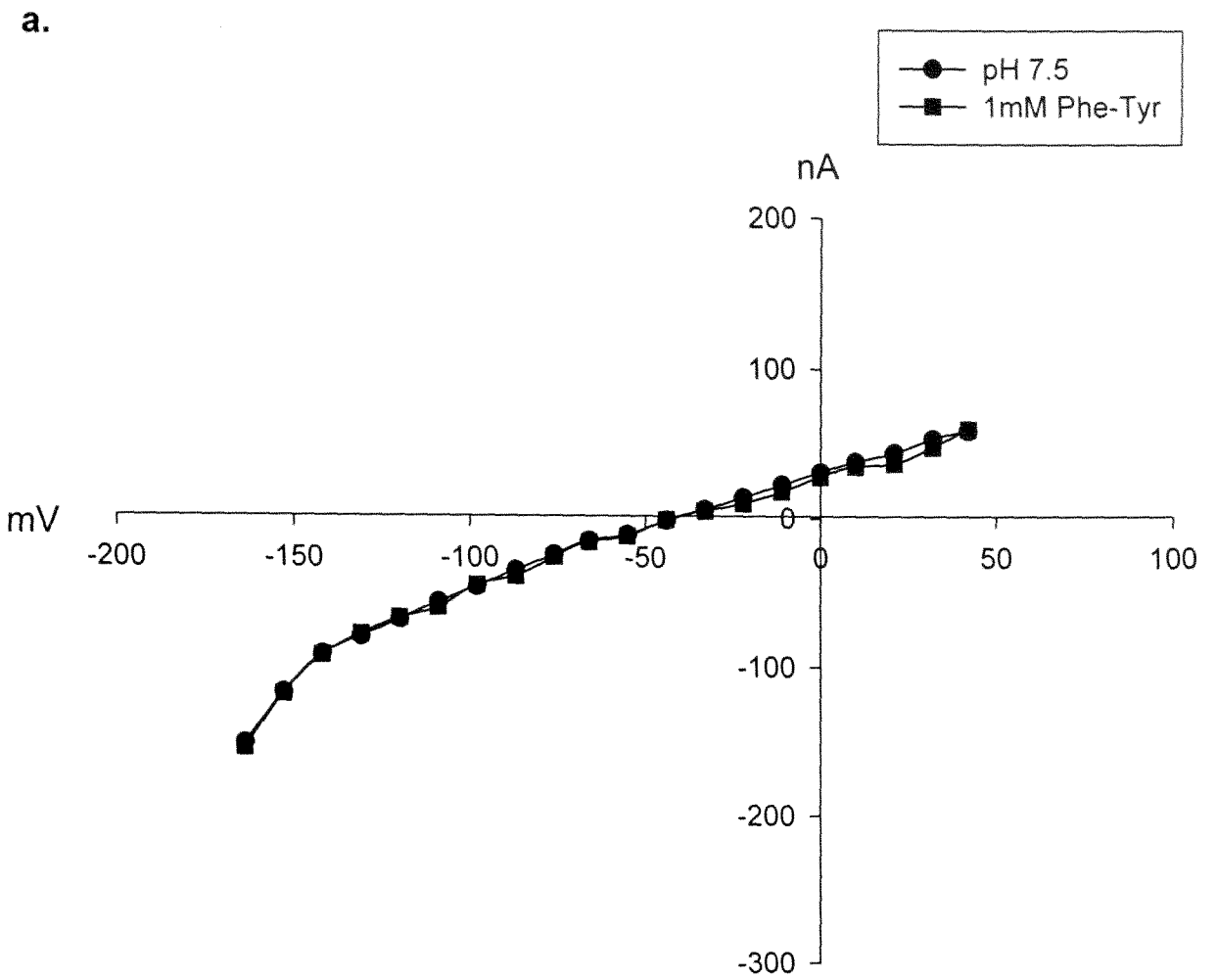


Figure 4.3a. Steady state I-V curves recorded in a control oocyte in the presence and absence of 1mM Phe-Tyr, at a. pH 7.5 and b. at pH 5.5.

to endogenous PepT1 transport. The steady state I-V curves showing no peptide-induced transport in these oocytes are seen in Figure 4.3a and b.

4.4 Responses induced by Phe-Tyr-NH_2 in PepT1 expressing oocytes

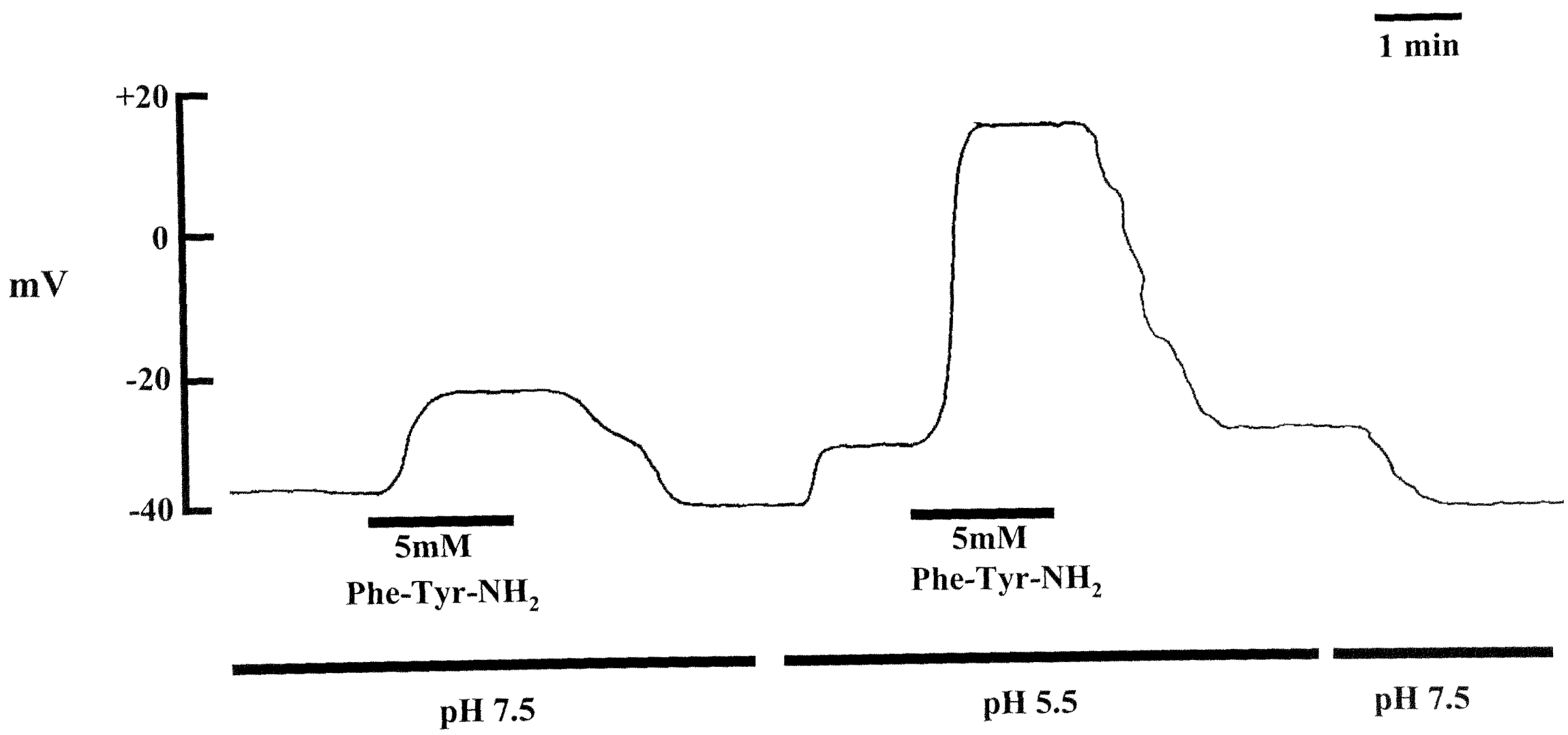
Similar experiments were carried out using a single saturating concentration of the modified peptide, Phe-Tyr-NH_2. The PepT1 expressing oocytes were subjected to pulses of 5mM Phe-Tyr-NH_2 at both pH 7.5 and 5.5 and two-electrode voltage clamps were carried out once steady state was reached. The electrophysiological protocol was identical to that stated in section 4.2, as was the experimental protocol, with the exception of the higher concentration of peptide being used.

Figure 4.4 shows the voltage trace recorded throughout the whole experiment. The changes to membrane potential upon addition of peptide substrate can be clearly seen, with greater depolarisations recorded at pH 5.5, values of 50 ± 7.5mV compared with 20 ± 6.5mV at pH 7.5, mean ± s.e.m, n = 10.

The steady state I-V curves recorded are shown in figure 4.5a and b. Maximal current values were observed at –150mV, as before. The data presented are that of one oocyte, but are representative of all oocytes tested.

The I_{max} values obtained at pH 7.5 were 118.8 ± 9nA compared with 302.2 ± 15.2nA at pH 5.5, mean ± s.e.m, n = 10. These results were expected since there was a greater inward proton driving force at pH 5.5, thus greater peptide induced currents were observed.

Figure 4.4. Voltage trace recorded in response to 5mM Phe-Tyr-NH_2 in a PepT1 expressing oocyte. A continuous voltage recording of an experiment was made with incubations in solutions of pH 7.5 and 5.5, with and without peptide substrate. Steady state I-V curves were carried out immediately before application of substrate, during substrate application and finally after the substrate had been removed from the media.


1 min
+20
0
mV
-20
-40
5mM
Phe-Tyr-NH2
5mM
Phe-Tyr-NH2
pH 7.5
pH 5.5
pH 7.5

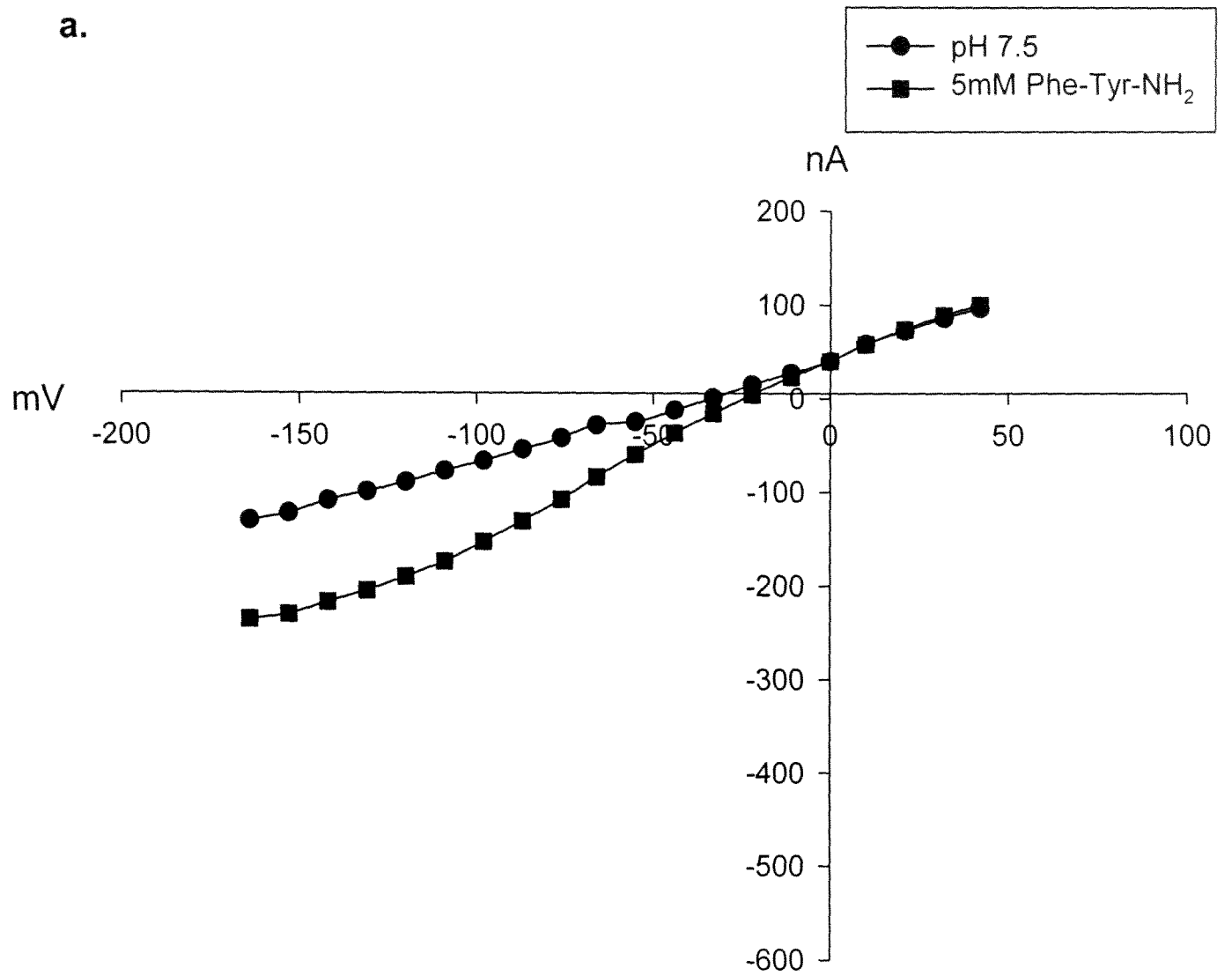


Figure 4.5a Steady state I-V curves recorded in a PepT1 expressing oocyte in the presence and absence of 5mM Phe-Tyr-NH_2, at pH 7.5.

b.

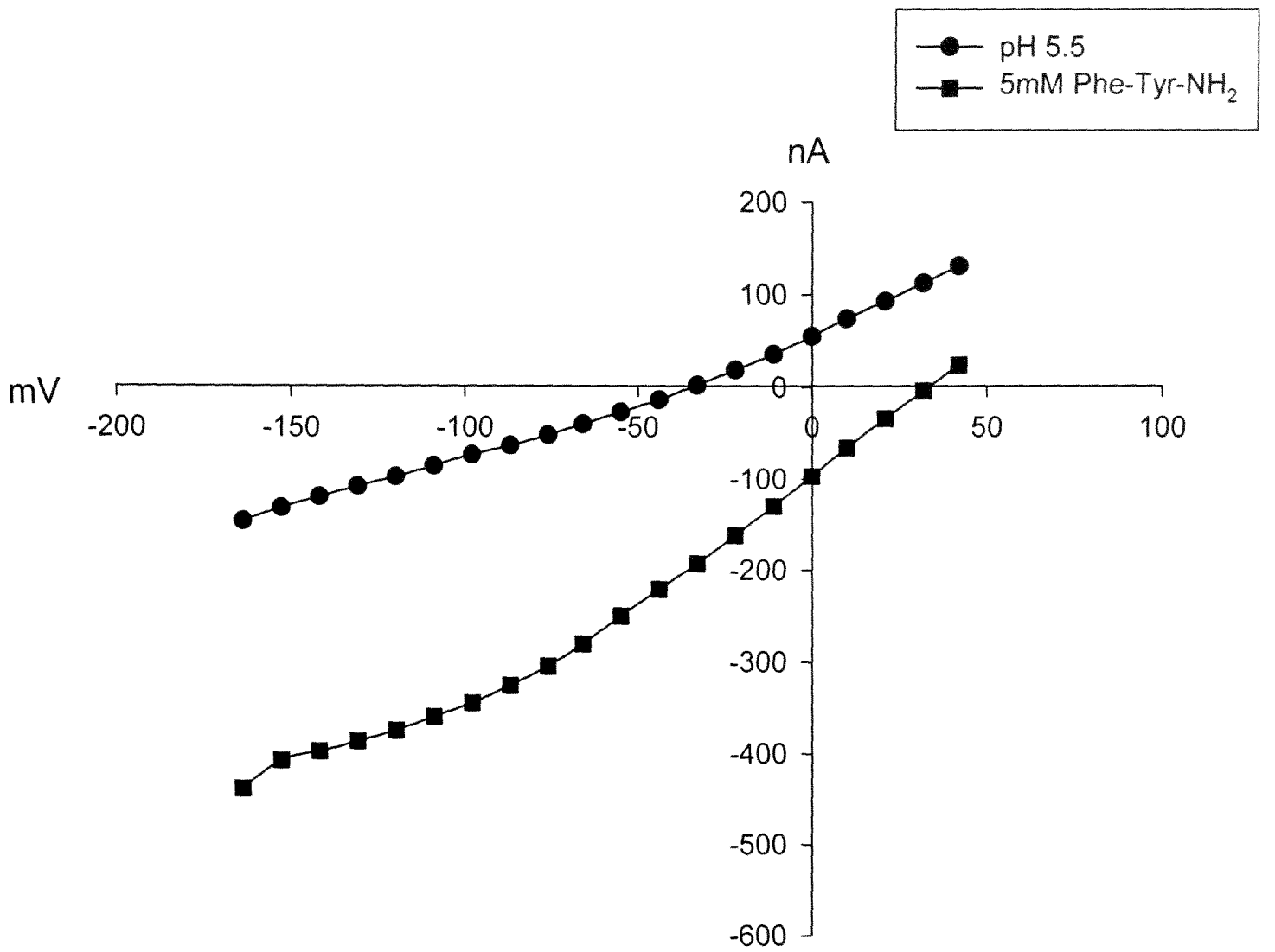


Figure 4.5b Steady state I-V curves recorded in a PepT1 expressing oocyte in the presence and absence of 5mM Phe-Tyr-NH_2, at pH 5.5.

4.5 Responses induced by Phe-Tyr-NH_2 in control oocytes

Again control experiments were carried out in water injected oocytes to ensure that the currents recorded were not due to endogenous PepT1 transport. There were no peptide-induced currents, as was the case with Phe-Tyr, (data not shown).

4.6 Comparison of responses induced by Phe-Tyr and Phe-Tyr-NH_2

The results presented in the previous sections for Phe-Tyr and Phe-Tyr-NH_2 provided evidence that the parent peptide was a better substrate for PepT1 than the modified molecule in agreement with Meredith *et al,* 2000. The currents evoked at both pH 7.5 and 5.5 were greater for Phe-Tyr than for Phe-Tyr-NH_2; 248.2 ± 11.2 compared to 118.8 ± 9nA at pH 7.5 and 446.8 ± 12.7nA compared to 302.2 ± 15.2 at pH 5.5, mean ± s.e.m, n = 10. This data shows a two-fold reduction in transport of Phe-Tyr-NH_2 compared to Phe-Tyr at pH 7.5 and a 1.5-fold reduction at pH 5.5.

However, the transport of both of the peptides was classical with the greatest transport seen at the more acidic pH, since there is a greater H^+ concentration gradient driving transport.

4.7 Dose-response curves of Phe-Tyr and Phe-Tyr-NH_2 transport

The two-electrode voltage clamp was employed in PepT1 expressing oocytes to record peptide-induced currents in response to increasing concentrations of Phe-Tyr and the modified Phe-Tyr-NH_2.

Steady state I-V curves were measured in response to both peptides at pH 7.5 and 5.5. The membrane potential was held at –50mV and stepped to test voltages between +50 and –150mV in 10mV increments. The concentrations of Phe-Tyr used were 0.03,

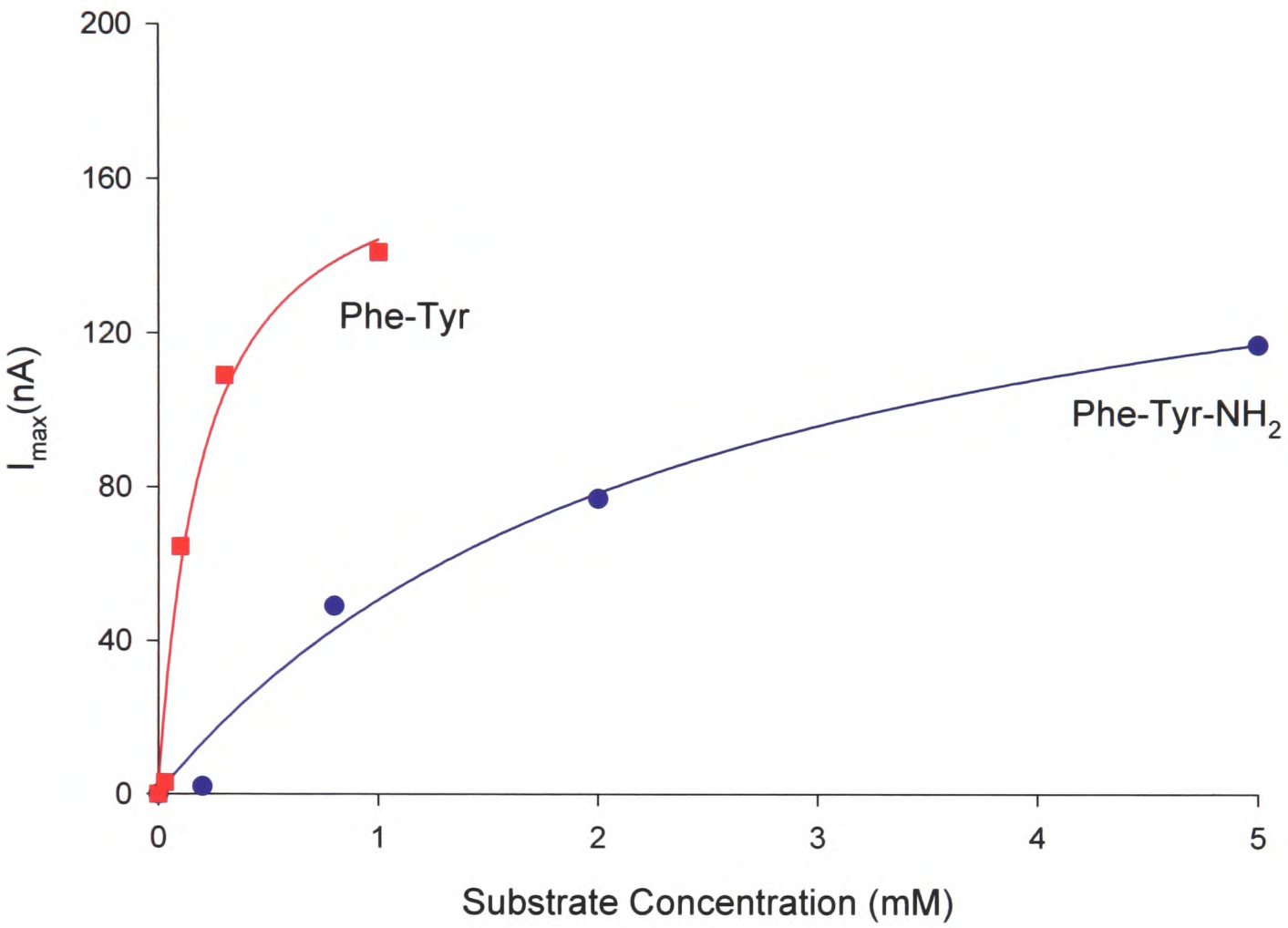


Figure 4.6 I_{max} for the peptide-induced currents at pH_o 7.5 (-150mV) were plotted as a function of substrate concentration for Phe-Tyr and Phe-Tyr-NH_2. Solutions contained in mM: NaCl 95, KCl 2, $CaCl_2$ 1, $MgCl_2$ 1, HEPES 20, pH adjusted with Tris.

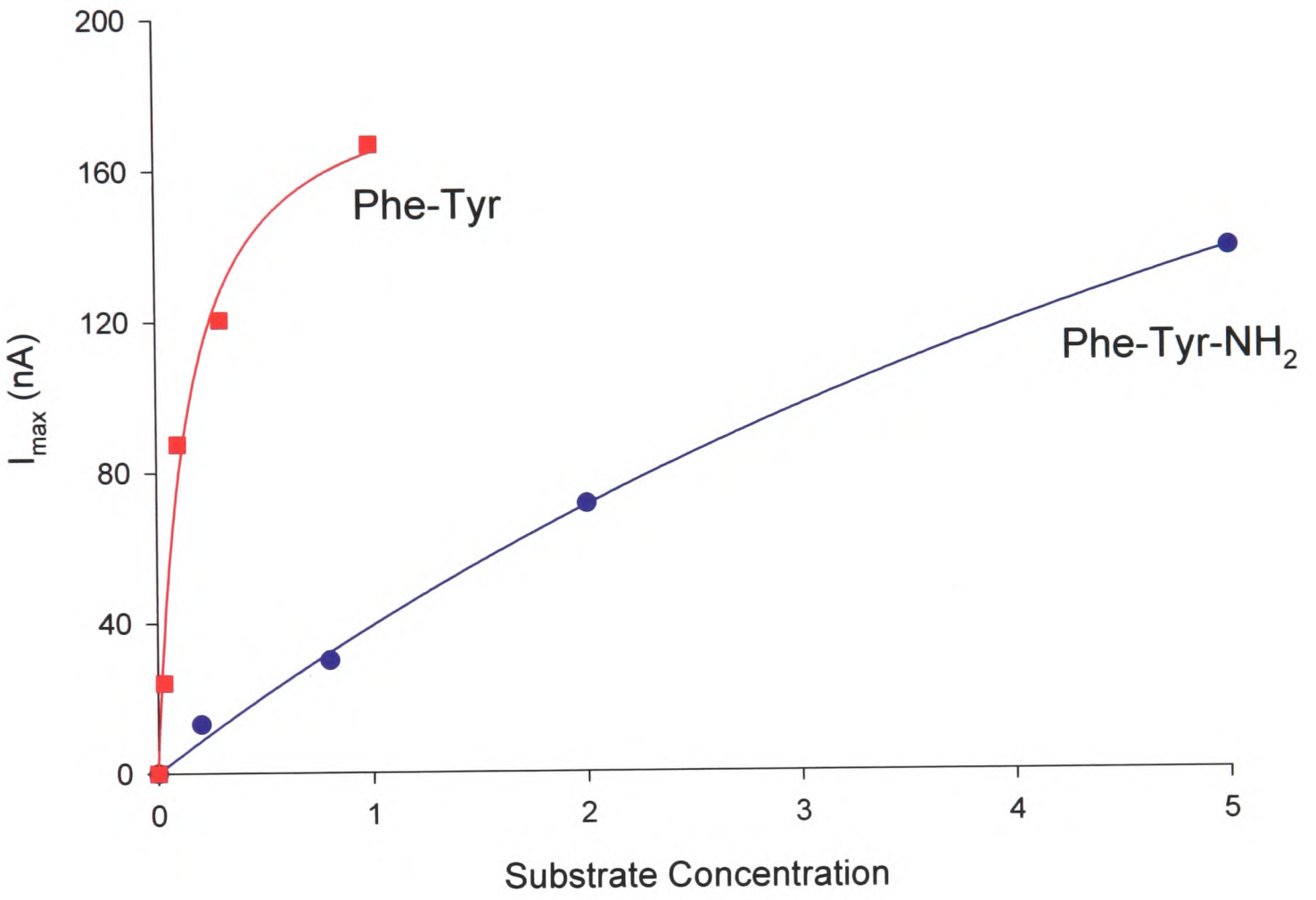


Figure 4.7 I_{max} for the peptide-induced currents at pH_o 5.5 (-150mV) were plotted as a function of substrate concentration for Phe-Tyr and Phe-Tyr-NH_2. Solutions contained in mM: NaCl 95, KCl 2, $CaCl_2$ 1, $MgCl_2$ 1, MES 20, pH adjusted with Tris.

Substrate	**pH**	**K_a (mM) ± s.e.m**
Phe-Tyr	7.5	0.59 ± 0.10
Phe-Tyr-NH_2	7.5	5.50 ± 1.60
Phe-Tyr	5.5	0.14 ± 0.03
Phe-Tyr-NH_2	5.5	5.25 ± 2.80

Substrate	**pH**	**I_{max}(nA) ± s.e.m**
Phe-Tyr	7.5	143 ± 29.47
Phe-Tyr-NH_2	7.5	92 ± 35.05
Phe-Tyr	5.5	232.5 ± 48.25
Phe-Tyr-NH_2	5.5	142 ± 32.20

Table 4.2 K_a and I_{max} values for Phe-Tyr and Phe-Tyr-NH2 at pH 7.5 and 5.5 in PepT1 expressing oocytes. Data presented are mean ± s.e.m, n = 5.

0.1, 0.3, and 1mM, and the concentrations of Phe-Tyr-NH_2 used were 0.2, 0.8, 2,and 5mM. All solutions were made up in uptake solution at pH 7.5 and 5.5.

Figure 4.6 and 4.7 show the dose response curves recorded at each pH for both peptides. Table 4.2 shows the values obtained for K_a and I_{max} for both of the peptide substrates at each pH.

Inward currents were observed for both substrates at pH 7.5 and pH 5.5. I_{max} values for Phe-Tyr and Phe-Tyr-NH_2 were 143 ± 29.47nA and 92 ± 35.05nA at pH 7.5; and 232.5 ± 48.25nA and 142 ± 32.20nA at pH 5.5 (± s.e.m n = 5).

The affinity for modified peptide was approximately 10 fold lower than for the free dipeptide, 0.59 ± 0.1mM compared with 5.5 ± 1.6mM at pH 7.5; and 0.14 ± 0.03mM and 8.8 ± 1.8mM at pH 5.5 (mean ±s.e.m, n = 5). Extracellular acidification substantially increased the affinity for Phe-Tyr. An increase in affinity was seen from 0.59 ± 0.1mM to 0.14 ± 0.03mM. Extracellular acidification appeared to have no similar effect on the affinity for Phe-Tyr-NH_2, (no significant difference using Students *t* test).

The finding that the affinity for Phe-Tyr-NH_2 did not increase upon external acidification suggested that the free carboxyl group of the substrate was involved in the protonation interaction with the PepT1 binding site (Bailey *et al*, 2000).

4.8 Template binding model for PepT1

At present there is no 3D structure for PepT1, but there is data available on several hundred substrates. Bailey *et al,* (2000), used this information to create a general

model for the affinity/transport of substrates. This binding template model was based on the binding and transport of nearly all of the published substrates whether obtained from brush border membrane vesicles, oocytes or intact rat jejunum. See figure 4.8. The template model has four main features, (Meredith *et al*, 2000), not including conformational requirements. They are as follows:

1. Glu_{595} secures the N terminus of the peptide.

2. A hydrogen bond stabilises the first peptide bond.

3. The first peptide bond can be *N*-alkylated, but the side chain of the residue must occupy a critical binding region.

4. A histidine residue could be involved here to account for the additional proton cotransported with Xaa-Glu peptides.

5. The C terminus binds to a positively charged site, perhaps protonated His_{57}, which provides hydrogen bonding potential for dipeptide amines.

This model for substrate binding takes into account the features of the PepT1 protein as seen in chapter 1 (Fig. 1.5) as well as the data obtained for the substrate binding and transport, and gives a valuable insight into how substrates interact with the transporter protein.

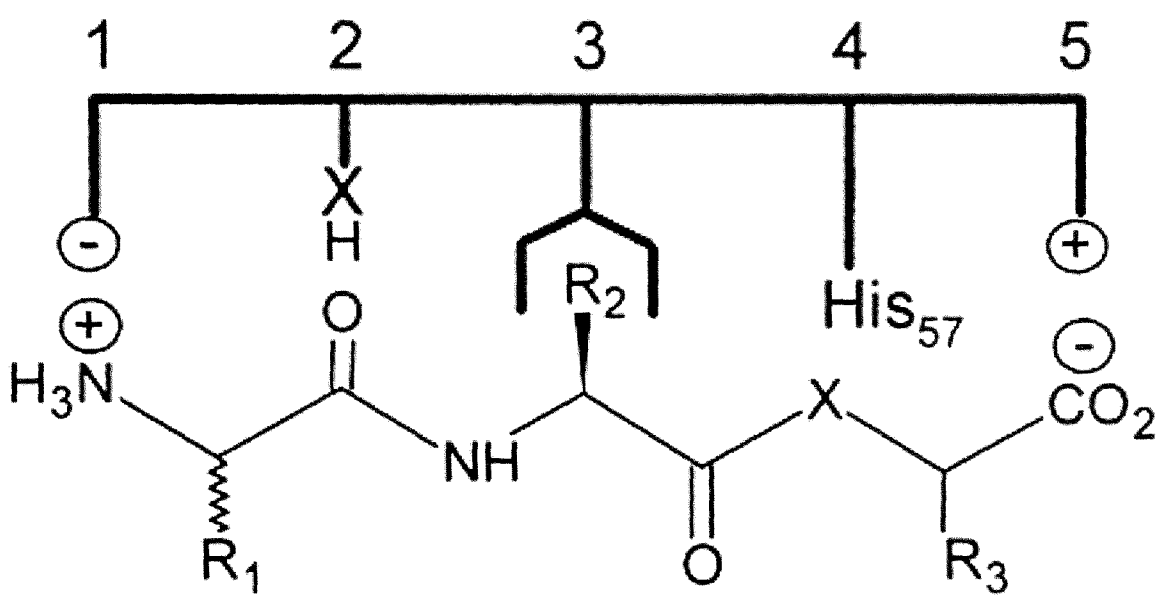


Figure 4.8 A model for substrate binding to PepT1 devised by Bailey *et al* and re-drawn from Meredith *et al, Eur. J. Biochem*, 2000.

4.9 Summary of Chapter

1. Phe-Tyr and Phe-Tyr-NH_2 were substrates for PepT1 and their transport was dependent on both membrane potential and pH_o.

2. The affinity for Phe-Tyr-NH_2 was approximately 10 fold lower than for the native dipeptide.

3. Extracellular acidification from pH 7.5 to pH 5.5 increased the affinity for Phe-Tyr six fold, but had no effect on the affinity for Phe-Tyr-NH_2.

4. The results suggest that the free carboxyl group of the unmodified substrate was involved in the protonation interaction with the PepT1 binding site (Bailey *et al* 2000).

CHAPTER 5

SUBSTRATE TITRATION IS NOT SOLELY RESPONSIBLE FOR THE EFFECT OF pH ON CHARGED PEPTIDE BINDING

5.1 Introduction

PepT1 displays a broad substrate range including neutral and charged dipeptides (Amasheh *et al*, 1997). However, the exact mechanism by which PepT1 transports charged peptides remains controversial. The study by Amasheh *et al* investigated transport characteristics of a neutral peptide, Gly-Gln, compared to those carrying a charge. Their study included the anionic dipeptide, Gly-Asp and the cationic peptide, Gly-Lys. Their transport characteristics were recorded in four different solutions ranging from pH 5.5-pH 8.0. These studies showed that maximal transport of the neutral dipeptide occurred at pH 6.5, compared to pH 8.0 for the cationic peptide and pH 5.5 for the anionic peptide. Clearly the charge on the peptide alters the characteristics of transport. However, in this study it was not investigated if the position of charge was an important factor in dipeptide recognition and transport by PepT1, as all the charged amino acid residues were at the amino terminal.

In this study we have investigated the importance of position of charge within a dipeptide using the anionic peptides Gly-Asp and Asp-Gly, and preliminary experiments have been carried out using the cationic peptides Gly-Lys and Lys-Gly.

5.2 Response to Gly-Asp and Asp-Gly by PepT1 expressing oocytes

Preliminary experiments were carried out using a single saturating concentration of the charged peptides, in this case 2mM. Experiments were carried out at both pH 5.5 and 7.5, and two-electrode voltage clamps were carried out once steady state had been reached. The membrane was held at –50 mV and stepped to test voltages of +50mV to –150mV in 10mV increments. In each case the charged peptide responses were bracketed with a pulse of 2mM Gly-Gln, to ensure the effects recorded were real. Table 5.1 shows the experimental protocol in detail. The charged peptides were introduced to the oocytes in the order shown in the table, and also in the opposite order, with the Asp-Gly pulse first. Changing the order in which the oocytes experience the peptides had no effect on the results observed.

5.3 Response to Gly-Asp and Asp-Gly at pH 7.5

See Figure 5.1 for the steady state I-V curves obtained by a pulse of each of the charged peptides at pH 7.5.

The maximal currents for all peptides were recorded at –150mV with the largest currents being evoked in response to the neutral peptide Gly-Gln. Average currents of 420.2 ± 12.2nA were recorded in response to the first pulse of Gly-Gln. In comparison, maximum currents induced by 2mM Gly-Asp were 55.7 ± 18.6nA and by 2mM Asp-Gly, 120.0 ± 15.7nA. Average currents induced in response to the second pulse of Gly-Gln were 415.4 ± 10.0. All data are quoted as mean ± s.e.m, $n = 7$. All values were statistically significant from each other with $P < 0.01$ in all cases as determined by the Students *t* test, see table 5.2.

Step	Condition
1	pH 7.5 uptake
2	pH 7.5 uptake + 2mM Gly-Gln
3	pH 7.5 uptake
4	pH 7.5 uptake + 2mM Gly-Asp
5	pH 7.5 uptake
6	pH 7.5 uptake + 2mM Asp-Gly
7	pH 7.5 uptake
8	pH 7.5 uptake + 2mM Gly-Gln

Table 5.1 Experimental protocol for the effect of a single saturating concentration of neutral and negatively charged peptides. The protocol was carried out at pH 7.5 (as shown), and also at pH 5.5.

The data for one oocyte were normalised. The maximal current from the first Gly-Gln pulse was set to 100% and the Gly-Asp and Asp-Gly and the second Gly-Gln pulse maximal currents were expressed as a percentage of this. The results of this can be seen in the bar chart, figure 5.2.

The Gly-Asp current was only 12.2% of the first Gly-Gln pulse, whereas the Asp-Gly current was 26.9% of the Gly-Gln pulse. The second Gly-Gln pulse was 99.8% of the first pulse. These values were representative of only one oocyte, but the same trend was found in all experiments. This trend was even the case when the oocyte experienced the charged peptides in the opposite order, i.e. when the Asp-Gly was introduced to the oocyte before the Gly-Asp.

pH 7.5

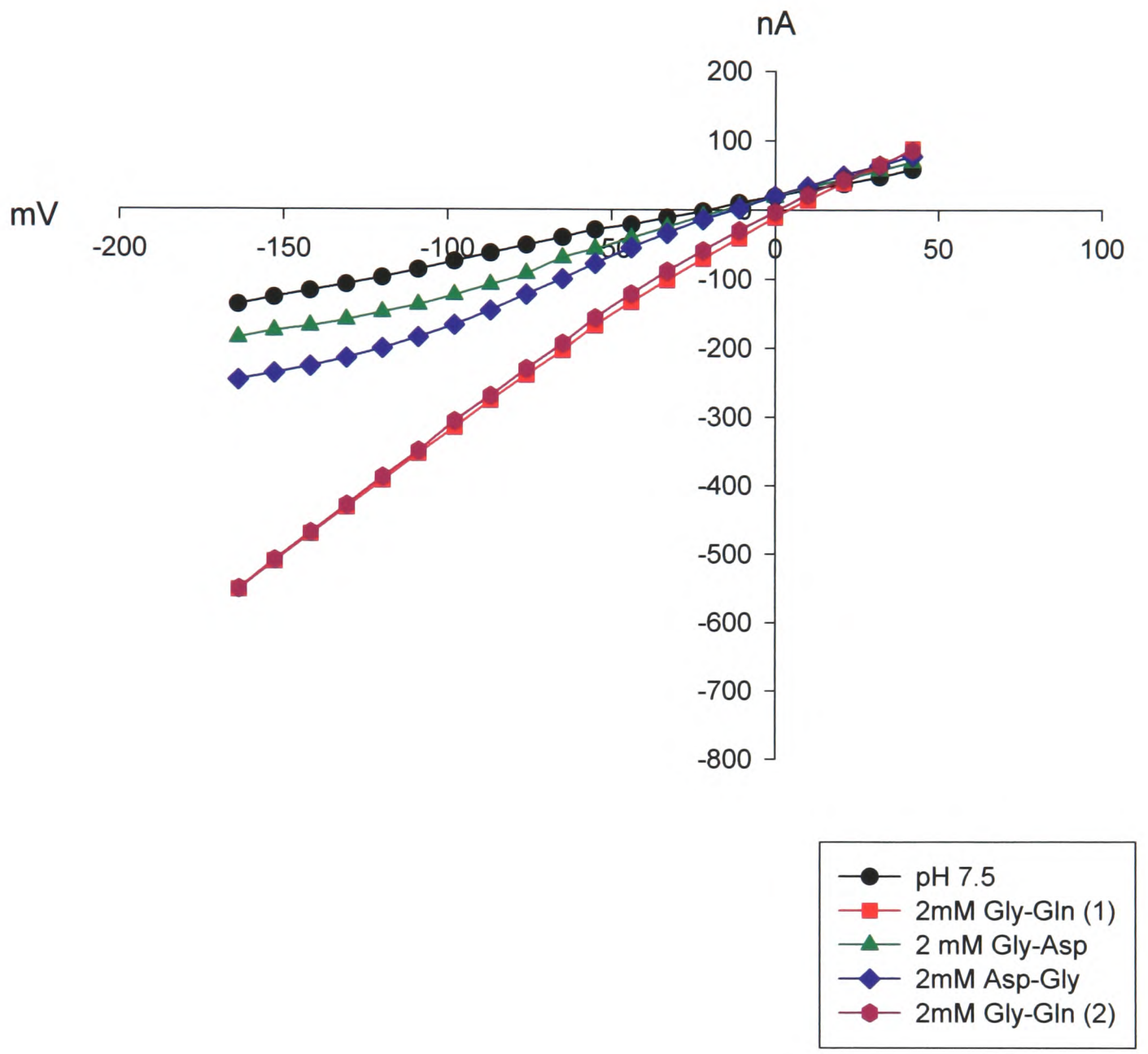


Figure 5.1 Steady state I-V curves recorded in PepT1 expressing oocytes in response to 2mM Gly-Asp and Asp-Gly, bracketed with two pulses of 2mM Gly-Gln, at pH 7.5.

Peptide	Maximal Current (nA)
Gly-Gln	420.2 ± 12.2
Gly-Asp	55.7 ± 18.6
Asp-Gly	120.0 ± 15.7
Gly-Gln	415.4 ± 10.0

Table 5.2 Maximal current values recorded in PepT1 expressing oocytes in response to 2mM Gly-Gln, Gly-Asp, Asp-Gly and then a second pulse of Gly-Gln at pH 7.5. Values are quoted as mean ± s.e.m, n=7.

pH 7.5

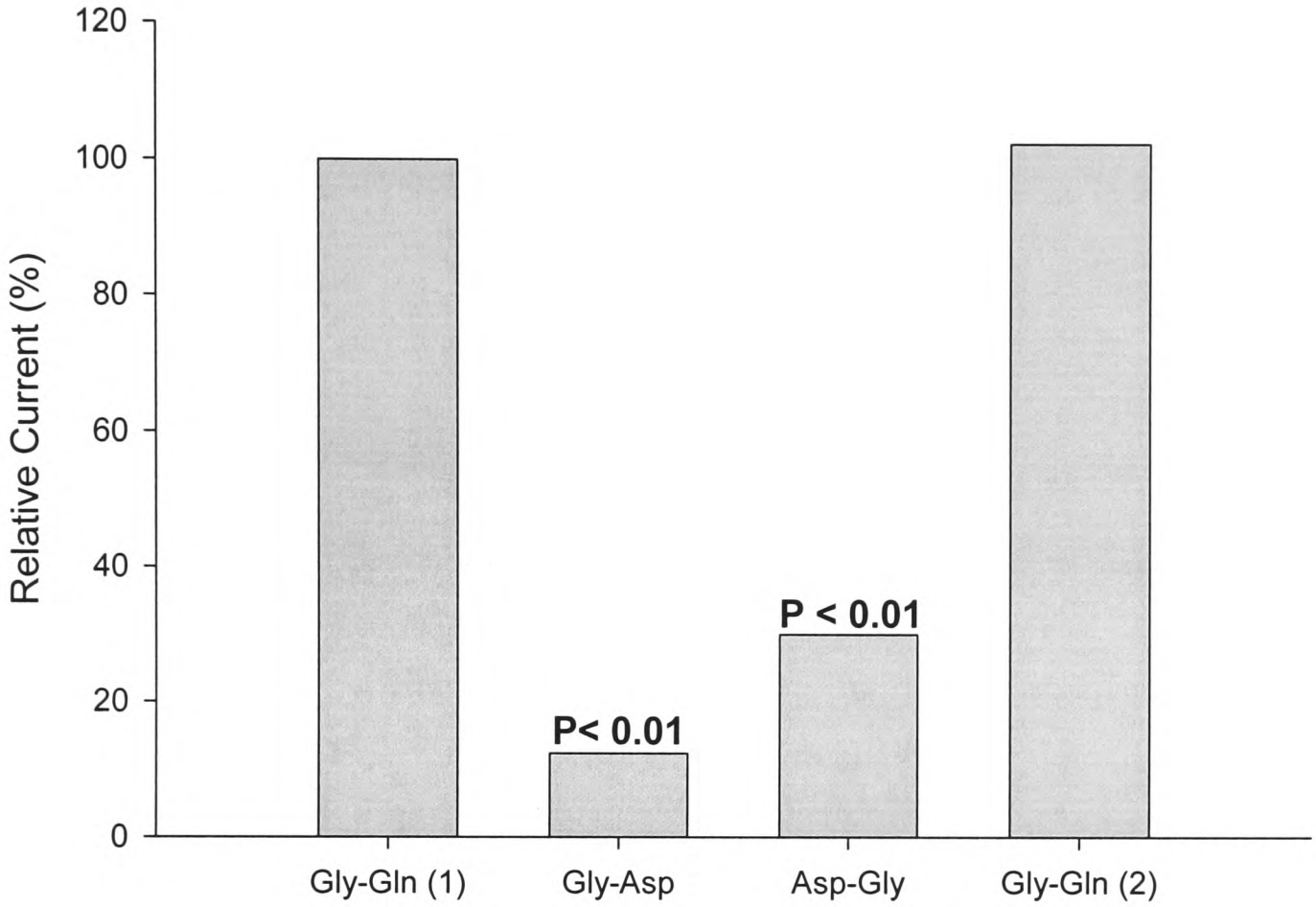


Figure 5.2 Relative currents induced by 2mM Gly-Asp, Asp-Gly and the second Gly-Gln pulse as a percentage of the first Gly-Gln pulse, at pH 7.5. Values for Gly-Asp and Asp-Gly are statistically significant, $P < 0.01$ as shown.

5.4 Response to Gly-Asp and Asp-Gly at pH 5.5 in PepT1 expressing oocytes

Again experiments were carried out using 2mM of both of the charged peptides. Two-electrode voltage clamps were carried out once steady state had been reached with the membrane held at –50 mV and stepped to test voltages of +50mV to –150mV in 10mV increments. As in the experiments carried out at pH 7.5, the charged peptide responses were bracketed with a pulse of 2mM Gly-Gln, to ensure the effects recorded were real.

Figure 5.3 shows the steady state I-V curves recorded in PepT1 expressing oocytes in response to 2mM Gly-Asp and Asp-Gly, compared to a pulse of Gly-Gln before and after.

The maximal currents in each case were observed at –150mV and again the largest response was evoked by 2mM Gly-Gln, with an average current of 591.5 ± 13.2nA being recorded. In comparison the charged peptide Gly-Asp elicited currents of 417.2 ± 8.5, an approximate reduction of 1.5 fold. The Asp-Gly however showed the most marked reduction compared to the Gly-Gln, with the average current observed being only 271.6 ± 15.1, an approximate 2.2 fold reduction. All data are quoted as mean ± s.e.m, $n = 7$. All values were statistically significant from each other with $P < 0.01$ in all cases as determined by the Students *t* test, see table 5.3.

The data for one oocyte were normalised by setting the Gly-Gln currents to 100% and the other values were expressed as a percentage of this to give the relative current (%), see figure 5.4.

The relative current for Gly-Asp was calculated to be 70.6% of the first Gly-Gln current, and the Asp-Gly current was 45.9%. The second Gly-Gln pulse evoked currents that were 99.8% of the first Gly-Gln pulse. As before, these values were representative of only one oocyte, but the same trend was found in all experiments. This was even the case when the oocyte experienced the charged peptides in the opposite order, i.e. when the Asp-Gly was introduced to the oocyte before the Gly-Asp.

pH 5.5

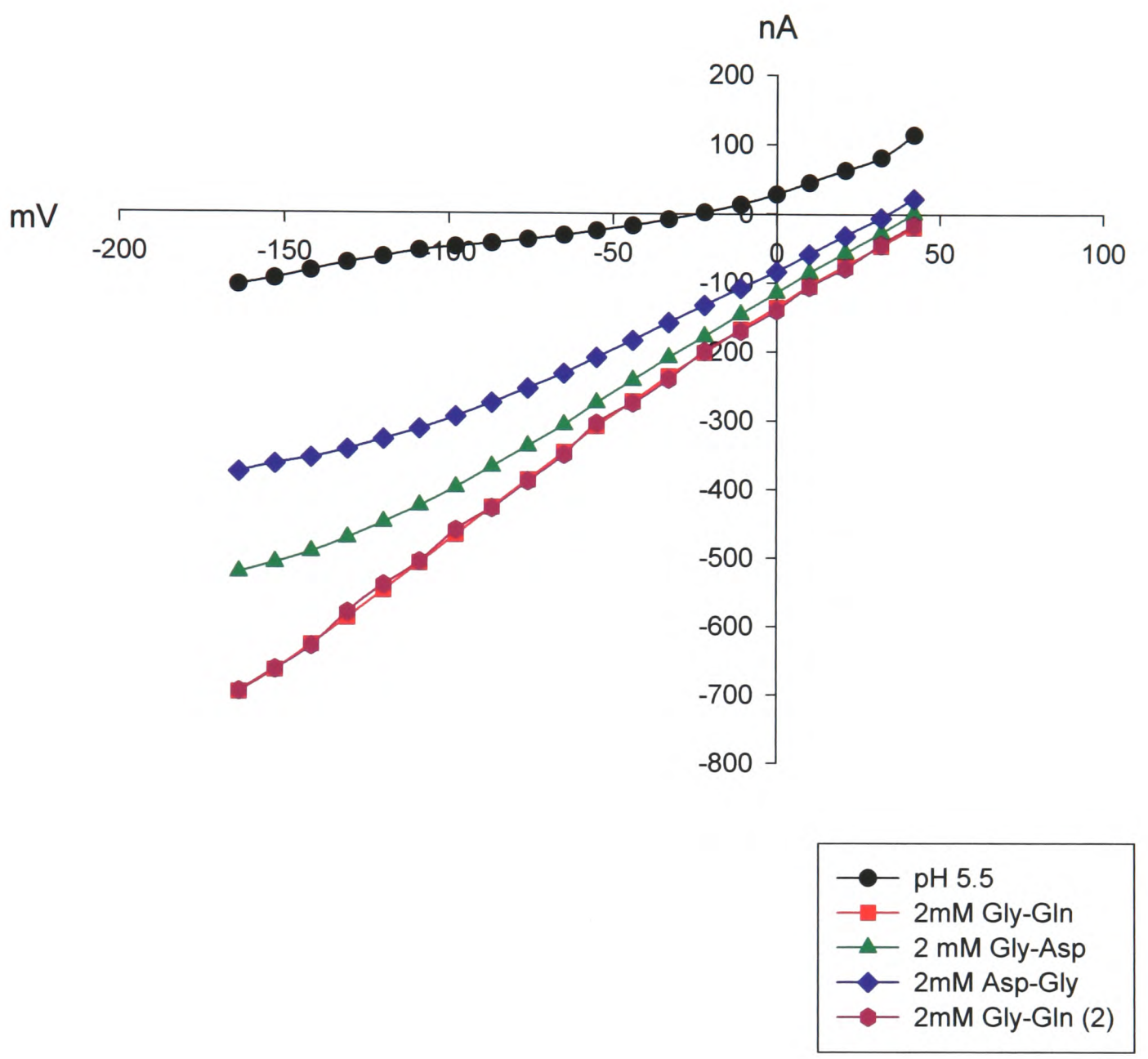


Figure 5.3 Steady state I-V curves recorded in PepT1 expressing oocytes in response to 2mM Gly-Asp and Asp-Gly, bracketed with two pulses of 2mM Gly-Gln, at pH 5.5.

Peptide	Maximal Current (nA)
Gly-Gln	591.5 ± 13.2
Gly-Asp	417.2 ± 8.5
Asp-Gly	271.6 ± 15.1
Gly-Gln	590.0 ± 11.7

Table 5.3 Maximal current values recorded in PepT1 expressing oocytes in response to 2mM Gly-Gln, Gly-Asp, Asp-Gly and then a second pulse of Gly-Gln at pH 5.5. Values are quoted as mean ± s.e.m, n=7.

pH 5.5

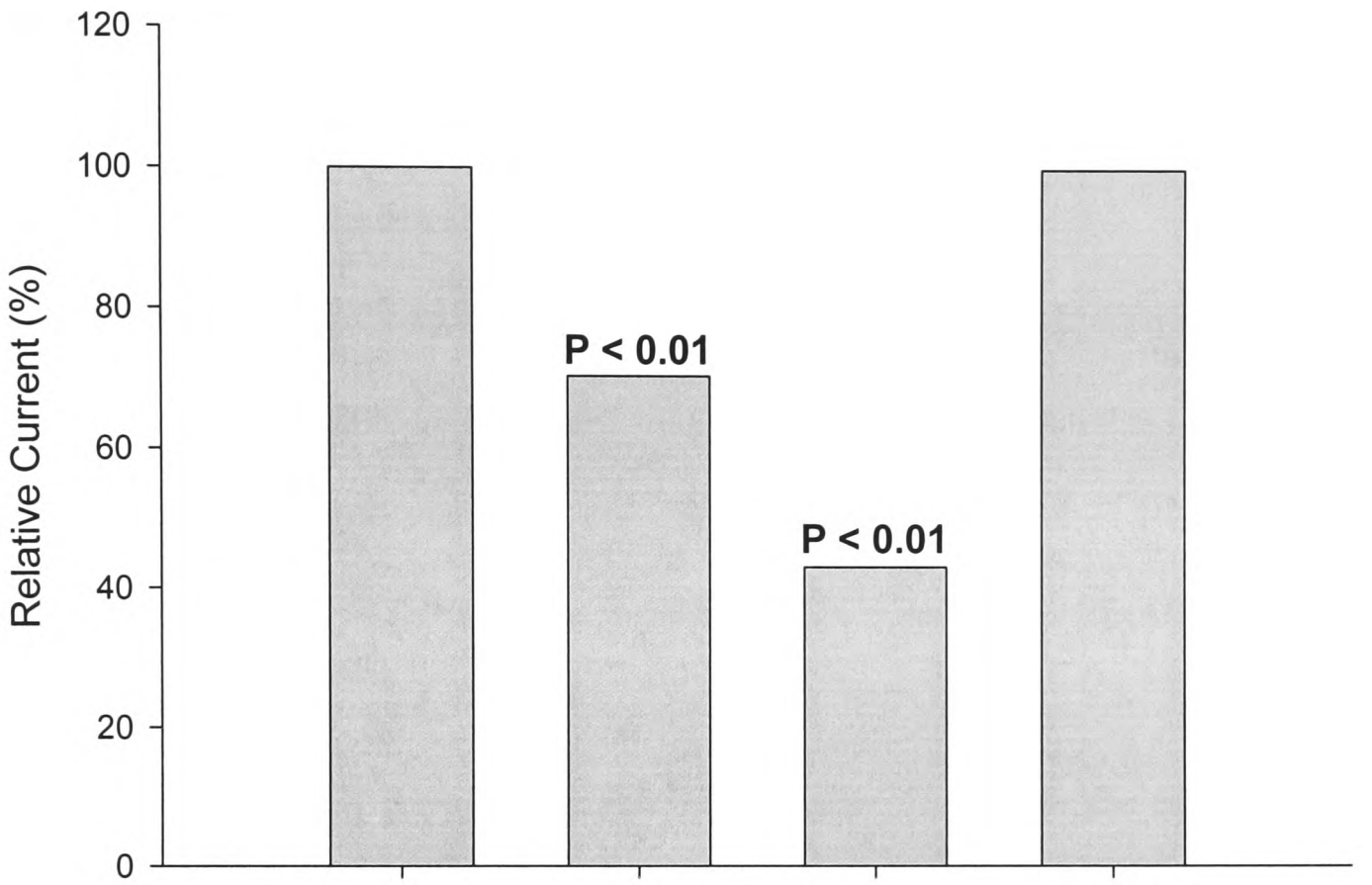


Figure 5.4 Relative currents induced by 2mM Gly-Asp, Asp-Gly and the second Gly-Gln pulse as a percentage of the first Gly-Gln pulse, at pH 5.5. Values for Gly-Asp and Asp-Gly are statistically significant, $P < 0.01$ as shown.

5.5 Comparison of Gly-Asp and Asp-Gly transport at pH 7.5 and 5.5

There were two main differences between the data obtained at pH 7.5 and pH 5.5. Firstly the currents evoked by Gly-Gln at pH 5.5 were 71% greater than those same currents evoked at pH 7.5, 591.5 ± 13.2nA compared to 420.2± 12.2. These results were what we would expect to obtain as there was a greater proton concentration gradient driving peptide transport at the more acidic pH.

The second major difference was based around the transport of the charged peptides. It is clear from the graphs and tables that Gly-Asp was transported to a higher degree at pH 5.5, with currents of 417.2 ± 8.5nA compared with 55.7 ± 18.6nA at pH 7.5. The transport of Asp-Gly was also greater at pH 5.5, but was 145nA less than that of the Gly-Asp at the same pH, however at pH 7.5 the transport of Asp-Gly was approximately 2 fold greater than Gly-Asp. Table 5.4 quotes the maximal currents for all peptides at both pH values.

5.6 Dose-response curves of Gly-Asp and Asp-Gly transport

The two-electrode voltage clamp was employed in PepT1 expressing oocytes to record peptide-induced currents in response to the charged peptides Gly-Asp and Asp-Gly.

Steady state I-V curves were measured in response to Gly-Asp and Asp-Gly at pH 7.5 and 5.5. Again the membrane potential was held at –50mV and stepped to test voltages between +50 and –150mV in 10mV increments. The concentrations of charged peptides used were 0.5, 1, 2, 5 and 10mM, all made up in uptake solution at pH 7.5 and 5.5. Maximal responses were not obtained at 10mM concentrations of

peptide substrate, but higher concentrations could not be obtained due to solubility constraints.

From this data, the maximal current evoked during the voltage clamp, in this case at –150mV, was plotted against the substrate concentration. This allowed estimation of the kinetic parameters of transport, K_a and I_{max}, and to observe how these parameters changed depending on the peptide substrate. Figures 5.5a and b shows the dose response curves recorded and the changes seen in K_a and I_{max}. Tables 5.5a and b shows the exact values for K_a and I_{max}.

At neutral extracellular pH, the I_{max} for Gly-Asp was 66 ± 9.25 compared to 417 ± 19.5nA at acidic pH, an approximate 6 fold increase in current. The transport of Asp-Gly was greater than Gly-Asp at pH 7.5 with maximal currents of 120 ± 15.1nA compared to 271 ± 17.3nA at pH 5.5 (mean ± s.e.m., n = 7). Although the currents for Asp-Gly were greater at pH 5.5, the maximal currents observed were only 65% of that obtained for the Gly-Asp.

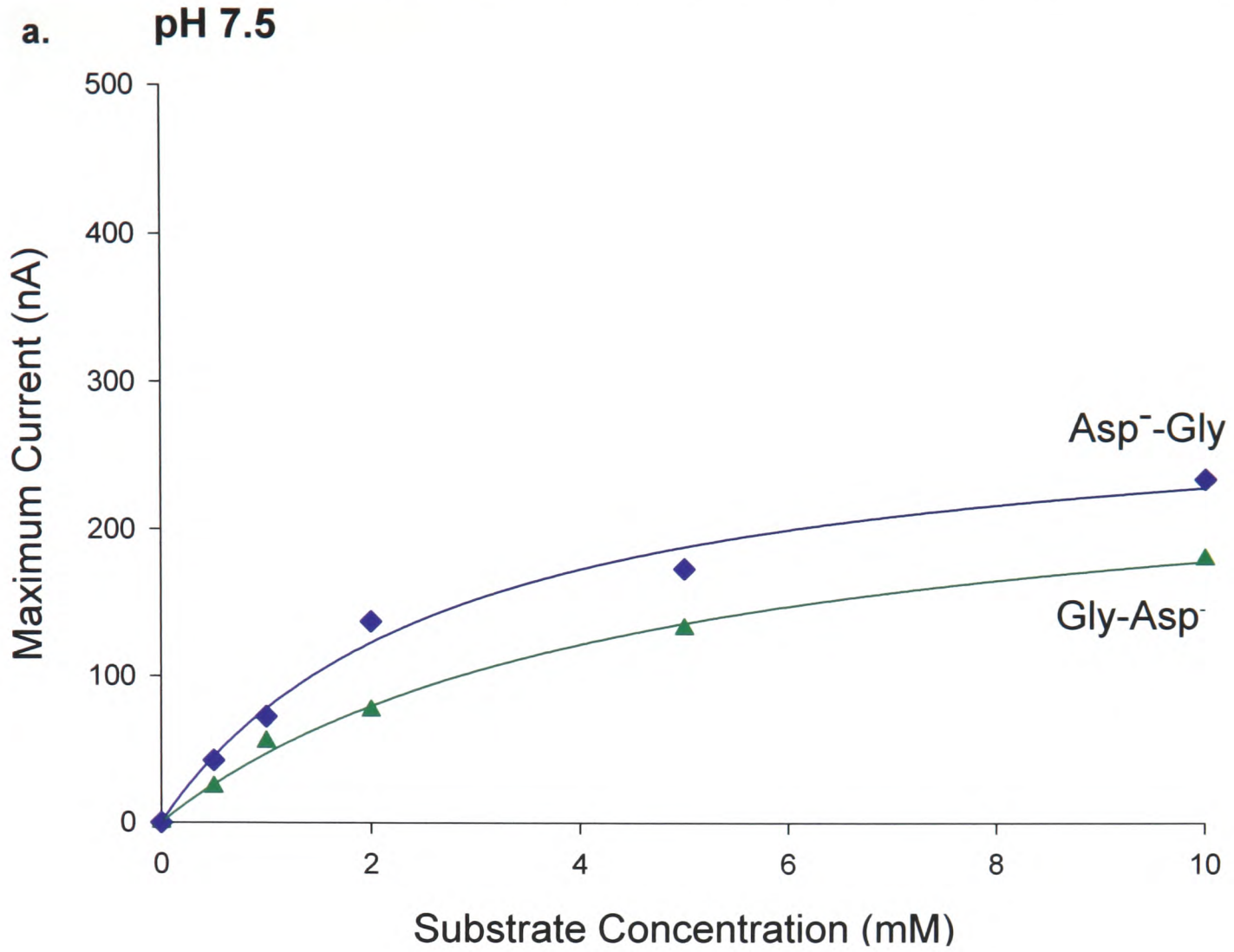
Upon extracellular acidification the affinity for Gly-Asp increased 5 fold, 7.96 ± 1.73mM at pH 7.5 compared with 1.50 ± 0.15mM at pH 5.5; whilst the affinity for Asp-Gly only increased 2-fold, 4.50 ± 0.82mM at pH 7.5 compared with 2.09 ± 0.15mM at pH 5.5 (mean ± s.e.m., n = 7).

The Gly-Asp/Asp-Gly affinity ratio at pH 7.5 was greater than 1, $P < 0.01$, whereas at pH 5.5 the ratio was less than 1, $P < 0.03$.

Since extracellular acidification reverses the order of affinity for the two peptides, the changes observed cannot simply be due to titration of the substrate. Therefore, it must be concluded that the position of the charged amino acid residue within the peptide determines how the transporter binds the peptide.

pH	2mM Gly-Gln (1^{st} pulse)	2mM Gly-Asp	2mM Asp-Gly	2mM Gly-Gln (2^{nd} pulse)
7.5	420.2 ± 12.2	55.7 ± 18.6	120.0 ± 15.7	415.4 ± 10.0
5.5	591.5 ± 13.2	417.2 ± 8.5	271.6 ± 15.1	590.0 ± 11.7

Table 5.4 Maximal current values in response to 2mM Gly-Gln, Gly-Asp, Asp-Gly and a second pulse of Gly-Gln at pH 7.5 and 5.5. Values are quoted as mean±s.e.m, n=7.



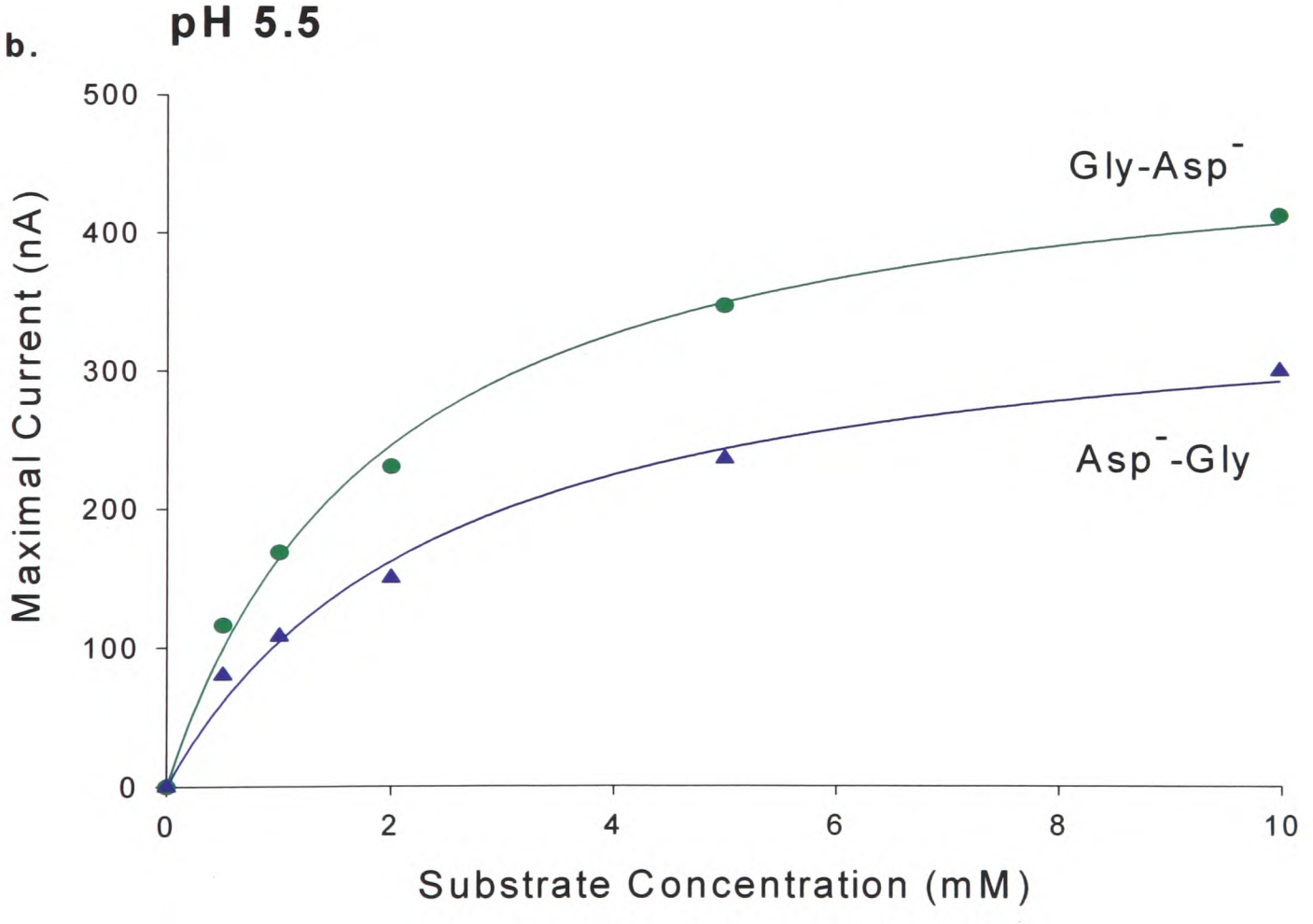


Figure 5.5 Dose-response curves for Gly-Asp and Asp-Gly at a. pH 7.5 and b. pH 5.5, recorded in PepT1 expressing oocytes, (data representative of one oocyte).

Substrate	pH	K_a (mM) ± s.e.m
Gly-Asp	7.5	7.96 ± 1.73
Asp-Gly	7.5	4.50 ± 0.82
Gly-Asp	5.5	1.50 ± 0.15
Asp-Gly	5.5	2.09 ± 0.15

a.

Substrate	pH	I_{max} (nA) ± s.e.m
Gly-Asp	7.5	66 ± 9.25
Asp-Gly	7.5	120 ± 15.1
Gly-Asp	5.5	417 ± 19.5
Asp-Gly	5.5	271 ± 17.3

b.

Table 5.5 a. K_a and b. I_{max} values for Gly-Asp and Asp-Gly at pH 7.5 and 5.5 in PepT1 expressing oocytes. Values quoted are mean ± s.e.m, n = 7.

5.7 Summary of Gly-Asp and Asp-Gly experiments

1. Gly-Asp and Asp-Gly were both substrates for PepT1.

2. Transport of both peptides was greater at pH 5.5 compared to pH 7.5.

3. The I_{max} of Asp-Gly was greater than Gly-Asp at pH 7.5, whereas the I_{max} of Gly-Asp was greater than Asp-Gly at pH 5.5.

4. The affinity of Asp-Gly was higher than Gly-Asp at pH 7.5 and the reverse was true for the same charged peptides at pH 5.5.

5. The apparent order of affinity reversed upon extracellular acidification, thus the position of charge within the peptide plays an important role in substrate binding.

5.8 Preliminary experiments with Gly-Lys and Lys-Gly

Following the findings from the experiments on anionic peptides, the transport of two cationic peptides were investigated. In these experiments the positively charged peptides Gly-Lys and Lys-Gly were used.

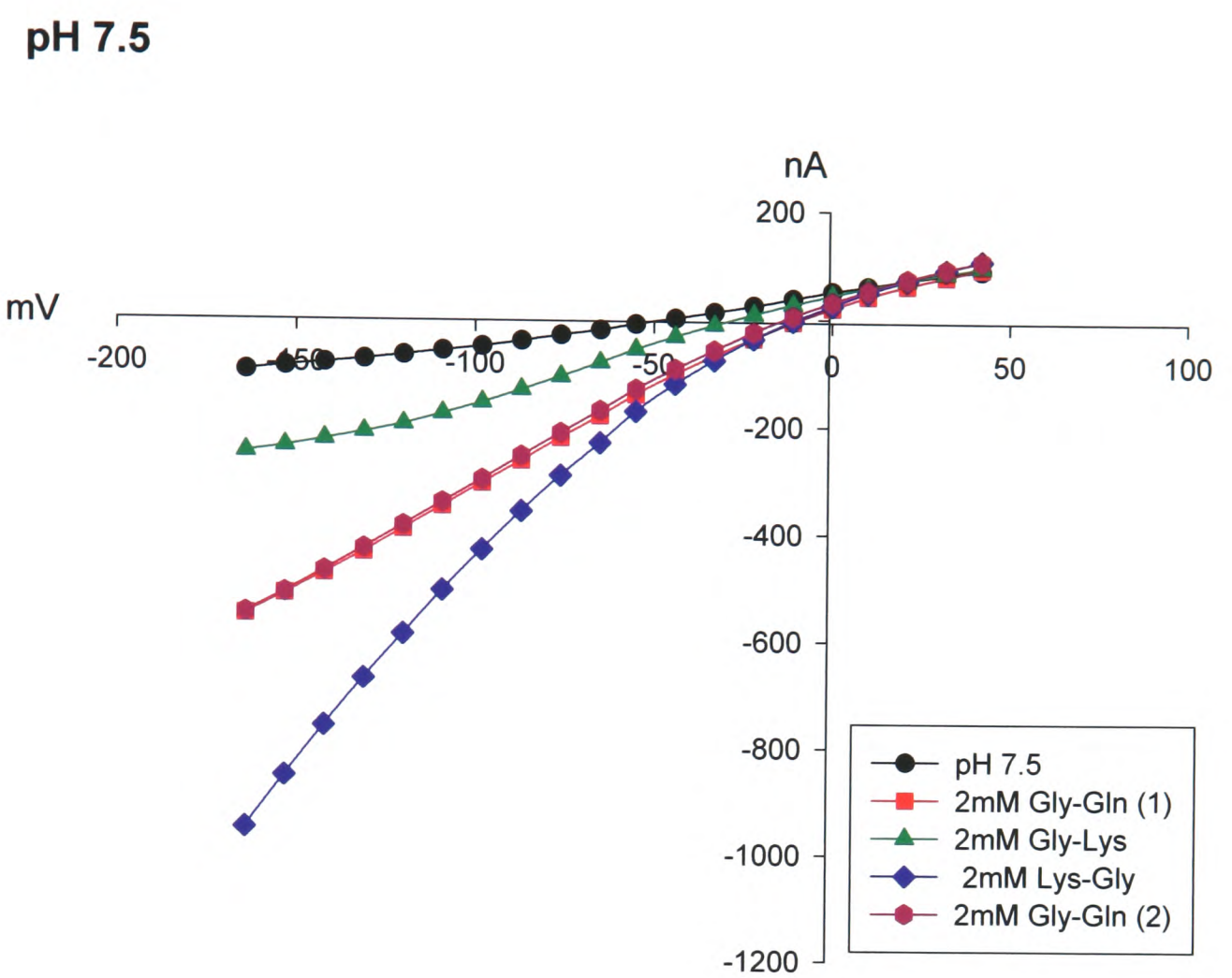
The two electrode voltage clamp was used as described earlier to characterise transport of these peptides at pH 7.5 and 5.5. A single saturating concentration of these peptides ,2mM, was used and steady state I-V recordings were carried out using PepT1 expressing *X.laevis* oocytes. As in the case of the anionic peptides, the pulses of Gly-Lys and Lys-Gly were bracketed with 2 pulses of Gly-Gln and the charged peptides were also introduced to the experimental system in both orders to detect any differences to the results obtained.

Figures 5.6 and 5.7 show the results obtained for both peptides, as compared to Gly-Gln, at pH 7.5 and 5.5.

Figure 5.6a shows the currents obtained during voltage clamp conditions of both Gly-Lys and Lys Gly. Maximal currents were obtained by 2mM Lys-Gly with values of 982 ± 16.0nA compared to 440 ± 19.6nA for Gly-Gln and 251 ± 11.2nA for Gly-Lys, mean ± s.e.m, n = 4.

The values for one oocyte were normalised, with the first pulse of Gly-Gln set to 100%, and all other values quoted as a percentage of this, see figure 5.6b. Clearly Lys-Gly is the best transported substrate with 186.7% of the transport of Gly-Gln, the 'model substrate'.

Figure 5.7a shows the curents obtained for these same substrates at pH 5.5. Maximal currents again were evoked by 2mM Lys-Gly, with values of 943 ± 17.3nA compared to 595 ± 30.0nA for Gly-Gln and 65 ± 24.6nA for Gly-Lys, mean ± s.e.m, n = 4. Figure 5.7b shows the normalised values for one oocyte expressed as a percentage of Gly-Gln transport, with Lys-Gly again evoking currents of 147.4% that of Gly-Gln.



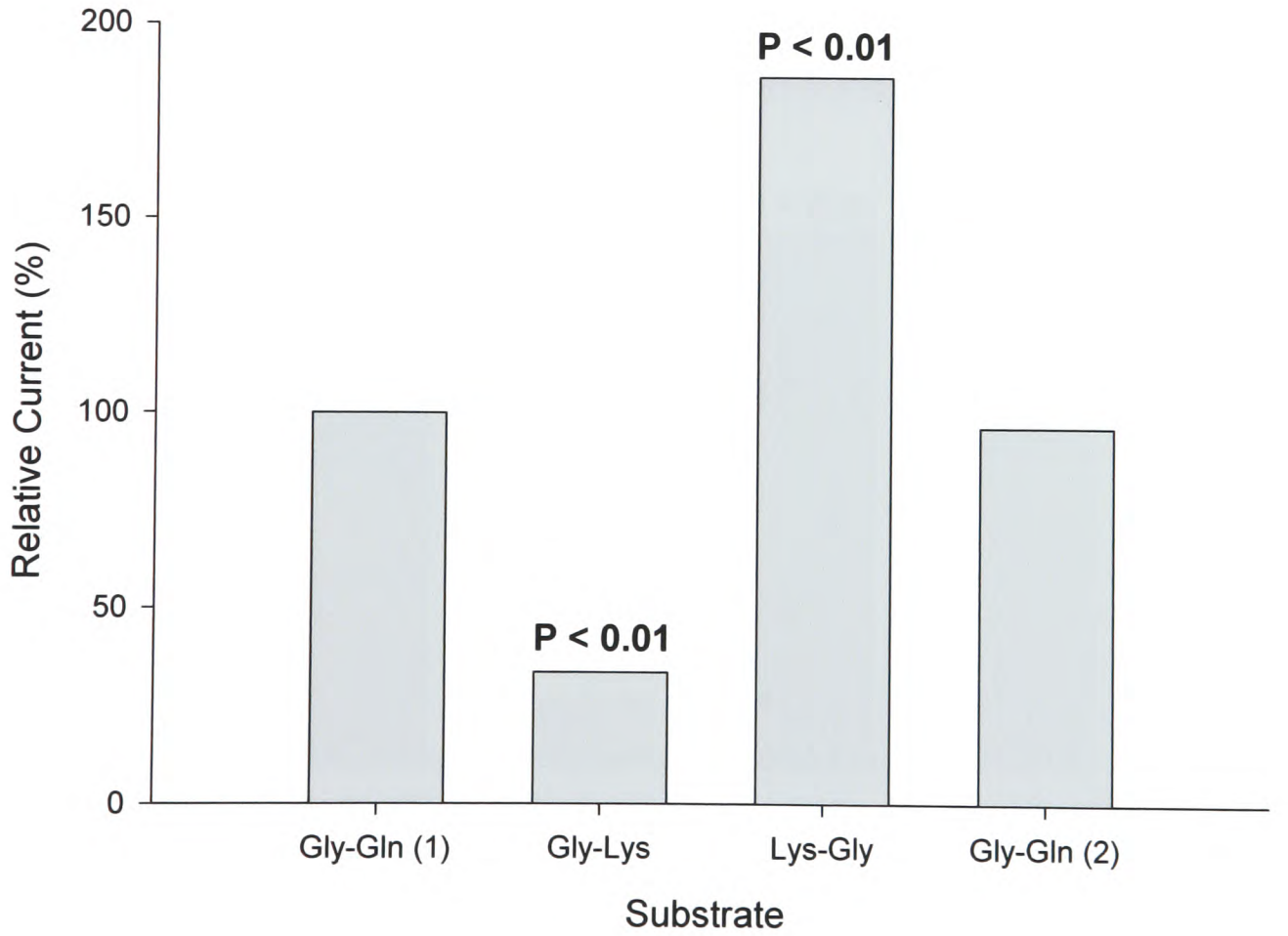
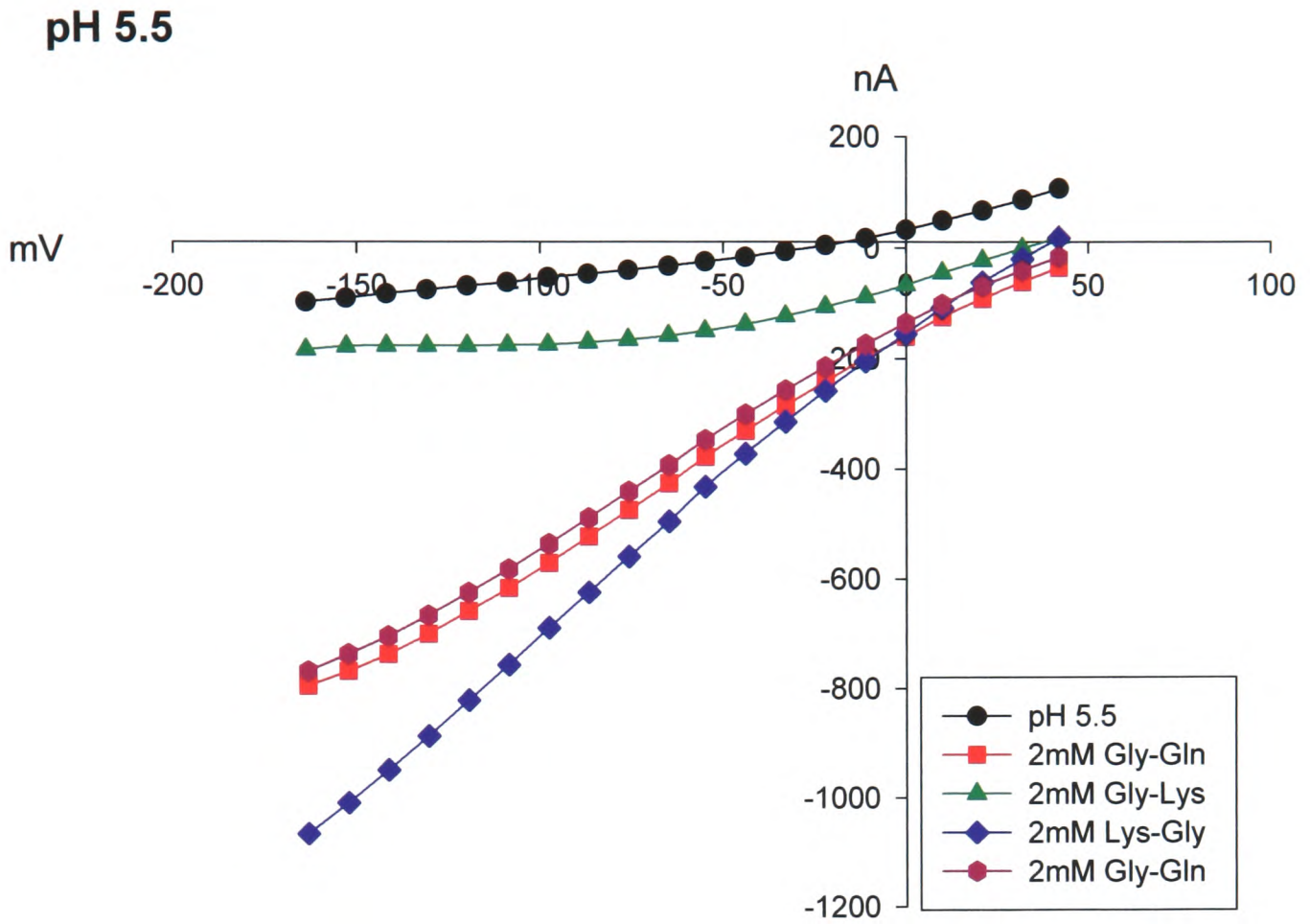


Figure 5.6. a. Steady state I-V curves in response to 2mM Gly-Lys and Lys-Gly, bracketed by 2mM Gly-Gln. b. Normalised values for I_{max}, at pH 7.5.



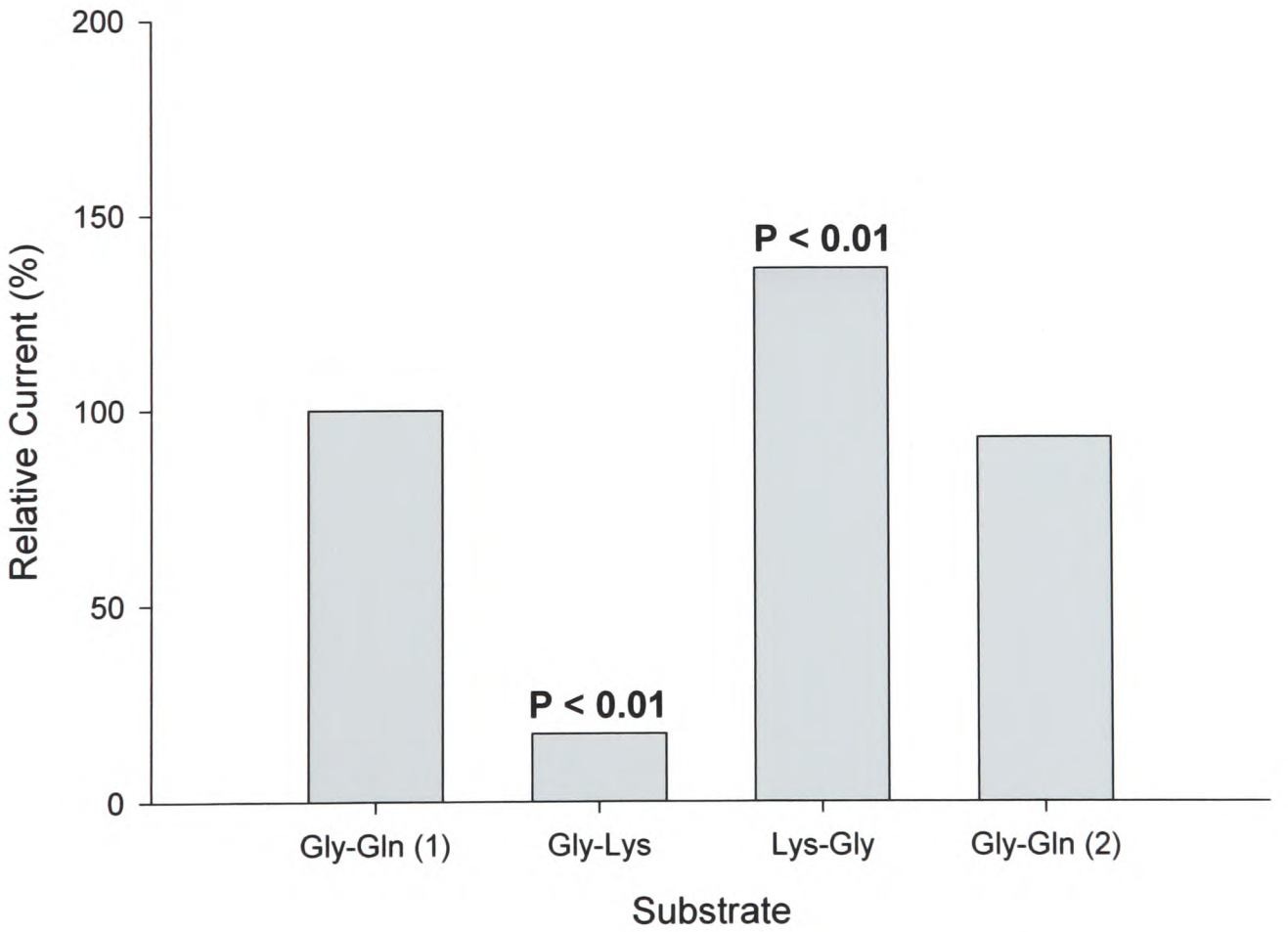


Figure 5.7. a. Steady state I-V curves in response to 2mM Gly-Lys and Lys-Gly, bracketed by 2mM Gly-Gln. b. Normalised values for I_{max}.

Substrate	pH 7.5	pH 5.5
Gly-Gln	440 ± 19.6nA	595 ± 30nA
Gly-Lys	982 ± 16.0nA	943 ± 17.3
Lys-Gly	251 ± 11.2nA	65 ± 24.6nA

Table 5.6 I_{max} values for Gly-Lys and Lys-Gly at pH 7.5 and 5.5. Values quoted are mean ± s.e.m, n = 4.

5.9 Summary of Gly-Lys and Lys-Gly experiments

1. Gly-Lys and Lys-Gly were both substrates for PepT1.

2. Currents induced by neutral Gly-Gln were greater at pH 5.5 than 7.5.

3. Currents induced by the charged peptides were greater at pH 7.5.

4. The difference between currents evoked by Gly-Lys at both pH values was small, only 39nA, whereas the difference for Lys-Gly was 186nA.

5. The trend seen with negatively charged substrates was not seen with positively charged peptides, (from preliminary data).

5.10 Summary of chapter

1. PepT1 transports a wide range of substrates, including neutral, anionic and cationic dipeptides.

2. For anionic peptides, the extent to which they are transported depends on both extracellular pH and the position of charge within the peptide, with maximal transport occuring at pH 5.5 in all cases (for the peptides tested).

3. The transport of cationic peptides appears to be greater at neutral pH (for the peptides tested), with the peptide with the charge in the amino terminal being the higher affinity substrate.

4. The apparent order of affinity of the two anionic peptides changed upon extracellular acidification, suggesting that substrate titration alone is not responsible for the changes observed.

5. The position of charge within a peptide therefore appears to play an important role in substrate binding to the transporter.

CHAPTER 6

REGULATION OF PEPT1: THE ROLE OF PHORBOL ESTERS

6.1 Introduction

Little research has been carried out into the acute regulation of the epithelial H^+/oligopeptide transporter, PepT1. Much of the research to date has focussed on substrate upregulation of peptide transport, (Erickson *et al*, 1995, Walker *et al*, 1998 and Shiraga *et al*, 1999), with one study on hormonal regulation of PepT1, (Thamotharan *et al*, 1999). However, one earlier study has shown downregulation of PepT1 activity in Caco-2 cells by activation of protein kinase C, but the exact mechanism by which it occurred remained unresolved (Brandsch *et al*, 1994).

In this study I have investigated electrophysiologically and using fluorescence immunocytochemistry the regulation of PepT1 by utilising phorbol esters. The activator of protein kinase C, PMA (phorbol 12 myristate, 13-acetate) and the inactive phorbol ester 4αPDD (4α–phorbol 12, 13-didecanoate) have been studied in PepT1 expressing *Xenopus laevis* oocytes. These compounds had been used successfully in studies on hCAT-1, (Closs *et al*, 2001).

6.2 Protein kinase C (PKC)

Protein kinase C was first identified in 1977 and is known to be ubiquitous in tissues and cells. There are many different subtypes of PKC, but all have a catalytic and a regulatory domain, (diagram 6.1a). Activation of PKC requires calcium,

phospholipid-phosphatidylserine and diacylglycerol, DAG, with only sn-1,2-DAG being active towards PKC. Diacylglycerol interacts with PKC in the regulatory domain. PKC is involved in many cellular processes, but it is also a receptor for tumour promoters and as such phorbol esters have been observed to act on PKC, (diagram 6.1a).

6.3 Phorbol 12 myristate, 13 acetate (PMA)

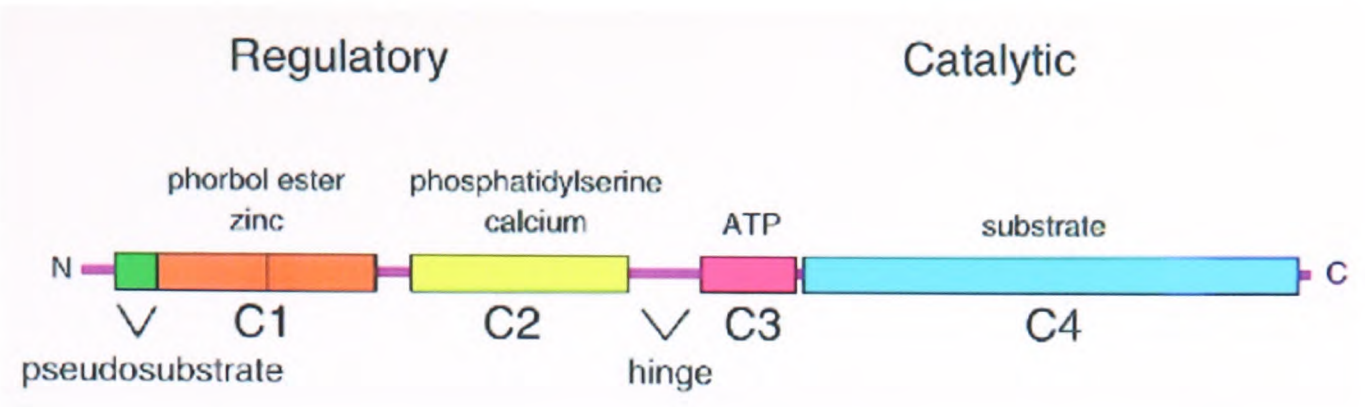
PMA is a specific activator of protein kinases A, B and C. It is active in the range 1-100nM and elicits its effect by mimicking diacylglycerol, a natural ligand and activator of protein kinases. See diagram 6.1b for the molecular structure of PMA. Phorbol esters act on the same site of PKC as DAG due to structural similarities between the molecules.

6.4 4α–phorbol 12, 13-didecanoate (4α PDD)

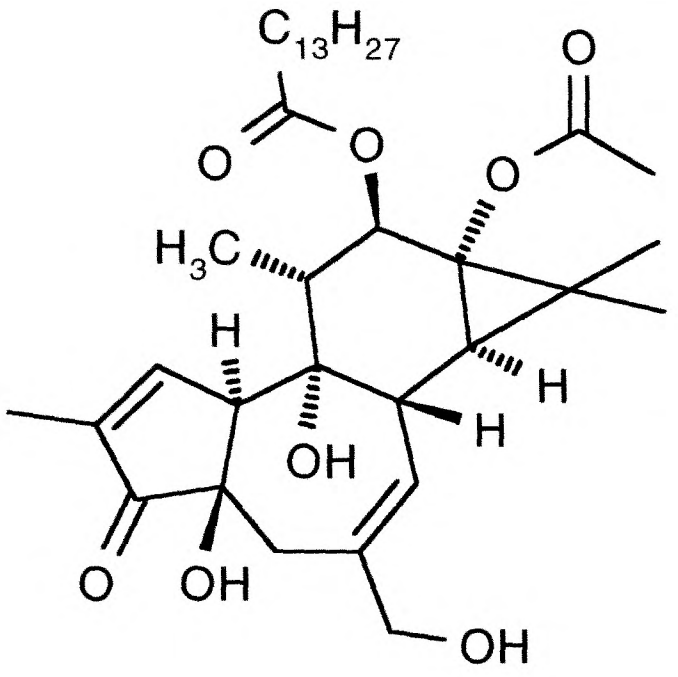
4α PDD is an inactive phorbol ester and it's structural similarities and differences to PMA can be seen in diagram 6.1c. As it is an inactive phorbol ester it was used as a negative control in the experiments detailed in this chapter.

6.5 Composition of solutions

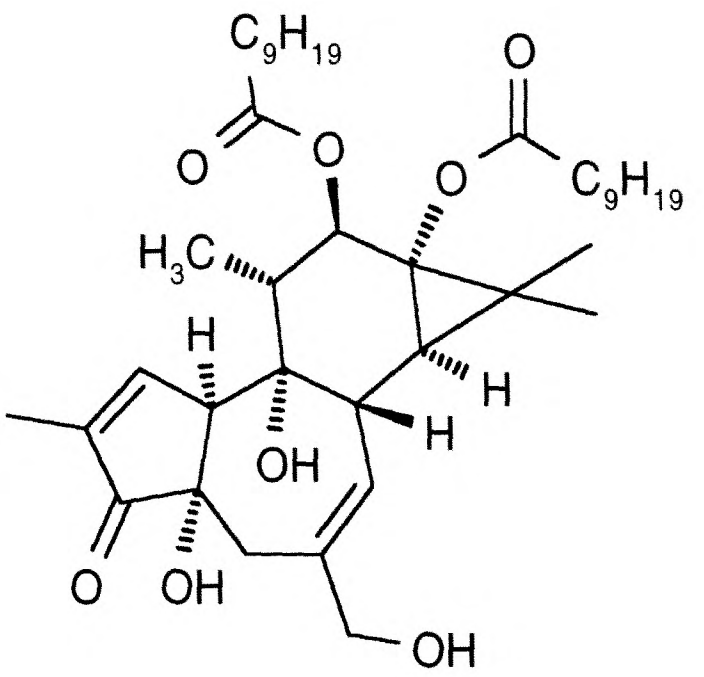
The phorbol esters were purchased from Sigma, Poole, Dorset, UK, and were dissolved in DMSO to a stock concentration of 1mM and stored at -20°C in the dark. These stock solutions were then dissolved to a concentration of 10nM in uptake solution. See table 6.1 for the composition of uptake solution.



a.



b.



c.

Diagram 6.1 a. Schematic diagram of PKC showing 4 conserved regions, C1-C4, reproduced from Newton, J. Biol. Chem, 1995. b. Molecular structure of PMA, an activator of PKC. c. Molecular structure of 4α PDD, an inactive phorbol ester.

Uptake Solution	Concentration (mM)	ml/litre
NaCl	95	19ml (5M stock)
KCl	2	10ml (0.2M stock)
$CaCl_2$	1	1ml (1M stock)
$MgCl_2$	1	10ml (0.1M) stock)
Tris-HEPES	20	40ml (0.5M stock)

Table 6.1 Composition of Uptake Solution. The stock solutions were made up in autoclaved double distilled water and filter sterilised. The volumes of stock solutions were added to a volumetric flask and made up to 1 litre with autoclaved double distilled water. Solutions were adjusted to pH 7.5 with Tris-HEPES. The appropriate phorbol ester was added to give a final concentration of 10nM.

6.6 Effect of PMA on Gly-Gln transport

6.6.1 Determining concentration of PMA and incubation period

The protocol for these experiments was based on studies on the human cationic amino acid transporter, hCAT-1, (Closs *et al*, 2001). In this study, the concentration of phorbol esters used was 100nM and the incubation time 30 minutes. Initial experiments were based upon this strategy, however it proved to be unsuccessful as the oocytes exhibited gross morphological changes almost immediately. This led to a change in the concentration of PMA used, with the eventual concentration of 10nM chosen. The incubation period was unchanged at 30 minutes.

6.6.2 Effect of PMA on 2mM Gly-Gln transport

Two-electrode voltage clamping was used to record the effect of 10nM PMA in PepT1 expressing *X.laevis* oocytes at three and four days post cRNA injection. The membrane potential of the oocytes were held at –50mV and then stepped from +50 to –150mV in 10mV increments. Initial experiments focussed on any change occurring at all upon incubation PMA. The experimental protocol involved comparing the Gly-Gln induced currents before and after PMA incubation, as well as monitoring the effect the phorbol ester had on currents induced in the absence of peptide. The oocytes were subjected to a third pulse of peptide to confirm if the effect of PMA was permanent. Voltage clamps were carried out in each case when the oocyte had reached steady state. A more detailed protocol can be found in table 6.2.

Figure 6.1 shows the effect of PMA on the peptide-induced currents. The first pulse of 2mM Gly-Gln induced a maximal current of 435nA, whereas after PMA treatment, this was reduced by 149nA to 286nA. Upon the third pulse of Gly-Gln this was

further reduced to only 214nA, only 50% of the original current evoked by Gly-Gln. The data quoted here are representative of one oocyte, but a similar trend was observed in all experiments.

The incubation in PMA had no effect on the underlying currents recorded when the oocyte was bathing in uptake solution, see figure 6.2, with the maximal current in all cases being approximately 120nA. Figure 6.3 shows the I-V curves recorded in the presence and absence of PMA, with and without Gly-Gln.

Step	Condition
1	pH 7.5 uptake
2	pH 7.5 uptake + 2mM Gly-Gln
3	pH 7.5 uptake
4	30 min. incubation in 10nM PMA
5	pH 7.5 uptake + 2mM Gly-Gln
6	pH 7.5 uptake
7	pH 7.5 uptake + 2mM Gly-Gln
8	pH 7.5 uptake

Table 6.2 Detailed protocol for voltage clamp experiments involving PMA. Voltage clamping for each condition occurred once steady state had been reached.

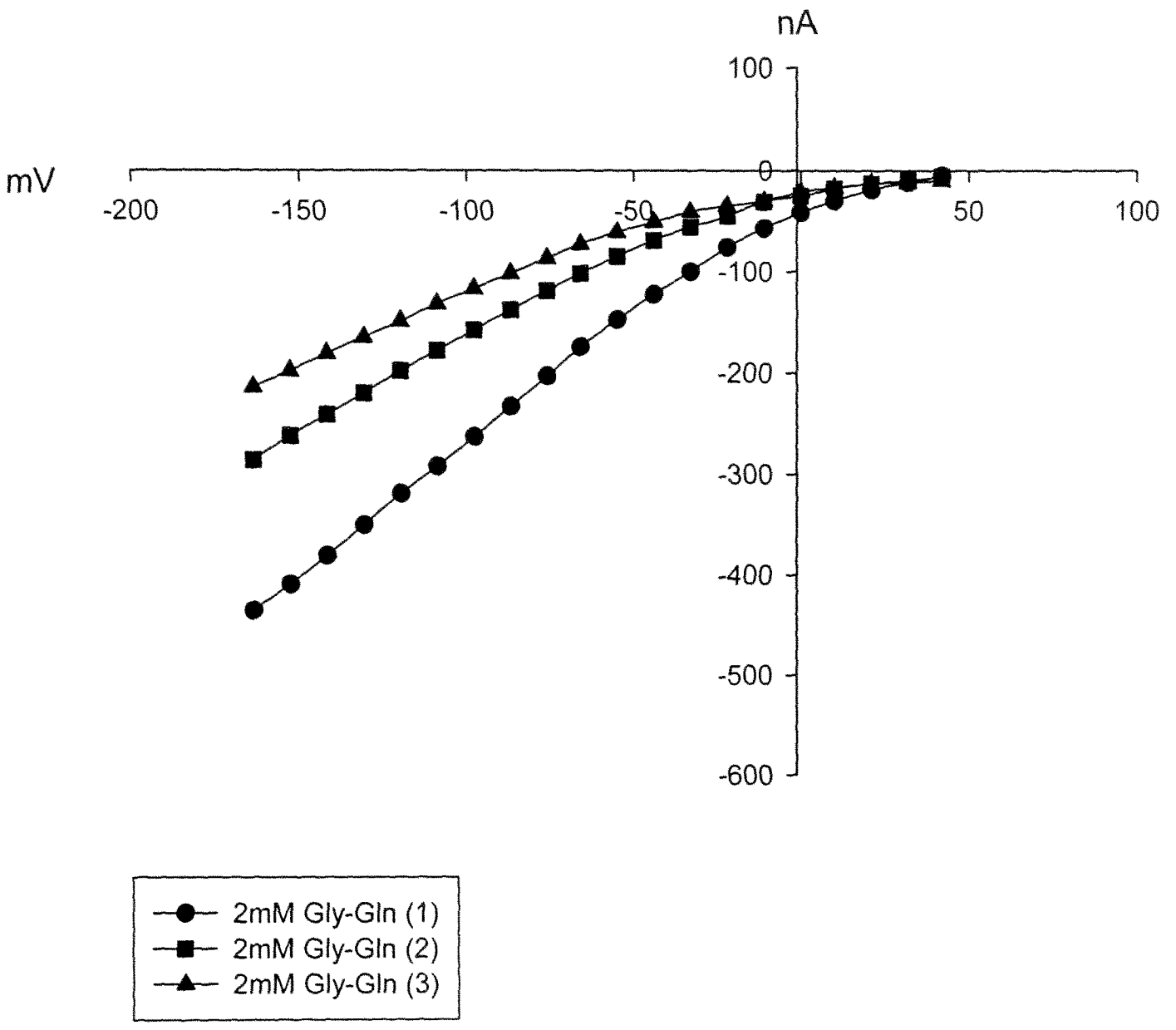


Figure 6.1 Peptide induced currents recorded from PepT1 expressing oocytes before, (1), immediately after, (2), and 30 minutes after, (3), treatment with the phorbol ester, PMA (data representative of one oocyte).

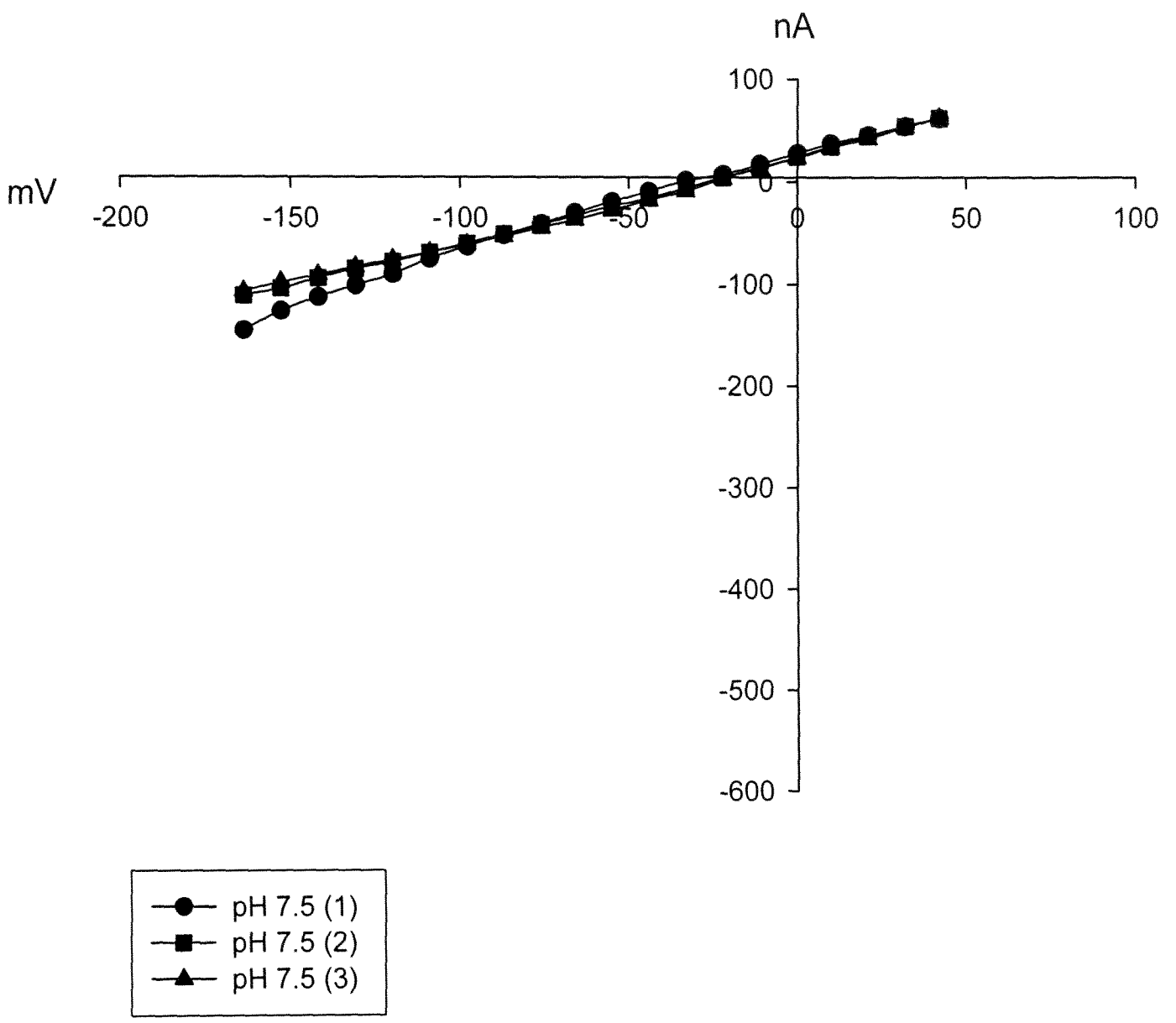


Figure 6.2 Steady state currents induced upon voltage clamping PepT1 expressing oocytes in uptake solution, pH 7.5, before, during and after PMA treatment.

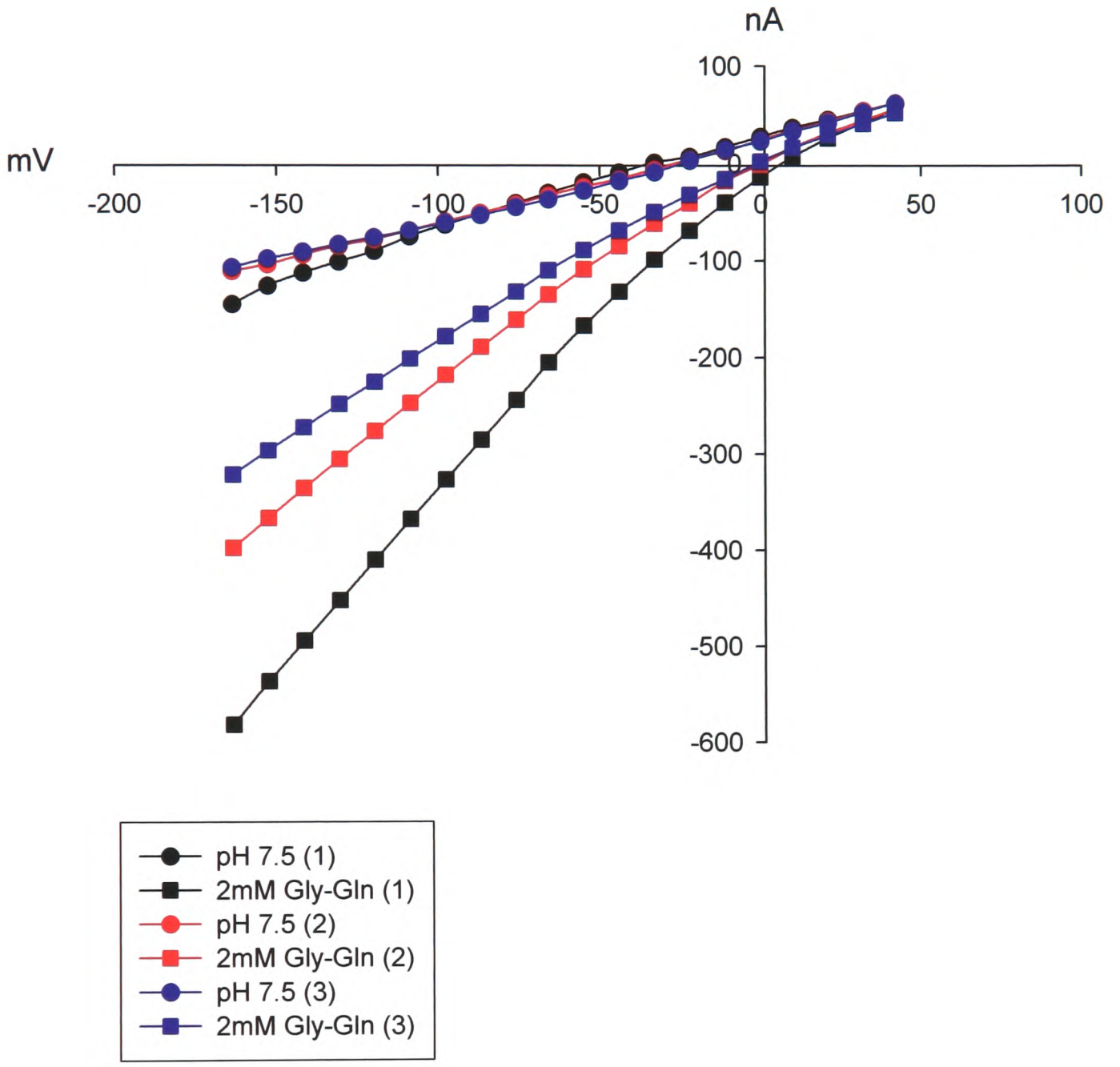


Figure 6.3 Steady state I-V relationship in the presence and absence of Gly-Gln before and after incubation with 10nM PMA.

6.7 Effect of PMA on Gly-Gln dose-response curve

The two-electrode voltage clamp was employed in PepT1 expressing oocytes to record peptide-induced currents in response to the neutral peptide Gly-Gln before and after treatment with PMA.

Steady state I-V curves were measured in response to Gly-Gln before and after PMA treatment. Again the membrane potential was held at –50mV and stepped to test voltages between +50 and –150mV in 10mV increments. The concentrations of Gly-Gln used were 0.1, 0.2, 0.5, 1 and 2mM, all made up in uptake solution at pH 7.5. Figures 6.4a and b show the differences in the currents generated before and after treatment with PMA.

From this data, the maximal current evoked during the voltage clamp, in this case at –150mV, was plotted against the substrate concentration. This allowed estimation of the kinetic parameters of transport, K_a and I_{max}, and to observe how these parameters changed upon treatment with the phorbol ester. Figure 6.5a shows the dose response curves recorded and the changes seen in K_a and I_{max}, while figure 6.5b shows the change in I_{max} before and 30 minutes after PMA treatment. Table 6.3 shows the exact values for K_a and I_{max}.

Following the incubation in PMA the K_a for Gly-Gln decreased by 50% from 0.6 ± 0.08mM to 0.3 ± 0.05mM, mean ± s.e.m, n = 4. The I_{max} also decreased by approximately 50% from 920.2 ± 39.3nA to 422.7 ± 16.8nA, mean ± s.e.m, n = 4. These values were statistically significant using the Student's *t* test with $P < 0.05$ for the K_a values and $P < 0.001$ for the I_{max} values.

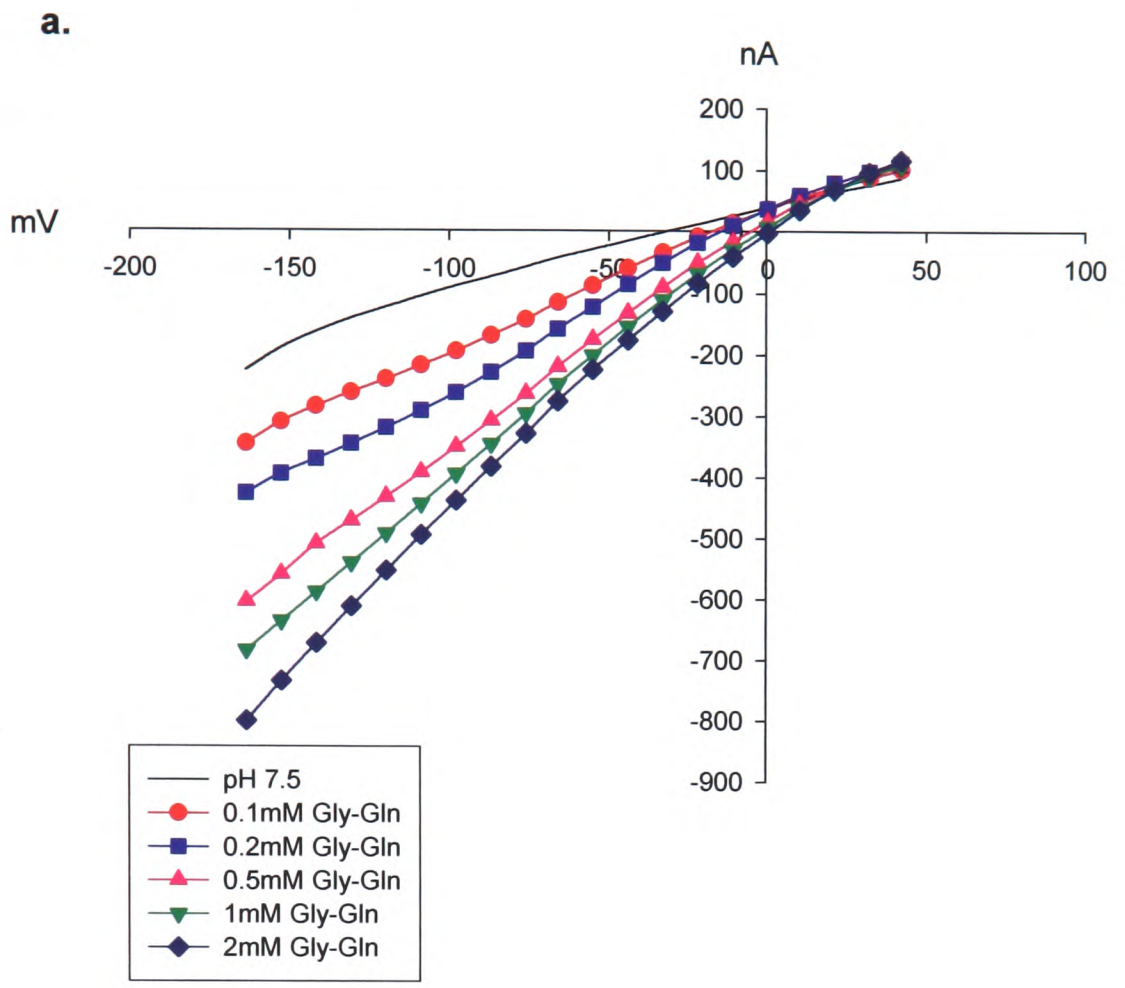
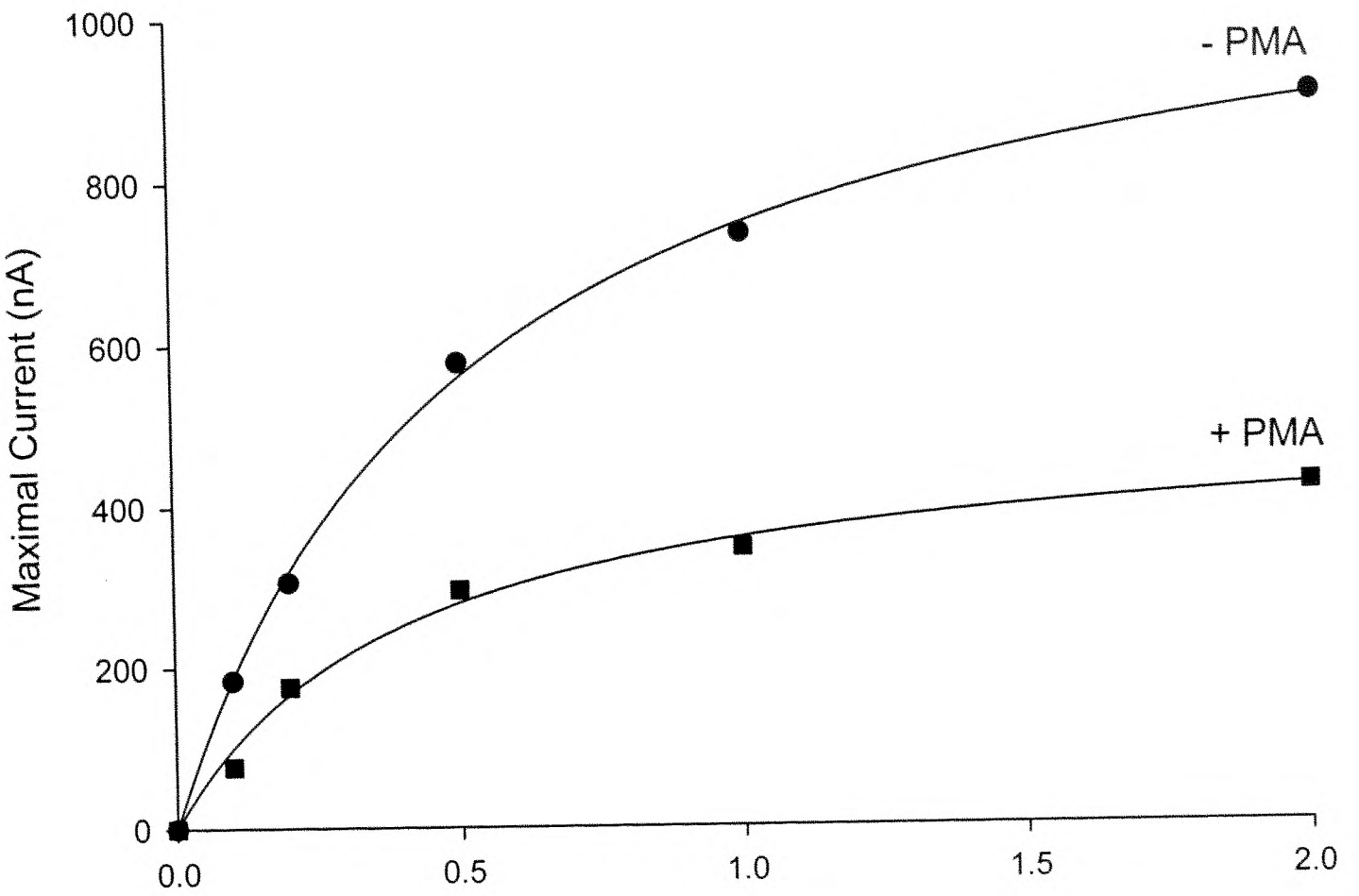


Figure 6.4a. Steady state I-V curves recorded in response to increasing concentrations of Gly-Gln. b. Steady state I-V curves recorded in response to increasing concentrations of Gly-Gln after PMA treatment.

a.



b.

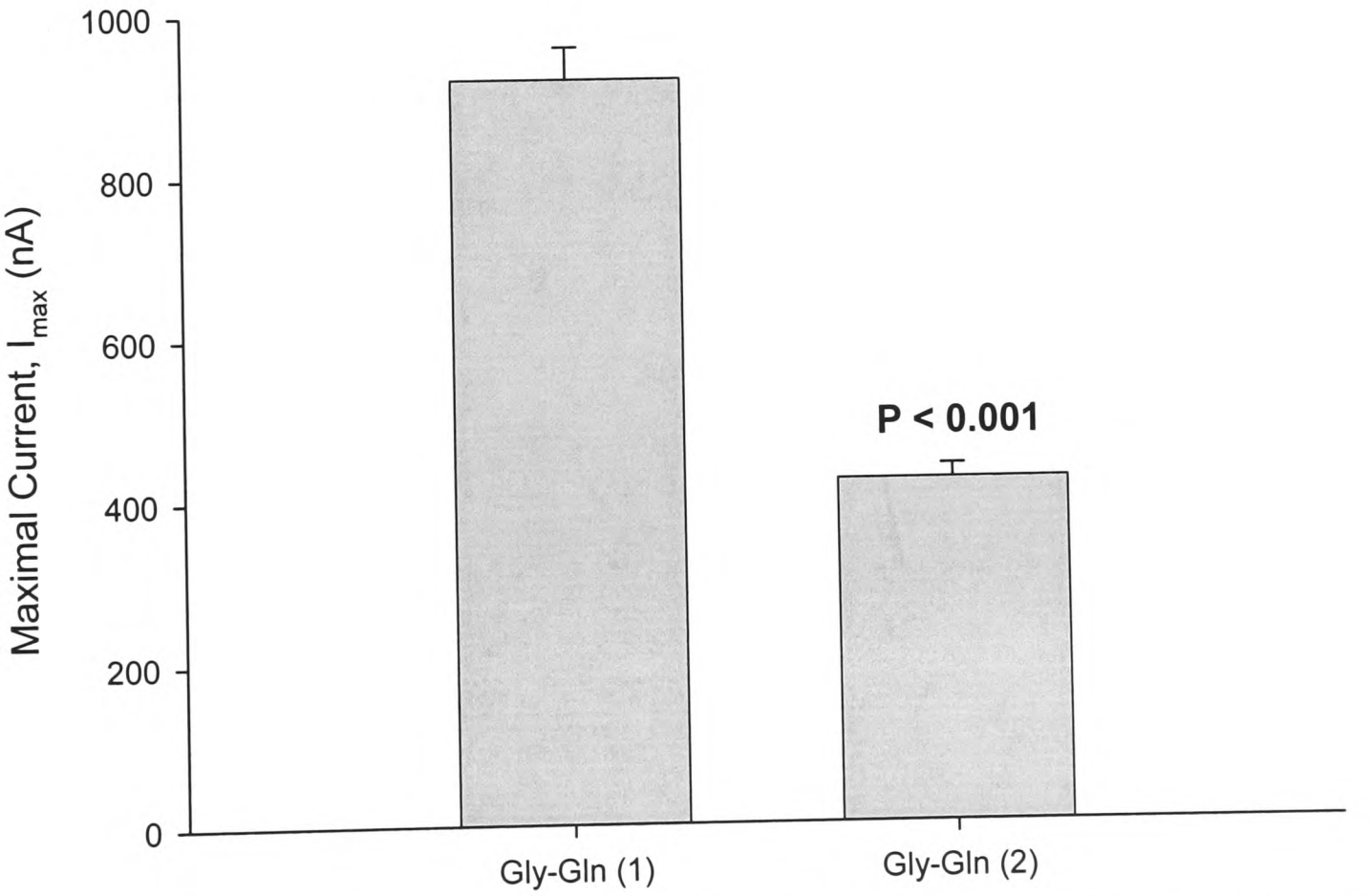


Figure 6.5a. I_{max} for the peptide-induced currents at pH 7.5 were plotted as a function of substrate concentration before and after treatment with the phorbol ester,(data shown representative of one oocyte). b. I_{max} for Gly-Gln pulses, recorded at –150mV, before and after PMA treatment, mean ± s.e.m, n = 4.

Substrate	Phorbol Ester	I_{max} (nA) mean ± s.e.m.	K_a (mM) mean ± s.e.m
Gly-Gln	None	920.2 ± 39.3	0.6 ± 0.08
Gly-Gln	PMA	422.7 ± 16.8	0.3 ± 0.05

Table 6.3 K_a and I_{max} values for Gly-Gln transport through PepT1 at pH 7.5 before and after PMA treatment. Values quoted are mean ± s.e.m, n=4.

6.8 Control Experiments

6.8.1 The effect of 4α PDD on Gly-Gln transport

As stated in section 6.4, 4α PDD is an inactive phorbol ester and as such can be used as a negative control. The two-electrode voltage clamp technique was used to record the effect of 10nM 4α PDD on Gly-Gln uptake in PepT1 expressing oocytes. The batches of oocytes used in these experiments were used 3 and 4 days post cRNA injection. Again the protocol for these experiments were based upon the techniques used by Closs *et al*, 2001.

The strategy employed was identical to the one for PMA, with incubations in 4α PDD lasting for 30 minutes and steady state recordings being taken before and after treatment by the phorbol ester. Figure 6.6 shows the effects of 4α PDD on currents induced by 2mM Gly-Gln and on currents in the absence of peptide at pH 7.5. There were clearly no significant changes to any of the currents recorded.

To ensure that no differences had occurred to the kinetic parameters, the effect of 4α PDD was also tested on the dose-response of Gly-Gln. The same concentrations were used as for the PMA experiments. Again the maximal currents were plotted against substrate concentration. Figures 6.7a and b show that there was no effect by 4α PDD on either K_a or I_{max}, and table 6.4 quotes the exact values for these parameters.

Following incubation for 30 minutes in 10nM 4α PDD both the I_{max} and the K_a were unchanged. The I_{max} before treatment was 988.2 ± 38.4nA compared to 990.5 ± 36.6nA after incubation with phorbol ester, mean ± s.e.m, n = 4. The K_a before 4α PDD treatment was 0.5 ± 0.05mM compared to 0.5 ± 0.04mM after incubation, mean

± s.e.m, n = 4. These values were tested statistically using the Student's *t* test, and were not found to be significantly different, $P > 0.1$ for both I_{max} and K_a values.

6.8.2 The effect of three consecutive pulses of Gly-Gln on transport through PepT1

To further clarify the results seen upon incubation in PMA, an extra set of control experiments were carried out. Three consecutive Gly-Gln pulses were carried out in the same oocyte to rule out accumulation of peptide inside the cell being responsible for the decrease in I_{max}. Figure 6.8a shows the results obtained.

6.8.3 The effect of three consecutive Gly-Gln dose-response curves on K_a and I_{max}

Figure 6.8b shows the results of the three consecutive Gly-Gln dose-response experiments carried out in a single oocyte. The I_{max} of the first pulse was 429.8 ± 6.06nA compared to 445.2 ± 5.20nA for the second and 435.7 ± 6.60nA for the third pulse. The K_a was unchanged at 0.6 ± 0.03mM for all three pulses. There was clearly no significant effect, with $P > 0.1$ for both K_a and I_{max}.

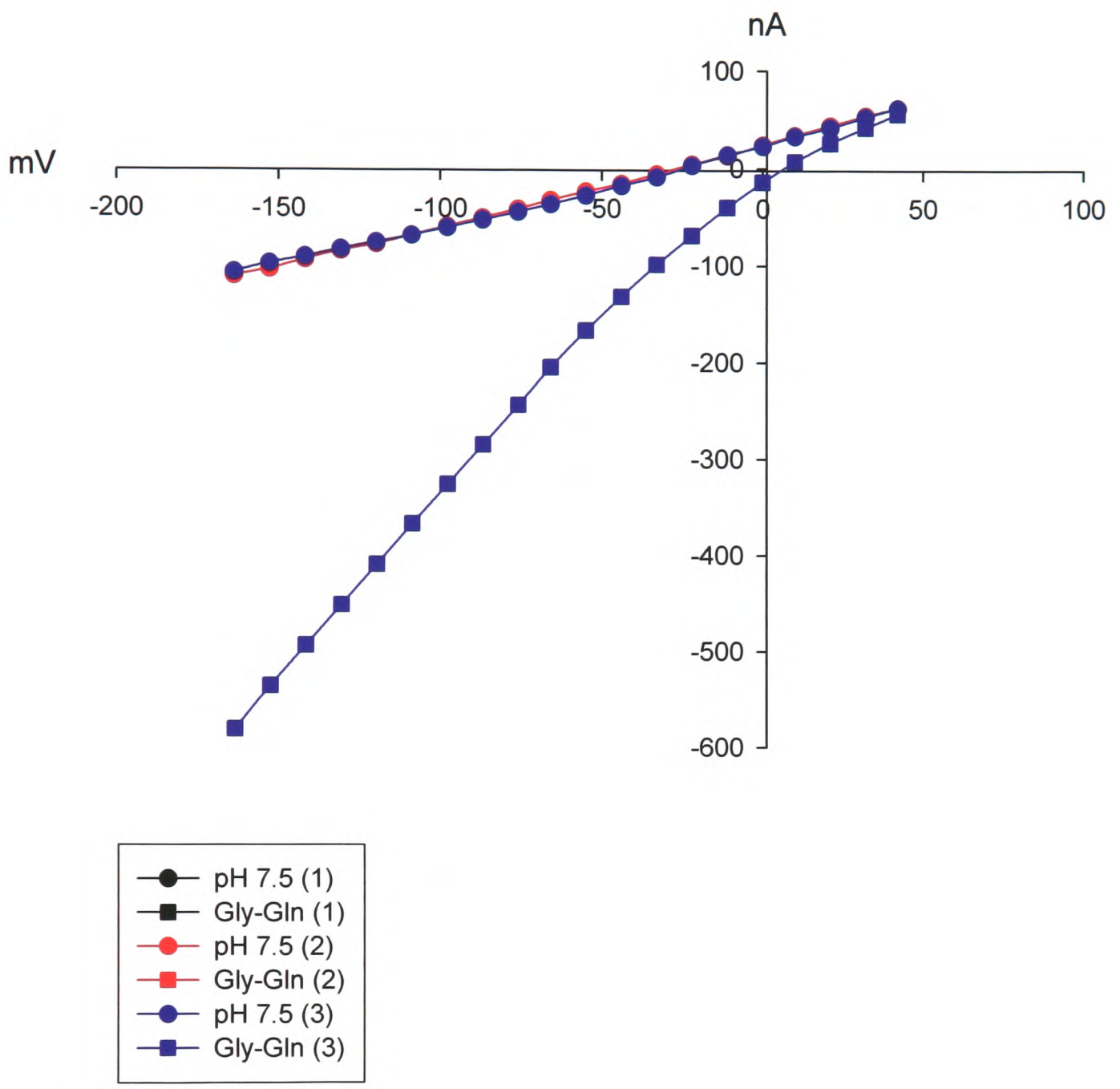


Figure 6.6 Steady-state I-V curves showing the effect of 4α PDD on currents induced by 2mM Gly-Gln and on those recorded in the absence of substrate at pH7.5. Experimental data for all three conditions overlay each other.

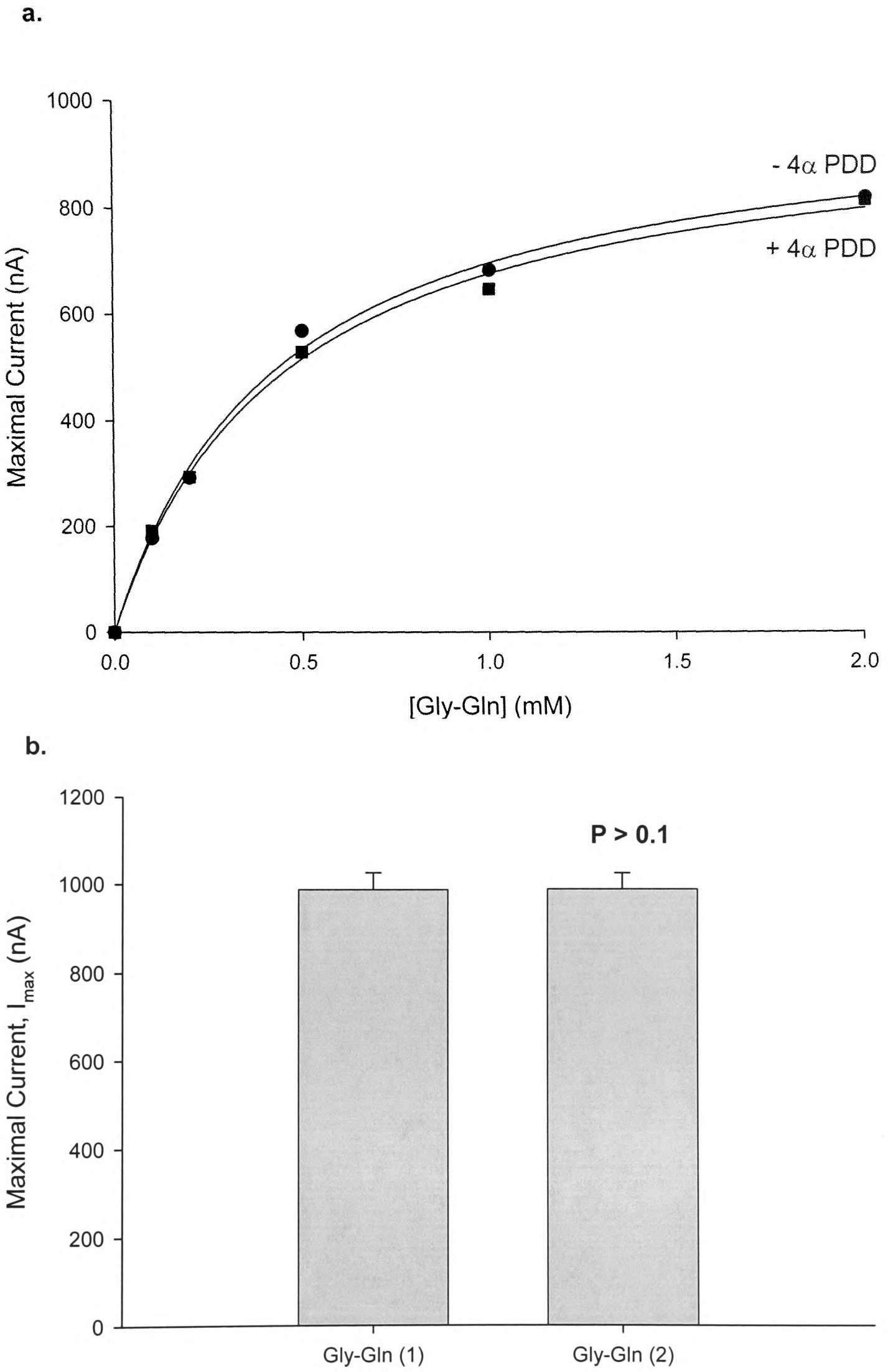
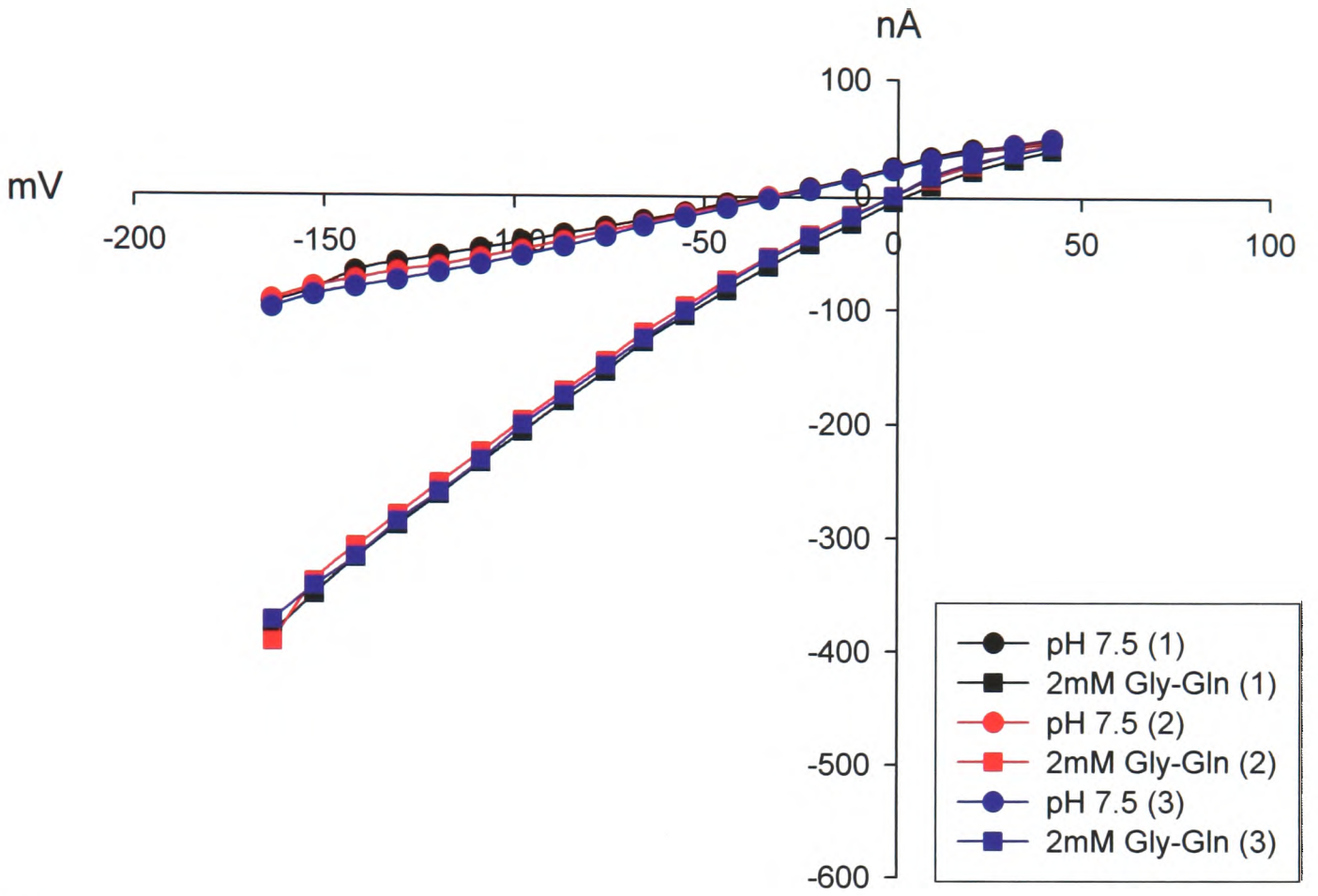


Figure 6.7 a. I_{max} for the peptide-induced currents at pH 7.5 were plotted as a function of substrate concentration, (data shown representative of one oocyte) before and after phorbol ester treatment and b. I_{max} values recorded in PepT1 expressing *X.laevis* oocytes (mean ± s.e.m, n=4).

Substrate	Phorbol Ester	I_{max} (nA) mean ± s.e.m.	K_a (mM) mean ± s.e.m
Gly-Gln	None	988.2 ± 38.4	0.5 ± 0.05
Gly-Gln	4α PDD	990.5 ± 36.6	0.5 ± 0.04

Table 6.4 K_a and I_{max} values for Gly-Gln transport through PepT1 at pH 7.5 before and after 4α PDD treatment. Values quoted are mean ± s.e.m, n=4.

a.



b.

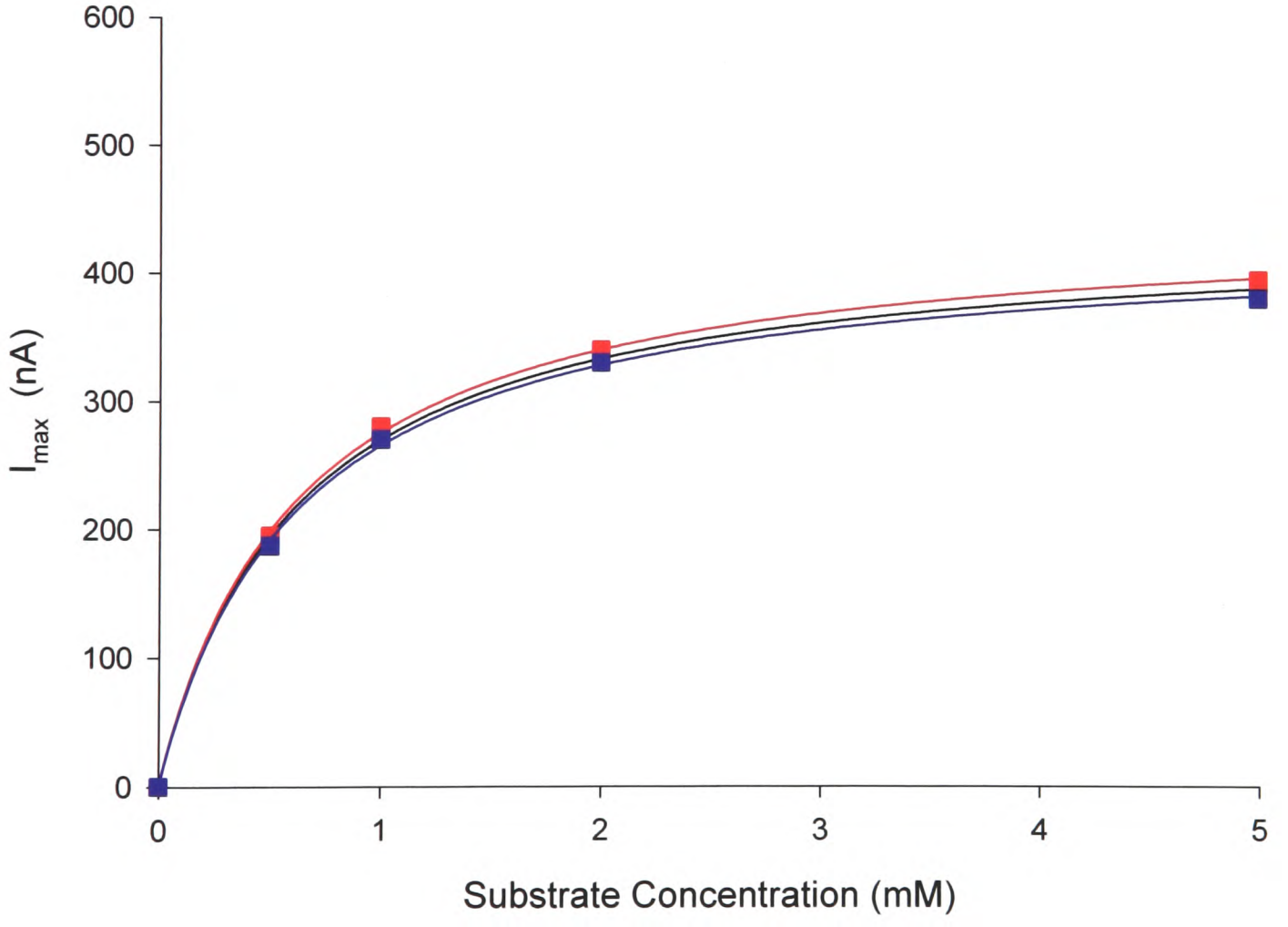


Figure 6.8 a. Currents induced by three consecutive pulses of 2mM Gly-Gln and also those currents recorded in the absence of peptide substrate, at pH 7.5, and b. three consecutive dose-response curves evoked by Gly-Gln, (data shown are representative of one oocyte).

6.9 Summary of electrophysiological results

1. Both K_a and I_{max} for Gly-Gln were decreased by approximately 50% upon incubation in 10nM PMA for 30 minutes.

2. Similar treatment with an inactive phorbol ester, 4α PDD, resulted in no significant change on K_a or I_{max}.

3. Three consecutive pulses of Gly-Gln also had no effect on the kinetic parameters of peptide transport.

4. PepT1 appears to be under the regulatory control of PKC. PMA downregulates PepT1 activity under conditions when driving forces are not altered, i.e. under voltage clamp conditions, suggesting that phosphorylation of the PepT1 protein itself may alter K_a and I_{max}.

6.10 Confocal analysis of PepT1 expression in *X.laevis* oocytes

6.10.1 Introduction

The effects of PMA and 4α PDD on PepT1 expression in oocytes were investigated using fluorescence immunocytochemistry. The oocytes were subjected to the same concentration and incubation period of PMA and 4α PDD as those used in the electrophysiology studies. Polyclonal antibodies were raised in rabbit against a synthetic peptide corresponding to the 15 C terminal amino acids of rat PepT1. This primary antibody was used in our studies in conjunction with FITC and TRITC-conjugated goat anti-rabbit secondary antibodies.

The FITC-conjugated secondary antibody was used primarily, based on the findings of a colleague in our laboratory. However it was difficult to get good images due to the excitation wavelength of FITC being in the same range as the natural autofluorescence of oocytes. As a result bright PepT1 fluorescence was observed, but green background staining was also present. To combat this, the fluorescent tag was changed to TRITC, which has an excitation wavelength that is further away from the biological autofluorescence wavelength. Despite the problems with secondary antibodies, the results in this section have been obtained with both FITC- and TRITC-goat anti-rabbit antibodies.

6.10.2 Effect of PMA and 4α PDD on PepT1 expression determined by FITC

Groups of 5 PepT1 expressing *X.laevis* oocytes were incubated in either:

(1) normal uptake solution, pH 7.5, (2) 10nM PMA or (3) 10nM 4α PDD. Water injected oocytes served as controls, as did oocytes that had no incubation in secondary antibody. Figure 6.9 shows the images obtained for these oocytes when stained with

FITC conjugated secondary antibodies. The images were obtained at x20 magnification, with all other parameters (e.g. zoom, accumulations etc) identical. Clearly PMA treatment reduces the amount of PepT1 expression at the membrane. Higher magnification of the samples could not be carried out, so it was unclear how this change in membrane expression occurred. However, it was clear that the PMA has had a marked effect on the expression of PepT1 whereas the 4α PDD has had no effect at all. The water controls exhibited no bright band of staining at the membrane, but there was some background staining – a problem mentioned in *6.10.1.*

Fluorescence readings were taken at 6 points around the oocyte. Table 6.5 details the exact values for maximum intensity of the fluorescence as calculated using TCS NT software. The PMA reduced the intensity of staining by 89 units ($P<0.01$) , whereas the value for the 4α PDD treated oocyte was the same as for the PepT1 control, 255 units. The water control exhibited only a sixth of the fluorescence of the PepT1 control, 40units ($P<0.01$), confirming the electrophysiological studies conclusion that there is no endogenous PepT1 in oocytes.

6.10.3 Effect of PMA and 4α PDD on PepT1 expression determined by TRITC

A protocol identical to that in section *6.10.2* was employed, but the secondary antibody was conjugated to TRITC. The samples were again viewed using the confocal microscope and figure 6.10 shows the images obtained. The PMA reduced the intensity of the PepT1 staining by 108 units ($P<0.01$), whereas there was only a small decrease of 10 units seen with 4α PDD. The controls were a water injected control, which had a fluorescence intensity of only 20 units ($P<0.01$), and a sample that had no incubation in secondary antibody. The fluorescence intensity of this control was 0. Table 6.6 shows the exact values for maximum fluorescence intensity.

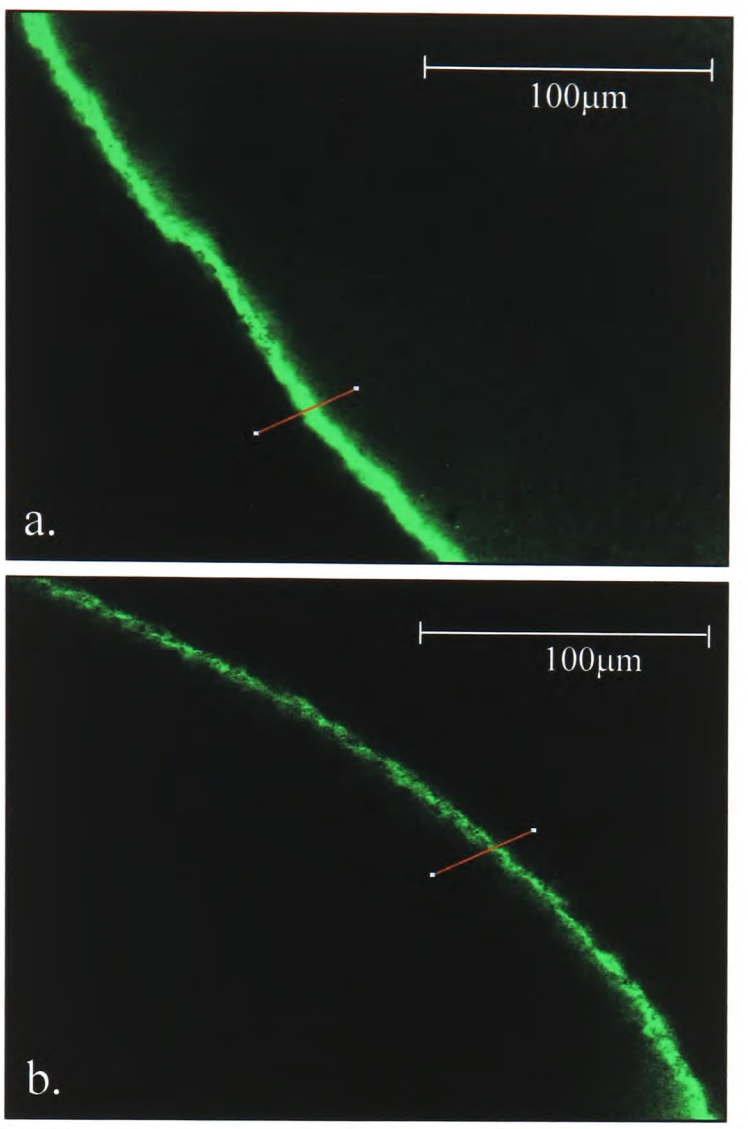
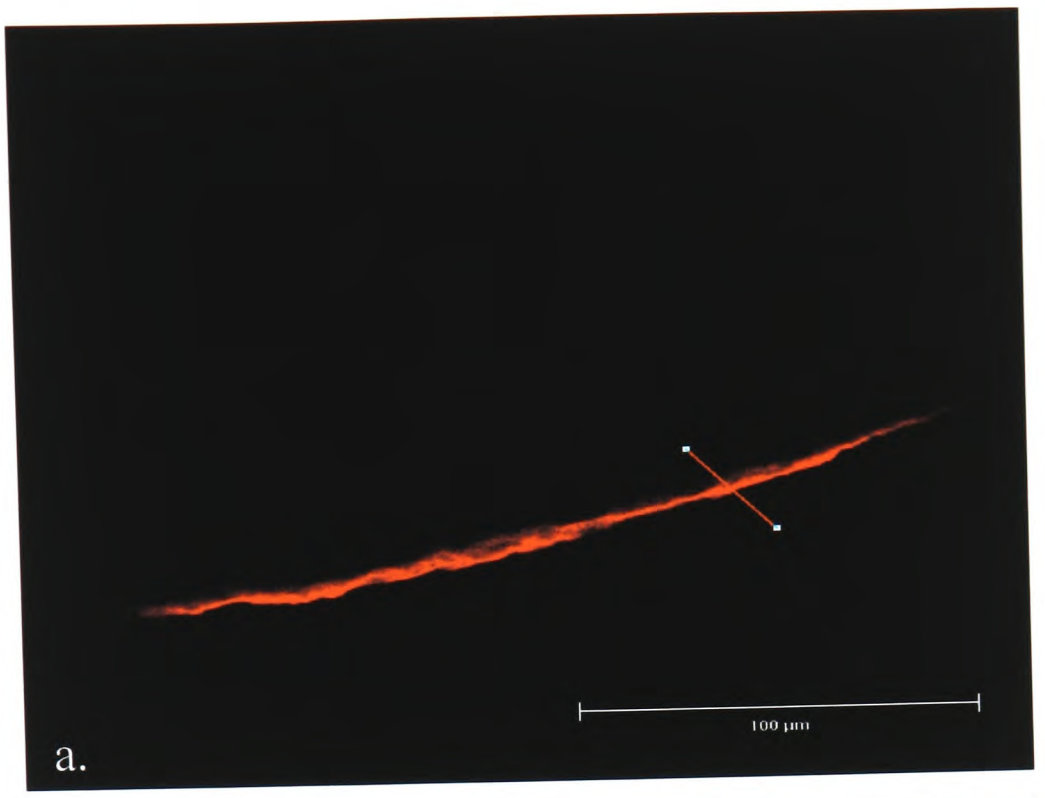


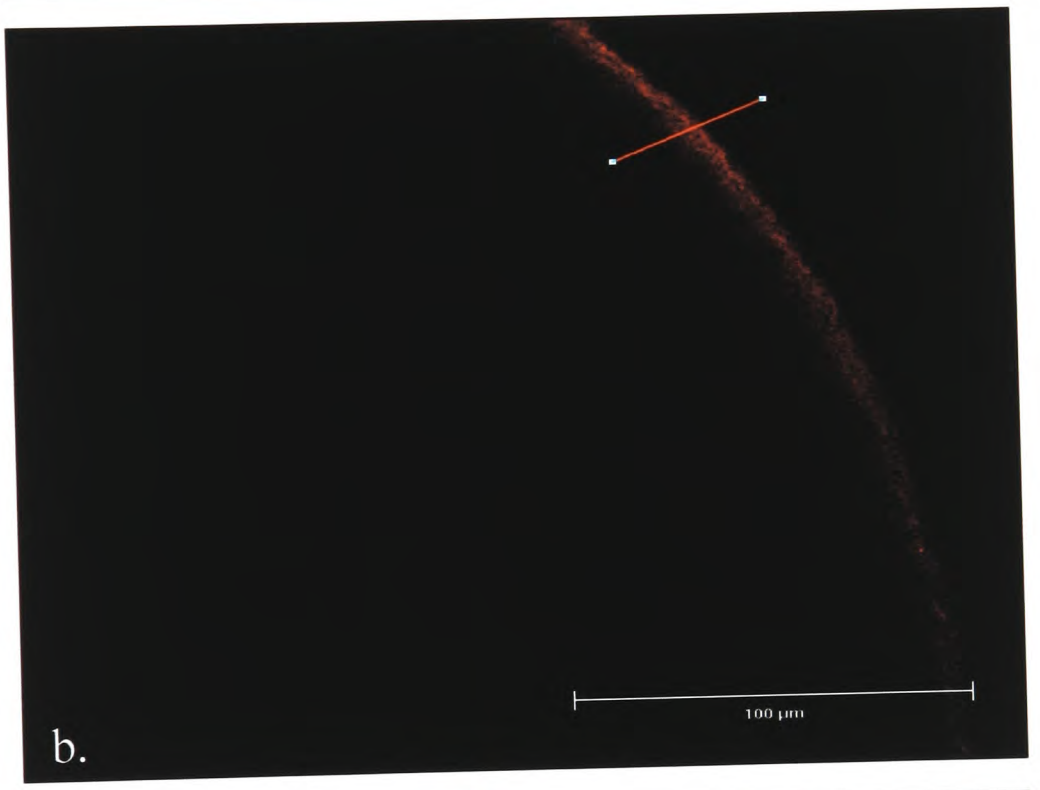
Figure 6.9 a. PepT1 control b. PMA treated c. 4α PDD treated d. H_2O control

Condition	Maximum fluorescence intensity
PepT1 control	255 ± 15
10nM PMA	166 ± 20
10nM 4α PDD	255 ± 13
H_2O control	40 ± 5

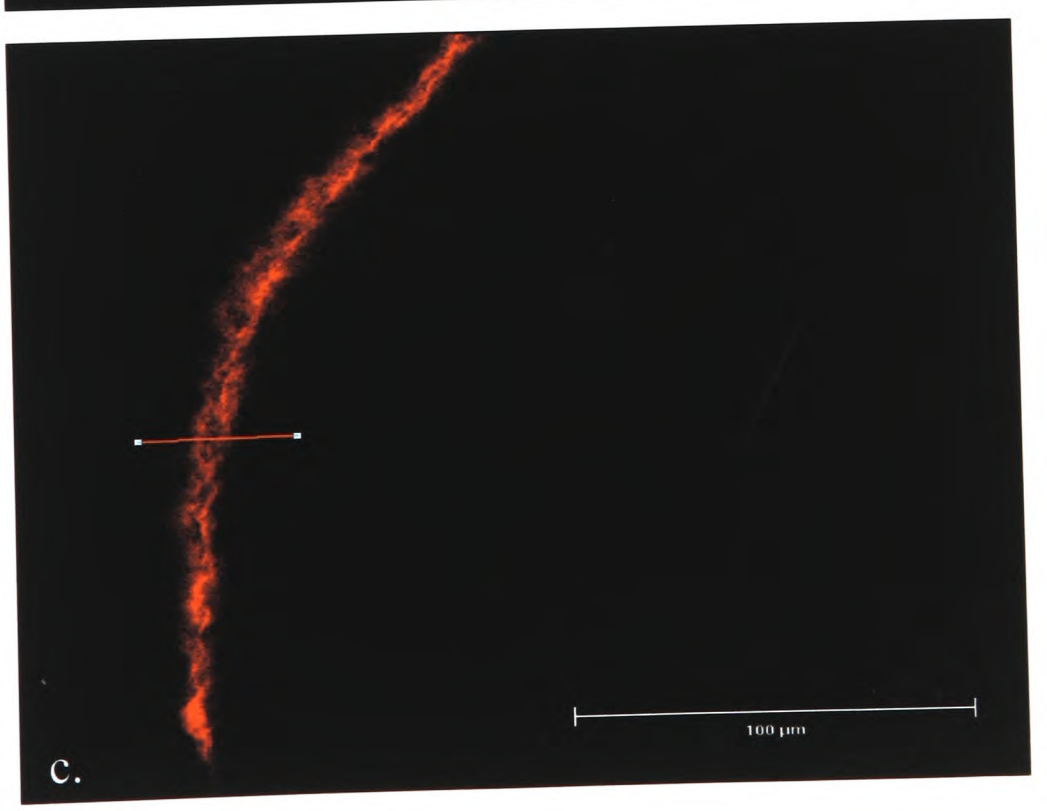
Table 6.5 Maximum intensity of fluorescence obtained for each experimental condition, using Leica TCS NT software. Six readings were taken per oocyte and data quoted is representative of one oocyte.



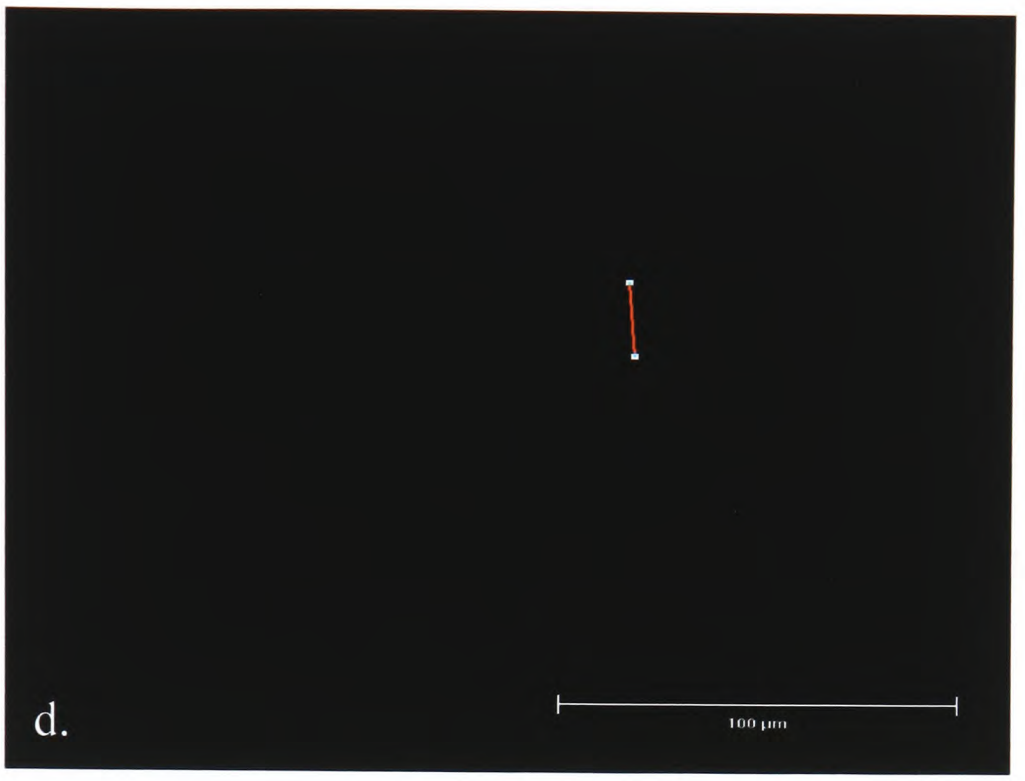
a.



b.



c.



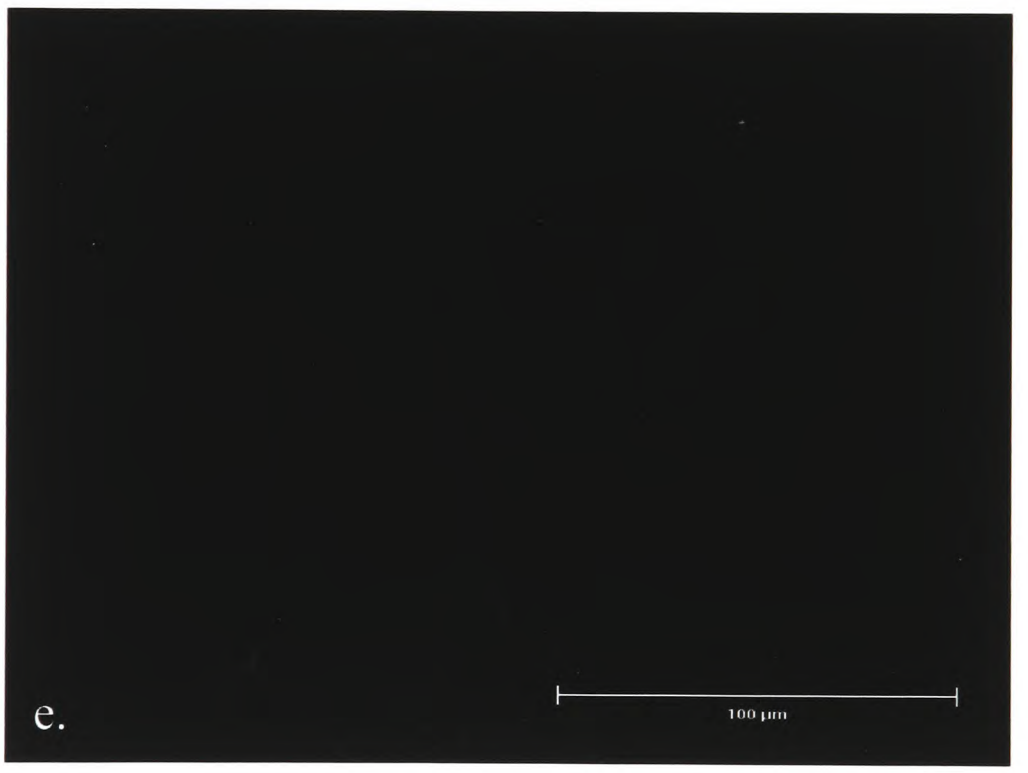


Figure 6.10 Confocal images obtained using TRITC at x20 magnification a. PepT1 control b. PMA treated c. 4α PDD treated d. Water control e. Omission of secondary, (data representative of one oocyte).

Condition	Maximum fluorescence intensity
PepT1 control	255 ± 18
10nM PMA	147 ± 11
10nM 4α PDD	245 ± 8
H_2O control	20 ± 5
Omission of secondary	0

Table 6.6 Maximum intensity of fluorescence obtained for each experimental condition, using Leica TCS NT software. Six readings were taken per oocyte and data quoted is representative of one oocyte.

6.11 Summary of confocal results

1. PepT1 expression has been visualised with both FITC and TRITC-labelled secondary antibodies, to differing degrees of success with PepT1 expression seen as a bright band of staining in the membrane of *X.laevis* oocytes.

2. No staining was seen in water injected control oocytes or those oocytes that had no incubation in secondary antibody.

3. PMA reduced the intensity of the staining seen in PepT1 expressing oocytes.

4. 4α PDD had no effect on the intensity of staining in PepT1 expressing oocytes.

5. The results obtained using immunocytochemical techniques agree with those observed from voltage clamping.

6. The decrease in V_{max} observed in the electrophysiology experiments confirms the finding of a decreased fluorescence at the membrane as determined by confocal analysis.

7. The results suggest that there is less PepT1 being inserted into the membrane, that there is a lower turnover rate of the existing protein or that the epitope that the antibody recognises no longer exists due to a conformational change by the PMA.

CHAPTER 7

GENERAL DISCUSSION

The intestinal isoform of PepT1 plays a vital role in the absorption of the end products of protein digestion, namely di- and tripeptides, as well as a large range of pharmacologically active molecules, (Fei *et al*, 1994, Boll *et al,* 1994). Transport of PepT1 substrates is novel in that it is Na^+-independent and is instead coupled to H^+ cotransport, (Ganapathy and Leibach, 1985). It was the first H^+ coupled peptide transporter to be identified in mammals, (Fei *et al*, 1994). PepT1 has little in common with other mammalian transporters, but has some homology with plant and bacterial transporters. It shows weak similarity to the H^+-dependent CHL1 transporter from plants and a peptide permease from *Saccharomyces cerevisiae,* as well as Dtp, a di/tripeptide transporter from *Lactococcus lactis* and YhiP a putative protein found in *Escherichia coli,* (Hediger *et al*, 1995).

In this thesis I have characterised PepT1, primarily using electrophysiological techniques, to investigate how PepT1 achieves the transport of such a wide range of molecules. To accomplish this, peptides that have been modified at their carboxyl terminus have been investigated, as well as a selection of charged peptides with the anionic or cationic residue at either the amino or carboxyl position within the peptide. The formulation of a template binding model for substrates of PepT1 aided in the characterisation of PepT1 substrates.

I have also investigated the regulation of PepT1 with respect to the role that PKC plays in this process. Rabbit intestinal PepT1 contains a putative PKC

phosphorylation at Ser_{357}, which is located between transmembrane domains 8 and 9, so activators of PKC, namely phorbol esters, were employed to investigate the acute regulation of PepT1.

7.1 Advantages and Disadvantages of electrophysiology

Electrophysiology has been used for decades to characterise electrogenic transport. Expression of membrane proteins results in a new conductance for the co-transported ions, and this new conductance can be recorded using electrophysiology. As peptides are co-transported with protons, PepT1-mediated peptide transport can be studied by employing the two-electrode voltage-clamp.

7.1.1 Advantages

The two-electrode voltage-clamp has been used in many laboratories to study transport characteristics of different electrogenic transporters; SGLT1 (Birnir *et al*, 1991), hCAT2A and hCAT2B (Nawrath *et al*, 2000), KAAT (Bossi *et al*, 1999) and TAUT (Loo *et al*, 1996). The technique allows measurements of voltage and current to be made upon application of substrates for the particular transporter. From standard two-electrode voltage-clamp experiments, the voltage dependence of transport can be determined, (see sections *1.1.4.3* and *1.1.4.4*) as well as the optimum pH for transport (see section 3.4), and the effect of pH on the reversal potential. Concentration-dependence of substrate transport using electrophysiology allows the determination of kinetic parameters, such as the affinity constant, K_a and the maximal current, I_{max}. Voltage-clamp experiments have one major advantage over other techniques, such as radiolabelled uptake studies, and that is that recordings are made when driving forces are not altered.

7.1.2 Disadvantages

Although electrophysiology can provide the researcher with valuable information about current and voltage changes, reversal potential and various kinetic parameters, it should be noted that there are limitations to the technique. Most notably in this thesis was that there was no direct evidence of peptide transport occurring in the oocytes. Although depolarisations and inward currents were observed upon the application to PepT1 oocytes, but not control oocytes, there was no conclusive proof that this was brought about by peptide entering the cell. In order to obtain this proof a technique such as HPLC would need to be carried out. Previous studies in this and other laboratories have however provided evidence of translocation of peptide substrates, so it is safe to assume that the depolarisations and currents observed are indeed due to electrogenic transport of peptides via PepT1.

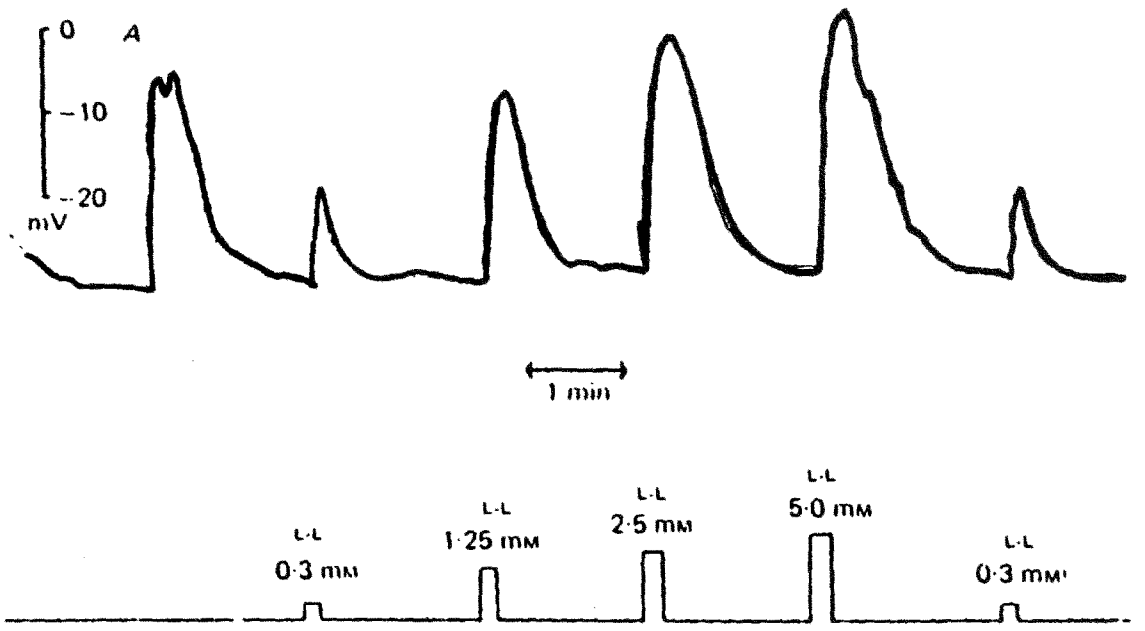
Secondly, it was impossible in my experiments to have much control over the intracellular environment of the oocytes e.g. the concentrations of ions and in the case of the regulation experiments, any second messengers. Combining techniques such as two-electrode voltage clamping, cut-open oocyte technique, immunocytochemistry, radiolabelled uptake experiments and HPLC should help us to obtain a full understanding of how PepT1 functions.

7.2 Evidence for proton dependence of peptide transport

7.2.1 Early evidence

For many years, protein absorption was thought to occur as a result of uptake of a mixture of amino acids, however this is now known not to be the case. However, during the 1950's and 60's some scientists did disagree with the classical hypothesis of peptide absorption, (Matthews, 1975). It was the largely the work of Newey and

Smyth in a series of papers during this period which brought about the change in the hypothesis to include the absorption of peptides as being an important occurrence in protein absorption. Important factors involved in the turnaround of the hypothesis included the finding that to hydrolyse all the protein ingested in a normal diet to amino acids would take days, rather than hours. However, most important was the finding that peptide absorption was independent of sodium. In 1982 a study by Ward and Boyd showed for the first time that peptide transport was independent of sodium, but was dependent on the transport of another cation. Figure 7.1 shows traces recorded in the presence and absence of sodium in the extracellular medium. Their study used hydrolysis-resistant peptides and focussed on making electrical recordings. They showed without doubt that the application of peptides to the test intestinal tissue, (*Necturus maculosus*), caused a depolarisation similar to that caused by the transport of amino acids, but that it persisted in the absence of sodium. Subsequent studies on purified brush border membrane vesicles (Ganapathy *et al*, 1983) and intact intestinal tissue, (Matthews and Burston, 1984) identified H^+ as the candidate cation involved in peptide transport. The role of pH was investigated and a proton gradient-induced stimulation of peptide transport was reported. This stimulation was abolished upon the addition of a proton ionophore. These studies provided the evidence required to completely overturn the classical hypothesis of protein absorption.



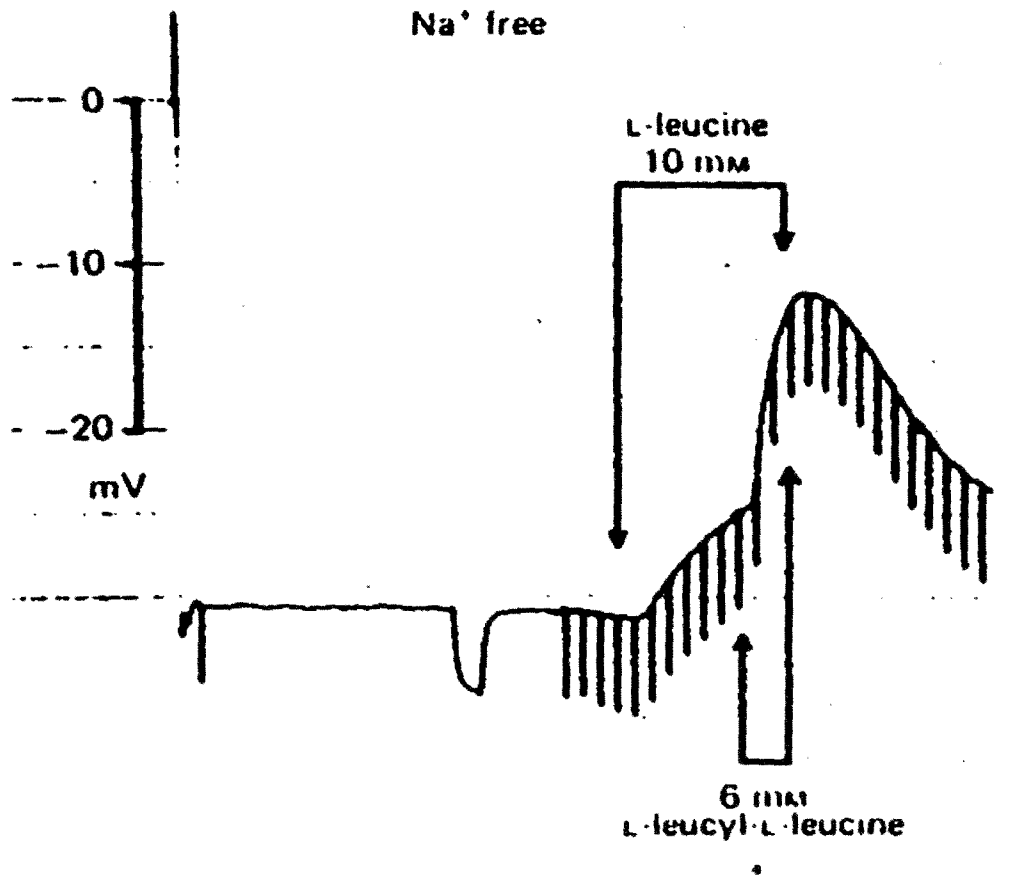


Figure 7.1 Top panel: Depolarisations induced by varying concentrations of Leu-Leu in *N.maculosus* in the presence of Na^+. Bottom panel: Depolarisation seen in *N.maculosus* in response to a single concentration of Leu-Leu in the absence of extracellular Na^+. Reproduced from Boyd and Ward, 1982.

7.2.2 Evidence presented in this thesis

In this thesis there is evidence of oligopeptide transport being dependent on H^+. I have presented data showing that the transport of various peptides causes a membrane depolarisation (Chapter 3) or generation of an inward current (Chapters 4-7), and that this transport is dependent on pH, (Chapter 3). In Chapter 3 I have shown that peptide transport is maximal at pH 5.5, 942.9 ± 7.07nA at pH 5.5 compared to 574.4 ± 7.64nA at pH 8.0. The data presented here is compatible with the presence of an acidic microclimate in the lumen of the intestine adjacent to the brush border membrane of the small intestinal epithelium that is precisely in the area of the intestine where PepT1 is found.

7.3 Structural requirements for PepT1 substrates

When PepT1 was cloned in 1994 it was known that the transporter would accept di- and tripeptides, as well as peptidomimetic drugs, such as β-lactam antibiotics, but that it would not transport peptides greater than three amino acids in length. It was assumed that a peptide bond was essential for a molecule to be a substrate for PepT1. It was not until 4 years later that Temple *et al*, (1998), reported for the first time transport of a substrate that although resembling a peptide, did not have a peptide bond. This molecule was a 'space mimic', and was modelled on the peptide D-Phe-L-Ala. The molecule was 4-Aminophenylacetic acid, and it was a translocated substrate as determined by HPLC. A paper published later the same year by Döring *et al,* reported that to be a substrate for PepT1, a molecule must have a distance of > 500 <630 pm between the ionised head groups. These studies were milestones in the advancement of understanding how PepT1 recognises its substrates. The

development of a substrate template binding model for PepT1 by Bailey *et al,* 2000, further advanced knowledge in this area.

7.4 Substrate template binding model for PepT1

7.4.1 Formulation of the model

Since a three dimensional structure of PepT1is lacking, in order to study how PepT1 manages to transport such a wide range of substrates Bailey *et al* devised a substrate template binding model. This model was based on studies in brush border membrane vesicles, intact rat jejunum and in PepT1 expressing *X.laevis* oocytes. The data used was from their collaborative groups, and also from other published data. Data from hundreds of substrates were used to formulate this substrate binding template model which can be seen in figure 7.2.

The model has been designed to take into account different combinations of potential binding features in 3 dimensional space. There are 4 main binding features of the template model:

(i) It possesses a strong binding site for NH_3^+

(ii) There is a hydrogen bond to the first peptide bond carbonyl group

(iii) It possesses a hydrophobic pocket

(iv) It possesses a carboxylate binding site.

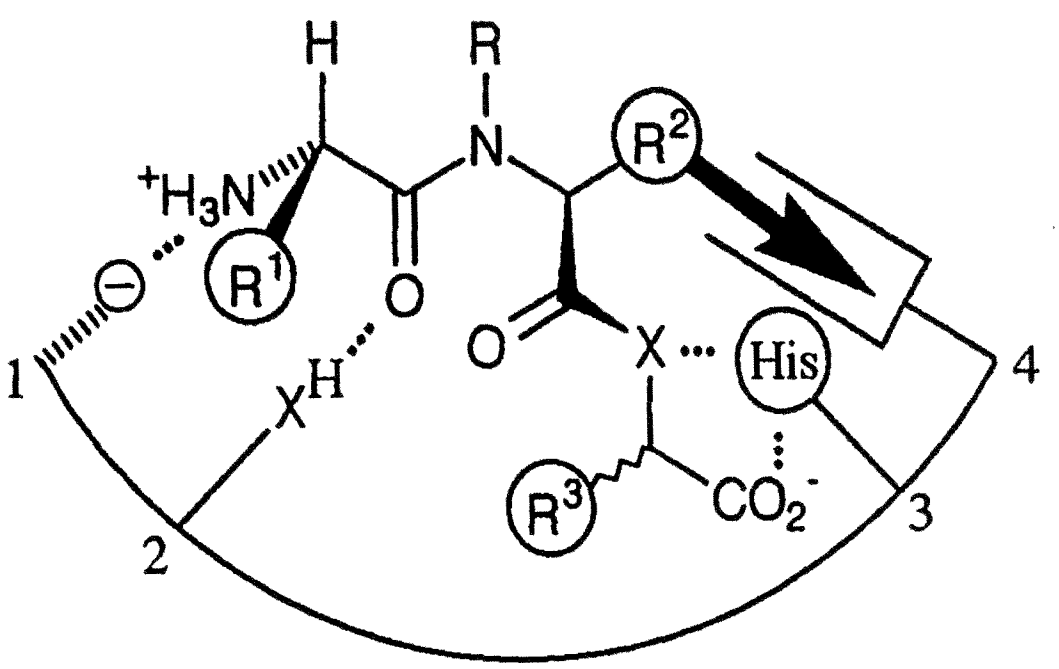


Figure 7.2 Substrate template for binding to PepT1. Free dipeptides terminate with O- at X, whilst tripeptides are extended via X = NH; for the 4 main binding features, possible complementarity to PepT1 is indicated; plain bonds (—) lie close to the plane of the paper. (Reproduced form Bailey *et al*, 2000)

7.4.2 Experimental evidence supporting the model

I have shown in Chapter 4 that modification of the carboxyl terminus of peptides affects the affinity of the substrate for the transporter. The parent peptide, Phe-Tyr, and the modified peptide, Phe-Tyr-NH_2, were both transported by PepT1. Inward currents were observed for both substrates at pH 7.5 and pH 5.5. The average maximal currents for the modified peptides were approximately $^2/_3$ that of the currents obtained for the parent peptide.

The affinity for the Phe-Tyr was 10 fold lower than for the free dipeptide, and extracellular acidification substantially increased the affinity of Phe-Tyr by approximately 4-fold. Extracellular acidification had no effect on the affinity for Phe-Tyr-NH_2.

The finding that the affinity for Phe-Tyr-NH_2 did not increase upon external acidification suggested that the free carboxyl group of the substrate was involved in the protonation interaction with the PepT1 binding site. This fits in very well with the model proposed by Bailey *et al* where one of the important binding features is a carboxylate binding site. The abolishment of the carboxyl group of the peptide results in the peptide binding more weakly to the transporter. This data correlates with previous radiolabelled uptake studies carried out in oocytes using the same molecules, (Meredith *et al*, 2000). Figure 7.3 shows the results from the radiolabelled uptake experiments. The results showed that Phe-Tyr was the best inhibitor of ^{3}[H]D-Phe-L-Gln transport, with inhibition by Phe-Tyr-NH_2 being markedly reduced in comparison, whilst Ac-Phe-Tyr and Ac-Phe-Tyr-NH_2 did not inhibit transport at all. These experiments have provided a simple test for the model, and the data obtained agreed with that predicted by the model. Thus the model could prove to be a significant factor in future drug design.

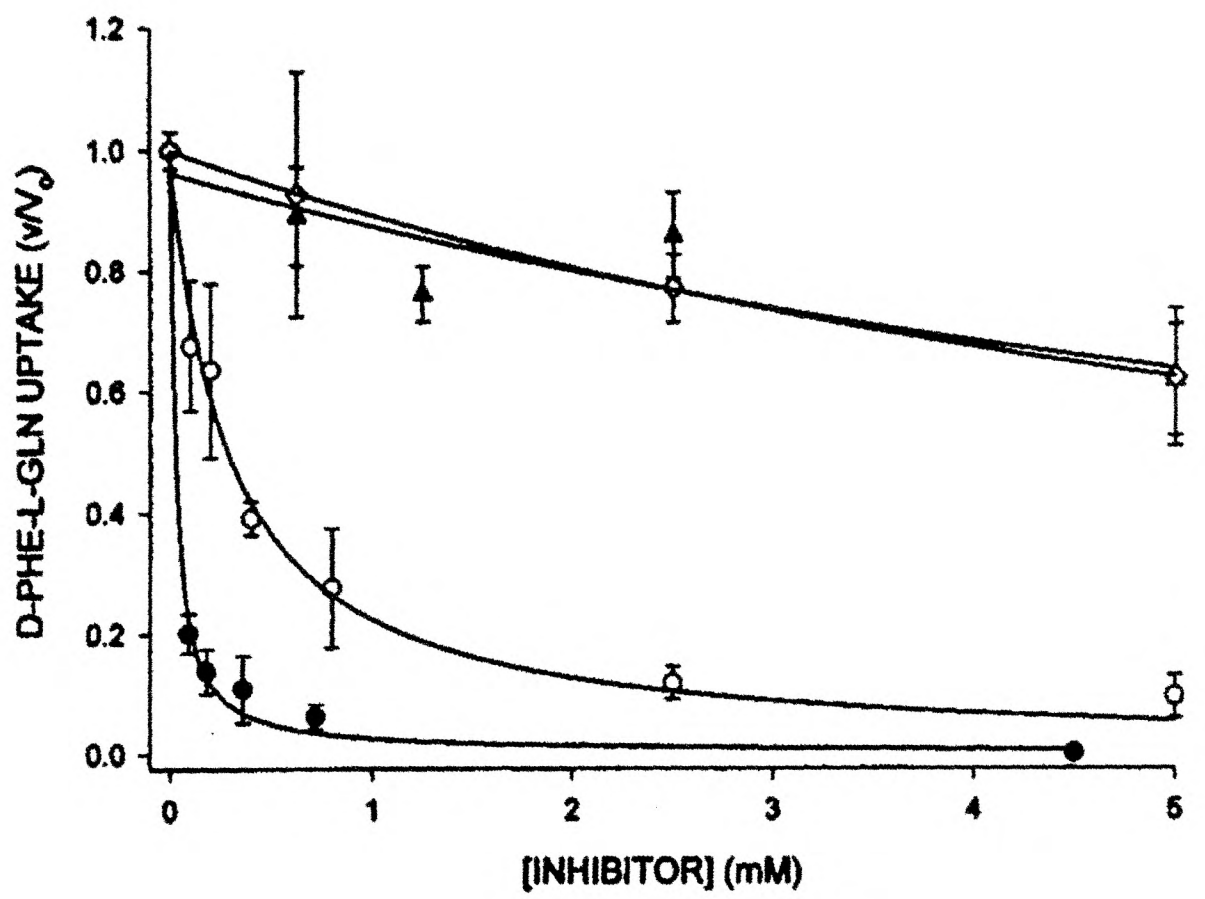


Figure 7.3 Inhibition of uptake of ^{3}[H]D-Phe-L-Gln into PepT1 expressing oocytes, where (●) is Phe-Tyr, (○) is Phe-Tyr-NH_2, (◊) is Ac-Phe-Tyr and (▲) is Ac-Phe-Tyr-NH_2. (Reproduced from Meredith *et al*, 2000)

7.5 Transport of charged peptides

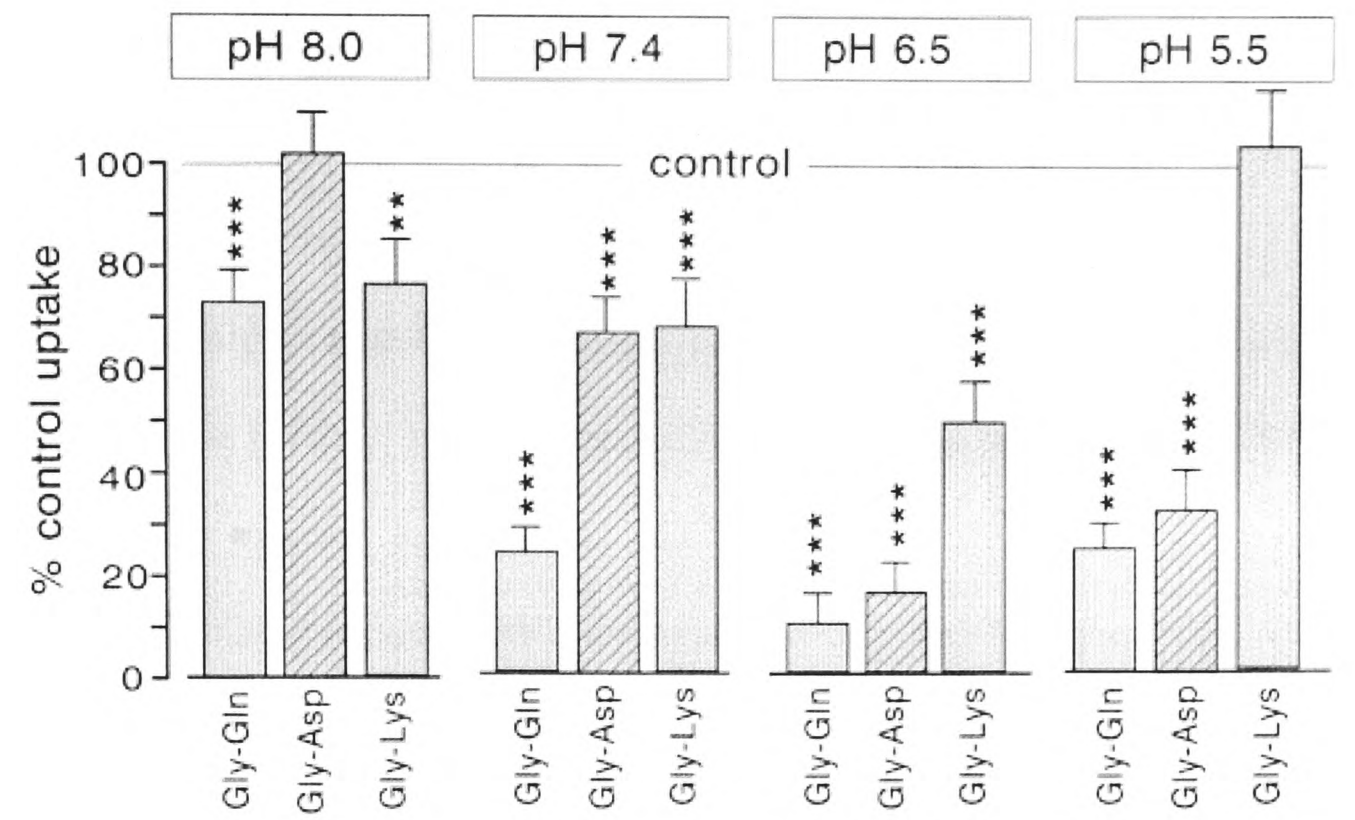
7.5.1 Evidence from previous research

Previous studies by Amasheh *et al*, 1997, have focussed on the pH dependence of transport of neutral, anionic and cationic peptides. The peptides in question were Gly-Gln, Gly-Asp and Gly-Lys, and some of the results of the research can be seen in figure 7.5. Their study concluded that transport of the neutral peptide, Gly-Gln, was mainly unaffected by pH, but that transport of the charged peptides was highly dependent on pH. The affinity of the anionic peptide for PepT1 was increased dramatically upon extracellular acidification with a concomitant increase of approximately 5-fold in the magnitude of the currents obtained. The cationic peptide however, showed only a weak affinity for PepT1 at all pH values, and evoked similar magnitude currents at pH 7.4 and 6.5 with currents decreased by 50% at pH 5.5. Gly-Lys exhibited its greatest currents at pH 8.0.

7.5.2 Evidence from this thesis

7.5.2.1 Transport of anionic peptides

In Chapter 5, I investigated the importance of position of charge in how PepT1 recognises and binds substrates. The experiments carried out in this thesis have been based on the transport of both anionic and cationic peptides. A more detailed study has been carried out on the anionic peptides, Gly-Asp and Asp-Gly, and preliminary experiments have been carried out on Gly-Lys and Lys-Gly. In chapter 5 it was shown that the currents evoked by Gly-Asp were greater at pH 5.5 than pH7.5, 417.2 ± 8.5nA compared to 55.7± 18.6nA respectively. The results obtained agreed in part with a previous study by Amasheh *et al*, 1997. The currents induced by Asp-Gly were also greater at pH 5.5, but were less than those observed for Gly-Asp. Asp-Gly



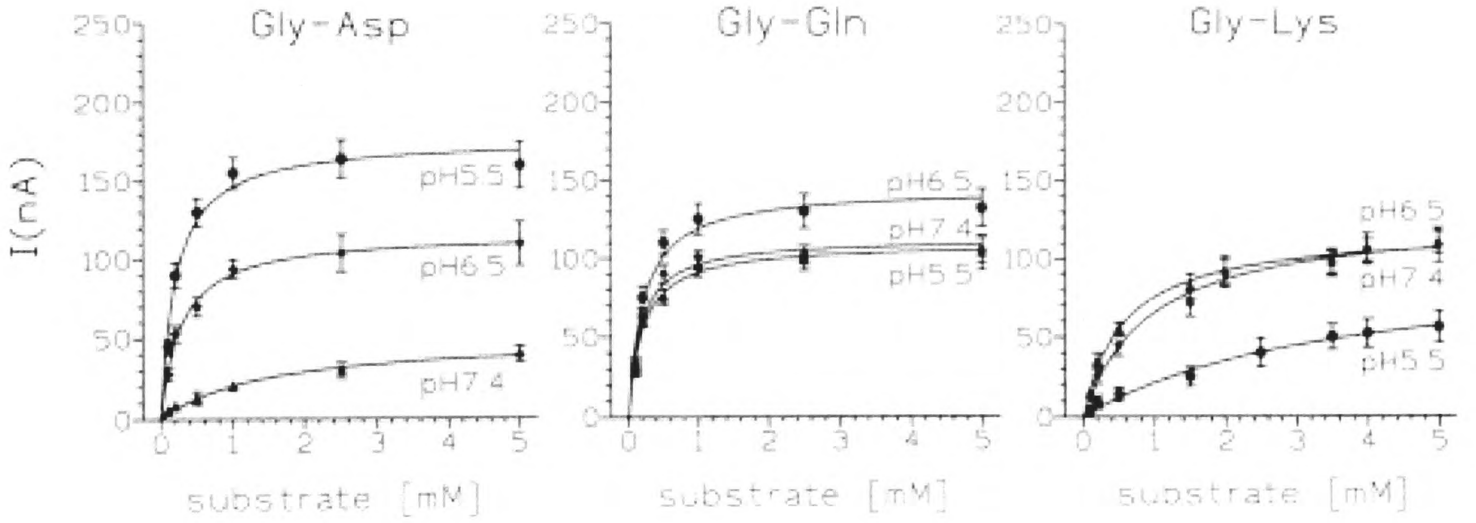


Figure 7.4 Top panel: Transport of differently charged peptides by PepT1 expressing oocytes at four pH values determined by uptake of radiolabelled D-Phe-L-Ala. Bottom panel: Concentration-dependence of transport of differently charged peptide substrates at different pH values, determined by two-electrode voltage clamping. (Reproduced from Amasheh *et al*, 1997).

was however transported to a greater degree than Gly-Asp at pH 7.5, with currents obtained being approximately 2-fold greater.

The affinity for the peptides was also altered upon extracellular acidification. The affinity for Gly-Asp increased 5-fold when the pH was changed from pH 7.5 to pH 5.5, whereas the affinity for Asp-Gly increased only 2 fold. However, the affinity for Asp-Gly was higher than Gly-Asp at pH 7.5, and the affinity of Gly-Asp was higher than Asp-Gly at pH 5.5. There is therefore a change in the order of affinity of the two peptides upon external acidification, and thus it is concluded that the position of charged amino acid residue within the peptide determines how the transporter binds the substrate.

7.5.2.2 Transport of cationic peptides

The results from the experiments using Gly-Lys and Lys-Gly were based on the currents evoked at a single concentration of peptide, therefore no data on the affinity of the molecules was available. Transport of the cationic peptides was greatest at neutral pH, again in agreement with the study by Amasheh *et al,* 1997. The transport of Gly-Lys was relatively independent of pH, with only 39nA difference between the values obtained at the two pH values, however, the transport of Lys-Gly was dependent on pH, with the transport at pH 7.5 being much greater than that seen at pH 5.5.

Time constraints meant that the concentration-dependence of peptide transport could not be carried out for Gly-Lys and Lys-Gly, and as a result no conclusions about the change, if any, in the affinity of the two substrates could be made. From preliminary data, it appeared that the trend seen for anionic peptides was not seen for positively

charged peptides. However, this topic requires further study before any solid conclusions can be made.

7.6 Regulation of PepT1

There have been a number of studies focussing on the regulation of PepT1, but none have addressed the acute regulation of PepT1. In this section the various theories for regulation will be outlined together with the evidence to support each theory. My data on regulation by protein kinase C will be incorporated into the existing theories based on regulation by phorbol esters.

7.6.1 Dietary regulation of PepT1

There have been several studies on the dietary regulation of PepT1 using either intact rat intestine, (Erickson *et al*, 1995, and Shiraga *et al*, 1999), or Caco-2 cells as the experimental model, (Walker *et al*, 1998). In each study an increase in PepT1 mRNA was observed. The study by Shiraga *et al*, however, suggested that specific amino acids and peptides were responsible for this substrate upregulation of the transporter. In particular the amino acids Phe, Lys and Arg and the peptides Gly-Sar, Gly-Phe, Lys-Phe and Ap-Lys were responsible for this stimulation of transcription of the PepT1 gene. Table 7.1 shows the data obtained in this study.

7.6.2 Hormonal regulation of PepT1

The study by Walker *et al*, mentioned above, concluded that the action of substrates on the regulation of PepT1 occurred as a direct result of action on the enterocytes themselves, with no neural or hormonal input. However, there have been two studies that provided evidence for the existence of hormonal regulation of PepT1,

Diet	Gly-Sar uptake	
	V_{max}	K_m
Protein free	2.1 ± 0.4	2.8 ±0.3
5% casein	2.0 ± 0.2	2.7 ± 0.2
20% casein	**3.6 ± 0.3***	2.7 ± 0.2
50% casein	**4.6 ± 0.2***	2.5 ± 0.2
10% Gly	2.2 ± 0.3	2.6 ± 0.3
10% Phe	**4.7 ± 0.3***	2.6 ± 0.2
20% Gly-Phe	**5.5 ± 0.4***	2.4 ± 0.5

Table 7.1 Values for uptake of 14[C]Gly-Sar in rat ileal brush border membrane vesicles from rats fed diets of different composition for 4 days. Numbers in bold are those that are significantly different from those fed no protein. Reproduced from Shiraga *et al*, 1999.

(Thamotharan *et al*, 1999 and Buyse et al, 2001). The first study was on Caco-2 cells and insulin was shown to have a rapid (within 60 minutes) stimulation of Gly-Gln uptake. The stimulation was brought about by a change in V_{max}, with no effect on K_m. In this case, there was no change seen in PepT1 gene expression, but instead there was an increase in the PepT1 protein at the apical membrane. It was concluded that when the insulin bound to its receptor, Gly-Gln uptake was stimulated by an increase of the membrane population of the transporter. A suggestion of the mechanism whereby this occurs was similar to that of GLUT 4, where there was increased translocation of PepT1 from a pre-formed cytoplasmic pool.

In the second study, Caco-2 cells and intact rat jejunum were used to study the effects of leptin on PepT1 function. Leptin significantly increased the V_{max} for Gly-Sar transport, whereas the K_m did not change. The conclusion of the study was that gastric leptin played an unexpected action in controlling ingestion of dietary proteins

7.6.3 Regulation of PepT1 by PKC

Protein kinase C (PKC) is a multifunctional protein kinase that plays a critical regulatory role in a wide variety of cellular signalling processes. PKC mediates cellular responses to second messengers and regulates a number of cellular functions including neurotransmitter synthesis and release, gene expression and ion channel function. PKC is activated physiologically by various hormones, neurotransmitters and growth factors, but as yet there is no direct evidence to link PKC activation to PepT1 activity.

Previously there have been two studies on the regulation of peptide transport by PKC. The first was a study by Brandsch *et al* in 1994 on Caco-2 cells. Treatment of the cells with phorbol esters resulted in a significant inhibition of the transport system.

Phorbol esters act on PKC by mimicking diacylglycerol. This inhibition was specific and could be blocked by addition of staurosporine, an inhibitor of PKC. In this particular case the inhibition was associated with a decrease in V_{max}, but the K_m remained the same.

In a subsequent study by Muller *et al* in 1996 also on Caco-2 cells, the cells were treated with cholera toxin, which increased cAMP levels and brought about an inhibition in PepT1 activity. Again the inhibition was associated with a decrease in V_{max}. Since there are no PKA sites in Caco-2 PepT1, it was concluded that inhibition of PepT1 by cholera toxin occurred through activation of PKC.

7.6.4 Evidence for regulation by phorbol esters

In Chapter 6 I investigated the role of phorbol esters in the regulation of PepT1. A combination of techniques was used, and inhibition of PepT1 activity by phorbol esters *X.laevis* oocytes was observed. The oocytes were incubated in the active phorbol ester, PMA, or the inactive ester, 4α PDD, for 30 minutes prior to measuring the concentration-dependence of Gly-Gln transport. The inactive ester was found to have no significant effect on either K_a or I_{max}, see table 6.4. However, PMA was found to have significant effects on both the K_a and the I_{max}, see table 6.3. These results agree in part with the previous studies where a decrease in I_{max} was observed, however this is the first study in which a decrease in K_a has also been observed. In the experiments in chapter 6 the I_{max} and K_a values decrease proportionately independent of membrane voltage. In figure 7.6 it is proposed that the $k_{1PKC} < k_{1CONTROL}$ and so the phosphorylation affects the rate of orientation of the carrier protein.

In addition, the immunocytochemical data showing a decrease in fluorescence intensity suggests that the decrease in I_{max} could be due to a decrease in the number of

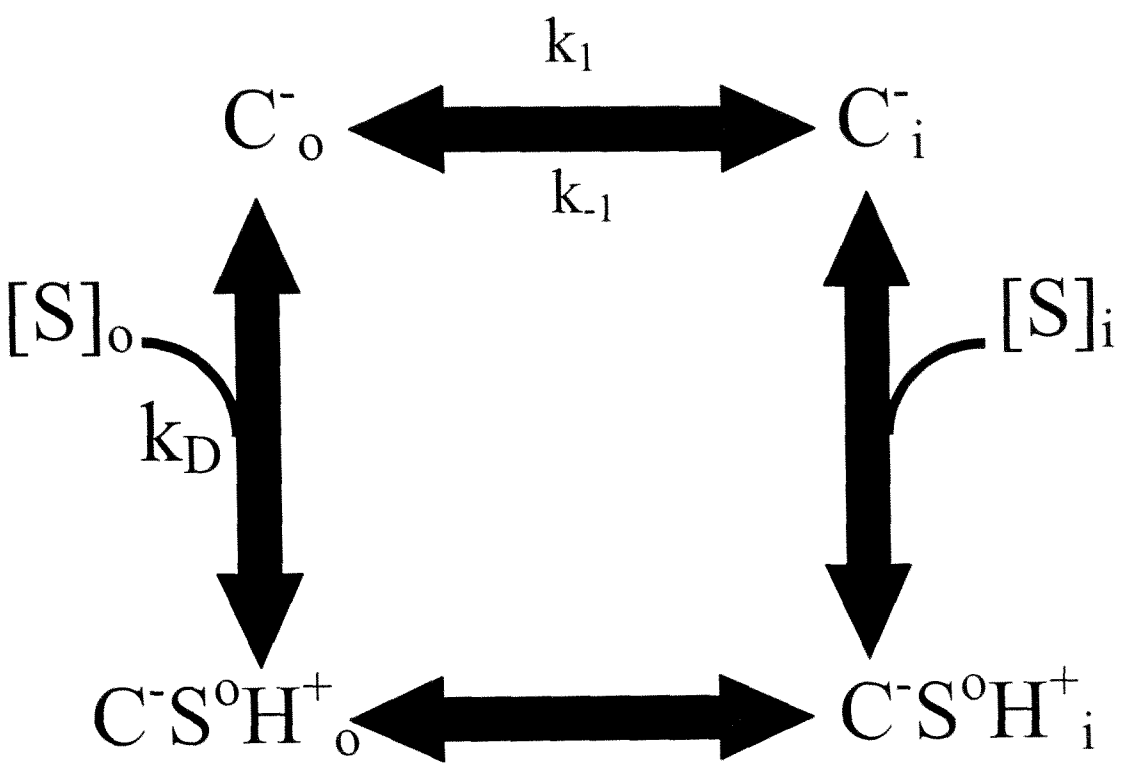


Figure 7.5 Putative model for the effects of phorbol esters on PepT1 function, where C^- is the negatively charged carrier (PepT1) and S is the substrate (peptide). The carrier alternates between C^-_o and C^-_I at a rate determined by k, and the rate of association/disassociation of the substrate with the carrier is determined by k_A/k_D.

transporters at the membrane, or that turnover of the transporter is lower. The decrease in intensity of the fluorescence could however be due to the epitope that the antibody recognises no longer existing due to a conformational change brought about by the PMA.

7.7 General conclusions and future work

This thesis has answered some of the fundamental questions of peptide transport through the intestinal PepT1 isoform. I have demonstrated that transport is electrogenic and that there is an optimum pH for peptide transport. In addition I have shown the importance of the presence of a free carboxyl terminus in substrate recognition and transport, as well as the importance of the position of charge within a peptide, and the effects on substrate transport when this charge is moved. Finally, I have demonstrated that PKC is involved in the acute regulation of PepT1. A question not yet answered is the relative importance of PepT1. The percentage of dietary protein absorbed as peptides remains elusive, although all the evidence points to PepT1 playing a major role. In 1954 it was reported that protein is absorbed within 4 hours of ingestion, however, if all the protein was to be broken down to amino acids by intestinal secretions before absorption, it would take approximately 96 hours (Fisher, 1954). The discovery of a high affinity inhibitor would greatly improve the likelihood of being able to answer this fundamental question.

There is scope for further investigation of this unique transporter. In the first instance transport of tripeptides and peptidomimetic drugs should be analysed electrophysiologically. In addition, further investigation of the regulation of PepT1 should be carried out, in particular using inhibitors of PKC to see if the inhibition observed can be abolished.

Other methods of investigation should also be considered, such as knockout mice (Rubio-Aliaga and Daniel, in press), and another new way to define the physiological functions of peptide transporters could be to use *Drosophila melanogaster* and *Caenorhabditis elegans*, both of which have homologues to mammalian PepT1.

7.8 Physiological implications

The experiments carried out in this study have furthered our knowledge of one of the most fundamental physiological processes, protein absorption. The mechanism by which protein uptake occurs is of major importance as it is a central nutritional pathway for all living organisms. Understanding how the protein we eat enters our bloodstream may help in the treatment of patients with abnormal absorption of protein e.g. Hartnup's disease. On a wider level, however, understanding the basic processes of one transporter may aid in the understanding of many of the other fundamental physiological processes of the human body.

This study has provided valuable information regarding how PepT1 recognises its substrates, as well as giving an insight into how its activity may be regulated. The formulation of the substrate template binding model has been instrumental in the design of many of the experiments in this thesis. With further study, the intricacies of protein absorption may soon be revealed.

J. Physiol. 528.P *GI Tract & Epithelial Transport* 99P

Analysis of currents induced in PepT1-expressing *Xenopus laevis* oocytes by native and carboxyl terminus modified peptides

L.A. Beattie and C.A.R. Boyd

Department of Human Anatomy and Genetics, University of Oxford, South Parks Road, Oxford OX1 3QX, UK

The electrogenic H^+–oligopeptide transporter PepT1 is required for intestinal absorption of the end products of protein digestion (Fei *et al.* 1994).

The two-electrode voltage-clamp technique was employed in oocytes expressing PepT1 to record currents evoked upon addition of free and modified peptides. As expected, these currents were dependent on both membrane voltage (V_m) and extracellular pH (pH_o).

Maximal currents I_{max} were always recorded at hyperpolarizing potentials (Fig. 1).

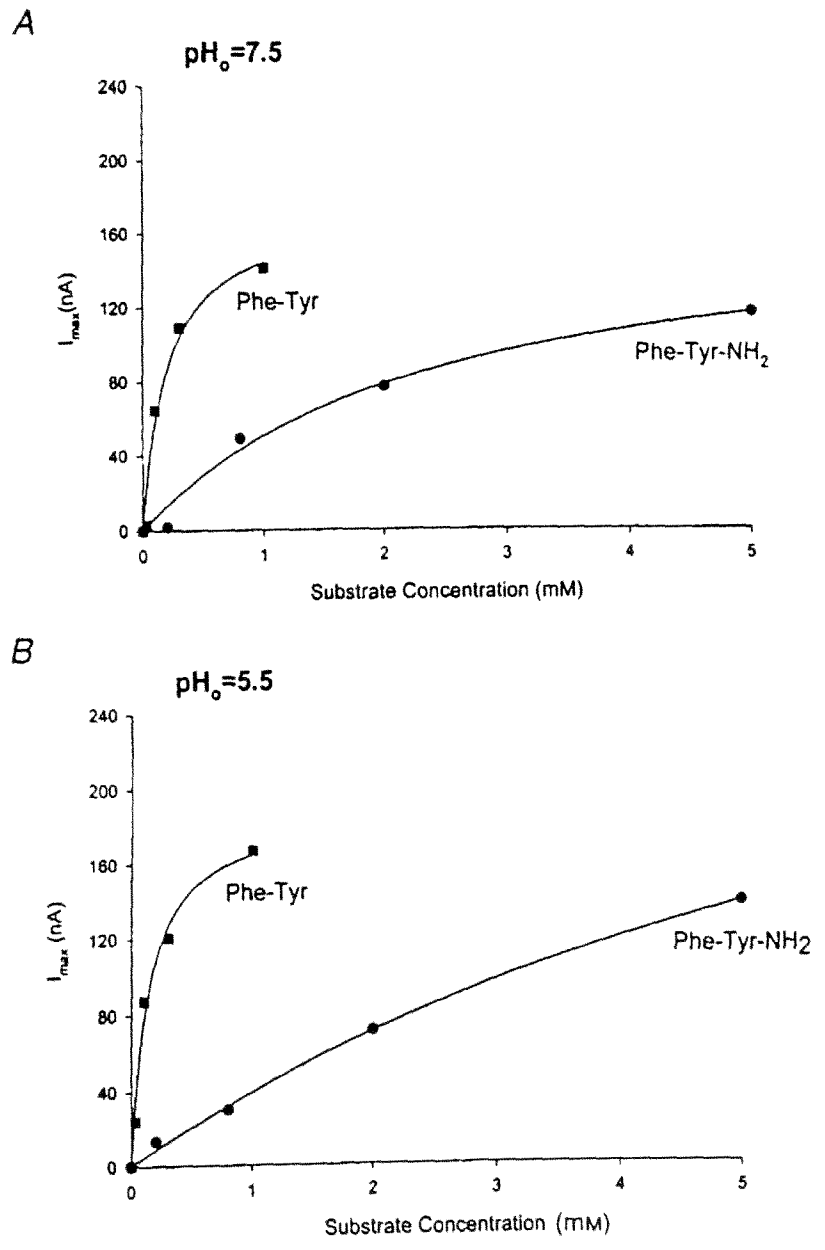


Figure 1. Steady-state current–voltage (I–V) relationships were measured in the presence and absence of the dipeptide and modified dipeptide in PepT1 oocytes. Membrane potential was held at −50 mV and stepped to test voltages between +50 and −150 mV in 10 mV increments. I_{max} for the peptide-induced currents at pH_o 7·5 (−150 mV) or 5·5 (−100 mV) were plotted as a function of substrate concentration. Solutions contained (mM): 95 NaCl, 2 KCl, 1 $CaCl_2$, 1 $MgCl_2$ and 20 Hepes or 20 MES; pH adjusted with Tris.

The affinity for modified peptide was approximately 10-fold lower than for free dipeptide, 0·59 ± 0·1 mM compared with 5·5 ± 1·6 mM at pH 7·5; and 0·14 ± 0·03 and 8·8 ± 1·8 mM at pH 5·5 (mean ± S.E.M., $n = 5$). Whereas extracellular acidification substantially increased the affinity for the native dipeptide, this was not seen for the modified peptide (no significant difference using Student's t test).

The finding that the affinity for Phe-Tyr-NH_2 does not increase on external acidification suggests that the free carboxyl group of the substrate is involved in the protonation interaction with the PepT1 binding site (Bailey *et al.* 2000).

Bailey, P.D., Boyd, C.A.R., Bronk, J.R., Collier, I.D., Meredith, D., Morgan, K.M. & Temple, C.S. (2000). *Angew. Chem. Int. Ed.* **39**, 505–508.

Fei, Y.J., Kanai, Y., Nussberger, S., Ganapathy, V., Leibach, F.H., Romero, M.F., Singh, S.K., Boron, W.F. & Hediger, M.A. (1994). *Nature* **368**, 563–566.

We thank M.A. Hediger for the PepT1 clone and The Wellcome Trust for financial support.

Modified dipeptides inhibit substrate uptake into PepT1-expressing *Xenopus* oocytes

C.J. Sword, A.A. Constantinou, I.D. Collier*, P.D. Bailey* and C.A.R. Boyd

*Department of Human Anatomy & Genetics, University of Oxford, South Parks Road, Oxford OX1 3QX and *Department of Chemistry, Heriot-Watt University, Edinburgh EH14 4AS, UK*

The epithelial peptide transporter PepT1 (Fei *et al.* 1994) has a uniquely broad substrate specificity. In addition to transporting small peptides, PepT1 is known to carry modified peptides and peptide mimics. In this study we examined quantitatively the ability of the cloned rabbit PepT1 transporter to interact with a series of modified dipeptides.

Inhibition studies between the unlabelled test compounds and tritiated D-Phe-L-Gln, a known PepT1 substrate, were carried out. Results are expressed as inhibition constants and are shown in Table 1. This series of molecules allows us to investigate the nature of PepT1 substrate binding as a function of the length of an added amino terminal hydrocarbon chain.

Berger, U.V. & Hediger, M.A. (1999). *Anat. Embryol.* **199**, 439–449.

Fujita, T., Kishida, T., Okada, N.,Ganapathy, V., Leibach, F.H. & Yamamoto, A. (1999). *Neurosci. Lett.* **271**, 117–120.

Hussain, I., Zanic-Grubisic, T. & Boyd, C.A.R. (2001). *J. Physiol.* **531.P**, 129*P*.

Takagi, H., Shiomi, H., Ueda, H. & Amano, H. (1979). *Nature* **282**, 410–412.

We thank The Wellcome Trust for financial support.

Evidence that substrate titration is not solely responsible for the effect of pH on charged peptide binding in PepT1-expressing *X. laevis* oocytes

L.A. Beattie and C.A.R. Boyd

Department of Human Anatomy & Genetics, University of Oxford, South Parks Road, Oxford OX1 3QX, UK

PepT1 displays a broad substrate range including neutral and charged dipeptides (Amasheh *et al.* 1997). However, the exact mechanism by which PepT1 transports charged peptides remains controversial. In this study we have investigated the importance of position of charge within a dipeptide using the anionic peptides Gly-Asp and Asp-Gly.

The two-electrode voltage clamp was employed in PepT1-expressing oocytes to record peptide-induced currents in response to the charged peptides at neutral and acidic extracellular pH (Fig. 1*A* and *B*).

Upon extracellular acidification, the affinity for Gly-Asp increased 5-fold, 7.96 ± 1.73 mM at pH 7.5 compared with 1.50 ± 0.15 mM at pH 5.5, whilst the affinity for Asp-Gly only increased 2-fold, 4.50 ± 0.82 mM at pH 7.5 compared with 2.09 ± 0.15 mM at pH 5.5 (mean $\pm$ S.E.M., $n = 7$).

The Gly-Asp/Asp-Gly affinity ratio at pH 7.5 is greater than 1, $P = 0.01$, whereas at pH 5.5 the ratio is less than 1, $P = 0.03$, using Student's t test.

Since extracellular acidification reverses the affinity for the two peptides, the changes observed cannot simply be due to titration of the substrate. Therefore, we must conclude that the position of the charged amino acid residue within the peptide determines how the transporter binds the peptide.

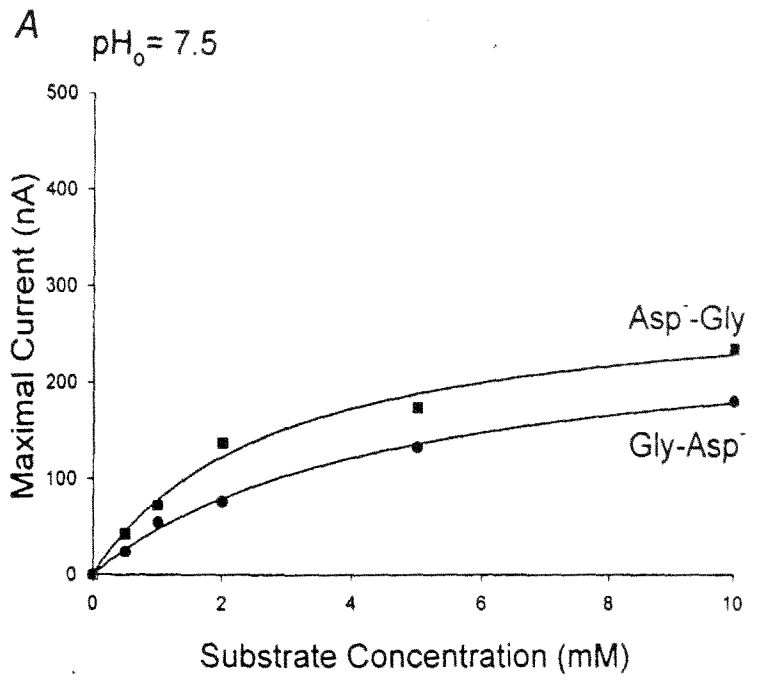


Figure 1. *A* and *B*, steady-state current–voltage (I–V) relationships were measured in the presence and absence of anionic dipeptides in PepT1 oocytes. Membrane potential was held at −50 mV and stepped to test voltages between +50 and −150 mV in 10 mV increments. I_{max} for the peptide-induced currents at pH$_o$ 7.5 or 5.5 (recorded at −150 mV) were plotted as a function of substrate concentration. Solutions contained (mM): NaCl 95, KCl 2, $CaCl_2$ 1, $MgCl_2$ 1, Hepes 20, or MES 20, pH adjusted with Tris.

Amasheh, S., Wenzel, U., Boll, M., Dorn, D., Weber, W., Clauss, W. & Daniel, H. (1997). *J. Membr. Biol.* **155**, 247–256.

We thank M.A. Hediger for the PepT1 clone and The Wellcome Trust for financial support.

Table 1. mRNA expression in PBMCs from 7 septic patients and 8 controls, expressed as % ± S.D. of that found in placental reference tissue

Transporter system	mRNA encoding protein with this activity	Control ($n = 8$)	Septic ($n = 7$)
y^+	CAT1	79 ± 40	84 ± 33
	CAT2	None detected in any sample	0.02 ± 0.03 (present in 5/7 samples)*
	CAT4	6.48 ± 10.2	0.005 ± 0.01
y^+L	CD98hc	90 ± 40	141 ± 56

*$P = 0.01$, Fisher's exact test. The possible decrease in CAT4 and increase in CD98hc expression in sepsis did not reach statistical significance.

mRNA for CAT2 is increased in PBMCs from septic patients. While the amount of CAT2 mRNA appears quantitatively small, it is not possible to conclude from this experiment whether this is functionally significant. We suggest the data presented here, combined with our previous functional data demonstrating increased y^+ activity in human PBMCs, show that CAT2 is an attractive target to selectively reduce the upregulated component of nitric oxide production in patients with septic shock.

Reade, M.C., Young, J.D. & Boyd, C.A.R. (2001). *J. Physiol.* **531.P**, 116*P*.

All work using human tissue was approved by the Central Oxfordshire Research Ethics Committee, which gave exemption from the need for informed consent from patients not competent to give it. M.C.R. is funded by a Brasenose College Oxford Graduate Scholarship and a University of Sydney Travelling Fellowship.

Protein kinase C activation directly alters the kinetics of PepT1-mediated peptide transport

L.A. Beattie and C.A.R. Boyd

Department of Human Anatomy and Genetics, University of Oxford, Oxford OX1 3QX, UK

Little research has been carried out into the acute regulation of the epithelial H^+/oligopeptide transporter, PepT1. However, one earlier study has shown downregulation of PepT1 activity in Caco-2 cells by activation of protein kinase C, but the exact mechanism by which it occurs remains unresolved (Brandsch *et al.* 1994). In this study we have investigated electrophysiologically the regulation of PepT1 using the activator of protein kinase C, PMA (phorbol 12-myristate, 13-acetate) and the inactive phorbol ester 4αPDD (4α-phorbol 12,13-didecanoate) in PepT1-expressing *Xenopus laevis* oocytes.

The two-electrode voltage clamp was employed in PepT1-expressing oocytes to record peptide-induced currents in response to the neutral peptide Gly-Gln before and after treatment with PMA and 4αPDD.

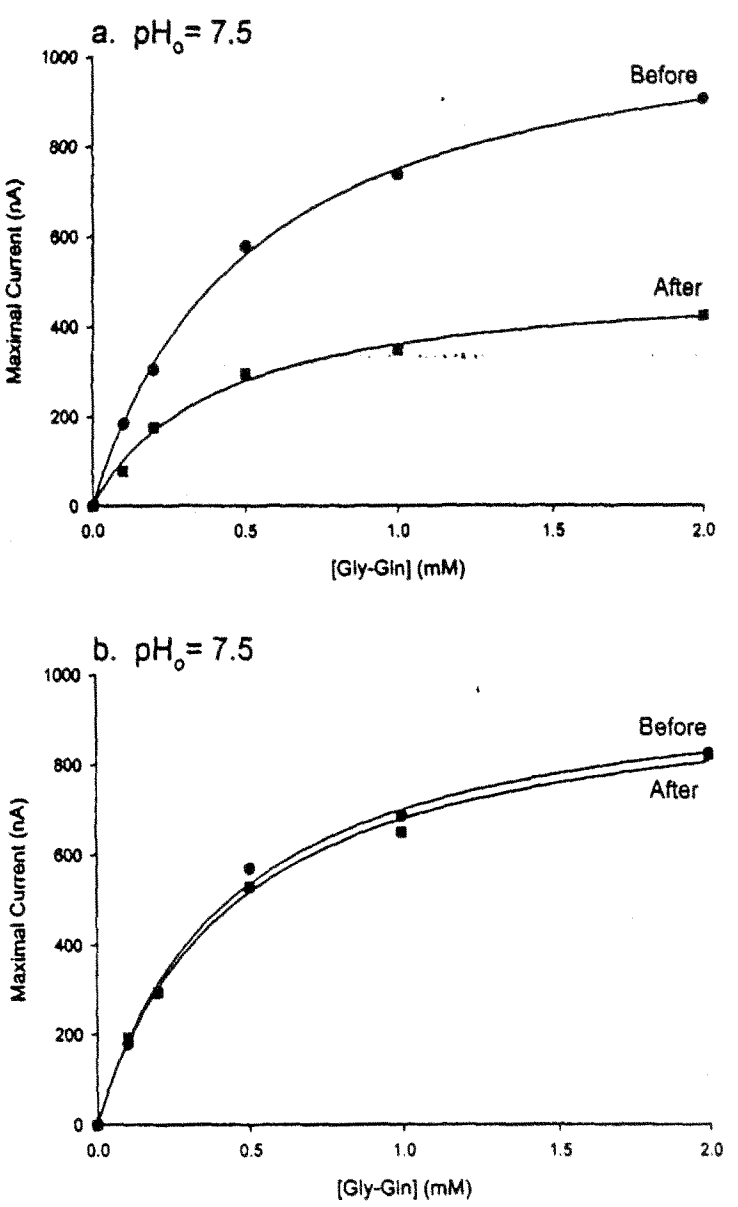


Figure 1. Steady-state current–voltage (I–V) relationships were measured in the presence of Gly-Gln in oocytes expressing rabbit PepT1 before and after (a) PMA or (b) 4αPDD treatment. Membrane potential was held at −50 mV and stepped to test voltages between +50 and −150 mV in 10 mV increments. I_{max} for the peptide-induced currents at pH$_o$ 7.5 were plotted as a function of substrate concentration ($n = 4$, mean ± S.E.M.). Solutions contained (mM): NaCl 95, KCl 2, $CaCl_2$ 1, $MgCl_2$ 1 and Hepes 20, pH adjusted with Tris, plus the appropriate concentration of Gly-Gln. Oocytes were incubated with 10 nM PMA or 4αPDD for 30 min.

Following incubation in PMA the K_m for Gly-Gln decreased 2-fold, 0.6 ± 0.08 mM compared with 0.3 ± 0.05 mM (mean ± S.E.M., $n = 4$). V_{max} decreased

2.2-fold upon treatment with PMA, 920.2 ± 39.3 nA compared with 422.7 ± 16.8 nA (mean ± S.E.M., $n = 4$). Values are statistically significant using Student's t test with $P < 0.05$ for K_m values and $P < 0.001$ for V_{max} values. Control experiments using 4αPDD showed no change in K_m or V_{max} (see Fig. 1*B*).

We conclude that PepT1 is under the regulatory control of protein kinase C. PMA downregulates PepT1 activity under conditions when driving forces are not altered, suggesting that phosphorylation of the PepT1 protein itself may alter the K_m and V_{max}.

Brandsch, M., Miyamoto, Y., Ganapathy, V. & Leibach, F. (1994). *Biochem. J.* **299**, 253–260.

We thank M.A. Hediger for the PepT1 clone and The Wellcome Trust for financial support.

Regulation of the vitamin C transporter SVCT1 in Caco-2 cells

Paul Sharp, Lauren MacDonald and Alfred Thumser

School of Biomedical and Life Sciences, University of Surrey, Guildford GU2 7XH, UK

Vitamin C (ascorbic acid) is an essential nutrient, which is involved in a number of cellular processes. However, unlike most mammals, humans are unable to synthesize vitamin C and it must therefore be acquired from the diet. This is thought to be achieved by two transporters, SVCT1 and SVCT2, recently cloned from rat (Tsukaguchi *et al.* 1999) and human kidney (Daruwala *et al.* 1999). Tissue distribution suggests that SVCT1 is the predominant transporter in the intestine (Tsukaguchi *et al.* 1999), and subsequent studies have shown that SVCT1 is functionally expressed in the human intestinal Caco-2 cell line (Wang *et al.* 1999). Vitamin C supplements are becoming increasingly common, adding greatly to the dietary load. However, little is known regarding the effects of vitamin supplements on intestinal physiology. There are reports that taking high doses of vitamin C can reduce the percentage absorption of the vitamin and that the unabsorbed fraction is retained within the intestine, producing mild diarrhoea (reviewed in Bates, 1997). The aim of our study was to investigate the effect of high doses of ascorbate on SVCT1 expression, using the Caco-2 cell model of small intestinal enterocytes.

Caco-2 cells were cultured for 21 days on Anapore inserts and incubated for the final 24 h in the presence of ascorbic acid (4.5 mg ml^{-1} of culture medium). L-[^{14}C]ascorbic acid uptake (100 μM) was measured by scintillation counting. The effects of ascorbate on SVCT1 expression were determined by RT-PCR using transporter-specific primers. Parallel experiments measured β-actin mRNA as a control. Band densities were analysed using Scion Image software and data expressed as a ratio of SVCT1 : β-actin for each sample. All data are the means ± S.E.M. of four experiments. Statistical analysis was performed using Student's unpaired t test.

Ascorbic acid uptake by Caco-2 cells showed typical exponential kinetics and had a half-time of 2.1 min. Following incubation with ascorbate for 24 h, uptake was decreased significantly (control, 0.37 ± 0.03 nmol cm^{-2} h^{-1}; ascorbate, 0.18 ± 0.01 nmol cm^{-2} h^{-1}, $P < 0.05$). Interestingly, expression of SVCT1 was also significantly reduced by exposure to elevated levels of ascorbate for 24 h (control, 71.8 ± 12.6 a.u.; ascorbate, 16.9 ± 5.0 a.u., $P < 0.01$), whereas β-actin levels were unaffected. Taken together, these data suggest that multi-gram supplements might not be the most appropriate way of increasing the body pool of vitamin C.

Bates, C.J. (1997). *Eur. J. Clin. Nutr.* **51**, suppl.1, S28–33.

Daruwala, R., Song, J., Koh, W.S., Rumsey, S.C. & Levine, M. (1999). *FEBS Lett.* **460**, 480–484.

Tsukaguchi, H., Toki, T., Mackenzie, B., Berger, U.V., Chen, X.-Z., Wang, Y., Brubaker, R.F. & Hediger, M.A (1999). *Nature* **399**, 70–75.

Wang, H., Dutta, B., Huang, W., Devoe, L.D., Leibach, F.H., Ganapathy, V. & Prasad, P.D. (1999). *Biochim. Biophys. Acta* **1461**, 1–9.

Neutral amino acid transport via system L at the basolateral membrane of human intestinal Caco-2 cell monolayers

Lee R.R. McCloy*, Peter M. Taylor† and David T. Thwaites*

**Department of Physiological Sciences, Medical School, Framlington Place, Newcastle upon Tyne NE2 4HH and †Division of Molecular Physiology, MSI/WTB Complex, University of Dundee, Dundee DD1 5EH, UK*

The recent explosion in molecular information has led to the suggestion that amino acid transport across epithelial cells is mediated at least partly by heterodimeric protein complexes (Verrey *et al.* 1999). To identify which putative transport proteins are involved in system L-like transport at the basolateral membrane of the human intestinal cell line Caco-2, we have investigated the Na^+-independent component of neutral amino acid transport. Specific PCR primers were designed using the published human sequences of the heavy chain subunits (rBAT and 4F2hc) and the system L-like light chain subunits (LAT1 and LAT2). RT-PCR using Caco-2 mRNA produced bands of the expected sizes for LAT1, LAT2, 4F2hc and rBAT when visualised after separation on a 1% agarose

APPENDIX II

PRELIMINARY STUDIES ON THE TRANSPORT OF N-FORMYL-MET-LEU-PHE - A BIOLOGICALLY ACTIVE MOLECULE

AII.1 Introduction

N-Formyl-L-methionyl-L-leucyl-L-phenylalanine, or N-Formyl-Met-Leu-Phe, is a chemotactic peptide produced by enteric flora. It has been implicated as being one of the major contributing factors in inflammatory bowel disease. It is a potent inducer of leukocyte chemotaxis and a macrophage activator. Receptors for formylpeptides have been found on phagocytic neutrophils and have recently been identified on cells of the intestinal mucosa, at the subepithelial level in the lamina propria (Anton *et al*, 1998). Studies of the structural requirements have shown that the formyl group is essential, as well as the methionine residue at position one, see figure AII.1 for the structure of N-Formyl-Met-Leu-Phe.

The transport of this chemotactic peptide has been studied electrophysiologically in PepT1 expressing *Xenopus laevis* oocytes.

AII.2 Methods

Currents were recorded using the two-electrode voltage-clamp technique in response to application of 2mM N-Formyl-Met-Leu-Phe to the experimental bath solution. The two-electrode voltage-clamp technique was used to record these currents induced by transport of the peptide at pH 7.5 and 5.5. Briefly the membrane was held at –50mV and stepped to test voltages between –150mV and +50mV in 10mV increments. The steady-state current-voltage relationships were plotted.

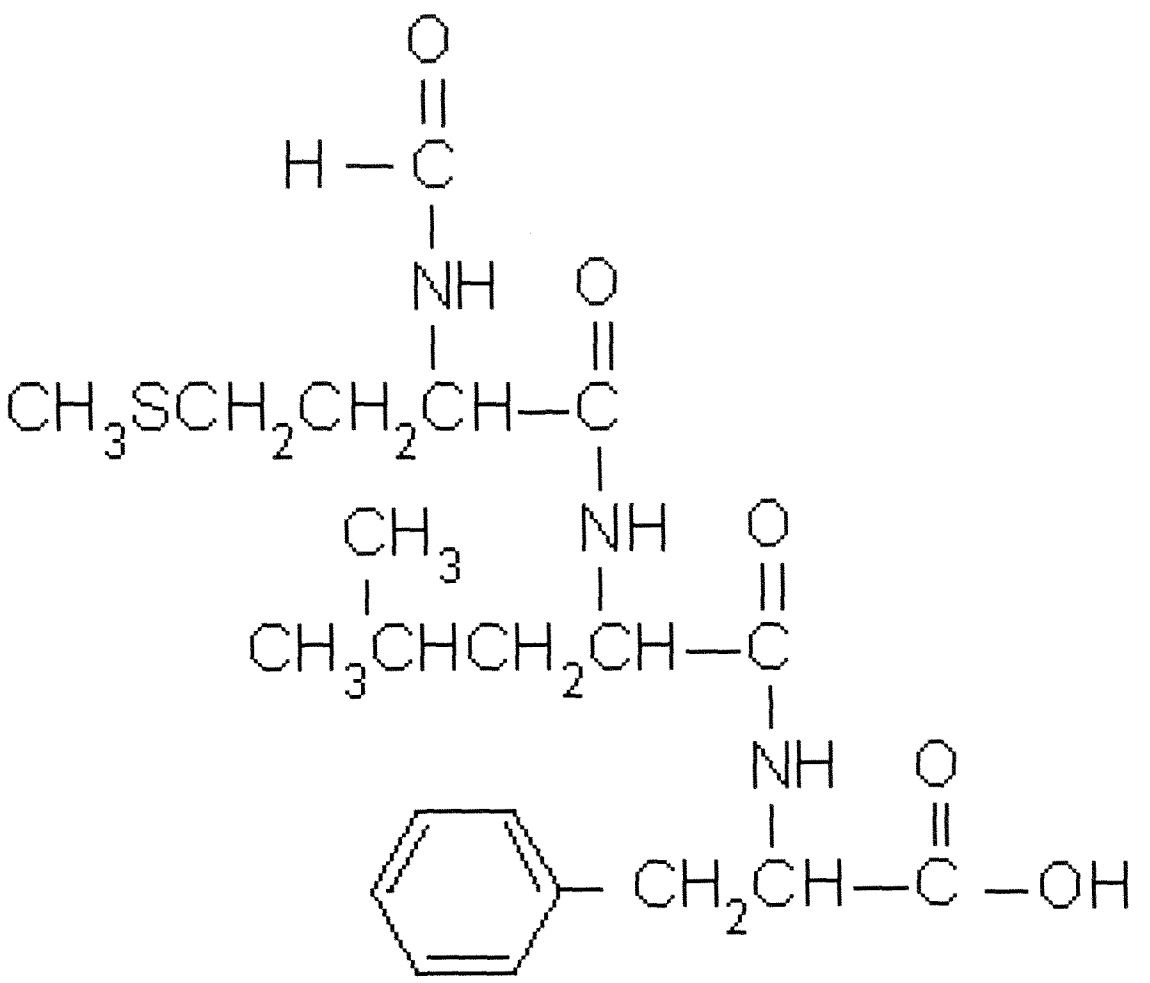


Figure AII.1 Structure of N-Formyl-Met-Leu-Phe (reproduced from www.sigma-aldrich.com.)

AII.2 .1 Solutions

The solutions used in these experiments composed of 95mM NaCl, 2mM KCl, 1mM $CaCl_2$, 1mM $MgCl_2$, 20mM HEPES, or 20mM MES adjusted to the appropriate pH with Tris. A single concentration of 2mM N-Formyl-Met-Leu-Phe was added to the solution, and the pH corrected to either pH 7.5 or 5.5.

AII.3 Results

There was a marked difference in the response to N-Formyl-Met-Leu-Phe between pH 7.5 and 5.5. The voltage at which maximal currents were observed in both cases were considerably different. The maximal current observed for 2mM N-Formyl-Met-Leu-Phe at pH 7.5 was observed at –150mV, which is in agreement with transport of most other peptides. However, at pH 5.5, the maximal current was observed at +50mV, a trend not previously seen for the transport of any peptide substrate. The maximal current obtained by N-Formyl-Met-Leu-Phe at pH 5.5 was in the opposite direction to all other peptide induced currents in this thesis, i.e. outward compared to inward.

The maximal currents obtained were also different at each pH, with a value of 14 ± 1.1nA recorded at pH 7.5 and 38 ± 2.7nA at pH 5.5. These currents are the smallest obtained for any substrate tested in this thesis. Figures AII.2 and AII.3 show examples of the I-V curves obtained for 2mM N-Formyl-Met-Leu-Phe at each pH in PepT1 expressing oocytes.

Similar experiments were carried out in control water injected oocytes, and the results can be seen in figures AII.4a and b. No currents in response to this peptide could be measured in control oocytes, in agreement with the results for all other peptides in control oocytes.

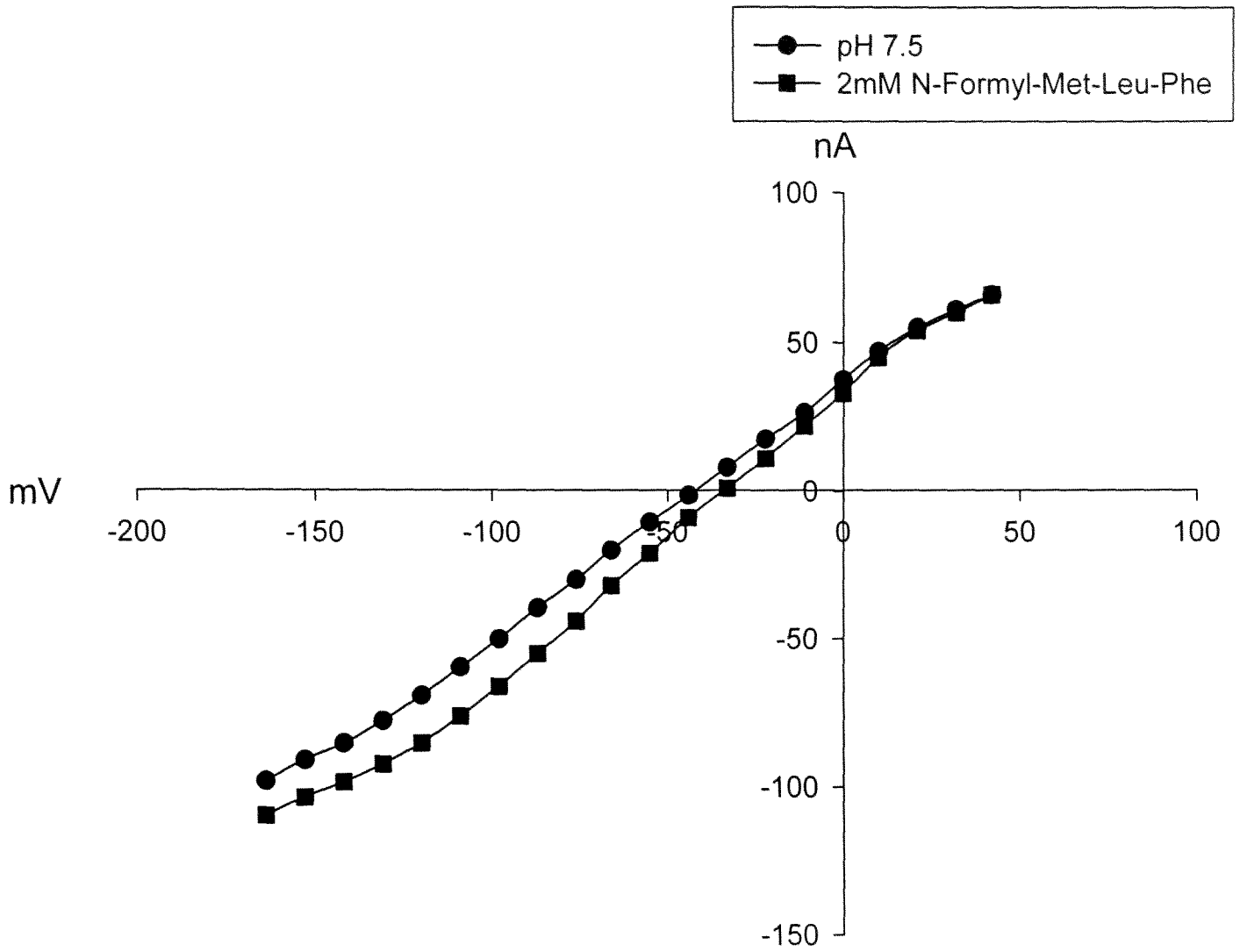


Figure AII.2 Steady-state I-V curves recorded in a PepT1 expressing oocyte in the presence and absence of 2mM N-Formyl-Met-Leu-Phe at pH 7.5 (data representative of one oocyte).

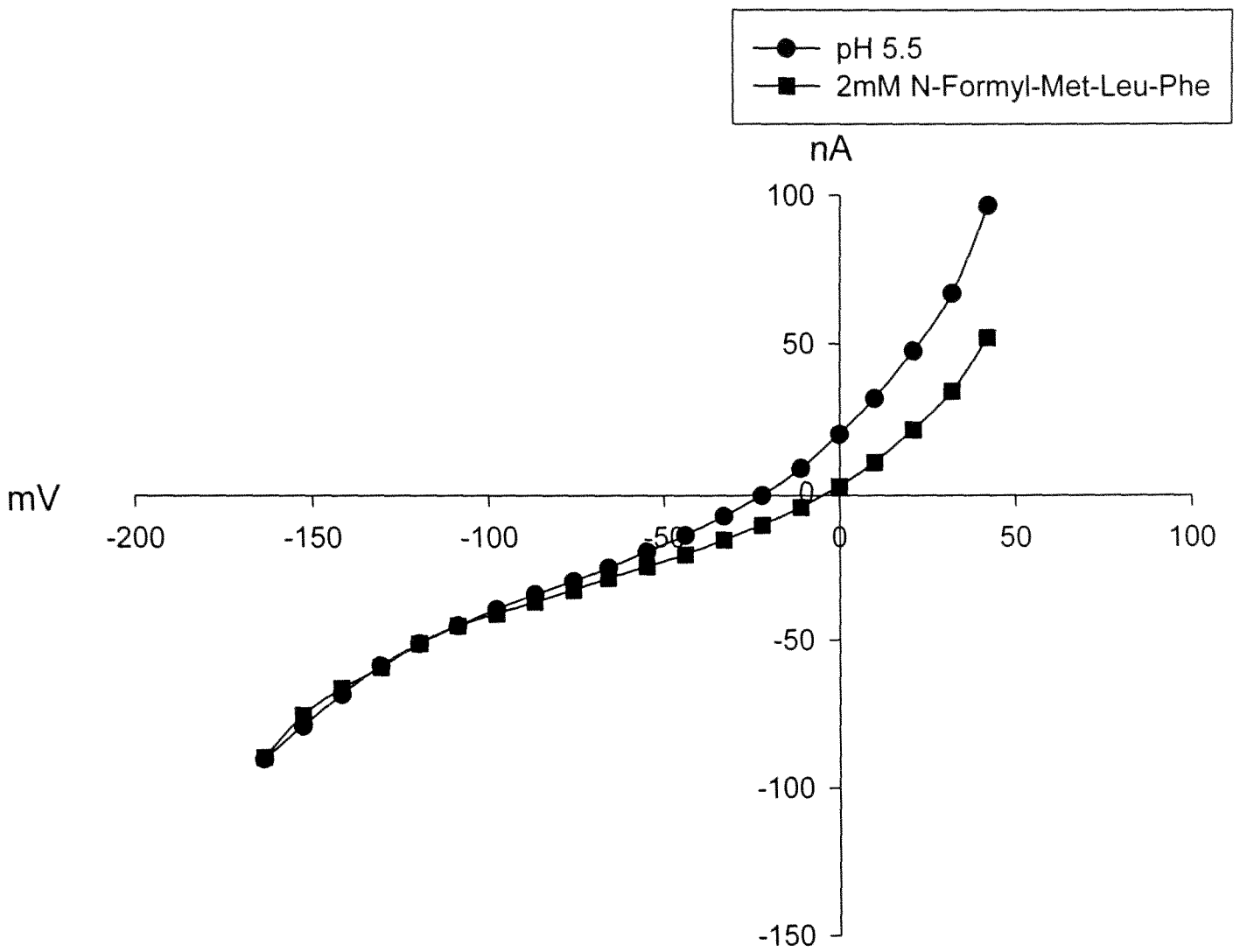
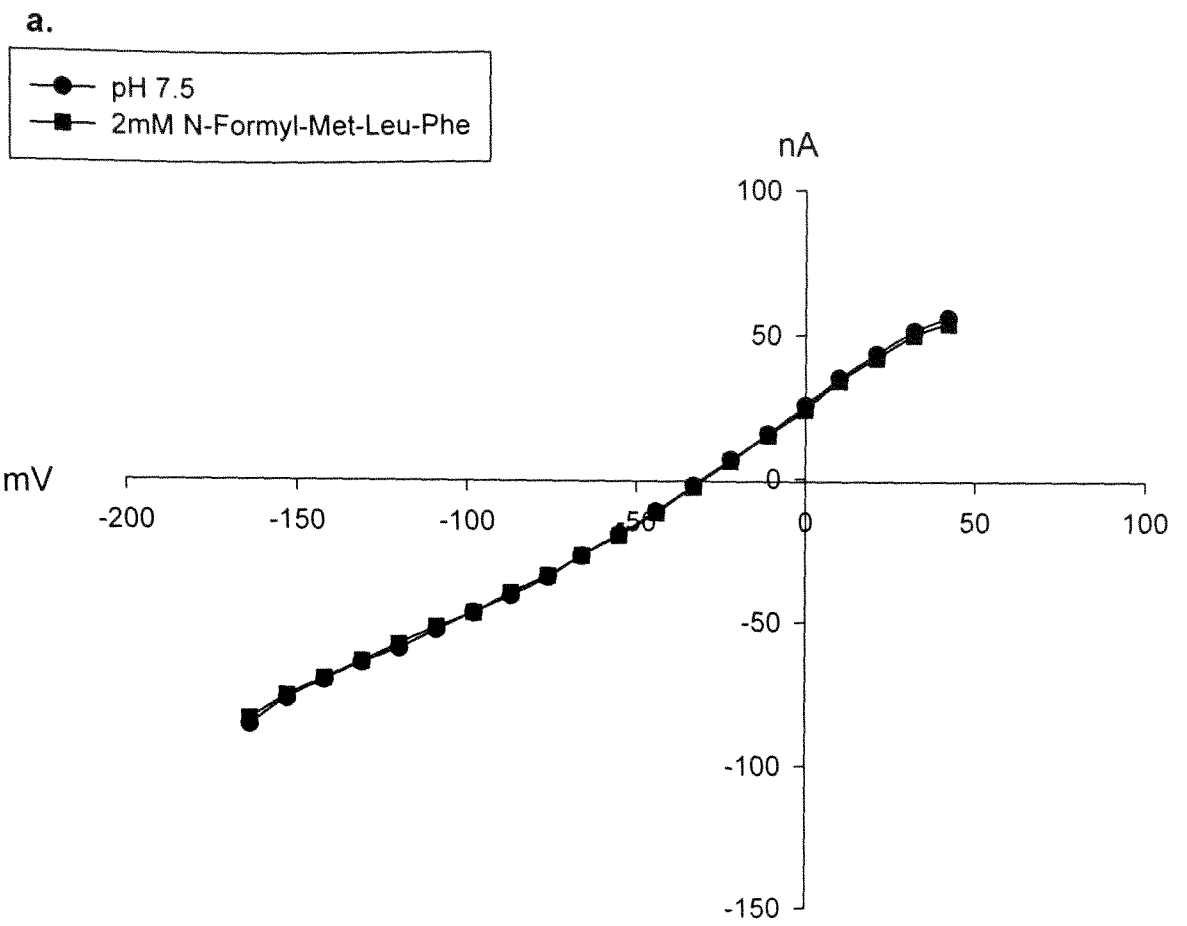


Figure AII.3 Steady-state I-V curves recorded in a PepT1 expressing oocyte in the presence and absence of 2mM N-Formyl-Met-Leu-Phe at pH 5.5 (data representative of one oocyte).

	Maximal current (nA)	**Voltage**
pH 7.5	14.4 ± 1.1 (inward)	-150mV
pH 5.5	38 ± 2.7nA (outward)	+50mV

Table AII.1 Maximal current values obtained, and the voltage at which they were recorded, in response to 2mM N-Formyl-Met-Leu-Phe, (mean ± s.e.m, n=5).



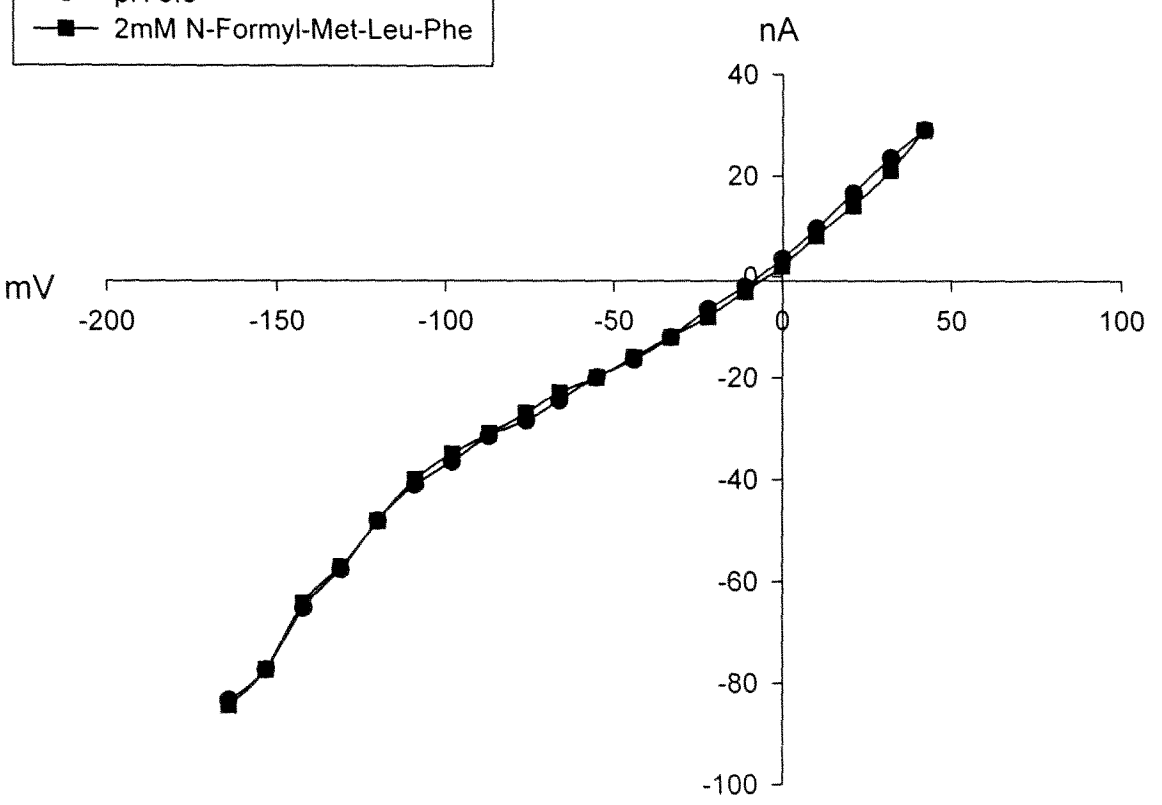


Figure AII.4a Steady-state I-V curves recorded in a control oocyte in the presence and absence of 2mM N-Formyl-Met-Leu-Phe at pH 7.5, and b. at pH 5.5 (data representative of one oocyte).

AII.4 Summary

1. N-Formyl-Met-Leu-Phe is a substrate for PepT1.

2. Transport of this peptide is markedly different at pH 7.5 compared to pH 5.5.

3. There are no peptide-induced currents recorded in control oocytes.

4. Further experiments are required, including the concentration-dependence of N-Formyl-Met-Leu-Phe transport before any additional conclusions can be made.

APPENDIX III

PRELIMINARY EXPERIMENTS INVESTIGATING THE ROLE OF INTRACELLULAR pH ON PEPTIDE TRANSPORT

AIII.1 Introduction

Transport of peptides via PepT1 is known to utilise the transmembrane proton gradient that exists across the brush border membrane of the small intestine. The extracellular pH plays an important role in this peptide uptake, with changes in pH greatly affecting the rate of peptide absorption. The role of extracellular pH has been investigated and pH 5.5-6.0 has been found to be the optimum pH for peptide transport. The part played by intracellular pH had not been investigated until the study reported by Kelly and Boyd, 2001. In this study the effects of changing intracellular pH on the influx of peptides into PepT1 expressing oocytes was investigated. The manipulation of intracellular pH (pH_I) was carried out using a method devised by Quick *et al,*2001 whereby sodium and potassium acetate were used to change decrease intracellular pH either in the presence or absence of a membrane potential.

The study by Kelly and Boyd will be reported here, in addition to the results of electrophysiological experiments based on this study.

AIII.2 Methods

AIII.2.1 Electrophysiology

The two-electrode-voltage clamp technique was used to record currents induced by Gly-Asp and Asp-Gly in the presence and absence of 25mM sodium acetate at pH 7.5 in PepT1 expressing oocytes. The concentration dependence of this transport was measured using the concentrations of peptides as follows; 0, 0.5mM, 1mM, 2mM, 5mM and 10mM, of the peptides in uptake solution comprising of 95mM NaCl, 2mM KCl, 1mM $CaCl_2$, 1mM $MgCl_2$, 20mM HEPES, or 20mM MES adjusted to the appropriate pH with Tris. Standard I-V curves were plotted for each separate concentration and concentration-dependence curves were plotted in order to determine the K_a and I_{max} values for each peptide in both conditions.

AIII.2.2 Radiolabelled influx studies

5 PepT1 oocytes were incubated for each experimental condition in 100µl uptake solution containing the appropriate test substrate and 0.42µM ^{3}[H]-D-Phe-L-Gln. The oocytes were incubated for 1 hour at 19°C and then immediately washed in ice-cold Barth's solution, (5 x 1ml), before being placed into individual scintillation vials. The oocytes were disrupted using 100µl of 2% SDS before 4ml of scintillation fluid was added and the radioactivity of the oocyte contents were measured in a liquid scintillation counter. Inhibition constants, K_I and V_{max} were calculated.

AIII.3 Results

AIII.3.1 Electrophysiology

The concentration-dependence of Gly-Asp and Asp-Gly in the presence and absence of 25mM sodium acetate can be seen in figure AIII.1. A similar experiment could not

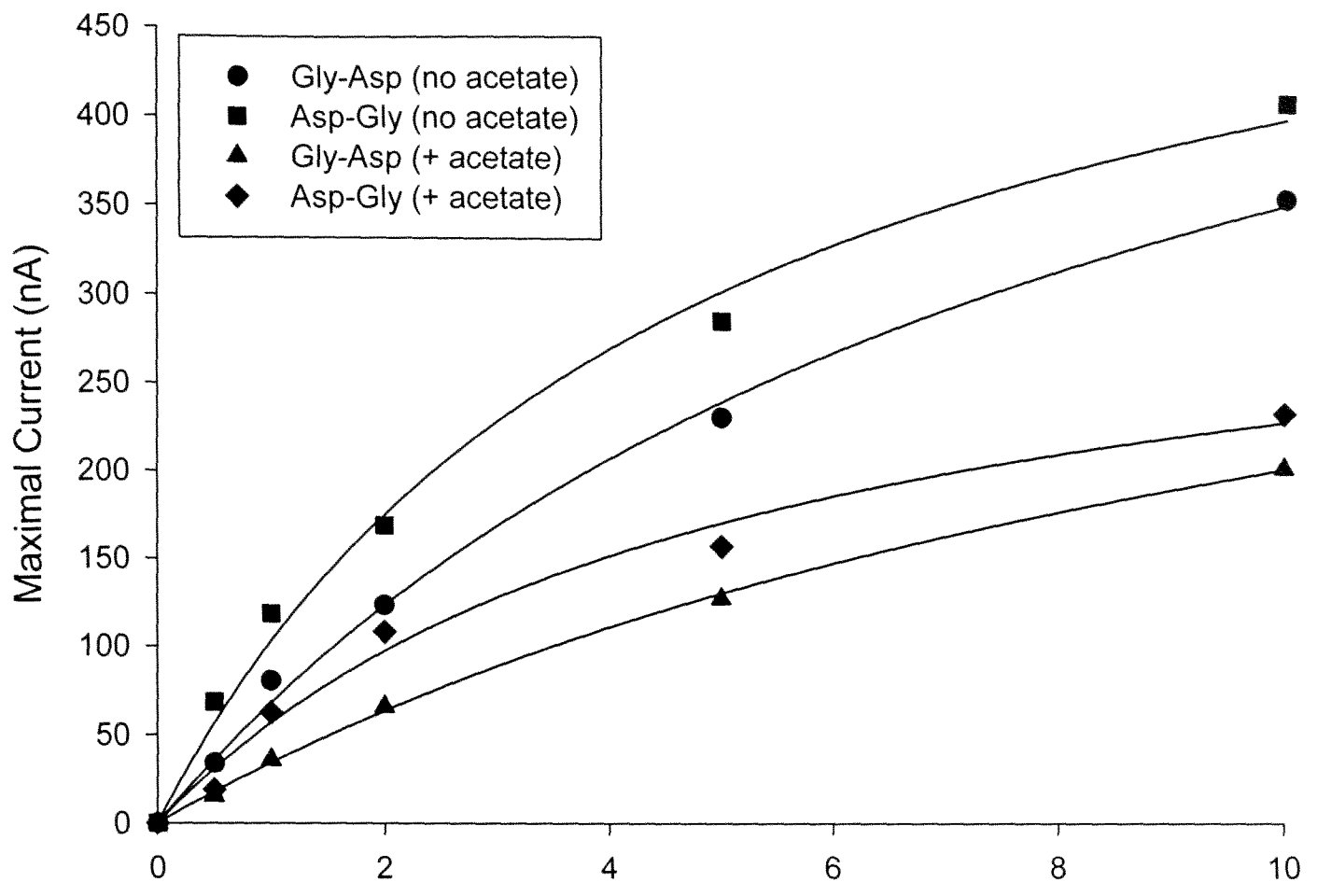


Figure AIII.1 Concentration dependence of Gly-Asp and Asp-Gly transport in the presence or absence of 25mM sodium acetate at pH 7.5 (data representative of one oocyte).

be carried out at pH 5.5 as the currents observed were very leaky, and eventually the oocytes burst.

The maximal currents obtained for Gly-Asp occurred at pH 7.5 (consistent with findings in Chapter 5) with values of 655.1 ± 52.2nA at pH 7.5 compared to 588.8± 46.3nA for Asp-Gly. The values for the K_a were also in agreement with previous studies with 8.6 ± 1.2mM for Gly-Asp and 4.7 ± 0.80mM for Asp-Gly, mean ± s.e.m, n=3.

When the intracellular pH was increased by the addition of 25mM sodium acetate to the extracellular solution, there were marked decreases in the I_{max} and increases in the values for K_a for both peptides. The maximal currents for Gly-Asp decreased from 655.1 ± 52.2nA to 445.6 ± 25.0nA, an approximate 1.5-fold reduction in I_{max}. Similarly the maximal current for Asp-Gly was reduced from 588.8 ± 46.3nA to 345.8 ± 39.5nA, an approximate 1.7-fold reduction in I_{max} in response to intracellular acidification, (mean ± s.e.m, n=3).

The K_a for Gly-Asp was increased 1.4-fold from 8.6 ± 1.2mM to 12.0 ± 1.1mM upon intracellular acidification, and the values for Asp-Gly also increased by approximately 1.1-fold from 4.7 ± 0.80mM to 5.1 ± 1.2mM, (mean ± s.e.m, n=3). Table AIII.1 shows the values for K_a and I_{max} for both peptides in both conditions.

Substrate	pH	K_a (mM)	I_{max} (nA)
Gly-Asp	7.5	8.6 ± 1.2	655.1 ± 52.2
Asp-Gly	7.5	4.7 ± 0.80	588.8 ± 46.3
Gly-Asp (acetate)	7.5	12.0 ± 1.1	445.6 ± 25.0
Asp-Gly (acetate)	7.5	5.1 ± 1.2	345.8 ± 39.5

Table AIII.1 K_a and I_{max} values for Gly-Asp and Asp-Gly transport in PepT1 expressing oocytes in the presence and absence of 25mM sodium acetate at pH 7.5, mean ± s.e.m, n=3.

AIII.3.2 Radiolabelled influx experiments

Radiolabelled influx experiments were carried out in the presence of increasing concentrations of either sodium or potassium acetate (E_m = negative or E_m = 0, respectively). The effect of this intracellular acidification on both the K_i and the V_{max} for influx of ^{3}[H]-D-Phe-L-Gln can be seen in figure AIII.2

Increasing the pH_i by addition of the acetate salts resulted in a decrease in the K_i from 0.95 ± 0.33mM with no sodium acetate present, to 0.17 ± 0.04mM with 75mM sodium acetate, and from 1.33 ± 0.33mM to 0.26 ± 0.18mM for potassium acetate (mean ± s.e.m, n=3).

The V_{max} values were also decreased substantially upon increased acetate salt composition of the extracellular medium. Indeed the V_{max} decreased from 1.35 ± 0.58 mmol/oocyte/hour to 0.01 ± 0.002 mmol/oocyte/hour upon increasing the concentration of sodium acetate from 0mM to 75 mM, and 0.95 ± 0.25mmol/oocyte/hour to 0.02 ±0.01mmol/oocyte/hour upon increasing the concentration of potassium acetate (mean ± s.e.m, n=3).

These results are consistent with those obtained by the two-electrode voltage clamp. The preliminary results are consistent with the model of transport reported by Temple *et al*, 1996, where an unloaded carrier carries a net negative charge and it is the conformational change of the carrier between inward and outward facing that is rate limiting. The increase in intracellular concentration of protons results in a decreased rate of influx of peptide and an increased affinity of the peptide for the transporter, PepT1.

A

[acetate] (mM)	K_i (mM)	
	E_m=-ve	E_m= 0
0	0.95 ± 0.33	1.33 ± 0.33
25	0.24 ± 0.06	0.74 ± 0.39
50	0.20 ± 0.02	0.30 ± 0.14
75	0.17 ± 0.04	0.26 ± 0.18

B

[acetate] (mM)	V_{max} (mmol/oocyte/hour)	
	E_m=-ve	E_m= 0
0	1.35 ± 0.58	0.95 ± 0.25
25	0.12 ± 0.03	0.10 ± 0.02
50	0.03 ± 0.01	0.04 ± 0.01
75	0.01 ± 0.002	0.02 ± 0.01

Figure AIII.2 K_i and V_{max} values for 3[H]-D-Phe-L-Gln uptake into PepT1 expressing oocytes in the presence of increasing concentrations of sodium (E_m = -ve) and potassium acetate (E_m = 0), (mean ± s.e.m, n=3) (reproduced from Kelly and Boyd, 2001).

APPENDIX IV

THE 'STATIC HEAD' METHOD TO ESTIMATE INTRACELLULAR PEPTIDE SUBSTRATE CONCENTRATION: A NOVEL ELECTROPHYSIOLOGICAL APPLICATION

AIV.1 Introduction

In Chapter 4, the role of pH in PepT1-mediated transport was investigated. Transport of 2mM Leu-Ala was recorded at various pH values between pH 5.0 and pH 8.0 in 0.5 unit intervals. This data can be used to investigate the effect of the change in extracellular pH on the static head condition, i.e. when the system is balanced and there is no net transport, this is analogous to the reversal potential, E_{rev} for an ion conductance through a channel.

AIV.2 Reversal potential and the Goldman-Hodgkin-Katz equation

The reversal potential for a membrane protein is the potential at which no net current is observed, that is, the potential that exactly balances the driving forces for ion flow across the membrane. As stated in Chapter 1, the Goldman-Hodgkin-Katz equation is used to calculate the resting membrane potential, or the potential at which no net current flow occurs. This equation below describes the resting membrane potential of a typical cell:

$$E_{rev} = \frac{RT}{F} \ln \frac{P_K [K]_o + P_{Na} [Na]_o + P_{Cl} [Cl]_i}{P_K [K]_i + P_{Na} [Na]_i + P_{Cl} [Cl]_o}$$

where E_{rev} is the reversal potential or zero-current potential. If only one permeant ion is present then E_{rev} becomes the Nernst potential for that ion. If there is more than one permeant ion present, then E_{rev} is a weighted mean of all the Nernst potentials.

AIV.3 Methods

The two-electrode voltage-clamp technique was used to record inward current induced by 2mM Leu-Ala at varying extracellular pH values in PepT1 expressing *Xenopus laevis* oocytes. Briefly, the membrane was held at –50mV and stepped to test potentials of +50mV to –150mV in 10mV increments. Steady-state I-V curves were plotted at each pH value in the presence and absence of peptide, (see figure 3.8 a-g). The reversal potential at each pH was plotted as a function of extracellular pH to determine the effect of pH on the reversal potential of PepT1.

AIV.4 Results

The absolute peptide-induced currents obtained at each pH value were plotted in figure AIV.1. Maximal currents were obtained at pH 5.5 with currents of 942.9 ± 7.07nA compared to the smallest currents obtained at pH 8.0, 574.4 ± 7.64nA, mean ± s.e.m, n = 5, (see table 3.6 in Chapter 3 for the maximal currents induced at each pH value).

The peptide-induced current measured at each pH when the membrane potential was 0mV was plotted against extracellular pH, and the theoretical reversal potential for peptide transport via PepT1 was calculated. The results can be seen in figure AIV.2. The solid line on the graph is a linear regression drawn using the experimental data points and the dashed line is a theoretical regression extrapolated beyond the data

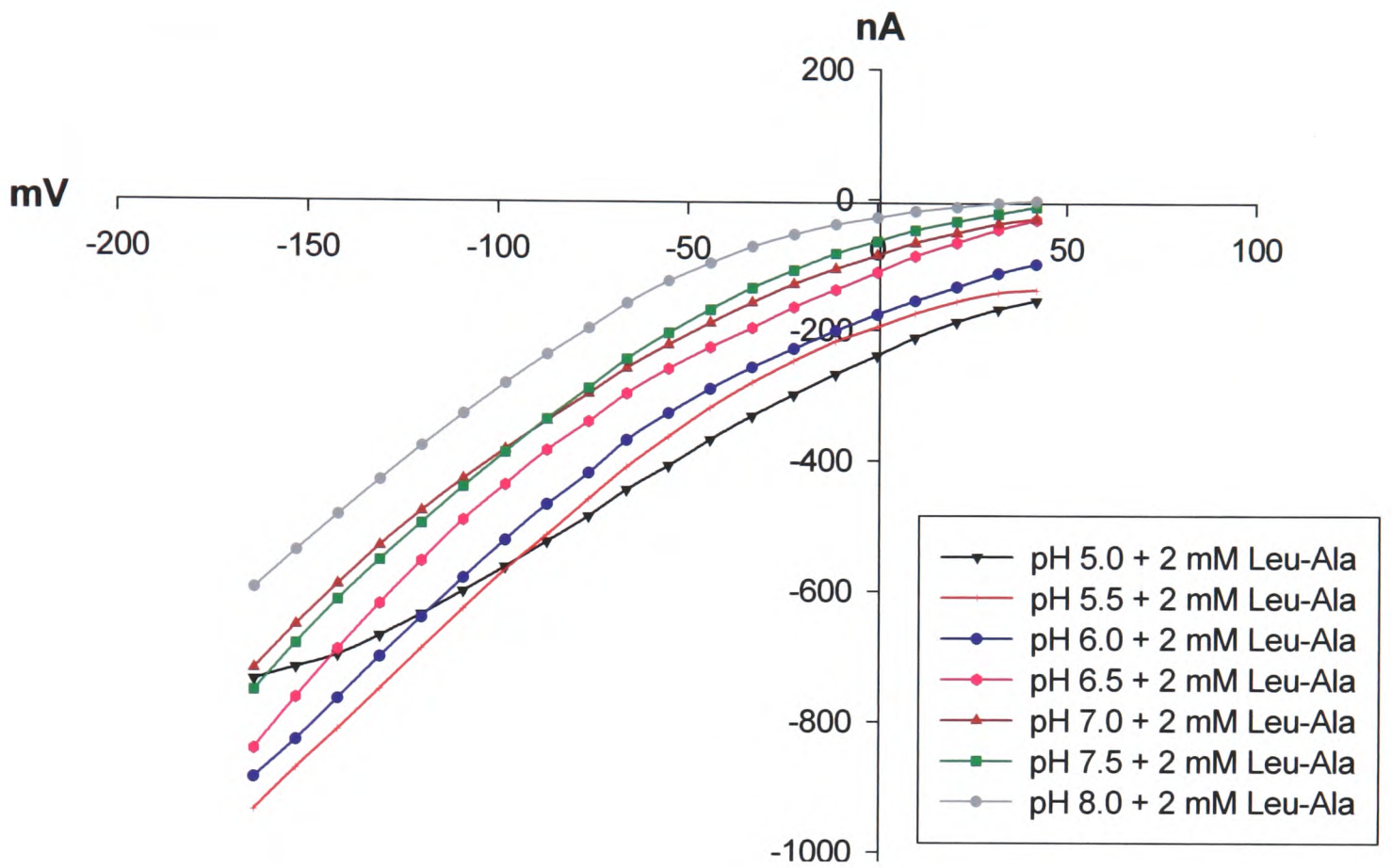


Figure AIV.1 Peptide-induced currents at different clamped voltages in response to 2mM Leu-Ala at various pH values from pH 5.0 to pH 8.0.

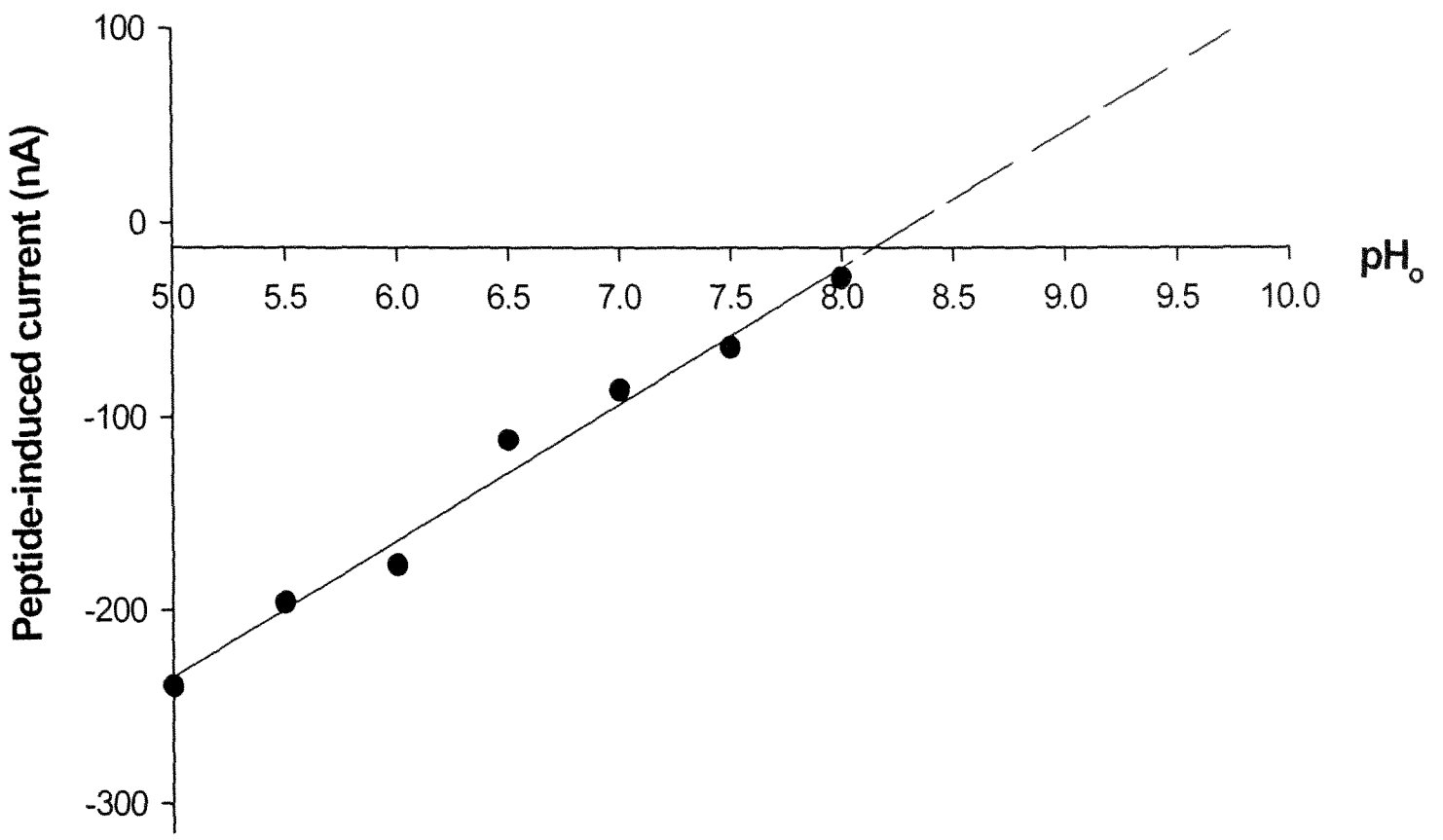


Figure AIV.2 Peptide induced currents, at zero membrane potential, evoked by 2mM Leu-Ala expressed as a function of extracellular pH. The solid line is a linear regression through the experimental data, the dashed line is thatextrapolated, showing the presumed 'static head' or electrochemical reversal potential of the transporter.

(since there are no data points above pH 8.0). Although the Goldman-Hodgkin-Katz equation predicts rectification for a system with net ion flow the voltage dependence of this rectification, however, is not steep. The extrapolation made is therefore a relatively safe prediction of what would happen in experimentally at slightly more alkaline external pH.

From figure AIV.2 the electrochemical reversal potential, E_{rev}, of PepT1-mediated peptide transport occurs at an external pH of approximately pH 8.2, that is, there is no net current flow at pH 8.2. This is the 'static-head' condition. The stoichiometry for proton:peptide coupling (for a neutral peptide being transported through PepT1) is 1:1, therefore at the electrochemical reversal potential, the following relationship applies:

$$\frac{[H^+]_o}{[H^+]_i} = \frac{[Peptide]_i}{[Peptide]_o}$$

Since we know the concentration of extracellular peptide (2mM) and pH (pH 8.2), and we have a safe assumption of intracellular pH in oocytes (pH 7.0) (based on other studies, Fei *et al*, 1994)), we can calculate the concentration of peptide inside the cell:

$$\mathbf{[Peptide]_i = 0.13mM}$$

This is the first estimate of the value in an intact cell with intact natural peptidase actvity.

AIV.5 Summary

1. The results above were carried out when the membrane potential was clamped to zero therefore the only transmembrane driving forces present were the pH gradient and the resulting transmembrane peptide gradient.

2. Experimentally a linear relationship between the extracellular pH and the peptide-induced currents at 0mV was found.

3. By making assumptions based on the Goldman-Hodgkin-Katz equation, the reversal potential for peptide transport via PepT1 was obtained, and an estimation of intracellular peptide concentration was made.

REFERENCES

Abe M., Hoshi T., Tajima A. (1987). Characteristics of transmural potential changes associated with the proton-peptide co-transport in toad small intestine. *J Physiol Lond* **394**: 481-99

Amasheh S., Wenzel U., Boll M., Dorn D., Weber W., Clauss W., Daniel H. (1997). Transport of charged dipeptides by the intestinal H+/peptide symporter PepT1 expressed in Xenopus laevis oocytes. *J-Membr-Biol* **155**: 247-56

Anton, P., O'Connell, J., O'Connell, D., Whitaker, L., O'Sullivan, G.C., Collins, J.K., Shanahan, F. (1998). Mucosal subepithelial binding sites for the bacterial chemotactic peptide, formyl-methionyl-leucyl-phenylalanine (FMLP). *Gut* **42**: 374-9.

Armstrong W. D. (1975). Electrophysiology of sodium transport by epithelial cells of the small intestine. *Intestinal absorption and malabsorption.*

Bailey P. D., Boyd C. A.R., Bronk J. R., Collier I. D., Meredith D., Morgan K. M., Temple C. S. (2000). How to Make Drugs Orally Active: A Substrate Template for Peptide Transporter PepT1. *Angew. Chem. Int. Ed.* **39**: 505-8

Balimane P. V., Tamai I., Guo A., Nakanishi T., Kitada H., Leibach F. H., Tsuji A., Sinko P. J. (1998). Direct evidence for peptide transporter (PepT1)-mediated uptake of a nonpeptide prodrug, valacyclovir. *Biochem-Biophys-Res-Commun* **250**: 246-51

Birnir B., Loo D. D., Wright E. M. (1991). Voltage-clamp studies of the Na+/glucose cotransporter cloned from rabbit small intestine. *Pflugers-Arch* **418**: 79-85

Boll M., Herget M., Wagener M., Weber W. M., Markovich D., Biber J., Clauss W., Murer H., Daniel H. (1996). Expression cloning and functional characterization

of the kidney cortex high-affinity proton-coupled peptide transporter. *Proc-Natl-Acad-Sci-U-S-A* **93**: 284-9

Boll M., Markovich D., Weber W. M., Korte H., Daniel H., Murer H. (1994). Expression cloning of a cDNA from rabbit small intestine related to proton-coupled transport of peptides, beta-lactam antibiotics and ACE-inhibitors. *Pflugers-Arch* **429**: 146-9

Bossi E., Centinaio E., Castagna M., Giovannardi S., Vincenti S., Sacchi V. F., Peres A. (1999). Ion binding and permeation through the lepidopteran amino acid transporter KAAT1 expressed in Xenopus oocytes. *J Physiol Lond* **515**: 729-42

Boyd C. A.R., Ward M. R. (1982). A micro-electrode study of oligopeptide absorption by the small intestinal epithelium of Necturus maculosus. *J Physiol Lond* **324**: 411-28

Brandsch M., Miyamoto Y., Ganapathy V., Leibach F.H. (1994). Expression and Protein Kinase C- dependent regulation of Peptide/H+ Co-transport System in the Caco-2human Carcinoma cell line. *Biochemical Journal* **299**: 253-60

Brandsch M., Thunecke F., Kullertz G., Schutkowski M., Fischer G., Neubert K. (1998). Evidence for the absolute conformational specificity of the intestinal H+/peptide symporter, PEPT1. *J-Biol-Chem* **273**: 3861-4

Bretschneider B., Brandsch M., Neubert R. (1999). Intestinal transport of beta-lactam antibiotics: analysis of the affinity at the H+/peptide symporter (PEPT1), the uptake into Caco-2 cell monolayers and the transepithelial flux. *Pharm Res* **16**: 55-61

Buyse M., Berlioz F., Guilmeau S., Tsocas A., Voisin T., Peranzi G., Merlin D., Laburthe M., Lewin, M.J.M., Roze C., Bado A. (2001). PepT1-mediated epithelial transport of dipeptides and cephalexin is enhanced by luminal leptin in the small intestine. *J.Clin.Invest* **108**:1483-1494.

Closs E., Graf P., Habermeier A., Cunningham J., Forstermann U. (1997). Human cationic amino acid transporters hCAT-1, hCAT-2A, and hCAT-2B: three related carriers with distinct transport properties. *Biochemistry* **36**: 6462-8

Colville C., Gould G.W. (1994). Expression of membrane transport proteins in Xenopus oocytes, form Membrane protein expression systems: A users guide. Ed. G.W.Gould.: 243-74

Daniel H., Adibi S. A. (1993). Transport of beta-lactam antibiotics in kidney brush border membrane. Determinants of their affinity for the oligopeptide/H+ symporter. *J-Clin-Invest* **92**: 2215-23

Daniel H. (1997). First insights into the operational mode of epithelial peptide transporters. *Journal of physiology* **498**: 561

Dascal N. (1987). The use of *Xenopus* oocytes for the study of ion channels. *Crit. Rev. Biochem.* **22**: 317-87

Deves R., Boyd C. A. R. (1998). Transporters for cationic amino acids in animal cells : Discovery, structure and function. *Physiological Reviews* **78**: 487-545

Döring F., Will J., Amasheh S., Clauss W., Ahlbrecht H., Daniel H. (1998). Minimal molecular determinants of substrates for recognition by the intestinal peptide transporter. *J-Biol-Chem* **273**: 23211-8

Erickson R. H., Gum Jr. J. R., Lindstrom M. M., McKean D., Kim Y. S. (1995). Regional expression and dietary regulation of rat small intestinal peptide and amino acid transporter mRNAs. *Biochem-Biophys-Res-Commun* **216**: 249-57

Fei Y. J., Kanai Y., Nussberger S., Ganapathy V., Leibach F. H., Romero M. F., Singh S. K., Boron W. F., Hediger M. A. (1994). Expression cloning of a mammalian proton-coupled oligopeptide transporter. *Nature* **368**: 563-6

Fei Y. J., Fujita T., Lapp D. F., Ganapathy V., Leibach F. H. (1998). Two oligopeptide transporters from Caenorhabditis elegans: molecular cloning and functional expression. *Biochem-J* **332**: 565-72

Fei Y. J., Romero M. F., Krause M., Liu J. C., Huang W., Ganapathy V., Leibach F. H. (2000). A novel H(+)-coupled oligopeptide transporter (OPT3) from Caenorhabditis elegans with a predominant function as a H(+) channel and an exclusive expression in neurons: *J-Biol-Chem*. **275**(13): 9563-71

Fei Y. J., Sugawara M., Liu J. C., Li H. W., Ganapathy V., Ganapathy M. E., Leibach F. H. (2000). cDNA structure, genomic organization, and promoter analysis of the mouse intestinal peptide transporter PEPT1: Biochim-Biophys-Acta. **1492**(1): 145-54

Freeman T., Bentsen B., Thwaites D.T., Simmons N.L. (1995). H+/di-tripeptide transporter (PepT1) expression in the rabbit intestine. *Pflugers Arch* **430**: 394-400

Ganapathy V., Leibach F. H. (1983). Role of pH gradient and membrane potential in dipeptide transport inintestinal and renal brush border membrane vesicles from the rabbit. Studies with L-carnosine and glycyl-L-proline. *J-Biol-Chem* **258**: 14189-92

Ganapathy V., Leibach F. H. (1985). Is intestinal peptide transport energized by a proton gradient? *Am-J-Physiol* **249**: G153-60

Ganapathy M. E., Prasad P. D., Mackenzie B., Ganapathy V., Leibach F. H. (1997). Interaction of anionic cephalosporins with the intestinal and renal peptide transporters PEPT 1 and PEPT 2. *Biochim-Biophys-Acta* **1324**: 296-308

Guo A., Hu P., Balimane P. V., Leibach F. H., Sinko P. J. (1999). Interactions of a nonpeptidic drug, valacyclovir, with the human intestinal peptide transporter (hPEPT1) expressed in a mammalian cell line. *J Pharmacol Exp Ther* **289**: 448-54

Han H. K., Rhie J. K., Oh D. M., Saito G., Hsu C. P., Stewart B. H., Amidon G. L. (1999). CHO/hPEPT1 cells overexpressing the human peptide transporter

(hPEPT1) as an alternative in vitro model for peptidomimetic drugs. *J Pharm Sci* **88**: 347-50

Hediger M.A., Coady M., Ikeda T., Wright E.M. (1987). Expression cloning and cDNA sequencing of the Na+/glucose co-transporter. *Nature* **330**: 379-81

Hediger M.A., Rhoads D. (1994). Molecular physiology of sodium-glucose cotransporters. *Physiol Rev* **74**: 993-1026

Hediger M. A., Kanai Y., You G., Nussberger S. (1995). Mammalian ion-coupled solute transporters. *J Physiol Lond* **482**: 7s-17s

Hussain I., Kellet G., Affleck J., Shepherd E. J., Boyd C. A.R. (2001). Expression and cellular distribution during development of the peptide transporter (PepT1) in the small intestine epithelium of the rat. *Cell and Tissue Research, in press*.

Kelly, S.L., Boyd, C.A.R. (2001). The effects of changing membrane potential and intracellular pH on the kinetic properties of labelled peptide influx into *Xenopus* oocytes expressing PepT1. *Proc. J-Physiol.* **533P.**

Kirk K.L., Halm D.R., Dawson D.C. (1980). Active transport by turtle colon via an electrogenic Na-K exchange pump. *Nature* **287**: 237-239.

Kusano K., Miledi R., Stinnakre J. (1977). Acetylcholine receptors in the oocyte membrane. *Nature* **270**: 739-741

Liang R., Fei Y. J., Prasad P. D., Ramamoorthy S., Han H., Yang Feng T. L., Hediger M. A., Ganapathy V., Leibach F. H. (1995). Human intestinal H+/peptide cotransporter. Cloning, functional expression, and chromosomal localization. *J-Biol-Chem* **270**: 6456-63

Lister N.A., Sykes A., Bailey P.D., Boyd C.A.R., Bronk J.R. (1995). Dipeptide transport and hydrolysis in isolated loops of rat small intestine: effects of stereospecificity. *J Physiol* **484**: 173-82

Liu W., Liang R., Ramamoorthy S., Fei Y.-J., Ganapathy M., Hediger M.A., Ganapathy V., Leibach F.H. (1995). Molecular cloning of PEPT 2, a new member of the H+/peptide cotransporter family, from human kidney. *Biochim Biophys Acta* **1235**: 461-6

Loo D. D., Hirsch J. R., Sarkar H. K., Wright E. M. (1996). Regulation of the mouse retinal taurine transporter (TAUT) by protein kinases in Xenopus oocytes. *FEBS-Lett* **392**: 250-4

Mackenzie B., Fei Y.J., Ganapathy V., Leibach F.H. (1996). The human intestinal H+/oligopeptide cotransporter hPEPT1 transports differently-charged dipeptides with identical electrogenic properties. *Biochim Biophys Acta* **1284**: 125-8

Mackenzie B., Loo D. D., Fei Y.J., Liu W. J., Ganapathy V., Leibach F. H., Wright E. M. (1996). Mechanisms of the human intestinal H+-coupled oligopeptide transporter hPEPT1. *J-Biol-Chem* **271**: 5430-7

Matthews D. M. (1975). Intestinal absorption of peptides. *Physiol-Rev* **55**: 537-608

Matthews D.M., Burston D. (1984). Uptake of a series of neutral dipeptides including L-alanyl-L-alanine, glycylglycine and glycylsarcosine by hamster jejunum in vitro. *Clin Sci (Colch)* **67**: 541-9

Matthews D.M. (1991). Protein Absorption: Development and present state of the subject.

Meredith D., Temple C. S., Guha N., Sword C. J., Boyd C. A.R., Collier I. D., Morgan K. M., Bailey P. D. (2000). Modified amino acids and peptides as substrates for the intestinal peptide transporter PepT1: *Eur-J-Biochem*. **267**(12): 3723-8

Meredith D., Boyd C.A.R. (2000). Structure and Function of Eukaryotic Peptide Transporters. *Cell.Mol.Life.Sci.* **57**: 754-78

Miyamoto K., Shiraga T., Morita K., Yamamoto H., Haga H., Taketani Y., Tamai I., Sai Y., Tsuji A., Takeda E. (1996). Sequence, tissue distribution and developmental changes in rat intestinal oligopeptide transporter. *Biochim-Biophys-Acta* **1305**: 34-8

Muller U., Brandsch M., Prasad P. D., Fei Y. J., Ganapathy V., Leibach F. H. (1996). Inhibition of the H+/peptide cotransporter in the human intestinal cell line Caco-2 by cyclic AMP. *Biochem-Biophys-Res-Commun* **218**: 461-5

Nawrath H., Wegener J.W., Rupp J., Habermeier A., Closs E. (2000). Voltage dependence of L-arginine transport by hCAT-2A and hCAT-2B expressed in oocytes from Xenopus laevis. *Am J Physiol Cell Physiol* **279**: C1336-44

Newton A. C. (1995). Protein kinase C: Structure, function, and regulation. *J-Biol-Chem*. **270**(48): 28495-28498

Ogihara H., Saito H., Shin B. C., Terado T., Takenoshita S., Nagamachi Y., Inui K., Takata K. (1996). Immuno-localization of H+/peptide cotransporter in rat digestive tract. *Biochem-Biophys-Res-Commun* **220**: 848-52

Paddock S.W (1999). Confocal Microscopy Methods and Protocols.

Pan Y. X., Wong E. A., Bloomquist J. R., Webb K. E., Jr. (2001). Expression of a cloned ovine gastrointestinal peptide transporter (oPepT1) in Xenopus oocytes induces uptake of oligopeptides in vitro: *Journal-of-Nutrition*. **131**(4): 1264-1270

Quick, M., Loo, D.D., Wright E.M., (2001). Neutralization of a conserved amino acid residue in the human Na^+/glucose transporter (hSGLT1) generates a glucose-gated H^+ channel. *J-Biol-Chem* **276**: 1728-34.

Roman G., Meller V., Wu K. H., Davis R. L. (1998). The opt1 gene of Drosophila melanogaster encodes a proton-dependent dipeptide transporter. *Am-J-Physiol* **275**: C857-69

Rubio-Aliaga I., Boll M., Daniel H. (2000). Cloning and characterization of the gene encoding the mouse peptide transporter PEPT2. *Biochem Biophys Res Commun* **276**: 734-41

Rubio-Aliaga I., Daniel H. (2001). Mammalian peptide transporters: New approaches for defining their physiological functions. *Proc. J Physiol (in press)*

Sai Y., Tamai I., Sumikawa H., Hayashi K., Nakanishi T., Amano O., Numata M., Iseki S., Tsuji A. (1996). Immunolocalization and pharmacological relevance of oligopeptide transporter PepT1 in intestinal absorption of beta-lactam antibiotics. *FEBS-Lett* **392**: 25-9

Saito H., Okuda M., Terada T., Sasaki S., Inui K. (1995). Cloning and characterization of a rat H+/peptide cotransporter mediating absorption of beta-lactam antibiotics in the intestine and kidney. *J-Pharmacol-Exp-Ther* **275**: 1631-7

Saito H., Terada T., Okuda M., Sasaki S., Inui K. (1996). Molecular cloning and tissue distribution of rat peptide transporter PEPT2. *Biochim Biophys Acta* **1280** : 173-7

Sanders D., Hansen U. P., Gradmann D., Slayman C. L. (1984). Generalised kinetic analysis of ion-driven cotransport systems: a unified interpretation of selective ionic effects on Michaelis parameters. *J-Membr-Biol* **77**: 123-52

Sawada K., Terada T., Saito H., Hashimoto Y., Inui K. (1999). Effects of Glibenclamide on Glycylsarcosine Transport by the rat Peptide Transporters PepT1 and PepT2. *British Journal of Pharmacology* **128**: 1159-64

Schultz S.G. (1980). Basic principles of membrane transport.

Sherwood L. (1993). Human Physiology: From cells to systems.

Shiraga T., Miyamoto K., Tanaka H., Yamamoto H., Taketani Y., Morita K., Tamai I., Tsuji A., Takeda E. (1999). Cellular and molecular mechanisms of dietary

regulation on rat intestinal H+/Peptide transporter PepT1. *Gastroenterology* **116**: 354-62

Steel A., Nussberger S., Romero M. F., Boron W. F., Boyd C. A.R., Hediger M. A. (1997). Stoichiometry and pH dependence of the rabbit proton-dependent oligopeptide transporter PepT1. *J-Physiol-Lond* **498**: 563-9

Stein W. (1990). Channels, Carriers and Pumps: An introduction to membrane transport.

Takahashi K., Nakamura N., Terada T., Okano T., Futami T., Saito H., Inui K. (1998). Interaction of beta-lactam antibiotics with H+/peptide cotransporters in rat renal brush-border membranes. *J-Pharmacol-Exp-Ther* **286**: 1037-42

Tamai I., Nakanishi T., Nakahara H., Sai Y., Ganapathy V., Leibach F. H., Tsuji A. (1999). Improvement of L-dopa absorption by dipeptidyl derivation, utilizing peptide transporter PepT1. *J Pharm Sci* **87**: 1542-6

Temple C. S., Bronk J. R., Bailey P. D., Boyd C.A.R. (1995). Substrate-charge dependence of stoichiometry shows membrane potential is the driving force for proton-peptide cotransport in rat renal cortex. *Pflugers-Arch* **430**: 825-9

Temple C. S., Bailey P. D., Bronk J. R., Boyd C.A.R. (1996). A model for the kinetics of neutral and anionic dipeptide-proton cotransport by the apical membrane of rat kidney cortex. *J-Physiol-Lond* **494**: 795-808

Temple C. S., Stewart A. K., Meredith D., Lister N. A., Morgan K. M., Collier I. D., Vaughan Jones R. D., Boyd C. A. R., Bailey P. D., Bronk J. R. (1998). Peptide mimics as substrates for the intestinal peptide transporter. *J-Biol-Chem* **273**: 20-2

Terada T., Sawada K., Saito H., Hashimoto Y., Inui K. (1999). Functional characteristics of basolateral peptide transporter in the human intestinal cell line Caco-2. *Am J Physiol* **276**: G1435-41

Thamotharan M., Bawani S. Z., Zhou X., Adibi S. A. (1999). Hormonal regulation of oligopeptide transporter PepT1 in a human intestinal cell line. *American Journal of Physiology* **276**: c821-c826.

Thorens B. (1993). Facilitated glucose transporters in epithelial cells. *Annual Review of Physiology* **55**: 591-608

Thwaites D.T., Hirst B.H., Simmons N.L. (1993). Direct assessment of dipeptide/H+ symport in intact human intestinal (Caco-2) epithelium: a novel method utilising continuous intracellular pH measurement. *Biochem Biophys Res Commun* **194**: 432-8

Thwaites D. T., Brown C. D., Hirst B. H., Simmons N. L. (1993). H(+)-coupled dipeptide (glycylsarcosine) transport across apical and basal borders of human intestinal Caco-2 cell monolayers display distinctive characteristics. *Biochim-Biophys-Acta* **1151**: 237-45

Walker D., Thwaites D. T., Simmons N. L., Gilbert H. J., Hirst B. H. (1998). Substrate upregulation of the human small intestinal peptide transporter, hPepT1. *J-Physiol-Lond* **507**: 697-706

Weber W. M. (1999). Ion currents of Xenopus laevis oocytes: State of the art. *Biochimica et Biophysica Acta Biomembranes* **1421**: 213-33

Wenzel U., Thwaites D. T., Daniel H. (1995). Stereoselective uptake of beta-lactam antibiotics by the intestinal peptide transporter. *Br-J-Pharmacol* **116**: 3021-7

Wenzel U., Gebert I., Weintraut H., Weber W. M., Clauss W., Daniel H. (1996). Transport characteristics of differently charged cephalosporin antibiotics in oocytes expressing the cloned intestinal peptide transporter PepT1 and in human intestinal Caco-2 cells. *J-Pharmacol-Exp-Ther* **277**: 831-9

Zhu T., Chen Xing Z., Steel A., Hediger M.A., Smith David E. (2000). Differential recognition of ACE inhibitors in xenopus laevis oocytes expressing rat PEPT1 and PEPT2. *Pharmaceutical-Research-New-York*. **17** (5): 526-532.

Zubay G., Salemme F. R. (1988). Biochemistry.